UNIVERSITAT POLITÈCNICA DE VALÈNCIA

ivia instituto valenciano de investigaciones agrarias

From root to fruit

Biotechnological tools applied to improvement of persimmon (*Diospyros kaki* Thunb.) culture

Francisco Gil Muñoz

Julio 2020

Directoras

Dra. Maria Luisa Badenes Catalá

Dra. María del Mar Naval Merino

Tutor

Dr. Jaime Prohens Tomás

Porque el 2020 no solo ha tenido cosas malas.

En los malos tiempos podemos lamentarnos, pero también podemos buscar oportunidades.

Agradecimientos

En primer lugar, he de agradecer a Marisa su dirección, apoyo y confianza que siempre ha depositado en mí. Sus ánimos y ayuda han permitido que esta tesis haya sacado lo mejor de mí. Siempre has sido mi apoyo en los momentos más difíciles durante estos años. También a Mar, por todo lo que me ha enseñado no solo a nivel laboral sino también a nivel personal, y sobre todo por su sinceridad. Gracias a tus ganas de enseñarme en todo momento y tu gran dedicación puesta en esta tesis. Espero haberos mostrado al menos parte de lo mucho que os agradezco vuestro trabajo.

He de mencionar también a Gabino por su gran apoyo científico, especialmente en la biología molecular y sobre todo por su buen humor que siempre alegra el día.

Jose y Julio, habéis sido una pieza fundamental en el desarrollo de muchos de los experimentos. Me llevo de vosotros grandes recuerdos de los días en el tórrido invernadero.

También al personal del departamento y el resto del IVIA con quienes he pasado grandes momentos y de quienes he aprendido mucho: Mati, Inma, Ana Conejero, Pepe, Elena, Alba, Helena, Mª Ángeles, Juan Gabriel, Amparo, Lidia, Mari-Rus, Jose Miguel, Dani, Estela, Carles, Cristina, Luis… Además, a Jesús Sánchez y al resto de personal del IBMCP que me ayudaron siempre de forma muy amable con los experimentos.

Aunque solo hayas llegado en mi última etapa de la tesis. Blasco, muchas gracias por confiar en mí en esta nueva etapa de mi carrera.

Después del largo viaje al frío y oscuro norte, he de agradecer profundamente a Sari, Nico, Sonali, Jesús y demás miembros del UPSC. A pesar de estar como en otro planeta me hicisteis sentir como en casa. No puedo no poner aquí a Josep y a Sonia, a pesar de que vi

auroras boreales, vosotros sois lo mejor que me llevo del fin del mundo.

En especial a mi familia, sobre todo a mis padres. Gracias a vosotros he podido llegar “tan lejos”. Por los muchos valores que me habéis enseñado, vuestra paciencia a la hora de educarme. Vuestro interés, y en general por todo. No puedo resumir lo mucho que tengo que agradeceros con unas pocas palabras. Además, a Lourdes, quien espero que sea mi compañera de vida. Hemos estado juntos en momentos muy difíciles y nos hemos apoyado siempre, los éxitos son de los dos porque somos un equipo.

También a mis amigos, porque sois quienes hacéis que la vida sea una aventura. Creo que sabéis que siempre me vais a tener para lo que necesitéis.

Gracias a todos y cada uno, me dejo a más personas que, de poneros a todos, llenaría otro documento del mismo volumen que esta tesis. Gracias a vosotros puedo decir que he crecido tanto o más a nivel personal que académico tras estos años.

…

Y el águila pasará horas posada en un risco escrutando los reinos del mundo hasta detectar algún movimiento lejano, y en ese momento de pronto se concentrará, concentrará, concentrará en el pequeño caparazón que se mece entre los arbustos allá abajo en el desierto. Y entonces el águila se lanzará desde lo alto del risco...

Y un minuto después la tortuga descubre que el mundo se está alejando de ella. Y ve el mundo por primera vez, ya no a unos centímetros del suelo sino a doscientos metros, qué gran amiga tengo en el águila.

Y entonces el águila la suelta.

Y casi siempre la tortuga se precipita hacia su muerte. Todo el mundo sabe por qué la tortuga hace esto. La gravedad es una costumbre a la que cuesta mucho renunciar. Nadie sabe por qué el águila hace esto. No cabe duda de que hay un buen almuerzo en una tortuga pero, teniendo en cuenta el esfuerzo que requiere, la verdad es que hay un almuerzo mucho mejor en prácticamente cualquier otra cosa. Lo que ocurre es, simplemente, que las águilas disfrutan atormentando a las tortugas.

Pero el águila, por supuesto, no es consciente de que está tomando parte en una forma muy tosca de selección natural.

Algún día una tortuga aprenderá a volar.

…

Terry Pratchett, *Dioses Menores*

Index

Figure Index

Table Index

Abbreviations

ABA: Abscisic Acid

AbA: Aureobasydin-A

ACT: Actine

AD: Activation Domain

Ade: Adenine

AFLP: Amplified Fragment Length Polymorphism

ALMT: Aluminum-Malate Transporter

AMOVA: Analysis of Molecular Variance

ANOVA: Analysis of Variance

ANR: Anthocyanidin Reductase

ANS: Anthocyanidin Synthase

ATPase: Adenosine Triphosphatase

AVP: Vacuolar H^+-translocase Pyrophosphatase

BAN: BANYULS

BC: *Diospyros kaki* x *Diospyros virginiana* Backcross

BD: Binding Domain

bHLH: Basic Helix-Loop-Helix

BiFC: Bimolecular Fluorescence Complementation

CCC: Chloride Channel

CCX: Ca^{2+}/ cation Exchanger

cDNA: Complementary DNA

CHI: Chalcone Isomerase

CHS: Chalcone Synthase

CHX: Cation/H^+ exchanger

CIPK: Calcineurin B-like Protein (CBL)-CBL-Interacting Protein Kinase

CLC: Chloride Channel

Ct: Carboxyl-*terminus*

CTAB: Cetrimonium Bromide

DFR: Dihydroflavonol Reductase

DK: *Diospyros kaki*

DL: *Diospyros lotus*

DNA: Deoxyribonucleic Acid

DV: *Diospyros virginiana*

EAR: Ethylene-Responsive Element Binding Factor-Associated Amphiphilic Repression

eGFP: Enhanced Green Fluorescent Protein

F3'H: Flavonoid 3´-Hydroxylase

FC: Fold Count

FW: Fresh Weight

GA: Gibberellin

Gal: Galactosidase

GFP: Green Fluorescent Protein

H: Histidine

HKT: High Affinity Potassium Transporter

BLAST: Basic Local Alignment Search Tool

IVIA: Valencian Institute of Agricultural Research

LAR: Leucoanthocyanidin Reductase

LSD: Least Significant Difference

LUC: Firefly luciferase

LWD: Light Regulated WD

MAPK: Mitogen-Activated Protein Kinase

MBW: MYB-BHLH-WDR protein complex

MCMC: Markov Chain Monte Carlo

MES: 2-ethanesulfonic Acid

MYB: Myeloblastosis family transcription factor

NHX: Na^+/H^+ antiporter

NIP: Nodulin-26 like Intrinsic Protein

NLS: Nuclear Localization Sequence

Nt: Amino-*terminus*

OD: Optical density

PA: Proanthocyanidin

PC: Principal Component

PCA: Pollination Constant Astringent

PCA: Principal Component Analysis

PCNA: Pollination Constant Non-Astringent

PCR: Polymerase Chain Reaction

PIC: Polymorphism Information Content

PIP: Plasma Membrane Intrinsic Protein

PP2A: Protein Phosphatase 2

PVA: Pollination Variant Astringent

PVNA: Pollination Variant Non-Astringent

Pwo: *Pyrococcus woesei*

QA: Quality Asessment

RAPD: Random Amplification of Polymorphic DNA

REN: *Renilla* Luciferase

RGR: Relative Growth Rate

RNA: Ribonucleic Acid

RNase: Ribonuclease

ROS: Reactive Oxygen Species

RT: Retrotranscription

RT-qPCR: Real-time Quantitative Polymerase Chain Reaction

SD: Nonselective medium

SIP: Small basic Intrinsic Protein

SOS: Saline Overly Sensitive

SRA: Sequence Read Archive

SSR: Single Sequence Repeat

TIP: Tonoplast Intrinsic Protein

TL: Transmitted light

TT2: Transparent Testa-2

TT8: Transparent Testa-8

TTG1: Transparent Testa Glabra-1

TUA: Tubulin Alpha Chain

UBC: Ubiquitin C

UPOV: International Union for the Protection of New Varieties of Plants

WD40: Beta-Transducin Repeat

WDR: WD40-Repeat Protein

WUE: Water Use Efficiency

YFP: Yellow Fluorescent Protein

ABSTRACT

Persimmon culture has vastly grown in the last 20 years as an alternative to citrus production in the Valencian region. However, its production faces three important problems. First, monovarietal production based on *Rojo Brillante* is a sanitary and market risk that requires to increase the number of varieties available. Second, climate change has threatened persimmon production in the Mediterranean areas because the salinity increase in water and soil. Salinity severely affects production, quality and postharvest life of the fruit. The lack of salt-tolerant rootstocks compatible with the cultural conditions aggravates the problem; hence clonal salt-tolerant rootstocks are needed. Third, persimmon industry relies on the postharvest deastringency treatment of the varieties. Even though there are varieties that are naturally non-astringent, its culture in the Mediterranean area is limited due to rootstock incompatibility. Additionally, the costly postharvest treatment is also affected by salinity. Consequently, more information is needed about the molecular mechanism of astringency biosynthesis in persimmon fruit in order to develop new varieties and/or more effective treatments for removing astringency of the fruit.

In the context of breeding and molecular biology, three goals need to be approached in order to improve the cultural conditions: development of new persimmon varieties with maturity date different from *Rojo Brillante*, development of salt-tolerant clonal rootstocks compatible with non-astringent varieties and research on

the molecular bases of the mechanism of astringency production to optimize the postharvest treatments. This research contributes and provides knowledge to address these goals.

Concerning breeding of new varieties, the IVIA persimmon germplasm collection is an important resource for breeding of new varieties. To ensure efficient breeding and avoid redundancy in the collection, a SSR analysis was carried out to solve this problem. This analysis has provided useful data, such as the discovery of unique alleles, that allows rapid identification of varieties or the division of the population according to its astringency type, confirming the common genetic background of the accessions concerning to this trait. The generated genetic diversity map will be useful for designing crosses in the breeding program.

To address the salinity problem, several salt-stress assays were done in greenhouse using different persimmon rootstocks populations: *Diospyros virginiana* (salt-tolerant), *Diospyros kaki* (salt-sensitive fully compatible) and *Diospyros lotus* (salt-sensitive). Furthermore, due to the desirable characters present in these species, a backcross progeny between *D. kaki* and *D. virginiana* was obtained and included in the salt-stress assays. Thus, several individuals from all the populations have been selected, which are tolerant to salinity and could meet the desired characteristics for appropriate persimmon clonal rootstocks. Furthermore we have used physiological, transcriptomic and mass transcriptome sequencing approaches in order to discover the physiological and genetic bases of salinity tolerance in these species. As a result, we described the

main facts related to salinity tolerance mechanisms in *Diospyros* species, such as ion compartmentalization, *HKT-1-like* root expression, abundancy of chloride channels and root architecture.

Finally, in order to get a deeper insight on the biosynthesis of proanthocyanidins, the responsible molecule of astringency, we hypothesized the presence of a MBW protein complex (MYB-bHLH-WD40) in persimmon fruit, involved in the regulation of the proanthocyanidins synthesis pathway in a similar way to other species. We firstly sequenced the putative persimmon *WD40* orthologue of *TTG1* gene from *Arabidopsis thaliana*. The role of this gene and other genes of the complex (*MYB2*, *MYB4* and *MYC1*) was studied through transcriptomic analysis in different stages of non-astringent and astringent fruit. Furthermore, we have observed through microscopy the subcellular localization of these genes using fluorescent protein fusions and transient expression in *Nicotiana benthamiana* leaves, and analyzed its interaction through yeast two-hybrid assays and BiFC (bimolecular fluorescence complementation) experiments in *Nicotiana benthamiana* leaves. In addition, we have analyzed the effects of these interactions in the pathway of proanthocyanidin biosynthesis using the *ANR* (anthocyanidin reductase) gene promoter and the promoters of some of these genes (*MYB4* and *MYC1*) fused with a luciferase reporter, together with the coexpression of the MBW genes using transient expression in *Nicotiana benthamiana* leaves. The results of these assays have confirmed the nuclear interaction of these genes and its role in the regulation of astringency biosynthesis, providing a basic model with

some differences with respect to the models proposed in other species.

RESUMEN

El cultivo del caqui ha crecido enormemente en la región Valenciana en los últimos 20 años al presentarse como una alternativa interesante al cultivo de cítricos. Sin embargo, su cultivo se enfrenta a tres problemas importantes. En primer lugar, su producción es monovarietal y se centra en la variedad *Rojo Brillante*, lo que conlleva un riesgo sanitario y de mercado importante que pone de manifiesto la necesidad de aumentar el número de variedades disponibles. En segundo lugar, el cambio climático pone en peligro la producción de caqui en zonas mediterráneas debido a un aumento en la salinidad del agua y suelo. La salinidad afecta especialmente al caqui debido a sus efectos sobre la producción, calidad y postcosecha de la fruta. La falta de patrones tolerantes a la salinidad compatibles con las condiciones de cultivo además agrava este problema, por lo que es necesario el desarrollo de patrones clonales tolerantes a la salinidad. En tercer lugar, la industria del caqui está basada en la aplicación de tratamientos postcosecha de desastringencia. Aunque existen variedades naturalmente no astringentes, su uso en el Mediterráneo es complicado debido a la incompatibilidad con los patrones existentes. Además, la salinidad afecta gravemente la eficacia del tratamiento de desastringencia. Por ello, cabe destacar que se necesita más información acerca de los mecanismos moleculares que controlan el desarrollo de la astringencia para poder desarrollar nuevas variedades y/o unos tratamientos de desastringencia más efectivos.

En el contexto de la mejora genética y la biología molecular, pueden distinguirse tres objetivos para mejorar las condiciones de cultivo en esta región: el desarrollo de nuevas variedades de caqui con una época de madurez distinta a *Rojo Brillante*, el desarrollo de patrones clonales tolerantes a la salinidad y compatibles con variedades no astringentes y la obtención de nuevos conocimientos acerca de las bases moleculares del mecanismo de regulación de la astringencia para optimizar los tratamientos postcosecha. La presente tesis ha contribuido a estos tres objetivos.

Respecto a la obtención de nuevas variedades, se ha desarrollado un análisis de diversidad genética del banco de germoplasma del IVIA, lo que es un recurso importante para la planificación de cruces. Para asegurar una mejora genética eficiente y evitar redundancias en la colección, se ha efectuado un análisis de diversidad usando secuencias microsatélites. El análisis ha arrojado datos de gran utilidad, como el descubrimiento de alelos únicos, que permiten la identificación rápida de variedades, o la división de la colección de acuerdo con el tipo de astringencia del fruto, confirmando el fondo genético común de las accesiones que comparten este carácter. Además, el mapa de las relaciones filogenéticas generado será de gran utilidad para la planificación futura de cruces dentro del programa de mejora de caqui.

Para abordar el problema de la salinidad, se han realizado distintos ensayos de estrés salino en invernadero con distintas poblaciones de especies utilizadas como patrón de caqui: *Diospyros virginiana* (tolerante a salinidad), *Diospyros kaki* (sensible a salinidad y

compatible) y *Diospyros lotus* (sensible a salinidad). Además, debido a los caracteres de gran interés presentes en estas dos especies, se incluyó en los ensayos una población proveniente de un retrocruce entre *D. kaki* y *D. virginiana*. Como resultado, varios individuos de estas poblaciones se han seleccionado debido a su tolerancia a la salinidad, ya que podrían tener las características adecuadas para ser patrones clonales. Complementariamente, se han usado aproximaciones fisiológicas, transcriptómicas y de secuenciación masiva de transcriptoma para hacer una primera descripción de los mecanismos de tolerancia a la salinidad presentes en estas especies. Como resultado, se han descrito los principales caracteres relacionados con la tolerancia a la salinidad en el género *Diospyros*, como la compartimentalización de iones, la expresión en raíz de un gen similar a *HKT-1,* la abundancia de canales de cloruro o la arquitectura de raíz.

Finalmente, para obtener más información sobre la biosíntesis de proantocianidinas, la molécula responsable de la astringencia, se formuló la hipótesis de la existencia de un complejo proteico del tipo MBW (MYB-bHLH-WD40) que podía regular la ruta molecular de forma análoga a la regulación existente en otras especies estudiadas. En primer lugar se secuenció un gen tipo WD40, posible ortólogo de *TTG1* de *Arabidopsis thaliana*. El papel de este gen y otros genes del hipotético complejo (*MYB2*, *MYB4* y *MYC1*) han sido estudiados mediante un análisis transcriptómico en distintos estadios de madurez de frutos astringentes y no astringentes. Además, se ha observado mediante microscopía la localización celular de estos

genes mediante la expresión transitoria con fusión con fluorescencia en hojas de *Nicotiana benthamiana* y hemos analizado su interacción mediante ensayos de doble híbrido en levadura y BiFC (complementación bimolecular de fluorescencia) mediante expresión transitoria en hojas de *Nicotiana benthamiana*. Finalmente, hemos analizado los efectos de estos genes y de sus interacciones en la ruta de biosíntesis de proantocianidinas usando el promotor del gen *ANR* (antocianidin reductasa) y promotores de los genes reguladores *MYC1* y *MYB4,* fusionándolos con una luciferasa como gen delator y coexpresándolos con distintas combinaciones de los genes del complejo MBW mediante expresión transitoria en hojas de *Nicotiana benthamiana.* Los resultados de estos ensayos confirman la interacción nuclear de estos genes y su papel en la regulación de la producción de la astringencia, dando lugar a un modelo básico con algunas diferencias a los propuestos en otras especies.

RESUM

El cultiu del caqui ha crescut enormement en la regió Valenciana en els últims 20 anys al presentar-se com una alternativa interessant al cultiu de cítrics. No obstant, el seu cultiu s'enfronta a tres problemes importants. En primer lloc, la seua producció es monovarietal i està centrada en la varietat *Rojo Brillante*, el que suposa un risc sanitari i de mercat important que posa de manifest la necessitat de augmentar el nombre de varietats disponibles. En segon lloc, el canvi climàtic posa en perill la producció de caqui a la zona mediterrània degut a un augment en la salinitat del aigua i del sòl. La salinitat afecta de forma especialment al caqui degut al seus efectes sobre la producció, qualitat i vida post collita de la fruita. La falta de patrons tolerants a salinitat compatibles amb les condicions de cultiu a més agreuja aquest problema, pel que es necessari el desenvolupament de patrons clonals tolerants a salinitat. En tercer lloc, la industria del caqui esta basada en la aplicació de tractaments post collita de deastringència. Encara que existixen varietats naturalment no astringents, el seu us al mediterrani es complicat degut a la incompatibilitat en els patrons existents. A més, la salinitat afecta gravement a la eficàcia del tractament post collita de deastringència. Per això, cal destacar que es necessita conèixer millor els mecanismes moleculars que controlen el desenvolupament de la astringència per a la obtenció de noves varietats i/o uns tractaments post collita més efectius.

En aquest context de millora genètica i biologia molecular, es poden distingir tres objectius per a millorar les condicions del cultiu en aquesta regió: el desenvolupament de noves varietats de caqui en una època de maduresa distinta a la de *Rojo Brillante*, el desenvolupament de patrons clonals tolerants a salinitat i compatibles amb varietats no astringents i la obtenció de nous coneixements sobre les bases moleculars del mecanisme de producció de astringència per optimitzar els tractaments post collita. La present tesi ha contribuït a aquests tres objectius.

En el que respecta a la obtenció de noves varietats, s'ha desenvolupat un anàlisi de diversitat genètica del banc de germoplasma de l'IVIA, el qual es un recurs important per a la planificació de creuaments. Per a assegurar una millora genètica eficient i evitar redundàncies a la col·lecció, s'ha efectuat un anàlisi en microsatèl·lits. El anàlisi ha resultat en dades de gran utilitat, com el descobriment de al·lels únics, que permiteixen la identificació rapida de varietats, o la divisió de la col·lecció d'acord en el tipus d'astringència del fruit, confirmant el fons genètic comú de les accessions que comparteixen aquest caràcter. A més, el mapa de les relacions filogenètiques elaborat serà de gran utilitat per a la planificació futura de creuaments dins del programa de millora de caqui.

Per a abordar el problema de la salinitat, s'han realitzat distints assajos d'estrés salí en hivernacle amb distintes poblacions de patró de caqui: *Diospyros virginiana* (tolerant a salinitat), *Diospyros kaki* (sensible a salinitat i amb compatibilitat) i *Diospyros lotus* (sensible a

salinitat). A més, degut als caràcters de gran interès presents en aquestes dos espècies, es va incloure en els assajos una població provenient de un retrocreuament entre *D. kaki* i *D. virginiana*. Com a resultat, diversos individus d aquestes poblacions s'han seleccionat degut a la seua tolerància a salinitat, ja que podrien tindre les característiques adequades per a ser patrons clonals. Complementàriament, s'han utilitzat aproximacions fisiològiques, transcriptòmiques i de seqüenciació massiva de transcriptoma per a fer una primera descripció dels mecanismes de tolerància a salinitat presents en aquestes espècies. Com a resultat s'han descrit els principals caràcters relacionats amb la tolerància a la salinitat en el gènere Diospyros, com la compartimentalització de ions, la expressió en arrel de un gen similar a *HKT-1*, la abundància de canals de clorur o la arquitectura de la arrel.

Finalment, per a obtenir mes informació sobre la biosíntesi de proantocianidines, la molècula responsable de la astringència, es va formular la hipòtesi de la existència de un complex proteic del tipus MBW (MYB-bHLH-WD40) que podria regular la ruta molecular de forma anàloga a la regulació existent en altres espècies estudiades. En primer lloc, es va seqüenciar el gen ortòlog putatiu del tipus WD40 de *TTG1* de *Arabidopsis thaliana*. El paper de aquest gen i altres gens del hipotètic complex (*MYB2*, *MYB4* i *MYC1*) han sigut estudiats mitjançant un anàlisi transcripcional en diferents estats de maduresa de fruits astringents i no astringents. A més, s'ha observat amb microscòpia la localització cel·lular de aquestos gens mitjançant la expressió transitòria amb fusió a fluorescència en fulles de Nicotiana

benthamiana i hem analitzat la seua interacció amb un assaig de doble híbrid en llevat i BiFC (complementació bimolecular de fluorescència) mitjançant expressió transitòria en fulles de *Nicotiana benthamiana*. Finalment hem analitzat els efectes de aquests gens i de les seues interaccions en la ruta de biosíntesi de proantocianidines utilitzant el promotor del gen *ANR* (antocianidin reductasa) i promotors dels gens reguladors *MYC1* i *MYB4* fusionant-los amb una luciferasa com a gen delator i coexpressant-los amb diferents combinacions dels gens del complex MBW mitjançant expressió transitòria en fulles de *Nicotiana benthamiana*. Els resultats de aquests assajos confirmen la interacció nuclear de aquestos gens i el seu paper en la regulació de la producció de la astringència, donant lloc a un model bàsic amb algunes diferències als proposats en altres espècies.

Introduction

Persimmon (*Diospyros kaki* Thunb.) has been cultivated in the Mediterranean area since the XVII century (Perucho, 2015). The species was introduced as a minor fruit tree for familiar consumption. In the XX century persimmon production was initiated in some regions of Spain. However, it was restricted to small orchards and the production sold in local markets. The astringency of the fruits from the Mediterranean varieties allowed consumption after over ripening, which limited marketing to long distances. Postharvest treatments for removing the fruit astringency (Pesis and Ben-Arie, 1984; Arnal and Del Río, 2003) provided non-astringent fruits that kept the firmness and fruit quality. The treated fruits have a longer post-harvest life, which enables their transport to mid and long-distance markets. This technology opened new markets for the persimmon industry and changed the paradigm of persimmon production, specifically at the Mediterranean basin in the 90s. Only in Spain, persimmon surface increased from 2,000 in 2004 to 13,000 ha in 2014 (Perucho, 2015), particularly in the Valencian region (Figure 1), that currently accounts for 90% of the Spanish production.

This market change has had a great impact over persimmon production. For instance, in the Protected Denomination of Origin "Ribera del Xúquer", inside one of the most important persimmon production regions, the production is nowadays almost exclusively based in the hard non-astringent treated fruit (branded as *Persimon*®), being the traditional soft form restricted (Figure 2).

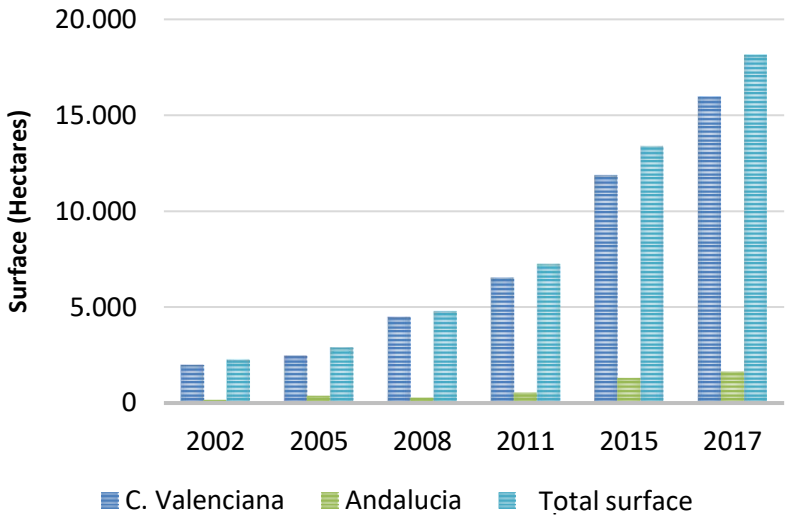

Figure 1. Evolution of persimmon production surface in Spain.

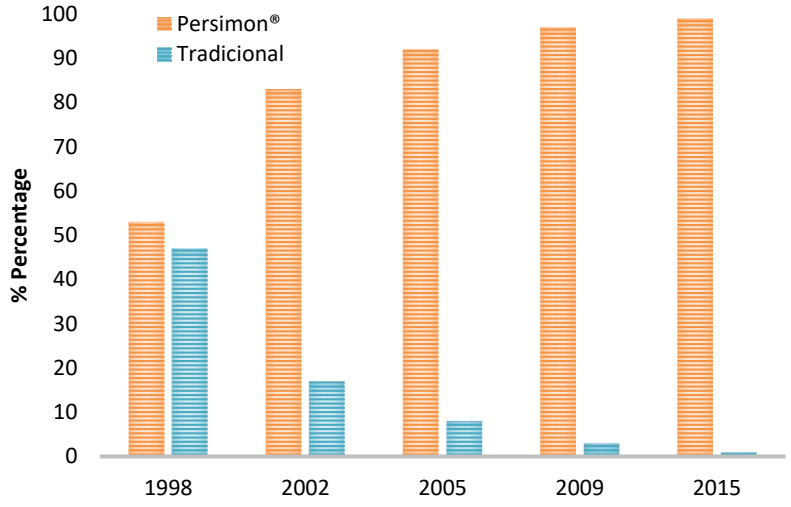

Figure 2. Hard-fruit versus soft-fruit evolution in the P.D.O. "Ribera del Xúquer"

Production at the Mediterranean basin is based on a few astringent varieties introduced from Asia by the merchants during the XVII century. Consequently, the genetic diversity present in Europe is limited. Furthermore, the European production relies mainly on three closed-related cultivars: *Triumph* in Israel, *Kaki Tipo* in Italy and *Rojo Brillante* in Spain (Perucho, 2015). This monovarietal-based production is both a sanitary and market risk for these regions.

Out of the center of origin (China) and diversification (South Korea and Japan), the Mediterranean basin produces the highest amount outside of Asia. Inside this region, Spain leads fruit production, even surpassing Japan production in the recent years (Figure 3). Spanish persimmon production is located in Valencia and Southwest Andalusia. In both regions the crop is based on astringent cultivars that need to be treated in postharvest for removing the astringency of the fruits devoted to export. Recently, market trends and climate change have threatened persimmon production. This fact makes necessary to analyze and solve the agronomical issues faced by the industry.

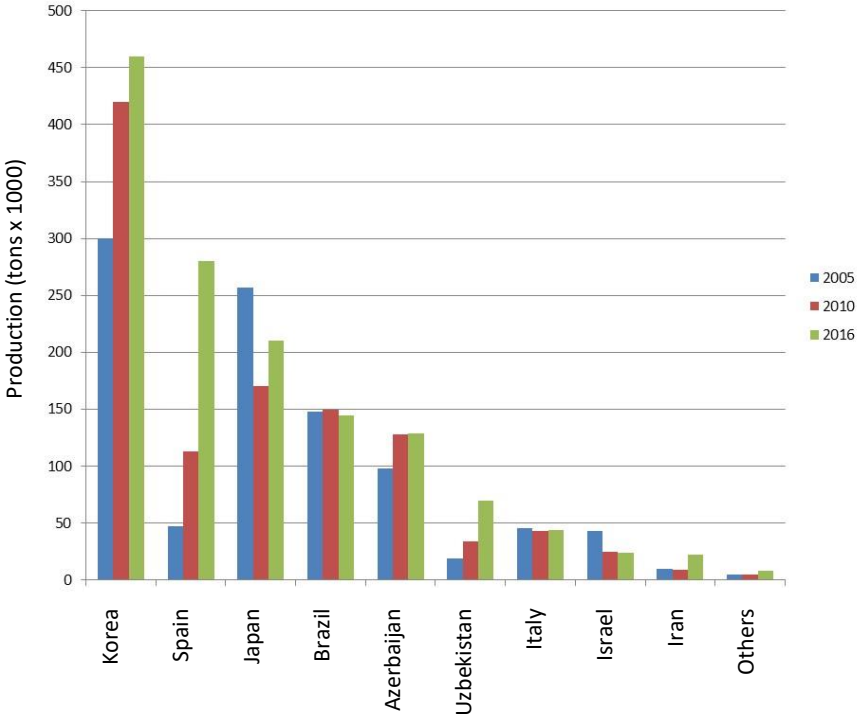

Figure 3. 2005 to 2016 evolution of persimmon production outside China

Genetic structure of persimmon varieties

Diospyros genus comprises more than 700 species, mainly native to the tropics, belonging to the family of Ebenaceae. Inside the family, only several species from this genus are exploited either for the quality of the wood (ebony) such as ceylon ebony (D*. ebenum*), benin ebony (*D. crassiflora*), makassar ebony (*D*. *celebica*) and mauritius ebony (*D. tesselaria*); or for fruit consumption such as persimmon (*D*. *kaki*), American persimmon (D. *virginiana*), date-plum (*D*. *lotus*), black sapote (*D. nigra*), Indian persimmon (*D*. *peregrine*) and Texan persimmon (*D*. *texana*). Interestingly, marble ebony (*D*. *leucomelas*) is used with pharmaceutical interest for betulinic acid extraction (Diospyros - Wikipedia).

Persimmon (*Diospyros kaki* Thunb.) origin is located at East Asia, where it was known around 2500 years B.C. and cultivated since approximately 200 years B.C (Wang et al., 2013); however it was not widely cultivated until the fifth century. On the seventh century it was introduced into Japan, where became widely cultivated (Kikuchi, 1948). In Japan, persimmon became the fourth most important fruit, being Japan an important source of genetic material. Only in East Asia more than 2.000 cultivars were described (Cho and Cho, 1965; Wang et al., 1997; Yamada et al., 2012). This species are hypothesized to have an autohexaploid origin (Tamura et al., 1998) (2n = 6x = 90), this ploidy difficults breeding and genome sequencing. Until now, no genome of any *Diospyros* species has been released, which slows the progress on genetic studies of persimmon. However, there is available a SRA from *D. lotus* (Akagi et al., 2014) (2n = 2x = 30).

Persimmon cultivars have been classified according to the loss of astringency during ripening and presence/absence of seeds from pollination. There are four types: pollination-variant astringent (PVA), pollination-constant astringent (PCA), pollination-variant non-astringent (PVNA) and, pollination-constant non-astringent (PCNA) (Kajiura, 1946; Kitagawa and Glucina, 1984; Yonemori et al., 2000) (Figure 4).

The pollination-variant and pollination-constant character is a seed-based trait, as persimmon seeds can produce different amounts of ethanol and acetaldehyde that naturally removes astringency in the flesh (Sugiura et al., 1979). According to the amount of astringency caused in the flesh, astringent cultivars are divided into PCA, PVA and PVNA (ordered from no emission to more) (Figure 5). The genetic base of this trait is not known yet and probably is a quantitative trait (Ikeda et al., 1985). However, it is known that PVNA cultivars (those in which the presence of seeds make the pulp no astringent) are a group originated in Japan, being 'Zenjimaru' cultivar the oldest described in XIII century (Sato and Yamada, 2016). Since then, this character has been widely introgressed into Japanese cultivars, resulting in wide genetic variation in this type, similar to the "wild type" PCA cultivars (Sato and Yamada, 2016).

PCA	PCNA	PVA	PVNA
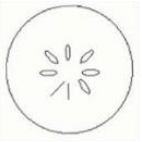	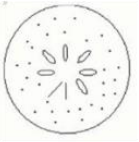	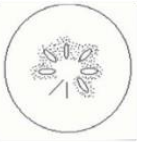	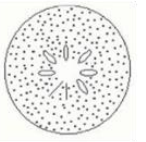
- Always astringent on commercial maturity, independent on pollination - Without brown stains in the flesh	- Always NON astringent on commercial maturity, independent on pollination - Some brown stains in the flesh	- Astringent on commercial maturity, except around the seeds, if present. - Brown stains in the flesh around the seeds	- Non astringents on commercial maturity if pollinated. - Big brown stains in the flesh around the seeds
			

Figure 4. Persimmon classification based on astringency and flesh color as defined by the guidelines of DHS from UPOV (31/03/2004), Geneva.

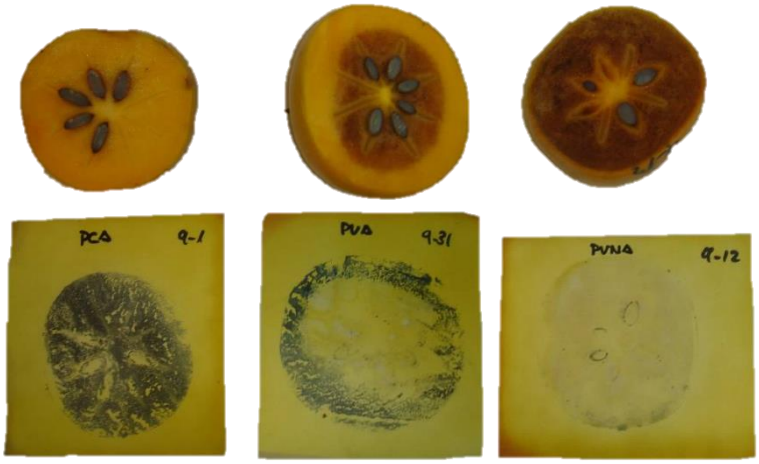

Figure 5. Three types of astringent persimmon according to the amount of astringency caused by the seed. The astringency distribution can be seen in blue the ferric chloride impregnated paper at the bottom (pictures provided by Jose Martínez-Calvo)

On the other hand, PCNA fruit are non-astringent during the most part of the ripening process. The genetic basis of this character is hypothesized to be caused by a single gene (Ikeda et al., 1985; Yamada and Sato, 2002; Akagi et al., 2010a). Two different known mutations cause this trait: a recessive one, caused by the ast/AST allele (Yonemori et al., 2000), which its non-astringent phenotype was firstly described in 'Gosho' variety at the XVII century (Parfitt et al., 2015) and a dominant one (so called Chinese-PCNA) discovered in China in 'Luo Tian Tian Shi' variety in 1983 (Wang, 1983).

Unfortunately, despite the development of molecular markers tightly linked to the PCNA character (Kanzaki et al., 2001; Kono et al., 2016; Sato and Yamada, 2016), the lack of a reference genome and the hexaploid genetic structure has avoided finding the mutation origin at gene-level. It is believed that all the Japanese PCNA cultivars are probably a result from inbreeding and backcrosses between an ancestor variety and other non-PCNA varieties, and their descendants resulted in the present Japanese PCNA cultivars (Ikeda et al., 1985; Yamada et al., 1993; Yamada, 2005). The oldest known Japanese PCNA is 'Gosho', that can be the original Japanese PCNA ancestor, but other known or unknown cultivars might have contributed to the formation of the Japanese PCNA varieties (Sato and Yamada, 2016). This inbreeding causes that PCNA cultivars usually have less production than other cultivars. This also has to be taken into account for breeding PCNA cultivars, as the risk of inbreeding depression is high (Yamada, 1993, 2005).

Furthermore, persimmon crosses are sometimes limited because of its reproductive biology. *Diospyros kaki* species has three types of flowers: female, male and hermaphrodite (Figure 6). Depending on the cultivar, we can find diclino-monoic (female and male flowers in the same tree), diclino-dioic (female and male flowers on different individuals) or polygamo-dioic (female, male and hermaphrodite flowers on the same individual). Even though a persimmon population of male-only flowers has been discovered (Xu et al., 2008; Zhang et al., 2016). Sex expression in persimmon is genetically determined and is associated with each cultivar. The genetic control

is based on a gene (MeGI) that triggers the production of both male and female flowers and a repressor (OGI) that regulates activity of MeGI gene therefore producing female-only flowers (Akagi et al., 2016). Both genes are epigenetically regulated by methylation, explaining the fact that sometimes viable male flowers can be found in female accessions (Yakushiji and Nakatsuka, 2007).

Figure 6. Female, male and hermaphrodite flowers in *Diospyros kaki* (pictures provided by Jose Martinez Calvo)

Persimmon cultivars have different levels of parthenocarpy. Some cultivars do not need pollination for fruit set and growth (Reig et al., 2018), being this characteristic a quantitative genetic trait (Kitajima

et al., 1992). In fruits from PVA and PVNA type, seeds produced acetaldehyde that insolubilizes tannins which removes the fruit astringency and browns the flesh color. In these types, pollination is necessary if a natural non-astringent hard brown spotted fruit is desired. If a non-brown flesh is wanted either for non-astringent over ripened fruit or for hard fruits that are going to be treated for deastringency, pollination needs to be avoided. In fact, in Spain most orchards produce the PVA *Rojo Brillante*, a very productive parthenocarpic fruit, and pollination should be avoided since pollination produces seeded fruits with brown flesh unpleasant for consumers. However, the number of PCA, PVA and PCNA accessions with only female flowers is much higher than the accessions with female and male flowers (Table 1).

Taking into account the low genetic diversity, persimmon breeding needs an increasing genetic knowledge of parentals for avoiding the high inbreeding risk. Furthermore, the sexual biology limits the availability of male parents and therefore restricts crossing possibilities.

Table 1. Flower type of the accessions described in the IVIA germplasm bank (data provided by Jose Martínez-Calvo, January 2020). Abbreviations: Brazil (BR), Spain (SP), Eastern Europe (E EUR), Italy (IT), Japan (JP), Russia (RU), Pakistan (PAK), Ukraine (UKR), France (FR).

Cultivar	Origin	Type	Flower types
Pomelo	BR	PCA	♀/♂/☿
Anheca	SP	PCA	♀
Ferrán-12	SP	PCA	♀
Garidells	SP	PCA	♀
Reus-6	SP	PCA	♀
Tomatero	SP	PCA	♀
Nikiskaja Bordobaja	E EUR	PCA	♀
Costata	IT	PCA	♀
Lycopersicon	IT	PCA	♀
Aizumishirazu-A	JP	PCA	♀
Fuji	JP	PCA	♀
Hachiya	JP	PCA	♀
Korea Kaki	JP	PCA	♀
Takura	JP	PCA	♀
Yokono	JP	PCA	♀
Russian Beauty	RU	PCA	♀
Ban Gosho	JP	PCNA	♀
Benisakigake	JP	PCNA	♀
Cal Fuyu	JP	PCNA	♀/♂
Fau Fau	JP	PCNA	♀/♂
Fukuro Gosho	JP	PCNA	♀/♂
Fuyu	JP	PCNA	♀
Giant Fuyu	JP	PCNA	♀
Hana fuyu	JP	PCNA	♀
Hana Gosho	JP	PCNA	♀/♂
Ichikikei Jiro	JP	PCNA	♀
Isahaya	JP	PCNA	♀
Jiro	JP	PCNA	♀
Jiro (C-24276)	JP	PCNA	♀

Kawabata	JP	PCNA	♀
Koda Gosho	JP	PCNA	♀
Maekawa jiro	JP	PCNA	♀
Mukaku jiro	JP	PCNA	♀
Nishijo (Saijo)	JP	PCNA	♀/♂
O'Gosho	JP	PCNA	♀
Suruga	JP	PCNA	♀
Tokio Gosho	JP	PCNA	♀
Yamato Gosho	JP	PCNA	♀
Giombo	BR	PVA	♀
Rama Forte	BR	PVA	♀
Bétera-2	SP	PVA	♀
Cristalino-B	SP	PVA	♀/♂/ ☿
Reus-15	SP	PVA	♀
Rojo Brillante	SP	PVA	♀
Xato de Bonrepós	SP	PVA	♀
Zuezdocka	E EUR	PVA	♀/♂
Triumph	IS	PVA	♀
Farmacista Honorati	IT	PVA	♀/♂/ ☿
Aizumishirazu-B	JP	PVA	♀
Atago	JP	PVA	♀
Hiratanekaki	JP	PVA	♀
Hiratanenashi	JP	PVA	♀
Koshu Hyakume	JP	PVA	♀
Maru	JP	PVA	♀/♂
Tone Hiratanenashi	JP	PVA	♀
Tone wase	JP	PVA	♀
Pakistan Seedless	PAK	PVA	♀
Bétera-3	SP	PVNA	♀
Constantí	SP	PVNA	♀
La Selva-14	SP	PVNA	♀
Cibaca	E EUR	PVNA	♀
Orest	UKR	PVNA	♀
Tardive des Charentes	FR	PVNA	♀
Brazzale	IT	PVNA	♀/♂/ ☿

Castellani	IT	PVNA	♀
Cioccolatino	IT	PVNA	♀/♂/ ☿
Edoichi	IT	PVNA	♀
Kaki Tipo	IT	PVNA	♀
Lampadina	IT	PVNA	♀
Mandarino	IT	PVNA	♀/♂/ ☿
Moro	IT	PVNA	♀/♂/ ☿
Vainiglia	IT	PVNA	♀/♂/ ☿
Agakaki	JP	PVNA	♀/♂
Akoumankaki	JP	PVNA	♀
Amahyakume	JP	PVNA	♀
Amankaki	JP	PVNA	♀
Giboshi	JP	PVNA	♀
Hyakume	JP	PVNA	♀
Kirakaki	JP	PVNA	♀
Kuro Kuma	JP	PVNA	♀
Mikatani Gosho	JP	PVNA	♀
Shogatsu	JP	PVNA	♀/♂

Salt-stress tolerance and climate change

Salinity stress effect in plants is a combination of osmotic stress and ion-toxicity stress. Osmotic stress affects firstly to the plants, decreasing shoot and plant growth. Ionic stress is caused by the accumulation of toxic concentrations of Na^+ and Cl^- at the tissues, causing premature organ senescence and tissue necrosis (Munns and Tester, 2008).

Solute presence in water reduces the availability of assimilable water in the soil by the plant, causing an osmotic stress. The reduced water availability causes an effect similar to drought, negatively affecting shoot and leaf growth in non-halophyte plants. The osmotic stress immediately causes a response in the stomatal aperture of the plant mediated by Abscisic acid (ABA) (Fricke et al., 2006). This effect is independent from the ion toxicity of the available water, since it has been observed that it might be regulated by root signals that are activated in drought conditions (Termaat et al., 1985; Davies et al., 2005).

Finally, overaccumulation of Na^+ and Cl^- ends in tissue necrosis, as these ions tend to be accumulated in old leaves (Sibole et al., 2003; Plett and Møller, 2010), leaf margins (Shapira et al., 2009), and epidermal cells (Huang and Van Steveninck, 1989; Karley et al., 2000a, 2000b; James et al., 2006). Probably this is due to an evolutive mechanism to protect photosynthetically active cells (Baetz et al., 2016).

Climate change has great impact on coastal regions due to inundations from sea-level rise and heightened storm damage. However, in these regions, soil salinization involves a great risk that should be taken into account (Brecht et al., 2012). In these regions, climate change usually involves a reduction in soil water availability and/or an increase of evapotranspiration, favoring saltwater intrusion in the land.

Currently, more than 600 million people live in worldwide coastal zones that will be affected by progressive salinization (Dasgupta et al., 2015). According to the climatic predictions, it is expected an increase in winter temperature in the Mediterranean region, combined with changes in rainfall amount and distribution (Mimi and Jamous, 2010).

Furthermore, anthropogenic practices such as agriculture can itself directly induce or accelerate the soil salinization process by using inorganic fertilization or by the irrigation system. The Mediterranean area is in consequence highly vulnerable to soil salinization due to climate change, agricultural system and climatic conditions. Historical evidences show this vulnerability since the times of the Ancient Mesopotamian civilizations, whose decline was accelerated by soil salinization through agriculture. More recently, in Egypt, the build of Aswan Dam in the Nile River has led to the salinization of 60% of the farmland in the Nile Delta (Postiglione, 2002), leading to a delicate situation of agriculture in this country. Inside Europe, Spain is one of the countries with the highest amount of saline land and highest saline risk (Figure 7) (Toth et al., 2008).

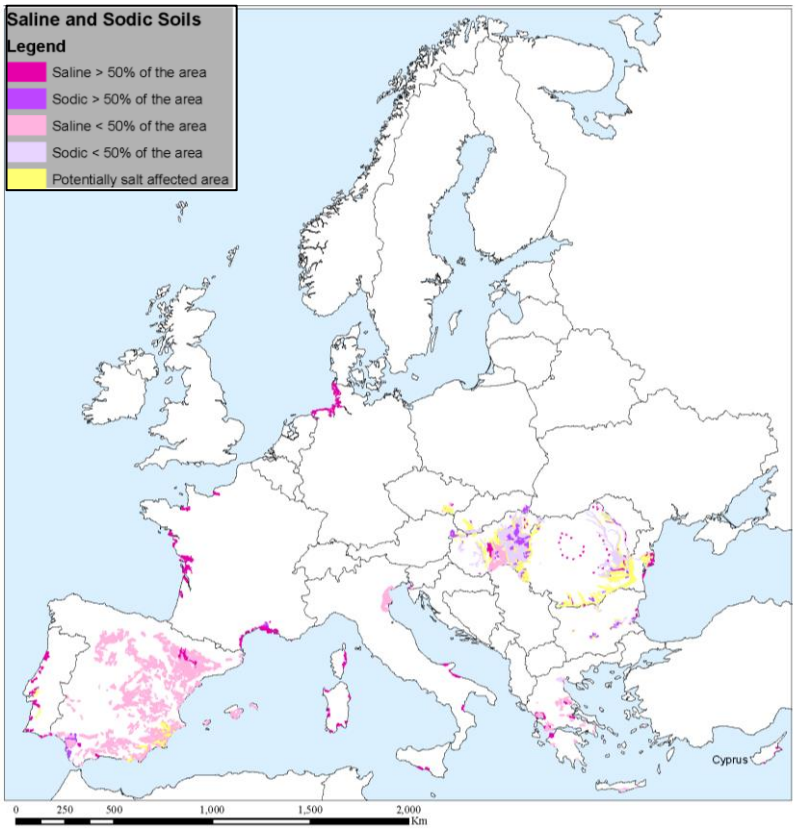

Figure 7. Saline, sodic and potentially saline areas inside the European Union (Toth et al., 2008)

In order to use saline areas for agriculture, several approaches could be applied, for instance the increase of soil drainage to ease salt leaching, the improvement of irrigation methods and the selection of salt tolerant species (Forner-Giner and Ancillo, 2013).

Three species are used worldwide as rootstock: *D. kaki*, *D. lotus* and *D. virginiana*. The most widespread used rootstock is *D. kaki*; however, it cannot be used in the Mediterranean basin countries due to the high levels of limestone in soil in this area. *D. lotus* is the most

used rootstock in Italy and Spain because of its tolerance to lime-filled soils; nevertheless, it is highly sensitive to salinity. On the other hand, *D. virginiana* is more tolerant to salinity and performs well on lime-filled soils, but confers too much vigor to the plant, and produce many suckers, making the crop management difficult (De Paz et al., 2016). Furthermore, PCNA varieties are not compatible with either *D. virginiana* or *D. lotus*, thus production of persimmon PCNA type in the Mediterranean area becomes difficult. Therefore, in this region, hard-fruit production is based on astringent varieties followed by deastringency postharvest treatment.

Persimmon production is being compromised by the increase of salinity in soil and water in areas where no salinity problems were previously reported (Visconti et al., 2015), causing severe damage to the trees (Figure 8). In these species, salinity causes a loss in production and premature fruit senescence, and hinders astringency removal by postharvest treatment (Besada et al., 2016), making salinity-affected fruits unusable. This fact is especially important in regions where persimmon marketing is based in the consumption of hard fruit and the production based on PCNA cultivars is not possible.

Figure 8. Damage in a persimmon orchard caused by salinity (picture provided by Jose Miguel de Paz)

Clonal rootstocks from persimmon species are not used due to the lack of efficient propagation methods. Nowadays, persimmon rootstocks are obtained from seeds that due to the heterozygosis of the species are highly variable. That situation may confer high heterogeneity to persimmon orchards. The availability of clonal rootstocks adapted to the soil conditions with easy propagation would be most desirable. Currently, there are few propagation protocols available for persimmon, which should be used for further propagation of selected genotypes from breeding (Giordani et al., 2012).

Proanthocyanidin biosynthesis and regulation

Persimmon production and marketing has evolved into a major preference of consumers for firm fruit, resulting either in the integration of postharvest treatments into the production system or the growth of PCNA cultivars (Yonemori et al., 2000; Bellini and Giordani, 2002).

Astringency is a tactile feel in the mouth surfaces of dryness caused by precipitation of saliva proteins (Lyman and Green, 1990). In persimmon, this precipitation is caused by the presence of soluble tannins in the fruit that are accumulated in the vacuoles of the 'tannin cells' (Gottreich and Blumenfeld, 1991; Yonemori et al., 1997; Salvador et al., 2007). Persimmon tannins belong to the group of the proanthocyanidins (PAs) (Matsuo and Itoo, 1978).

Naturally, persimmon PAs are in a soluble form. However, acetaldehyde exposure leads to PAs polymerization in the form of insoluble complexes that don't produce astringency. This reaction is produced in persimmon during maturity (Salvador et al., 2007; Tessmer et al., 2016), by the oxidation of the endogenous ethanol or by decarboxylation of pyruvic acid (Sugiura et al., 1979; Sugiura and Tomana, 1983). These reactions can be induced either by endogenous ethanol application or by anaerobiosis conditions (Besada et al., 2015). Commercial deastringency treatments are usually based in the last one, treating the fruits for several hours in a rich CO_2 or N_2 atmosphere.

PA biosynthesis is part of the flavonoid biosynthesis route, sharing pathways with the flavonol and anthocyanin routes. In *Arabidopsis thaliana*, such as in many other species, PAs are accumulated in the coat of the seeds, providing protection to microbial pathogens, pests and herbivores (Dixon et al., 2005). This accumulation can be also present in leaves, bark and fruits.

Analysis of *Arabidopsis thaliana* and other species seed coat mutants has allowed dissecting the biosynthetic pathway of PAs (Leipiniec et al., 2006). These molecules are formed by condensation of *trans*- and *cis*-flavan-3-ols units, synthesized respectively by stereospecific leucoanthocyanidin reductase (LAR) and anthocyanidin reductase (ANR) enzymes (Tanner et al., 2003; Xie et al., 2003) (Figure 9).

In *Arabidopsis,* those genes are regulated by a protein ternary complex named MYB-bHLH-WD40 (MBW), formed by a R2R3-MYB transcription factor, a basic helix-loop-helix (bHLH) transcription factor and a WD40-repeat (WDR) protein (Baudry et al., 2004). MBW complexes contribute to PAs production in edible fruits of crop plants such as grapevine (Hichry et al., 2010), strawberry (Schaart et al., 2013) and apple (Gesell et al., 2014).

This route is highly conserved among plants, including persimmon, and some of these genes have been identified. Furthermore, its expression has been analyzed in both astringent and non-astringent fruit during development. In the case of the Japanese non-astringent fruit, the absence of astringency is caused by both an interruption in the development of the tannin cells related to a reduction in the

expression of PA biosynthesis genes in early growth stages. This causes a dilution of the PAs in the fruit during the growth (Yonemori and Matsushima, 1985; Yonemori and Matsushima, 1987).

Interestingly, in the Chinese non-astringent fruit, it is observed an interruption in the development of the tannin cells, but the expression of PA biosynthesis related genes is not concomitantly reduced (Kanzaki et al., 2000; Ikegami et al., 2005).

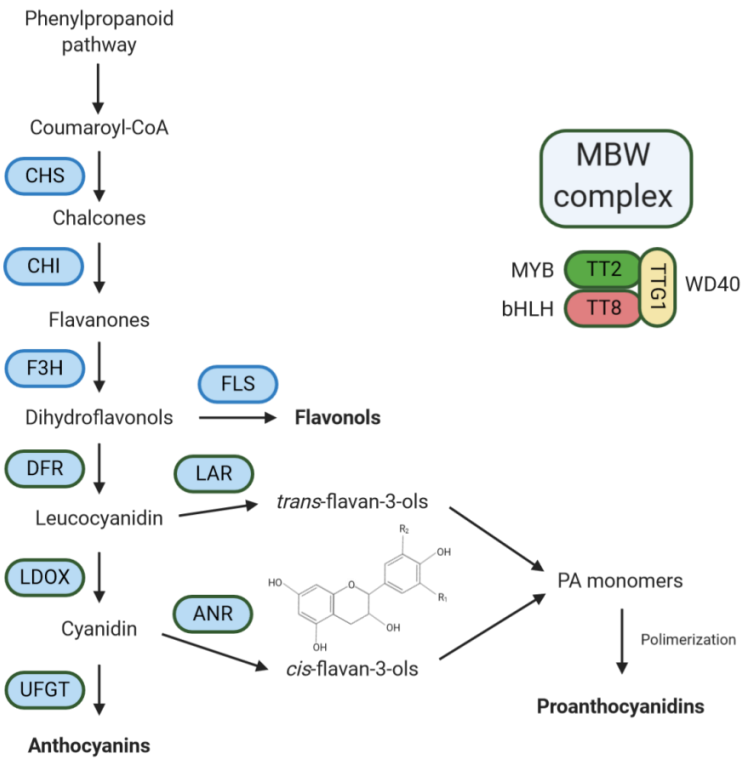

Figure 9. Scheme of Proanthocyanidin biosynthesis route in *Arabidopsis thaliana*. Green-bounded genes are controlled by a MYB-bHLH-WD40 (MBW) ternary complex formed by TT2, TT8 and TTG1 proteins.

Astringency removal in persimmon production and marketing is very important, understanding PA biosynthesis and regulation of this pathway can provide a key knowledge for breeding non-astringent varieties.

Main objectives

The objectives of this thesis are focused in three main goals:

- Elucidate the genetic structure of the IVIA persimmon germplasm bank compared with traditional cultivars aimed at identifying the most convenient parents for breeding.
- Unravel the mechanisms of salinity tolerance present in *Diospyros* species for establishing the basis of a persimmon saline-tolerant rootstock breeding program.
- Identify the WD40 orthologous protein that takes part of an hypothetical MBW complex involved in regulation of proanthocyanidin biosynthesis in persimmon, and characterize the possible complexes that regulate this pathway.

CHAPTER 1: Analysis of genetic diversity among a set of accessions of the IVIA's persimmon collection

The results presented in this chapter were published in a scientific paper and presented in an international symposium:

Francisco Gil-Muñoz, Elena Zuriaga, María Luisa Badenes, María del Mar Naval. 2018. Analysis of genetic diversity among a set of accessions from the IVIA's persimmon collection. Acta Horticulturae, (1195), 43–50. doi:10.17660/actahortic.2018.1195.7

Francisco Gil-Muñoz, Elena Zuriaga, María Luisa Badenes, María del Mar Naval. 2016. Analysis of genetic diversity among a set of accessions of the IVIA persimmon collection. VI International Symposium on Persimmon. Valencia.

Abstract

In Spain, persimmon (*Diospyros kaki* Thunb.) [2n = 6x = 90] production has become an alternative to the major fruit crops. The Instituto Valenciano de Investigaciones Agrarias (IVIA, Valencia, Spain) is carrying a persimmon breeding program aimed at increasing the range of varieties available in the crop. Genetic resources collections are an important tool for breeding. Knowledge of genetic structure of the germplasm is valuable information for better management of plant material in a breeding program. In this work, new accessions incorporated into the IVIA's germplasm bank were analyzed by molecular markers. A total of 48 accessions from different origins and two rootstock species have been studied using 18 polymorphic microsatellite markers. Genetic structure was estimated using a Bayesian-based model clustering method while a Neighbor-Joining phylogenetic tree was constructed to visualize the genetic relationship among samples. Evanno's test of the Bayesian-based model estimation resulted in 3 populations as the most informative. Persimmon cultivars are classified in 4 types according to its astringency into PCNA, PVNA, PCA and PVA. According to that, most of PVNA and PCNA accessions were grouped apart from PVA and PCA accessions, regardless of its origin.

Introduction

Persimmon (*Diospyros kaki* Thunb.) is an edible fruit belonging to the genus *Diospyros*, in the family Ebenaceae. This genus occurs worldwide in tropical and subtropical regions and contains more than 400 species with different ploidy levels, ranging from diploid (2n = 2x = 30) to nonaploid (2n = 9x = 135). From them, persimmon is the most widely cultivated species, and is mainly hexaploid (2n = 6x = 90) (Tamura et al., 1998). This species is native to Eastern Asia, being these regions very rich in germplasm resources (Yamada et al., 2012).

Persimmon cultivars are classified according to its astringency loss in the fruit and change in flesh color into four types: pollination-constant non-astringent (PCNA), pollination-variant non-astringent (PVNA), pollination-constant astringent (PCA) and pollination-variant astringent (PVA) (Yonemori et al., 2000). Fruits from pollination variant cultivars change their flesh color when pollination occurs, becoming darker. Non-astringent cultivars lose astringency naturally during growth, being edible at maturity, whereas astringent cultivars remain astringent until fruit softening (Parfitt et al., 2015). The trait of natural astringency loss in fruits is controlled by a single gene (AST), being the PCNA trait recessive (Yonemori et al., 2000). The inheritance of the AST/ast allele in this hexaploid context forces breeding programs to either intercrossing PCNA type cultivars or backcrossing the offspring of a PCNA x non-PCNA to a PCNA genotype. However, due to the limited number of PCNA cultivars available, crossing this type of cultivars could result in inbreeding depression in progenies (Yamada et al., 1994). Modern PCNA

breeding programs often include non-PCNA genotypes to increase the genetic pool and avoid this problem (Akagi et al., 2010b; Sato and Yamada, 2016).

In order to incorporate efficiently new accessions into a breeding program, it is important to clarify the genetic relationships between the available germplasm. A previous work (Naval et al., 2010) analyzed the genetic diversity of the IVIA's persimmon germplasm collection using simple sequence repeat (SSR) markers (Soriano et al., 2006). However, since 2010 new germplasm accessions have been introduced in the collection, hence new analyses are needed in order to update the information that could allow making a more effective use of these new materials.

Materials and methods

Plant material and DNA extraction

Forty-seven persimmon accessions from different countries belonging to the IVIA's germplasm collection were analyzed (Table 1). Seedlings from *Diospyros lotus* L. and *Diospyros virginiana* L. were included as reference outgroups. Fully expanded leaves from fruit-mature trees were sampled and kept at -20ºC until DNA extraction, using the CTAB method (Doyle and Doyle, 1987) with minor modifications (Soriano et al., 2006).

Table 2. List of persimmon cultivars analyzed in this study

Cultivar	Type	Origin	Cultivar	Type	Origin
Farmacista Honorati	PCA	Italy	Yamato Gosho	PCNA	Japan
Garidells	PCA	Spain	Youhou	PCNA	Japan
Korean Kaki	PCA	Japan	Yubeni	PCNA	Japan
Lycopersicon	PCA	Italy	Betera-2	PVA	Spain
Nikita Gift	PCA	Eastern Europe	Rama Forte	PVA	Brasil
Pomelo	PCA	Brasil	Reus-15	PVA	Spain
Russian Beauty	PCA	Eastern Europe	Taigetsu	PVA	Japan
Takura	PCA	Japan	Taiten	PVA	Japan
Yokono	PCA	Japan	Tone Wase	PVA	Japan
Fau Fau	PCNA	Portugal	Triumph	PVA	Israel
Giant Fuyu	PCNA	Japan	Xato del Bonrepos	PVA	Spain
Hana Fuyu	PCNA	Japan	Zuezdocka	PVA	Eastern Europe
Hana Gosho	PCNA	Japan	Agakaki	PVNA	Japan
Isahaya	PCNA	Japan	Akoumankaki	PVNA	Japan
Izu	PCNA	Japan	Brazzale	PVNA	Italy
Kanshu	PCNA	Japan	Cibaca	PVNA	Eastern Europe
Kawabata	PCNA	Japan	Giboshi	PVNA	Japan
Kishu	PCNA	Japan	Kirakaki	PVNA	Japan
Maekawa Jiro	PCNA	Japan	Kurokuma	PVNA	Japan
Shogatsu	PCNA	Japan	Moro	PVNA	Italy
Siushuu	PCNA	Japan	Orest	PVNA	Eastern Europe
Soshuu	PCNA	Japan	Tardif des Charentes	PVNA	France
Suruga	PCNA	Japan	*D. Lotus*	-	
Taishuu	PCNA	Japan	*D. virginiana*	-	

Microsatellite analysis

Eighteen polymorphic microsatellite loci previously employed in *D. kaki* (Naval et al., 2010) were used following the PCR conditions described by Soriano *et al.* (2006). Each reaction was performed with three primers: the specific forward primer of each microsatellite with M13(-21) tail at its 5'end, the sequence-specific reverse primer, and the universal fluorescent-labeled M13(-21) primer (Schuelke, 2000). Allele lengths were determined using an ABI Prism 3130 Genetic Analyzer with the aid of GeneMapper software, version 4.0 (Applied Biosystems).

Data analysis

For each microsatellite, the presence or absence of each single fragment was coded as 1 or 0, respectively, to generate a binary data matrix. In order to evaluate the informativeness of the microsatellites employed, the number of alleles per locus and the polymorphism information content (PIC) (Weir, 1990) were calculated.

Possible population substructure was estimated using the Bayesian-based model procedure from STRUCTURE v2.3.4 software (Pritchard et al., 2000) assuming admixture. Degree of admixture (λ) was inferred for K=1 assuming the same admixture in all populations using the mean from 15 runs (burn-in period length $1x10^5$, MCMC repetitions $5x10^5$). Test runs for estimating number of clusters (K) were conducted from K=1 to K=10 in 20 independent runs (Falush et al., 2003) (burn-in period length = $1x10^5$, MCMC repetitions = $5x10^5$). The most informative K was identified by using the Evanno's test (ΔK)

(Evanno et al., 2005). Subsequently, population structure was inferred for K = 3 with a burn-in period length of $5x10^5$ and $4x10^6$ MCMC repetitions. Analyses of molecular variance (AMOVA) (Excoffier et al., 1992) were carried out using GeneAlEx v.6.41 (Peakall and Smouse, 2012).

In order to visualize the genetic relationship between samples, Nei's genetic distance (Nei, 1972) was calculated using the Phylogenetic Computer Tools v. 1.3 software (Buntjer, 1997) and a Neighbor-Joining dendrogram was constructed using the PHYLIP v. 3.695 package (Felsenstein, 2005). The stability of the tree was tested with 1000 bootstrapped data matrices. Also, a Principal Component Analysis (PCA) was carried out using GeneAlEx v.6.41 (Peakall and Smouse, 2012).

Results

Genetic variation of SSR markers

A total of 208 alleles were amplified from the 47 persimmon cultivars and 2 rootstock species using 18 SSRs polymorphic markers (Table 2). The number of alleles per locus ranged from 3 (ssrdk-29) to 20 (ssrdk-03). PIC results confirmed the suitability of these markers for the analysis in this study, ranging from 0.537 (ssrdk-29) to 0.918 (ssrdk-37) with an average of 0.83. The highest number of rare alleles (6) was obtained for ssrdk-03 and ssrdk-26, whereas lowest was for ssrdk-14 (0). Unique alleles were obtained in some accessions with all markers except ssrdk-14, ssrdk-17, ssrdk-25, ssrdk-29 and ssrdk-32 as indicated in Table 3.

Table 3. Summary of SSRs results. Number of alleles obtained, polymorphism information content (PIC), rare alleles (freq < 0.02) and alleles exclusive for one accession (name between brackets) are indicated.

Marker	No. of alleles	PIC	Rare alleles	Unique alleles
ssrdk-01	13	0,8926	2	2 (Giboshi and Agakaki)
ssrdk-02	13	0,8803	3	1 (Triumph)
ssrdk-03	20	0,9145	6	3 (Triumph, Tone Wase and Kawabata)
ssrdk-04	9	0,8166	2	1 (Maekawa Jiro)
ssrdk-06	14	0,8969	2	2 (Giboshi and Agakaki)
ssrdk-10	9	0,8082	2	1 (Russian Beauty)
ssrdk-14	9	0,8509	0	0
ssrdk-15	9	0,7519	3	2 (Rama Forte)
ssrdk-16	11	0,8406	2	1 (Tone Wase)
ssrdk-17	8	0,7839	1	0
ssrdk-25	9	0,8303	2	0
ssrdk-26	18	0,9062	6	3 (Korean Kaki, Reus-15 and Rama Forte)
ssrdk-28	11	0,7918	2	2 (Korean Kaki)
ssrdk-29	3	0,5368	1	0
ssrdk-30	12	0,8536	3	1 (Garidells)
ssrdk-32	9	0,7942	2	0
ssrdk-36	13	0,8837	1	1 (Takura)
ssrdk-37	18	0,9184	4	2 (Tone Wase and Betera-2)

Population structure and genetic diversity

In order to analyze the significance of the partitioning of genetic variance according to its astringency (19 PCNA accessions, 10 PVNA accessions, 9 PVA accessions and 9 PCA accessions) (Table 2), an AMOVA was carried out. As a result, 15% of the total variation resided between persimmon types and 85% was present within groups. A PCA analysis showed that PCNA and PVNA accessions were partially differentiated from the rest of accessions (Figure 10). In order to elucidate an alternative partitioning of the samples, a Bayesian clustering approach was carried out to make a probabilistic assignment of individuals to groups based on its genotype using the software STRUCTURE 2.3.4. Both ln P(X/K) and Evanno's test indicated that the most informative number of clusters (K) was 3 (pop1 to pop3). The clustering showed an alpha value of 0.17, showing a low level of admixture between clusters. Each individual was classified inside each cluster according to the highest cluster importance into the genotype. Cluster 1 contained 21 accessions, 16 of them belonging to the PCNA type. Cluster 2, with 9 accessions, contained 8 PVNA accessions. Cluster 3 contained the rest of accessions (19) (Figure 11 and 12). Twenty-nine accessions had a membership coefficient (qi) to one of the populations higher than 0.8, while the other 18 could be considered as admixted ($qi \leq 0.8$). An AMOVA analysis was repeated assuming STRUCTURE given populations. Similar results were obtained to those using classification of samples by astringency type, with 15% of total variation between populations and 85% within groups.

Table 4. Parameters of the obtained Principal Components Analysis.

Axis	1	2	3
% of variability	32,73	17,25	14,63
Cumulative %	32,73	49,98	64,61
EigenValue	29,828	15,718	13,327

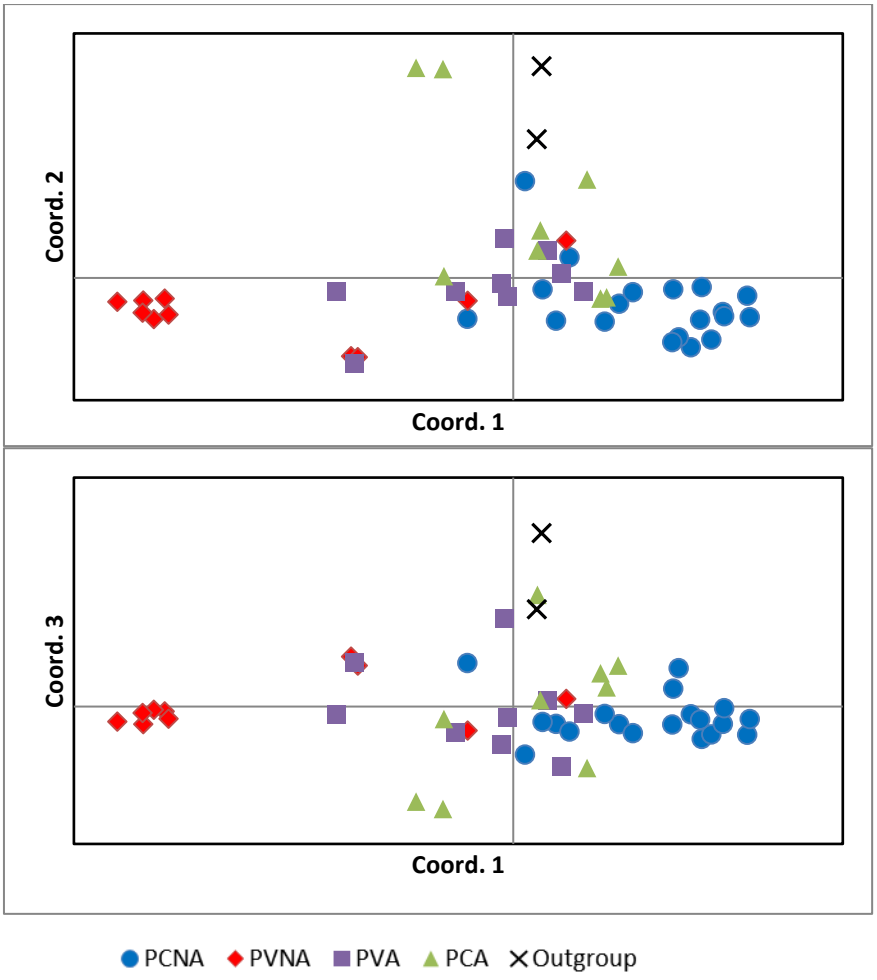

Figure 10. Representation of the first three components of Principal Component Analisys.

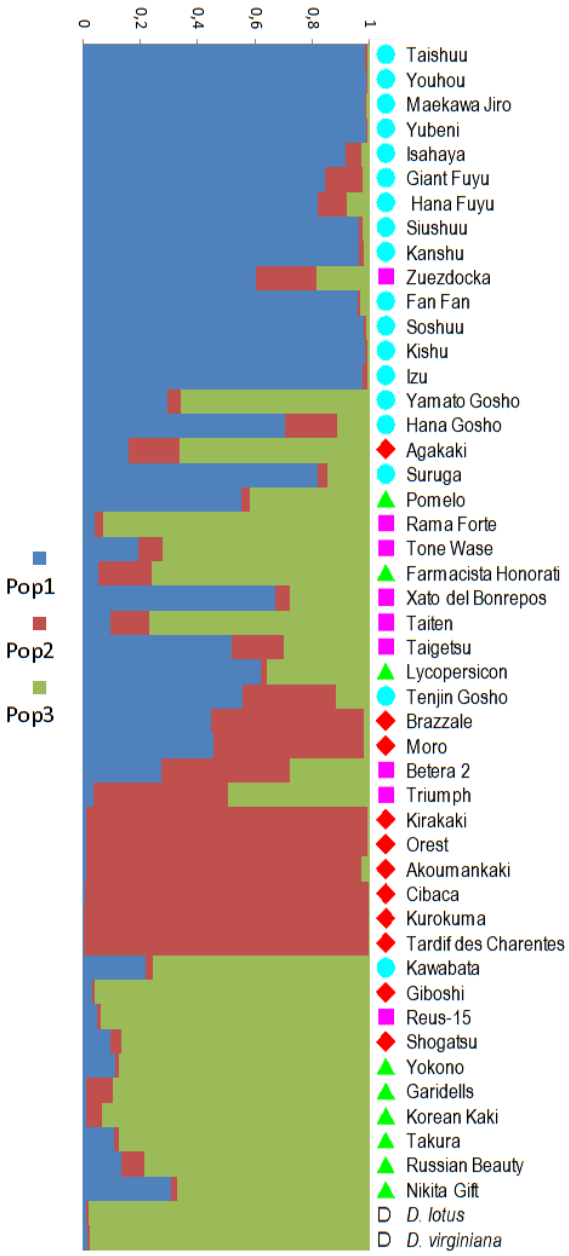

Figure 11. Clustering distribution of the accessions from the Bayesian STRUCTURE analysis. Each symbol represent different astringency trait. Each color represents different clusters.

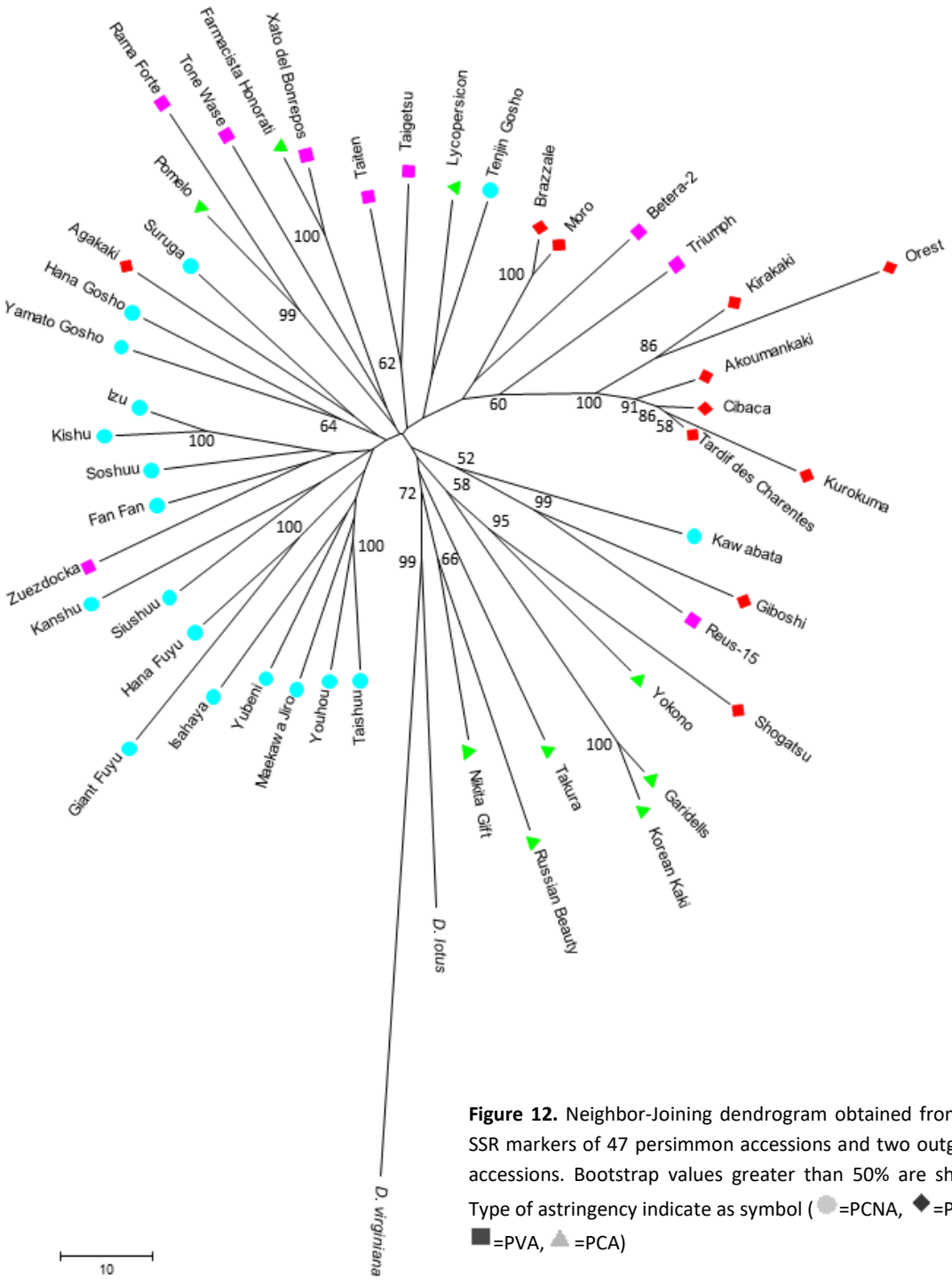

Figure 12. Neighbor-Joining dendrogram obtained from the SSR markers of 47 persimmon accessions and two outgroup accessions. Bootstrap values greater than 50% are shown. Type of astringency indicate as symbol (●=PCNA, ◆=PVNA, ■=PVA, ▲=PCA)

The neighbor-joining dendrogram generated using Nei's genetic distance showed two major clusters. (Figure 12). Bootstrap values only gave an acceptable support for most of PVNA accessions. Even though, two clusters could be elucidated from the dendrogram. First cluster comprised almost all PCNA accessions, but without bootstrap support. The second cluster includes most of PVNA accessions, with an acceptable bootstrap support (60%).

Discussion

Due to recent incorporation of new persimmon accessions to the IVIA's germplasm bank, this study aims to update the information about the genetic diversity maintained in this collection. For this purpose, different molecular markers have been used previously in persimmon such as RAPD (Luo Zheng-Rong et al., 1995; Badenes et al., 2003; Yamagishi et al., 2005) and AFLP (Kanzaki et al., 2000; Yonemori et al., 2008; Parfitt et al., 2015). Also, the use of SSR markers has showed satisfactory results in previous works (Naval et al. 2010). Markers employed in this work might be useful to distinguish some accessions, as the presence of unique alleles has been observed on 13 of 47 accessions. Furthermore, as expected in a germplasm bank, any accessions with identical genotype were found among the studied accessions.

Traditionally, astringency loss and change in flesh color in persimmon fruits allow classifying cultivars into 4 groups: PVNA, PCNA, PVA and PCA (Yonemori et al., 2000). AMOVA analysis determined that the highest percentage of the total genetic diversity was distributed

within astringency groups, rather than between astringency groups. Similar results were obtained by Naval et al. (2010) and Parfitt et al. (2015). In order to elucidate an alternative classification of the samples, the STRUCTURE clustering method was applied, classified the accessions into 3 groups. However, this classification into 3 groups was similar to the traditional classification by astringency types: first group = PCNA, second group = PVNA, third group = PVA and PCA. AMOVA analysis using this classification showed similar results than by partitioning in astringency types. In spite of the low diversity between groups, astringency classification has shown to be the most informative classification method for persimmon cultivars. The Neighbor-Joining dendrogram and PCA analysis showed a close relationship between all samples analyzed that prevent to define well supported groups. Similar results were obtained by Naval et al. (2010) and Parfitt et al. (2015). Yamada et al. (1994) described PVNA group as the most diverse group compared to the narrow genetic variability of PCNA group, according to that, our PVNA accessions showed more variability than our PCNA accessions. The analysis showed a well-supported group formed mostly by PVNA accessions in contrast to the poorly-supported group formed by PCNA accessions. These results are similar to those described by Naval et al. (2010) in their neighbor-joining analysis.

CHAPTER 2: Salt-tolerance mechanisms present in persimmon species and rootstock breeding

The results presented in this chapter were published in several scientific papers and presented in a national and an international symposium:

Francisco Gil-Muñoz, Pedro Maranha Peche Mª Ángeles Forner, María L. Badenes,Mª del Mar Naval. 2017. Respuesta a la salinidad de diferentes patrones de caqui. Phytoma. 286:42-45

Gil Muñoz, Francisco & Peche, Pedro & Climent, J & Forner, M.A. & Naval, Mar & Badenes, María. (2018). Breeding and screening persimmon rootstocks for saline stress tolerance. Acta Horticulturae. 1195. 105-110. 10.17660/ActaHortic.2018.1195.18.

Francisco Gil-Muñoz, Ana Quiñones, Amparo Primo-Capella, Jaime Cebolla, Mª Ángeles Forner-Giner, Maria L. Badenes, Mª del Mar Naval (2020) A cross population between D. kaki and D. virginiana shows high variability for saline tolerance and improved salt stress tolerance. PLOS ONE https://doi.org/10.1371/journal.pone.0229023.

Francisco Gil-Muñoz, Pedro Maranha Peche, María del Mar Naval, María Ángeles Forner María Luisa Badenes. 2016. Breeding and Screening Persimmon Rootstocks for Saline Stress Tolerance. VI International Symposium on Persimmon. Valencia.

Francisco Gil-Muñoz, María del Mar Naval, Pedro Maranha Peche, María Ángeles Forner, María Luisa Badenes. 2016. Efecto de la salinidad en diferentes patrones de caqui. VIII Congreso de Mejora Genética de Plantas. Vitoria-Gasteiz.

A cross population between *D. kaki* and *D. virginiana* shows high variability for saline tolerance and improved salt stress tolerance.

Abstract

Persimmon (*Diospyros kaki* Thunb.) production is facing important problems related to climate change in the Mediterranean areas. One of them is the soil salinization caused by the decrease and change of the rainfall distribution. Salinity tolerance is a quantitative trait controlled by several genes. Many traits contribute to salinity tolerance, thus development of tolerant rootstocks is possible and required for adaptability to the challenged soil conditions. In this study, two populations differing in salinity tolerance from two species used as a rootstock in persimmon, *D. kaki* and *D. virginiana* and a backcross between both species were analyzed for unraveling the mechanism involved in salinity tolerance. Variables related to growth, leaf gas exchange, leaf water relations and content of nutrients were significantly affected by saline stress. Water flow regulation appears as a mechanism of salt tolerance in persimmon via differences in water potential and transpiration rate, which reduces ion entrance in the plant. Genetic expression of eight putative orthologous genes involved in different mechanisms leading to salt tolerance was analyzed. Differences in expression levels among populations and between saline and control treatment were found. Gene expression of the 'High affinity potassium transporter' (*HKT1-like*) in roots linked with salinity tolerance, reduced its expression levels in all the

populations studied. Results obtained allowed selection of tolerant rootstocks genotypes and describe hypothesis about the mechanisms involved in salt tolerance in persimmon that will be useful for breeding salinity tolerant rootstocks.

Introduction

Persimmon, *Diospyros kaki* Thunb., has become one of the most dynamic tree crops in the world. According to the data available (www.fao.org/faostat), global cultivated surface has increased 43% in the last 10 years (2006-2016) and world production increased 59%, which demonstrates an important improvement in crop yield.

This trend has been highly relevant in some countries. For instance, in the Mediterranean basin, the cultivated surface has been increased by four times and production near to five times (Perucho, 2018), Despite the recent and fast increase in persimmon production in the Mediterranean, the persimmon industry is facing important problems, related to climate change. One of them is the soil salinization caused by the decrease and change of the rainfall distribution which is causing an increase of salts in the water available for irrigation (Visconti et al., 2015). In order to keep the production in these areas, availability of rootstocks tolerant to salinity is required (Forner-Giner and Ancillo, 2013).

The most commonly used rootstocks for persimmon production in these areas are seedlings from *Diospyros lotus* species, because of its tolerance to lime-filled soils and its adaptability to the Mediterranean conditions. Furthermore, *D. lotus* has a root system that does not

produce basal shoots (Bellini and Giordani, 2002), facilitating the management of the orchards. However, this species is highly sensitive to salinity (De Paz et al., 2016; Visconti et al., 2017). Other species used as rootstocks in some countries is *Diospyros virginiana*. This species is tolerant to salinity and performs well on lime-filled soils, but confers too much vigor to the plant, and produces many basal shoots, thus hindering crop management (Incesu et al., 2014; de Paz et al., 2016). The most used rootstock around the world are seedlings from *D. kaki,* which is not tolerant to salinity (Gil-Muñoz et al., 2018a). Additionally, *D. kaki* is high sensitive to lime-filled soils and produces tap-roots with few lateral roots, which are rather fine and broke easily, all together makes difficult the plant management in the nurseries. Consequently, seeds from D*. kaki* are not commonly used in the Mediterranean Basin countries. On the other hand, *D.kaki* exhibits compatibility with all cultivars, while *D. virginiana* can be graft-incompatible with a wide range of varieties, hence the graft-compatibility needs to be checked for each variety (Bellini and Giordani, 2002). No data have been reported about Na^+ toxicity in *D. kaki*, either by the absence of high Na^+ accumulation in the soils where they are cultivated or because the higher tolerance of tree plants to Na^+ toxicity. On the other hand, Cl^- accumulation has been reported problematic in persimmon for production and postharvest management (Besada et al., 2016)

In order to confer salinity tolerance, rootstocks should be able to overcome the two components of salinity stress: the osmotic effects and ion-toxicity. Osmotic effects are caused by the total

concentration of salt around the roots, which restricts extraction of water by roots and results in reduced plant growth. The osmotic stress immediately causes a response in the stomatal aperture of the plant mediated by abscisic acid, ABA (Fricke et al., 2006). On the other hand, ionic effects are caused by the accumulation of toxic concentrations of Na^+ and Cl^- ions in plant tissues, causing premature organ senescence and tissue necrosis (Munns and Tester, 2008).

It remains unclear if the reduction of growth rate causes a reduction of photosynthesis or the reduction of photosynthesis is the cause of the diminished growth rate (Munns and Tester, 2008). Some studies related salinity stress with an increase of stored carbohydrate (Munns et al., 2000), causing a reduction in sink demand that may downregulate photosynthesis. Other possible hypothesis that explains photosynthesis reduction is related to Na^+ inducing K^+ deficiency and both ions, Na^+ and Cl^- over-accumulation, producing ion toxicity (Forner-Giner and Ancillo, 2013). However, the mechanism to explain how toxicity affects the cell remains unknown (Munns and Tester, 2008). Finally, accumulation of Na^+ and Cl^- results in tissue necrosis. These effects are visible in older leaves where these ions tend to be accumulated (Sibole et al., 2003; Plett and Møller, 2010), leaf margins (Shapira et al., 2009), and epidermis (Huang and Van Steveninck, 1989; Karley et al., 2000a, 2000b; James et al., 2006) probably as result of an evolved mechanism for protecting photosynthetically active cells (Baetz et al., 2016).

To overcome these effects, plants use complex mechanisms including changes in morphology, water relations, photosynthesis, respiration

and toxic ion distribution, among others (Acosta-Motos et al., 2017). The decrease of photosynthesis rate comes with an increase of reactive oxygen species (ROS) production. At reduced photosynthesis activity, photoinhibition might occur due to the light excess. Under this scenario, plants have two mechanisms to prevent oxidative damage to photosystems: heat dissipation by pigments and electron transfer to oxygen acceptors. Genetic differences in salinity tolerance are probably not associated with differences in the ability of detoxifying ROS and could be related to differences in stomatal closure or CO_2 fixation, as these mechanisms are essential for plant survival under natural variable situations (Munns and Tester, 2008).

A reduction in root hydraulic conductance can be observed in roots grown with salt presence (Joly, 1989; Zekri and Parsons, 1989). This effect might be related to aquaporin activity. They are membrane intrinsic proteins involved in transport of water and small neutral solutes through the cells (Maurel et al., 2008). According to its amino acid sequences and subcellular localizations, plant aquaporins are classified into four subfamilies: plasma membrane intrinsic proteins (PIPs), tonoplast intrinsic proteins (TIPs), NOD26-like intrinsic proteins (NIPs) and small basic intrinsic proteins (SIPs) (Johanson et al., 2001). In fact, it has been observed that reduction of the hydraulic conductance can be linked to a lowered plasma-membrane intrinsic protein (PIP) aquaporin activity (Martínez-Ballesta et al., 2003). Also, reduction in PIP aquaporin gene expression has been observed under salinity stress (Martínez-Ballesta et al., 2003; Boursiac et al., 2005; López-Pérez et al., 2009). Interestingly, in citrus rootstocks, PIP

expression has been reported to be higher in tolerant genotypes compared to sensitive ones (Rodríguez-Gamir et al., 2012). However, experiments on yeast and *Xenopus oocytes* have shown a strong Na^+ conductance of AtPIP2;1 from *Arabidopsis thaliana,* suggesting that orthologues of PIP2;1 may act as a gate for Na^+ influx into the plant (Chaumont and Tyerman, 2014).

Prevention of the toxicity effect might be related to a mechanism of exclusion of toxic ions or their compartmentation. In this context, Na^+ access to the plant vascular system is mediated by non-selective cation channels (Amtmann and Sanders, 1998). Once inside the outer part of the root, the majority of the Na^+ is pumped out from the cells via plasma membrane Na^+/H^+ antiporters in a high energy demanding process (Tester and Davenport, 2003). In *Arabidopsis thaliana*, a plasma membrane encoding gene (SOS1) has been identified with Na^+/H^+ antiporter activity (Qiu et al., 2003). This gene has been also related to the elimination of Na^+ from the xylem (Shi et al., 2002). The SOS1 gene is the final part of a proposed signal transduction pathway responsible of maintaining ion homeostasis during salt stress (Zhu et al., 1998). Under high concentrations of Na^+ in the cytoplasm, a Ca^{2+} increase is triggered. The excess of Ca^{2+} ions are bound with a myristoylated calcium-binding protein CBL4 (SOS3) that acts as a sensor to perceive the Na^+ mediated Ca^{2+} spike. At this point, *CBL4* gene is able to interact with a serine/threonine protein kinase CIPK24 (SOS2) (Liu and Zhu, 1998; Halfter, 2000; Liu, 2000; Hrabak et al., 2003) that activates the target gene *SOS1* (Shi et al., 2000; Qiu et al., 2002; Quintero et al., 2002, 2011; Quan et al., 2007), activating the

retrieval of Na^+ from the cytosol. Furthermore, SOS pathway has been proposed to be part form a signaling network, and other genes might be implicated in activation of SOS pathway, such as SCaBP8 or MPK6. Furthermore, *SOS2* and *SOS3* genes seem to induce changes in the cytoskeleton that would cause root architectural changes in order to overcome the saline stress (Ji et al., 2013). However, the SOS pathway consumes plasma membrane H^+ gradient, and increased SOS1 expression may increase Na^+ tolerance, but at the expense of plant growth (Isayenkov and Maathuis, 2019). This mechanism of Na^+ removal from apoplast to cytosol is particularly important in root tip cells, due to the lack of vacuoles (Evans et al., 2012).

Other genes have been related with Na^+ exclusion from the xylem, such as some members of the *HKT* (High affinity potassium transporter) family (Munns and Tester, 2008) and *CHX* [cation/H^+ exchanger] family (Pardo et al., 2006). In *Arabidopsis*, *AtHKT1* has been identified as a Na^+ selective uniporter with some role in K^+ transport (Uozumi et al., 2000). Also, *hkt1;1 Arabidopsis* mutants showed hyper accumulation of Na^+ at the shoots while showing less Na^+ accumulation on the roots (Mäser et al., 2002; Berthomieu et al., 2003; Rus et al., 2004), suggesting a role on Na^+ long transport via xylem and phloem (Berthomieu et al., 2003; Sunarpi et al., 2005). Furthermore, multiple isoforms have been isolated in monocots (Garciadeblás et al., 2003; Huang et al., 2006, 2008; Byrt et al., 2007) and in several cereals HKTs can mediate Na^+ uptake (Horie et al., 2007; Almeida et al., 2013; Isayenkov and Maathuis, 2019). Under K^+ starvation and Na^+ stress, it has been observed increased transcript

abundance of *AtCHX17* (Cellier et al., 2004). Furthermore, AtCHX23 and AtCHX20 have been located in the chloroplast envelope (Song et al., 2004) and endosomal membranes (Padmanaban et al., 2007), suggesting intracellular functions. However, *CHX* family genes might be limited to cellular K^+ homeostasis (Szczerba et al., 2009), as experiments using *GsCHX19.3* from cotton have shown increased K^+ deficiency tolerance in yeast (Jia et al., 2017). NHX type antiporters have been also proposed to have a role in salt tolerance [66]. Its role seems to be related to maintaining Na^+/K^+ homeostasis rather than extruding or sequestrating Na^+ from the cytosol. Furthermore, it seems to have also a crucial role in stomatal closure via turgor regulation at guard cells (Barragán et al., 2012).

As the plants have complex Na^+ exclusion pathways, Cl^- accumulation becomes potentially more toxic than Na^+ accumulation. Cl^- influx into the plant has been proposed to depend on a passive mechanism via anion channels that are downregulated by ABA (Munns and Tester, 2008). Furthermore, Chloride Channel (CLC) family has been found in the tonoplast of various plant species. Cation/Cl^- cotransporter (CCC) might be involved in Cl^- sequestration into other types of intracellular compartments (Isayenkov and Maathuis, 2019).

Another strategy used by plants when the ion exclusion is not possible is the vacuole compartmentation of toxic ions. In *Arabidopsis,* for Na^+, this function is believed to be carried out by Ca^{2+}/cation exchangers (CCXs) as vacuolar Na^+ sequestration (Isayenkov and Maathuis, 2019). In the case of Cl^-, the ALMT (Aluminum-activated Malate Transporter) protein family encodes

anion transmembrane channels (Barbier-Brygoo et al., 2011). Furthermore, the *Arabidopsis* vacuolar H^+-translocase pyrophosphatase (AVP) has a role in pumping Na^+ into the vacuole through enhancing the H^+ electrochemical potential difference, improving salinity tolerance (Apse et al., 1999; Gaxiola et al., 2001). In *Arabidopsis*, tonoplast *ALMT9* gene knock-out mutants shown shoot accumulation of both Cl^- and Na^+. On the other hand, *almt9* plants complemented with a mutant variant of *ALMT9* that exhibits enhanced channel activity showed higher Cl^- and Na^+ accumulation (Baetz et al., 2016), suggesting a role of ALMT9 on ion compartmentation.

In this context, this study was aimed at identification of salinity tolerant rootstocks for persimmon production, combining the high salinity tolerance of *D. virginiana*, and the positive traits of *D. kaki*. For this purpose, a progeny (*D. virginiana* x *D. kaki*) x *D. kaki* was generated and phenotyped for salinity tolerance. The objectives are to explore the mechanisms involved in salinity tolerance in persimmon and develop alternative rootstocks for saline environments.

Material and methods

Plant material and salinity treatment

The *D. kaki* population (DK) was obtained from open pollination of different accessions of female trees with several accessions of male-flowering *D. kaki* trees in the IVIA germplasm bank. The *D. virginiana* (DV) population was obtained from a single female tree with a single male *D. virginiana*. A third population was obtained from the cross between open pollinaition *Diospyros kaki* population and a hybrid obtained between *D. kaki*, as a male parent and *D. virginiana* as a female parent. Both parents were single individuals from open pollination populations. The population obtained is therefore considered as interspecific backcross of *D. kaki* (BC). At the end of March, seeds were stratified for 30 days in plastic bags filled with perlite in a cold chamber at 4ºC. After stratification, seeds were transferred to trays containing peat-moss and perlite (4:1 ratio, respectively) and kept in a greenhouse at 18-24ºC during two months (from April, 29, to June, 27, 2016).

Sixty-five seedlings of each parental line and 420 seedlings of the BC line were transplanted into 1-L pots containing coarse sand. The plants were distributed randomly in the greenhouse and watered with a nutrient solution (3% Cristaljisa 18-18-18, soluble fertilizer with micronutrients) for one week, to acclimate the plants before exposition to the salinity treatment. After the acclimation week the plants were submitted to a salinity treatment for 72 days (from July, 5, 2016 to September, 15, 2016). The treatment consisted in 40 mM

NaCl added to the nutrient solution. The controls remained watered with the standard nutrient solution. The amount of NaCl added came from the results obtained in a previous experiment (Gil-Muñoz et al., 2018a).

Morphological phenotyping

Over all the indivuduals from all the populations, the variables measured were: height (cm), leaves (no.), nodes (no.), internodes (cm) and defoliation (1-no. leaves/no. nodes). They were recorded at the beginning of the experiment (day 0) and at the end of the salinity treatment (day 72). The ratio between initial and final value of variables related to growth was also calculated.

Based on visual symptoms, salinity injury was rated from 0 to 4: 0 – no symptoms, 1 – leaf turgor loss, 2 – leaf tip necrosis, 3 – leaf margin necrosis, 4 – defoliated plant.

This data was used to divide BC population into three groups according to its salt tolerance into tolerant, sensitive and intermediate phenotypes. Only tolerant and sensitive groups were used in further analyses.

Leaf gas exchange parameters

Stomatal conductance (g_s), leaf net CO_2 assimilation rate (A_{CO2}), leaf transpiration rate (E) and internal CO_2 concentration (C_i) were measured on single attached leaves from glasshouse-cultured plants. Intrinsic leaf water use efficiency (WUE) was calculated as A_{CO2} and g_s ratio. All measurements were carried out in a sunny day between

9:30 a.m. and 12:30 p.m. at the end of the salt treatment (day 72). Photosynthetically active radiation (PAR) at the leaf surface was adjusted to a photon flux density of 1.000 µmol m^{-2} s^{-1}. A closed gas exchange CIRAS-2 (PP-systems, Hitchin, UK) was used for the measurements. Leaf laminae were fully enclosed within a PLC 6 (U) universal leaf autocuvette in a closed-circuit model and kept at 25 ± 0.5 ºC, with a leaf-to-air vapor deficit of about 1.7 kPa. The air flow rate through the cuvette was 0.5–1.5 L min^{-1}. Determinations were performed using uniform fully expanded leaves from the mid-stem zone of each of 57 BC treated plants (28 tolerant and 29 sensitive), 15 of BC control, 19 DK treated, 9 DK control, 26 DV treated and 10 DV control.

Leaf water relations

Leaf stem water potential ψ_H, MPa) was measured in fully expanded leaves in a sunny day using a Model 600 Schölander Pressure Chamber (PMS Instrument Company, Albany, OR, USA) at the end of the salinity treatment (day 72), on the same plants used for the leaf gas exchange parameters. Previously, the leaf was kept in a reflective plastic bag for 30 minutes to remove water loss. For osmotic potential, after the same procedure, the leaf was introduced into microcentrifuge tubes and frozen immediately to -80ºC for breaking the cells by ice crystallization. After 48h, frozen samples were centrifuged at room temperature to extract the cell sap (modified from Callister et al. (Callister et al., 2006)). Leaf osmotic potential (ψ_π, MPa) of the leaf sap was calculated by van´t Hoff equation after measuring sap osmolarity (mmol kg^{-1}) using an automatic osmometer

(Wescor, Logan, USA). Leaf turgor potential (ψ_t, MPa) was estimated as the difference between ψ_H and ψ_π.

Proline content and ion analysis

At the end of the treatment, adult leaves were collected from all survival plants from parental populations: treated and control DK (19 and 13, respectively), DV (26 and 15, respectively), 32 tolerant BC, 46 sensitive BC plants and BC control (25).

Proline content of leaves (mg g^{-1} of dry weight) was measured by the method of Bates et al. (Bates et al., 1973). Dried leaves (250 mg) were homogenized in 1.5 mL of 3% (w/v) aqueous sulphosalicylic acid. The homogenate was centrifuged and 0.2 mL of supernatant was mixed with 0.7 mL of ninhydrin acid and 0.6 mL of glacial acetic acid. The mixture was incubated at 100°C for 1 h and the reaction was cooled in an iced bath. The chromophore was extracted using toluene and its absorbance at 520 nm was determined by spectrophotometry (Lambda 25, PerkinElmer, Shelton, CT, USA).

For ion analysis, collected samples were washed; fresh and dried (oven-dried for 48 h at 65ºC) weight was recorded. Dried leaves were ground to powder. For chloride determination (mg Cl^- g^{-1} of dry weight), 25 mg of leaf powder was diluted in 20 mL of combined acid buffer (Sherwood Scientific Ltd. Cambridge. UK). Chloride concentration (mg mL^{-1}) of the filtered solution was determined by silver ion-titration [73] with a Corning 926 automatic chloridometer (Corning Ltd. Halstead Essex, UK). A portion of dried leaves (0.5 g) were burnt in a muffle furnace for 12 h at 550 ºC. Remaining ashes

were digested with HNO_3 1M solution. Na^+, Ca^{2+}, K^+, Mg^{2+}, P and S ions were quantified (mg g^{-1} dry wt) using a multiple-collector inductively coupled plasma mass spectrometry (MC-ICP MS, Thermo Finnigan Neptune).

Gene expression analysis

A subset of each group was selected for gene expression analysis (Table 5). Root tip tissue was collected after 72 days of salt treatment and immediately frozen and powdered using liquid nitrogen. Control samples from the three populations were collected and processed. RNA was isolated according to Gambino et al. (2008). DNA was removed with the RNase-Free DNase Set (Qiagen, Valencia, CA, USA), using the RNeasy Plant Mini Kit (Qiagen). Purified RNA (500 ng) was reverse transcribed with PrimeScript RT Reagent Kit (Takara Bio, Otsu, Japan) in a total volume of 10 µL.

Eight putative orthologous genes involved in different mechanisms leading to salt tolerance were analyzed. *Arabidopsis* genes *SOS1* (AF_256224.1), *SOS2* (AF_237670.1), *SOS3* (HE_802983.1), *NHX1* (AF_106324.1), *HKT1* (AK_228564.1) and *ALMT9* (NM_112729.4) were blasted against the SRA archive of *D. lotus* (SRA ID: SRP045872) cv. Kunsenshi (Akagi et al., 2016). The output fragments were manually assembled to complete putative orthologous genes. Specific persimmon primers were designed using the sequences obtained (Table 6).

Table 5. Selected plants (tolerant and susceptible) for gene expression analysis

	D. virginiana	*D. kaki*	Backcross line (BC)			
			BC_t*		BC_s**	
Treated plants	V10	K9	BC11	BC312	BC61	BC198
	V14	K23	BC61	BC315	BC77	BC236
	V20	K26	BC127	BC323	BC90	BC237
	V23	K34	BC175	BC359	BC95	BC301
	V37	K44	BC291	BC375	BC172	BC333
Untreated plants	V4	K4	BC2			
	V5	K6	BC5			
	V7	K7	BC16			
	V11	K9	BC22			
	V15	K14	BC25			

*BC_t: tolerant backcross line

**BC_s: susceptible backcross line

For plasma membrane intrinsic (PIP) aquaporins, *Arabidopsis PIP1* (NM_001084854.2, NM_130159.4, NM_100044.5, NM_116268.4, NM_118469.4) and *PIP2* (NM_001035774.1, NM_129273.5, NM_129274.4, NM_125459.4, NM_115339.3, NM_129458.3, NM_001203991.1, NM_127238.3) family sequences were aligned and conserved regions within families identified. Each conserved region was blasted against *D. lotus* SRA archive. The output fragments were

manually assembled and specific primers designed at the conserved region, obtaining specific primers for each putative aquaporin family (Table 6).

Table 6. Primers used for RT-qPCR analysis

Gene name	Sequence (5'-3')
SOS1-Like	F:GGATTTTCTCTGGAAGGAAAGTGCTA
	R:GGAGATGTAATCAGTTCCTCTTTGACAC
SOS2-Like	F:TTAGAGTTTGTTACTGGAGGGGAACT
	R:CACTCAGTCCAAAGTCAGAAACCTTCA
SOS3-Like	F:GAAGTTGAGGCCTTGTATGAGCTATTT
	R:CCTAATGAACGAACAAATTCTCCAAACTC
HKT1-Like	F:GATTCCTAACCCTGCAGATAAACCCATT
	R:GTTGCAGACACAGAGGTAAAGAACAAG
NHX1-Like	F:CACCAAAGAACTTGACAAGAATGCTG
	R:CCAATAGTAGTGCACGGTACGAG
ALMT9-Like	F:TCACTTATGCAAAACTATACCCCACAATG
	R:GTAGATAAACATATTCACCACCAAACACAC
PIP1 Family-Like	F:GTCTTCTACATGGTGATGCAGTGC
	R:AGTGGCAGAGAAGACAGTGTAGAC
PIP2 Family- Like	F:GCATGATCTTCATCCTCGTCTACTGCAC
	R:TTGGGATCAGTGGCGGAGAAGAC

The first-strand cDNA was 60-fold diluted, using 1 µL as template in a final volume of 20 µL. Quantitative real-time PCR was performed on a StepOnePlus Real-Time PCR System (Life Technologies, Carlsbad, CA, USA), using SYBR premix Ex Taq (Tli RNaseH plus) (Takara Bio). The PCR protocol consisted of 10 min at 95 ºC, followed by 40 cycles of 15 s at 95 ºC, and 1 min at 60 ºC. The specificity of the reaction was assessed by the presence of a single peak in the dissociation curve and through size estimation of the amplified product by agarose electrophoresis. Four different genes were screened with Normfinder (Andersen et al., 2004) for use as reference genes: *DkACT* (Akagi et al., 2009b), *DkUBC*, *DkPP2A*, and *DkTUA* (Wang et al., 2016) and two of them selected as reference: *DkACT* and *DkTUA*. The normalization factor was calculated by the geometric mean of the values of relative expression of both genes. Expression analysis was carried out in 5 treated and untreated DV and DK plants, 10 tolerant BC plants and 10 susceptible BC plants as biological replicates (Table 1). Results were the average of 3 technical replicates.

Statistical analyses

Within treatment (saline vs saline and non-saline vs non-saline) parameters were statistically tested by Analysis of Variance (ANOVA) and averages were compared with the Least Significant Differences (LSD) method at 95% confidence level ($P \leq 0.05$). When comparing with the non-saline conditions, the parameters were found to not fit normal distribution and therefore were compared with Kruskal-Wallis test ($P \leq 0.05$) and median notch method (Chambers et al., 2018). Statgraphics Centurion, 16.1 version (Statistical Graphics, Englewood

Cliffs, NJ, USA) was used for performing the statistical analyses. Principal component analysis (PCA) was carried out using S-Plus 8.0 (Insightful Corp., Seattle, USA). The variables included were: morphological traits, leaf gas exchange and leaf water relations parameters, proline and ion contents. The number of components retained was defined by the inflection point of the corresponding screen plot. A biplot of individual scores and loadings was obtained. An average plant for each population was included in the analysis representing the average of each variable for the population.

Plants from the BC population were classified as tolerant or susceptible to salinity according to the phenotyping data and the distance to the average plant in the PC analysis.

Results

Populations phenotyping

Control plants from the three populations studied: *D. virginiana* (DV), *D. kaki* (DK) and the backcross (BC) grown in non-saline conditions were measured to address differences among populations. The variables were studied using PCA in which 63.2% of the total variance was explained by the two first components (Figure 13a). The average value of each variable/population was included in the analysis (referred as average plant). Plants from DV were the tallest at both the initial (day 0) and at the end of the experiment (day 72). They also had more leaves and nodes, with shorter internode length than those from DK. Although differences in the speed of growth were not considerable (bold letters in the figure of

variable loadings indicate significant differences, ANOVA $p<0.05$), plants from DV tended to show higher ending to initial height and nodes ratios. The plants from the BC resulted in values between DV and DK populations. In fact, the mean average plant of BC was closer to *D. kaki* than to *D. virginiana* population. This distribution was expected attending to the higher participation of the *D. kaki* genome in the backcross.

Differences in leaf gas exchange and leaf water relations were similar among populations. (Figure 13b). DV plants have higher A_{CO2} and lower C_i than DK and BC plants. No significant differences (non-bold letters) were observed in g_s and E and, ψ_π between the three populations. BC plants have lower ψ_H and ψ_t.

Regarding the accumulation of salt, nutrients (Cl^-, Na^+, Ca^{2+}, K^+, Mg^{2+}, P, S) and proline in the leaves showed a similar pattern to the one observed with morphological data. Plants from *D. virginiana* population were the most different in the PCA plot, while BC and *D. kaki* population plants were grouped (Figure 13c). For these variables PC1 and PC2 explained 46.7% and 17.3% of variability respectively. *D. virginiana* plants accumulate lower amounts of ions (especially of Cl^-, Na^+, Ca^{2+}, P and K^+) and higher amounts of proline than *D. kaki* population and BC plants.

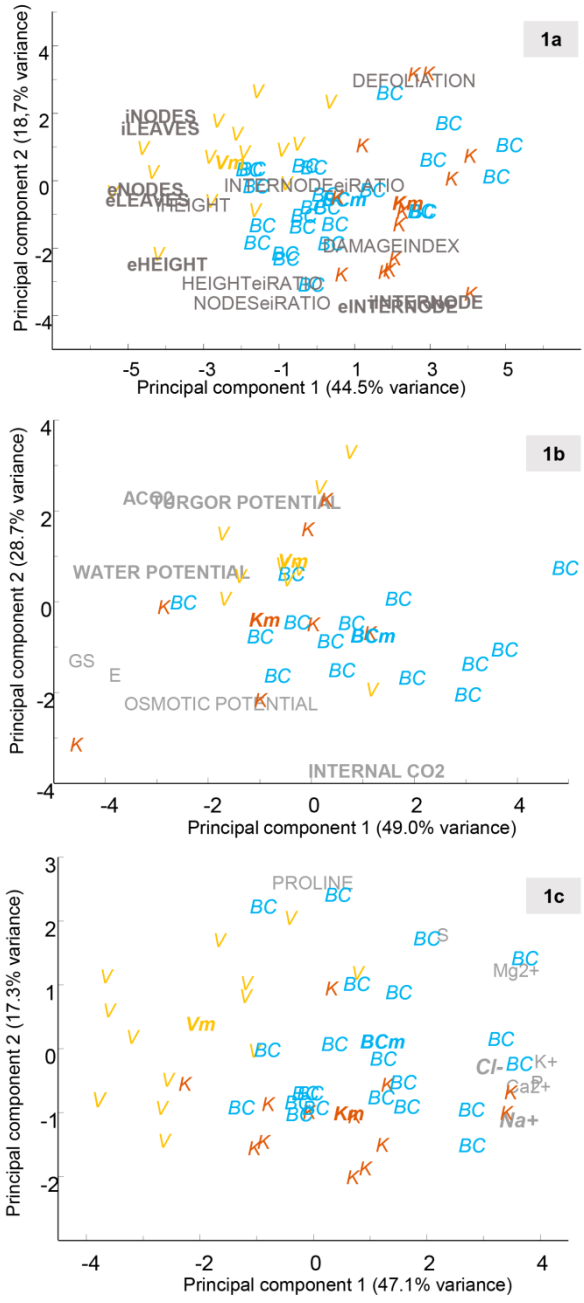

Figure 13. Plot of the first two components from a principal component analysis of morphological (a), leaf gas exchange and leaf water relations (b) and ionic and proline content (c) of the three populations in non-saline conditions. Each letter represents each population: V – *D. virginiana* population (yellow), K – *D. kaki* population (brown) and BC – Backcross population (blue). Vm, Km and BCm in bold represents the mean of the individuals. Gray letters represent each of the measured variables. The most important variables identified in each PCA are in bold type.

Evaluation of tolerance to salinity

A subset of 127 plants from each population (*D. virginiana*, *D. kaki* and BC) were grown under saline conditions (40mM) to evaluate tolerance to salinity. The variables studied were height, nodes number, internode length, defoliation and damage index. All measurement aimed at addressing the effect of salinity on growth rates and plant damages (Figure 14a). Values of ending/initial (e/i) ratio were used. The height, number of nodes and internode length were selected as variables for rating the saline stress effect on plant growth. The initial and end values were excluded in the PCA, as the differences between the populations in non-saline conditions were considerable and would mask the specific effect of salinity (Figure 14a). In the PCA, mean values of the average plant corresponding to non-saline conditions were included to enable a comparison between non-saline and saline conditions.

The tolerance to salinity of DV population plants was evident. In the analysis of the Principal Components related to morphological variables, the first two components explained 77.9% of variance (Figure 14a), these plants appear near the DV average plant under non-saline conditions (V_m), reflecting that the growth rate and damages were not considerably altered by saline treatments. On the other hand, *D. kaki* plants showed high susceptibility to salinity, with lower growth rates and higher levels of defoliation and damage under saline conditions compared to the average plant of the *D. kaki* population under non-saline conditions (K_m) (Figure 14a).

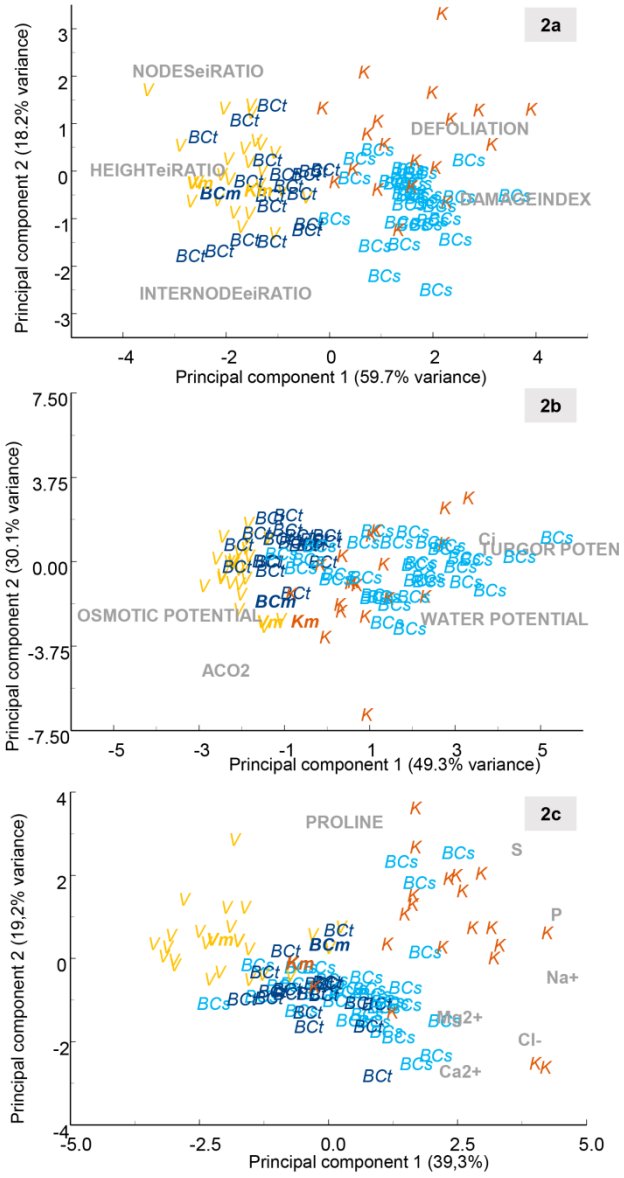

Figure 14. Plot of the first two components from a principal component analysis of morphological variables (a), leaf gas exchange and leaf water relations (b) ionic and proline content (c) of the three populations under saline conditions. Each population represented by letters: V – *D. virginiana* population (yellow), K – *D. kaki* population (brown) and BC – Backcross population (blue). BCt are the Backcross plants that showed a salt tolerant phenotype and BCs the plants salt sensitive. Vm, Km and BCm in bold represents the mean of the individuals under control treatment. Gray letters represent each of the measured variables.

In the BC population, important differences among plants grew under saline and non-saline conditions were obtained. The plant distribution overlaps the distributions of DV and DK population plants. According to the PC1 some plants showed similar behaviour than *D. virginiana* under saline conditions and some are located close to the BC average plant under non-saline conditions (BC_m), resembling the behaviour of the susceptible DK population plants (Figure 14a). Based on these results, BC plants were classified as tolerant (BC_t) and susceptible (BC_s) to salinity (Figure 15). The tolerance of DV, the susceptibility of DK, and the tolerance and susceptibility of BC plants were confirmed with ANOVA tests (Table 7). The values and the ratios between them and the average values in non-saline conditions (saline/non-saline ratios, s/ns ratios) were used. Plants of *D. virginiana* population showed values for morphological variables similar to those obtained in control conditions, being the s/ns ratios close to 1 for most variables (Table 7). The s/ns ratio of the damage index was higher than the control (1.79 folds), but the value was low (0.13) (Table 7).

D. kaki population plants were very affected by salinity with high values of defoliation (0.17) and damage index (2.26) (Table 7).

Figure 15. Phenotype of the saline tolerant (up) and sensitive (down) backcross population (BC) plants after 72 days of irrigation with 40mM NaCl.

Table 7. Phenotype of each population under saline and non-saline conditions for all the measured variables. Morphological variables are expressed as the ratio of each individual at the end of the treatment (saline conditions) and the beginning of the experiment (non-saline conditions). Different letters represent significant differences between populations ($p<0.05$).

	D. kaki	***D. virginiana***
Agro-morphological data	**Mean (s/ns ratio*)**	**Mean (s/ns ratio)**
Initial Height (iH, cm)	17.22^{a} (1.15^{ab})	21.00^{ab} (1.06^{a})
End Height (eH, cm)	42.21^{a} (0.62^{a})	92.63^{c} (0.87^{b})
$Height_{ei}$Ratio (eH:iH)	2.44^{a} (0.55^{a})	4.46^{c} (0.83^{b})
Initial Leaves (iL, nº)	5.58^{a} (1.00^{a})	10.54^{c} (1.01^{a})
End Leaves (eL, nº)	13.63^{a} (0.77^{a})	38.54^{c} (0.96^{ab})
Initial Nodes (iN, nº)	5.57^{a} (1.01^{a})	10.54^{c} (1.01^{a})
End Nodes (eN, nº)	16.11^{a} (0.84^{a})	40.50^{c} (0.94^{ab})
$Nodes_{ei}$Ratio (eN:iN)	3.04^{b} (0.84^{b})	3.88^{d} (0.94^{c})
Initial Internodes (iI, cm)	3.27^{c} (1.14^{a})	2.02^{a} (1.04^{a})
End Internodes (eI, cm)	2.59^{a} (0.73^{a})	2.32^{a} (0.92^{bc})
$Internode_{ei}$Ratio (eI:iI)	0.82^{a} (0.65^{a})	1.16^{c} (0.86^{bc})
Defoliation (eN:eL)	0.17^{c} (2.07^{c})	0.05^{a} (0.71^{a})
Damage Index	2.26^{b} (4.19^{b})	0.13^{a} (1.79^{a})
n (treated/control)	28/13	42/15
Leaf gas exchange		
A_{CO2} (μmol CO_2 m^{-2} s^{-1})	3.01^{a} (0.44^{a})	6.67^{b} (0.74^{b})
g_s (mmol H_2O m^{-2} s^{-1})	51.74^{c} (0.86^{bc})	41.75^{b} (0.74^{ab})
E (mmol H_2O m^{-2} s^{-1})	1.37^{b} (0.86^{b})	0.82^{a} (0.54^{a})
C_i (μmol CO_2 m^{-2} s^{-1})	304.90^{b} (1.67^{b})	124.17^{a} (1.09^{a})
n (treated/control)	19/9	26/10
Leaf water relations		
Water pot. (ψ_H, MPa)	-0.71^{b} (1.33^{b})	-1.13^{a} (1.63^{c})
Osmotic pot. (ψ_π, MPa)	-2.53^{b} (1.59^{b})	-2.06^{c} (1.23^{a})
Turgor pot. (ψ_t, MPa)	1.83^{c} (1.72^{b})	0.93^{a} (0.94^{a})
n (treated/control)	19/9	26/10
Proline (mg g^{-1} dry wt)	2.14^{b} (1.35^{b})	2.56^{b} (1.12^{b})
n (treated/control)	19/13	26/15
Ion analysis		
Cl^- (mg L^{-1})	2.50^{c} (11.05^{c})	1.18^{a} (6.38^{a})
Na^+ (mg g^{-1} dry wt)	1.85^{d} (13.43^{b})	0.23^{a} (4.13^{a})
Ca^{2+} (mg g^{-1} dry wt)	0.39^{ab} (0.73^{a})	0.34^{a} (0.88^{bc})
K^+ (mg g^{-1} dry wt)	2.60^{c} (1.07^{b})	1.81^{a} (1.09^{b})
Mg^{2+} (mg g^{-1} dry wt)	0.11^{b} (0.98^{c})	0.09^{a} (0.81^{b})
P (mg g^{-1} dry wt)	1.40^{d} (1.70^{c})	0.38^{a} (0.97^{b})
S (mg g^{-1} dry wt)	0.17^{c} (1.43^{c})	0.09^{ab} (0.86^{b})
n (treated/control)	19/13	26/15

* s/ns ratio (saline/non-saline ratio): ratio between value at the end of the treatment and the average value in non-saline conditions

	D. kaki x D. virginiana	
	Sensible	**Tolerant**
Agro-morphological data	**Mean (s/ns ratio)**	**Mean (s/ns ratio)**
Initial Height (iH, cm)	33.35^{c} (2.23^{c})	23.69^{b} (1.38^{b})
End Height (eH, cm)	82.51^{b} (1.22^{d})	92.16^{bc} (1.05^{c})
$Height_{ei}$Ratio (eH:iH)	2.48^{a} (0.56^{a})	4.01^{b} (0.78^{b})
Initial Leaves (iL, nº)	10.85^{c} (1.96^{c})	8.84^{b} (1.32^{b})
End Leaves (eL, nº)	24.79^{b} (1.41^{c})	28.37^{b} (1.10^{b})
Initial Nodes (iN, nº)	11.00^{c} (1.99^{b})	9.00^{b} (1.28^{c})
End Nodes (eN, nº)	27.55^{b} (1.44^{c})	30.11^{b} (1.10^{b})
$Nodes_{ei}$Ratio (eN:iN)	2.49^{a} (0.69^{a})	3.41^{c} (0.87^{bc})
Initial Internodes (iI, cm)	3.04^{c} (1.06^{a})	2.71^{b} (1.10^{a})
End Internodes (eI, cm)	3.02^{b} (0.85^{b})	3.16^{b} (0.99^{c})
$Internode_{ei}$Ratio (eI:iI)	1.00^{b} (0.80^{b})	1.19^{c} (0.89^{c})
Defoliation (eN:eL)	0.11^{b} (1.35^{b})	0.06^{a} (0.96^{ab})
Damage Index	2.67^{c} (4.94^{b})	0.05^{a} (0.26^{a})
n (treated/control)	53/15	38/15
Leaf gas exchange		
A_{CO2} (µmol CO_2 m^{-2} s^{-1})	2.96^{a} (0.45^{a})	4.23^{a} (0.64^{ab})
g_s (mmol H_2O m^{-2} s^{-1})	47.79^{bc} (0.96^{c})	29.58^{a} (0.59^{a})
E (mmol H_2O m^{-2} s^{-1})	1.28^{b} (0.91^{b})	0.77^{a} (0.55^{a})
C_i (µmol CO_2 m^{-2} s^{-1})	278.94^{b} (1.67^{b})	163.58^{a} (0.98^{a})
n (treated/control)	29/15	28/15
Leaf water relations		
Water pot. (ψ_H, MPa)	-0.68^{b} (0.78^{a})	-1.04^{a} (1.20^{b})
Osmotic pot. (ψ_π, MPa)	-3.09^{a} (1.91^{c})	-2.40^{b} (1.48^{b})
Turgor pot. (ψ_t, MPa)	2.42^{d} (3.21^{c})	1.36^{b} (1.81^{b})
n (treated/control)	29/15	28/15
Proline (mg g^{-1} dry wt)	1.41^{a} (0.67^{a})	1.44^{a} (0.69^{a})
n (treated/control)	46/25	46/25
Ion analysis		
Cl^- (mg L^{-1})	2.59^{c} (9.43^{b})	2.00^{b} (7.28^{a})
Na^+ (mg g^{-1} dry wt)	1.41^{c} (13.05^{b})	0.44^{b} (4.10^{a})
Ca^{2+} (mg g^{-1} dry wt)	0.43^{b} (0.83^{ab})	0.50^{c} (0.97^{c})
K^+ (mg g^{-1} dry wt)	2.12^{b} (0.83^{a})	2.56^{c} (1.00^{b})
Mg^{2+} (mg g^{-1} dry wt)	0.09^{a} (0.63^{a})	0.08^{a} (0.57^{a})
P (mg g^{-1} dry wt)	0.75^{c} (0.78^{a})	0.62^{b} (0.64^{a})
S (mg g^{-1} dry wt)	0.11^{b} (0.85^{b})	0.08^{a} (0.66^{a})
n (treated/control)	46/25	32/25

* s/ns ratio (saline/non-saline ratio): ratio between value at the end of the treatment and the average value in non-saline conditions

The classification of the BC plants according to the PCA was validated with ANOVA analysis. The BC group classified as tolerant (BC_t) showed values of the s/ns ratios of e/i ratios statistically equal to those of the DV population, while the performance of the BC susceptible group (BC_s) was closer to the DK population (Table 7). BC_s and BC_t plants exhibited a decrease in growth speed compared to the control grow in non-saline conditions, with s/ns ratios lower than 1 for height, nodes and internodes (Table 7), being those corresponding to BC_t significantly higher than those of BC_s. Additionally, BC_s plants exhibited a significant increase in defoliation and damage index, with values of 0.11 and 2.67 respectively, compared to BC_t, with values of 0.06 and 0.05 respectively (Table 7).

Regarding leaf gas exchange and leaf water relations parameters, the variability explained by the two first components was 79.4%. The plot showed different distribution between the populations of *D. virginiana* and *D. kaki* (Figure 14b). This difference was not so evident under non-saline conditions (Figure 13b), thus reflecting that *D. virginiana* population exhibited a clear response to salinity conditions. BC_t plants plotted within *D. virginiana* population, while most BC_s plants plotted within *D. kaki* population.

Almost all s/ns ratios of leaf water relations parameters (ψ_H, ψ_π, ψ_t) were higher than 1 in all the populations (Table 7). Only in the case of DV the ψ_t ratio was similar to non-saline conditions and in the case of BC_s plants the ψ_H ratio was lower than 1. DV plants exhibited significantly lower values of ψ_H and ψ_t, and significantly higher values of ψ_π than the rest of populations, while BC_s plants showed

significantly lower ψ_π and significantly higher ψ_H and ψ_t (Figure 16, Table 7).

The population of *D. virginiana* and BC_t subset under salinity conditions showed a reduction of the A_{CO2}, g_s and E (s/ns ratios lower than 1), while the C_i had a similar value to control conditions (Figure 17, Table 7). The reduction of s/ns ratio experimented by *D. kaki* population and BC_s plants was significantly higher in the case of A_{CO2}but lower in the case of g_s and E, which showed values similar to control conditions (Table 7). On the other hand, in these plants the C_i was higher under saline conditions (s/ns ratio > 1). DV plants had higher values of A_{CO2} and g_s, compared to BC_t (Figure 17). No significant differences were found between *D. kaki* and BC_s for leaf gas exchange parameters (Table 7). Under salinity conditions the leaf WUE of DV and BC_t plants was similar to the non-saline plants; however, it was decreased in *D. kaki* population BC_s plants (Figure 17).

Regarding leaf salt and nutrients (Cl^-, Na^+, Ca^{2+}, K^+, Mg^{2+}, P, S) and proline accumulation, the first two components of the PCA explained 58.8% of total variance. *D. virginana* population was separated from *D. kaki* population. DV plants plotted near its average plant under non-saline conditions (Vm), suggesting that these variables were not greatly affected by saline conditions. On the other hand, DK plants plotted away from its average plant under non-saline conditions (Km). The plants from the BC spanned between both populations without a clearly differentiation between BC_s and BC_t plants (Figure 14c)

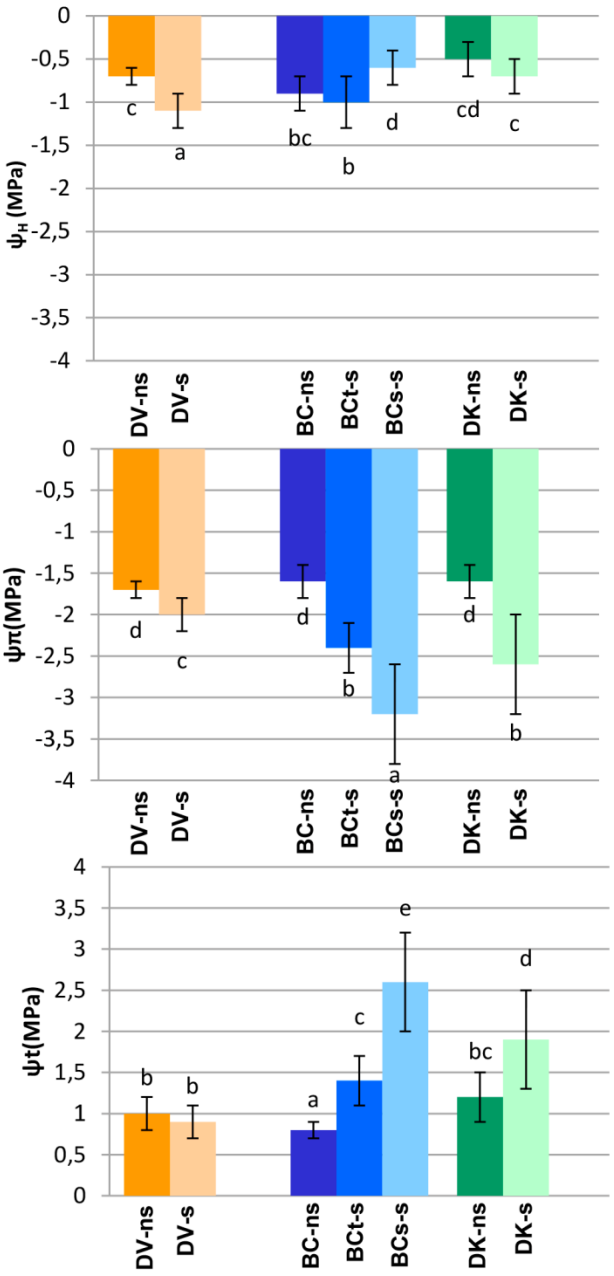

Figure 16. Leaf water relations measured on a pool of samples from each population under saline (s) and non-saline (ns) conditions: V – *D. virginiana* population (orange), K – *D. kaki* population (green) and BC – Backcross population (blue). The number of plants measured were 57 BC treated plants (28 tolerant and 29 sensitive), 15 of BC control, 19 DK treated, 9 DK control, 26 DV treated and 10 DV control. The vertical bars represent standard deviation. Different letters represent significant differences ($p<0.05$).

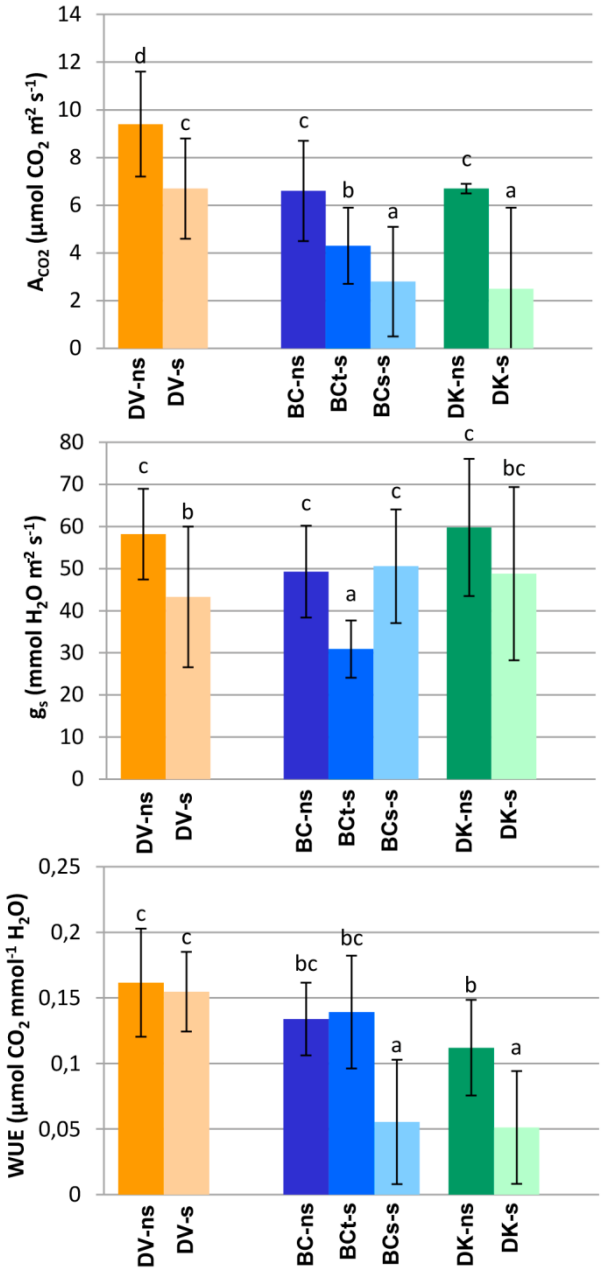

Figure 17. Leaf net CO2 assimilation rate (ACO2), stomatal conductance (gs) and intrinsic leaf water use efficiency (WUE), measured on a pool of samples from each population under saline (s) and non-saline (ns) conditions: V – D. virginiana population (orange), K – D. kaki population (green) and BC – Backcross population (blue The number of plants measured were 57 BC treated plants (28 tolerant and 29 sensitive), 15 of BC control, 19 DK treated, 9 DK control, 26 DV treated and 10 DV control. The vertical bars represent standard deviation. Different letters represent significant differences ($p<0.05$)

Regarding to proline content, DK plants tended to accumulate higher amounts under saline conditions (1.35 fold), while BC_s and BC_t plants accumulated lower amounts (0.67 and 0.69 fold respectively) *D. virginiana* plants tended to accumulate similar amounts (1.12 fold) in saline and non-saline conditions (Table 7). Plants from *D. kaki* and *D. virginiana* populations showed significantly higher content than BC_s and BC_t plants (Figure 18).

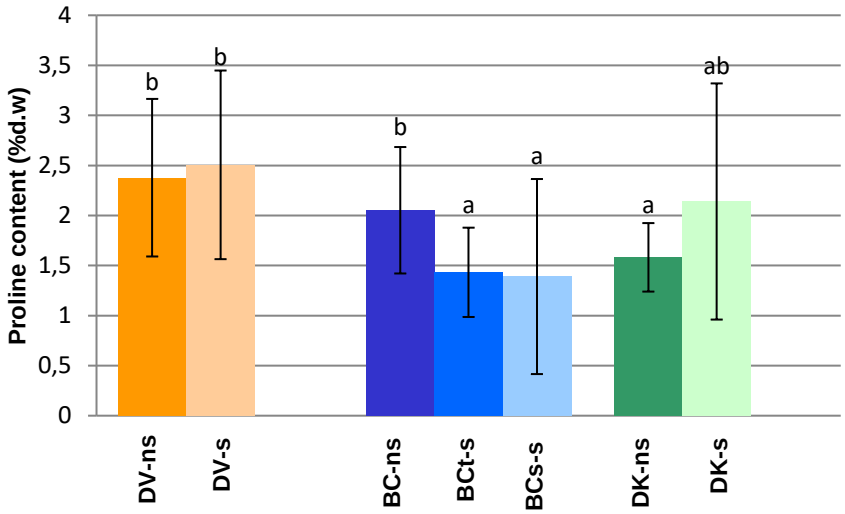

Figure 18. Leaf proline content on a pool of samples from each population under saline (s) and non-saline (ns) conditions: V – *D. virginiana* population (orange), K – *D. kaki* population (green) and BC – Backcross population (blue). The number of plants measured were treated and control DK: 19 and 13, respectively; DV: 26 and 15, respectively; 32 tolerant BC, 46 sensitive BC plants and 25 BC control. The vertical bars represent standard deviation. Different letters represent significant differences ($p<0.05$)

All populations showed s/ns ratios of Cl^- and Na^+ contents higher than 1. Concerning to Ca^{2+} and K^+ contents the s/ns ratios were close to 1, thus they were not affected by saline conditions (Table 7). DK and BC_s plants exhibited significantly higher values of Cl^- and Na^+ when compared to DV and BC_t plants (Figure 19). The highest mean content of Ca^{2+} was found in the leaves of BC_s and BC_t, while the highest contents of K^+ and Mg^{2+} were found in the leaves of DK (Table 7, Figure 20).

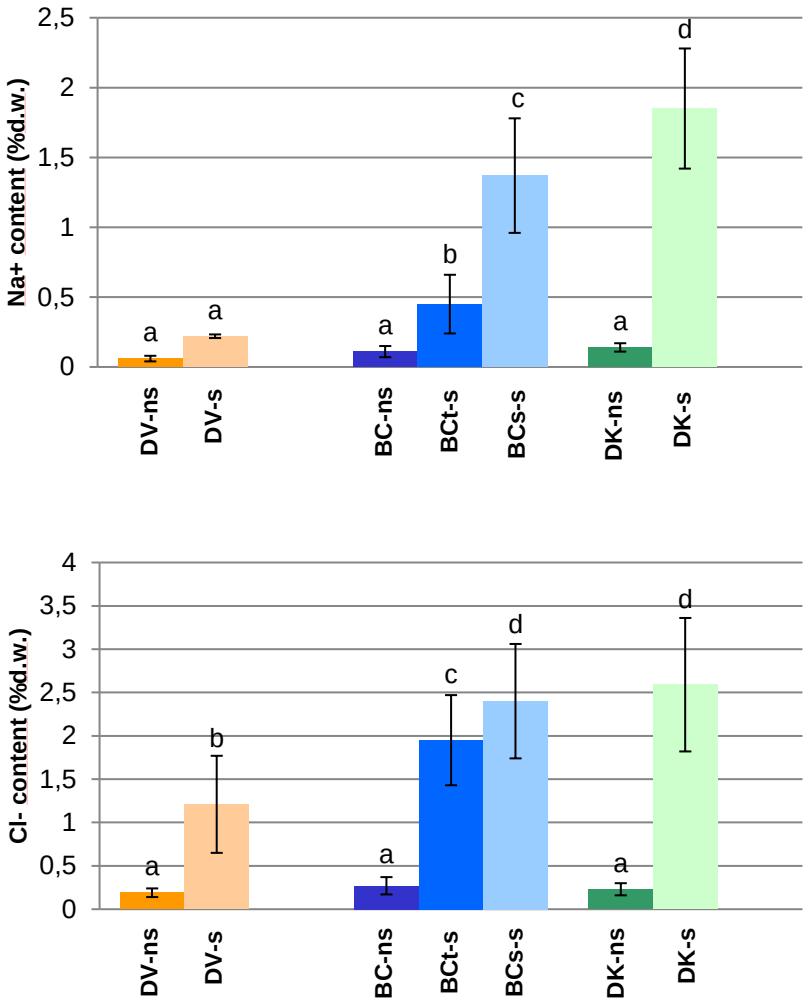

Figure 19. Na^+ and Cl^-, K^+ and Ca^{2+} leaf content on a pool of samples from each population under saline (s) and non-saline (ns) conditions: V – *D. virginiana* population (orange), K – *D. kaki* population (green) and BC – Backcross population (blue). The number of plants measured for treated and control DK were: 19 and 13, respectively; DV: 26 and 15, respectively; 32 tolerant BC, 46 sensitive BC plants and 25 BC control. The vertical bars represent standard deviation. Different letters represent significant differences ($p<0.05$).

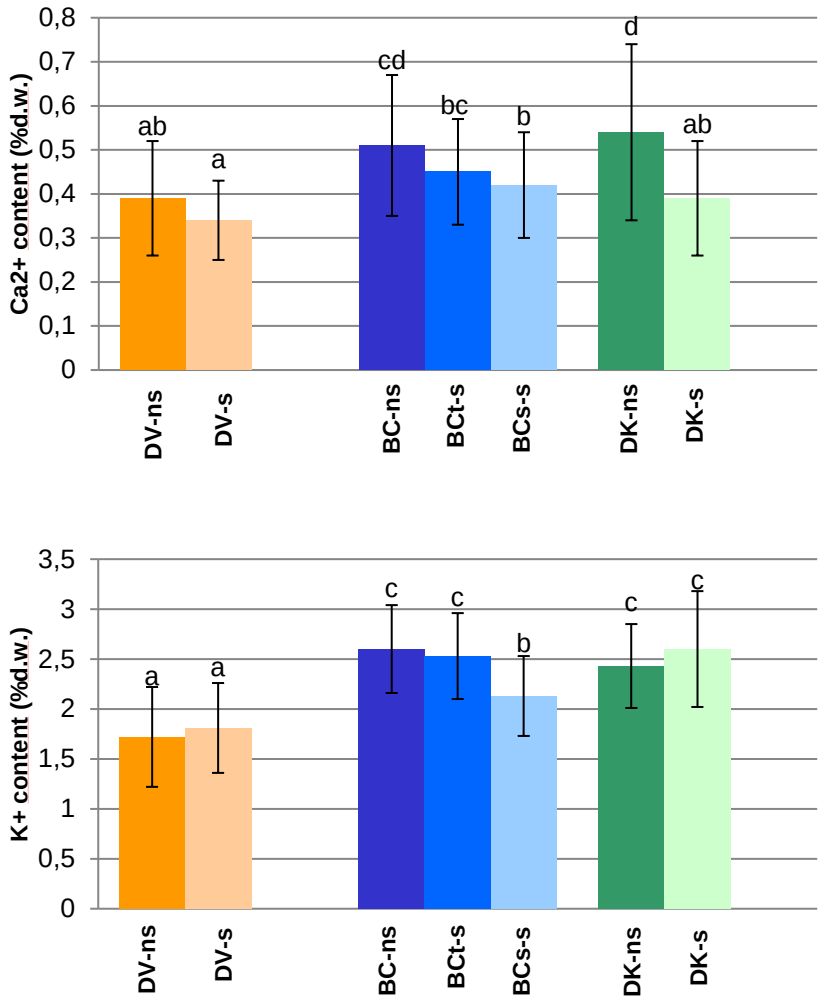

Figure 20. K^+ and Ca^{2+} leaf content on a pool of samples from each population under saline (s) and non-saline (ns) conditions: V – *D. virginiana* population (orange), K – *D. kaki* population (green) and BC – Backcross population (blue). The number of plants measured for treated and control DK were: 19 and 13, respectively; DV: 26 and 15, respectively; 32 tolerant BC, 46 sensitive BC plants and 25 BC control. The vertical bars represent standard deviation. Different letters represent significant differences ($p<0.05$).

Gene expression analysis

In the case of the salt overly sensitive pathway SOS, while the differences in the expression level of *SOS2* and *SOS3* between populations were limited, the expression of *SOS1* was considerably higher in DV root tissues, in saline and non-saline conditions (Figures 21a, 21b and 21c). Regarding the comparison of gene expression between saline and non-saline conditions, no differences were found in the expression levels of *SOS2* and *SOS1* for DV, DK and the BC groups (Figures 21a and 21b). In the case of *SOS3*, DK showed expression levels considerably higher under saline conditions, while DV showed slightly reduced expression under saline conditions, no differences were found in the BC groups (Figure 21c).

In the case of the anion vacuolar channel *ALMT9*, the expression levels were lower in DK both in saline and no saline conditions, but the effect of saline conditions was not significant for any population (Figure 21d). The expression levels of the Na^+/H^+ antiporter *NHX1* in *D. virginiana* were again higher than *D. kaki* and the BC populations (Figure 21e). In the last two cases salinity did not increase expression levels, but in the case of DV, the expression increased in saline conditions (Figure 21e).

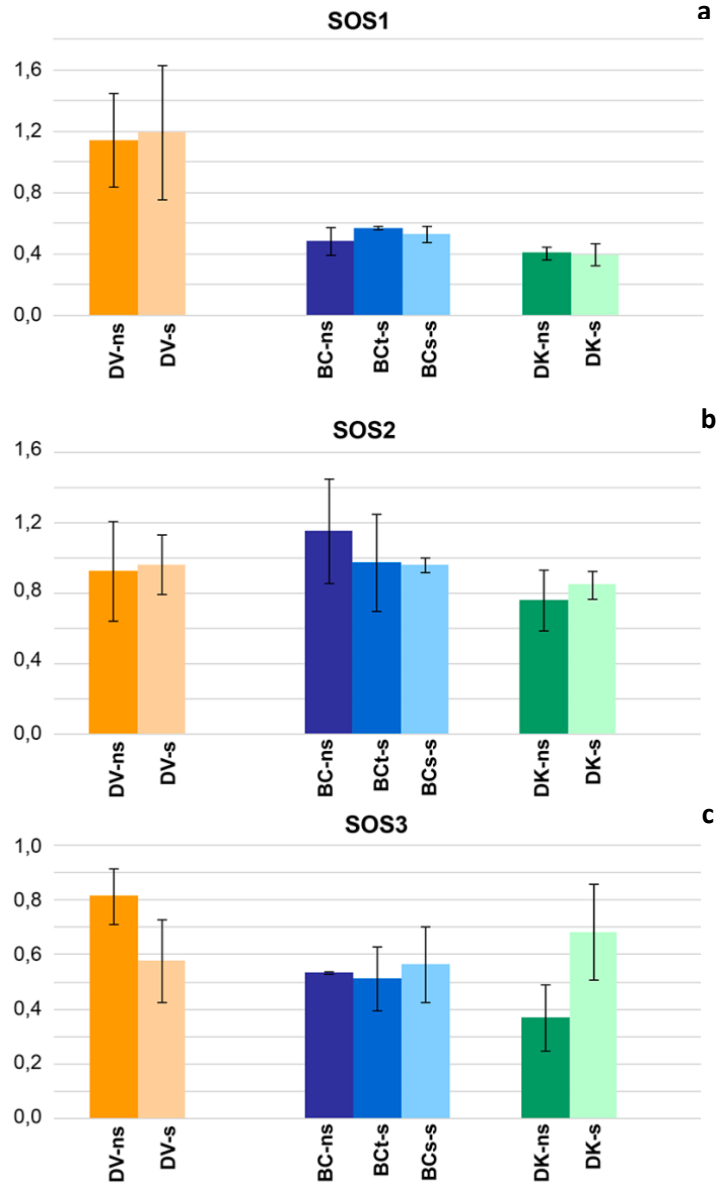
a
SOS1
1,6
1,2
0,8
0,4
0,0
DV-ns
DV-s
BC-ns
BCt-s
BCs-s
DK-ns
DK-s
b
SOS2
1,6
1,2
0,8
0,4
0,0
DV-ns
DV-s
BC-ns
BCt-s
BCs-s
DK-ns
DK-s
c
SOS3
1,0
0,8
0,6
0,4
0,2
0,0
DV-ns
DV-s
BC-ns
BCt-s
BCs-s
DK-ns
DK-s

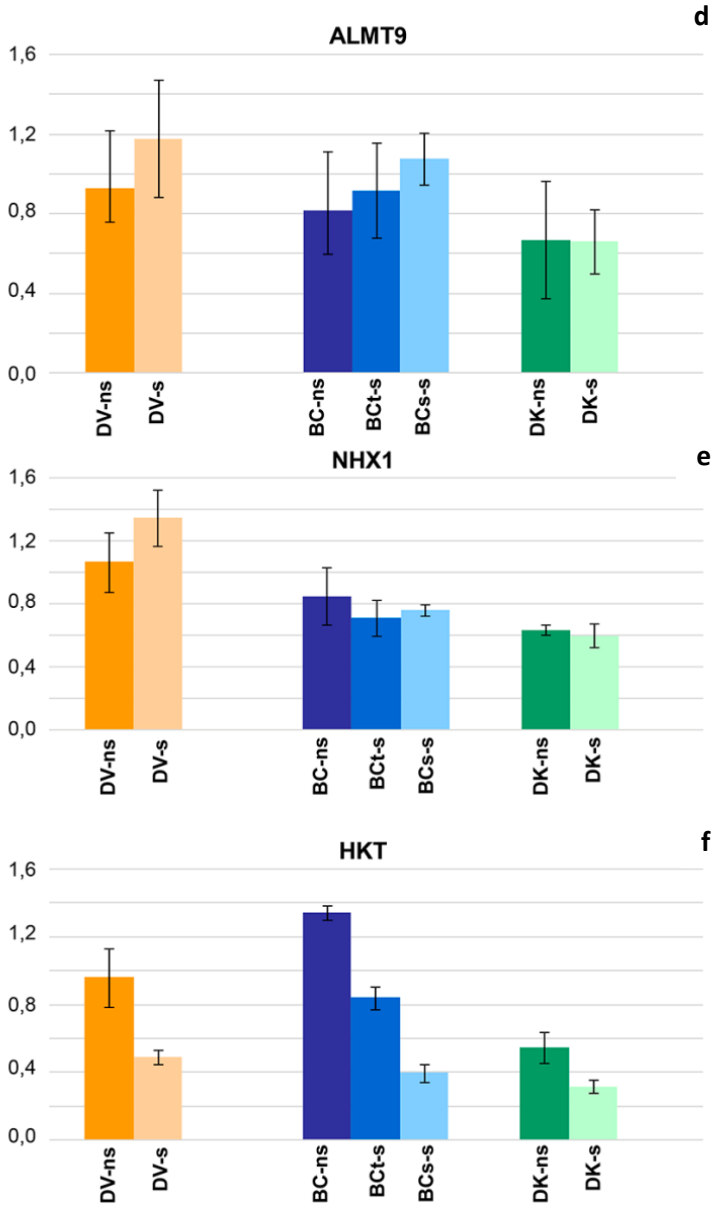

Figure 21. Relative expression of the genes SOS1-like (a), SOS2-like (b), SOS3-like (c), ALMT9-like (d), NHX1-like (e) and HKT-like (f) measured on a pool of samples of each population under saline (s) and non-saline (ns) conditions: V – *D. virginiana* population (red), K – *D. kaki* population (green) and BC – Backcross population (blue). The vertical bars represent standard deviation.

A different pattern was found in the high affinity potassium transporter *HKT*; the expression levels were higher in the BC than in any other populations (Figure 21f). Saline conditions showed a reduction of expression levels of *HKT* from 40% to 50% in all populations. Interestingly, differences were found in the expression levels of BC tolerant and susceptible plants under saline conditions. While BC_t plants reduced expression levels in a 40% compared to non-saline conditions, this reduction was much higher in BC_s plants, reaching a 70% decrease. Despite the reductions observed due to saline conditions, the expression levels of DV and BC_t plants were higher than those of DK and BC_s plants (Figure 21f).

In reference of plasma membrane intrinsic proteins PIPs, expression levels of both (*PIP1* and *PIP2*) in DV were higher under saline conditions, while in DK the expression were slightly reduced under saline conditions (Figure 22). No differences were found in the expression levels of *PIP1* and *PIP2* in BC tolerant and susceptible plants under saline conditions, while the expression under non-saline conditions was reduced (Figure 22).

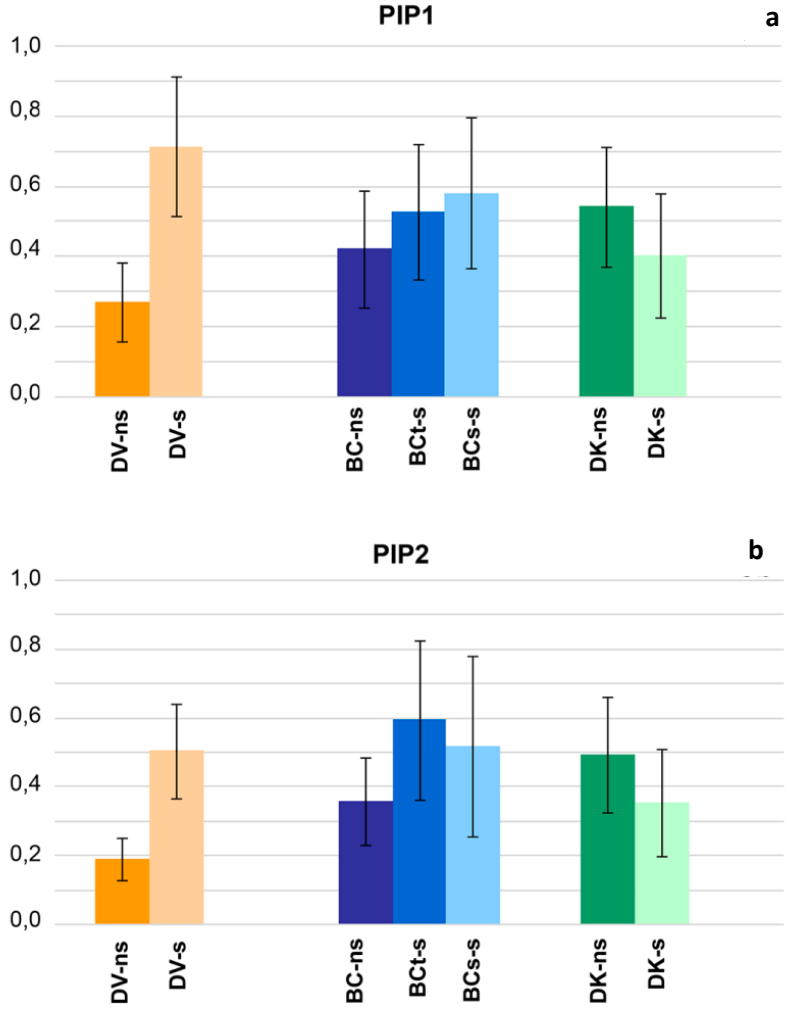

Figure 22. Relative expression of the PIP1-like (a), PIP2-like (b) families measured on a pool of samples of each population under saline (s) and non-saline (ns) conditions: V – *D. virginiana* population (orange), K – *D. kaki* population (green) and BC – Backcross population (blue). The vertical bars represent standard deviation.

Discussion

Previous studies have analyzed the salt tolerance of different species, and the authors concluded that tolerant plants make different morphological, physiological and biochemical changes that allowed them to adapt to salinity conditions (Acosta-Motos et al., 2017). Experiments of salinity tolerance using saline water have shown different effects between species of the same genus, and between cultivars from the same species (Flowers and Colmer, 2008; Munns and Tester, 2008).

The *Diospyros* genus includes more than 400 species while only three species are widely used as rootstock: *D. lotus*, *D. virginiana* and *D. kaki* (Bellini and Giordani, 2002). Species of the genus *Diospyros* show different degrees of tolerance to salt stress. *D. lotus* is the most common rootstock used for persimmon propagation in the Mediterranean basin. However, important damages attributed to ion toxicity has been reported in persimmon orchards grafted on *D. lotus*, which points out the need of selection of salinity tolerant rootstocks in the Mediterranean environments (Badenes et al., 2015; Visconti et al., 2017). *D. kaki* is the most used in persimmon orchards around the world because the affinity with all cultivars (Bellini and Giordani, 2002) and the lack of salinity problems in the areas where persimmon is most grown. *D. virginiana* has been described as more salt tolerant than *D. kaki* (Incesu et al., 2014). In a context of climate change and increase of salinity in soil and irrigation water, selections of tolerant rootstocks are required for maintaining the crop. In this study, salinity tolerance has been evaluated in plants from *D. virginiana*, *D. kaki* and

a backcross population (BC) between both species aimed at identifying tolerance to salinity suitable for rootstock breeding in persimmon. Analysis of effects on morphology, physiological parameters and transcriptomic on plants after saline treatment were used for tolerance evaluation.

Effects on morphology

The effects of salinity on growth rate have been widely reported for different species (Munns and Tester, 2008). The main effect of stress on plants is the progressive inhibition of growth as a consequence of an osmotic effect, that reduces the ability of the plant to absorb water, and a toxic effect by salt accumulation, that can produce the necrosis of leaves reducing the total photosynthetic leaf area (Munns, 2002). At the end of the treatment with saline water, our results showed inhibition of vegetative growth in the populations studied; indicated by reduction of several variables: plant height, number of leaves and nodes and internodes length. Moreover, the responses differed significantly between the two populations; *D. virginiana* (DK) population was less affected than *D. kaki* (DK). After the salt treatment, some backcross plants showed severe symptoms on plant growth and were classified as susceptible (BC_s), while others showed moderate symptoms and were classified as tolerant (BC_t). This fact indicates the presence of diversity within this population related to the response to salinity, enabling breeding for salinity tolerance.

Osmotic stress responses

In salinity conditions, growth rate reduction could be a consequence of an inadequate photosynthetic activity, as a result of stomatal and non-stomatal factors (Munns and Tester, 2008). All populations studied showed a reduction in the A_{CO2} compared to controls. In treated plants, salinity induces stomatal closure and reduction of C_i (Table 7 and Fig. 17), similarly to the effects described in other species (Brugnoli and Lauteri, 1991). In persimmon, besides of differences between saline treated and control plants, persimmon tolerant genotypes showed a significant higher reduction of g_s and E compared to sensitive genotypes. Interestingly, under salinity conditions, the tolerant populations maintained values of WUE similar to the control, which means that the reduction of A_{CO2} and g_s was proportional (Figure 17), indicating that stomatal closure in tolerant genotypes was the main limiting factor of photosynthesis. These responses are mechanisms described for adaptability to osmotic stress caused by excessive salt environments (Koyro, 2006). Reduction of g_s could be used as an indicator of the tolerance to osmotic stress in *D. kaki*, *D. lotus* and *D. virginiana* (Rahnama et al., 2010). Changes in g_s are always accompanied by changes in leaf water relations (Gimenez et al., 2004; Zhu et al., 2018). In agreement with previous studies in other species, significant differences in ψ_H between tolerant and sensitive populations were found in persimmon. The higher values of ψ_H found in tolerant plants (DV and BC_t) (Figure 16) indicates that salinity conditions affected much more plant water status in tolerant than in sensitive plants. This different response found was due to the osmotic adjustment mechanism

developed in sensitive plants, favored by the higher accumulation of ions such as Cl^-, that permitted maintain high ψ_t (Figure 16). In saline soils, 2% intake of the NaCl is used by the plant for osmotically adjust of Na^+ and Cl^- in vacuoles (Munns et al., 2020).

Ionic stress responses

Tolerance to salinity involves as well important mechanisms for prevention of ion toxicity. This prevention effect might be related to a mechanism of exclusion of toxic ions or their compartmentation. Energy-efficient osmotic adjustment requires compartmentation of Na^+ and Cl^- in vacuoles, and of K^+ and compatible organic solutes in the cytoplasm (Munns et al., 2020). The Na^+ content in leaves from tolerant populations (DV and BCt) was much lower than in sensitive (DK and BCs), which indicates that persimmon species are able to prevent Na^+ toxicity. Similar results would be expected in roots; however, the size of the plants did not allow sampling of ions in roots. To unravel this question, transcriptomic experiments using orthologues of genes described in model plants involved in ion transportation were made. The access to the plant vascular system of Na^+ is mediated by non-selective cation channels, but the exclusion from the cell is via a high energy demanding process of Na^+/H^+ transporters. In Arabidopsis, SOS1 has antiporter activity, it has been demonstrated to play a role in Na^+ transport outside the cells under salt conditions (Qiu et al., 2002; Shi et al., 2002). Increase of *SOS1* expression should increase salinity tolerance. In persimmon, the transcriptomic study revealed a higher *SOS1* expression in the tolerant *D. virginiana* genotypes; however this increase of expression

is not related to the salinity treatment. No differences were obtained among the BCt and the rest of sensitive populations, which seems to indicate that in these species salt conditions does not seem to trigger the SOS pathway response. The tolerant plants had lower content of Na^+ in leaves and are the ones in which the growth and leaf damage were less affected by salinity. Those tolerant plants presented higher values ofA_{CO2} than sensitive ones. The hypothesis is that tolerance in persimmon is based on reduction of hydraulic conductance and transpiration to overcome the osmotic stress. This reduction is not damaging the photosynthesis system and affect in a lower scale the plant growth, all together would allow reduction of toxic ions concentration like Na^+. Another fact supporting this mechanism is that tolerant DV population showed the ψ_t similar in control and saline conditions. The exposition to saline stress in tolerant persimmon is not causing an increase of Na^+ in leaves or an increase of the osmotic potential.

Regarding to the *HKT1* (high affinity potassium transporter) gene expression, this gene has been linked many times to salinity tolerance in several species, and it is believed that participates in Na^+ exclusion from the shoot via phloematic transport to the roots (Horie et al., 2008). *HKT1* expression prevents Na^+ accumulation in the higher parts of the plant such as stem and leaves, preventing toxic accumulation on sensible organs. Exposition to salinity environment causes a reduction of gene expression. In persimmon, *HKT1* expression was reduced in saline conditions in all populations. However, the root expression was higher in roots of tolerant plants compared to

sensitive which may explain its involvement in tolerance. As *HKT1*-driven tolerance is linked to the tissue-specific expression in other species (An et al., 2017; Han et al., 2018; Hazzouri et al., 2018), leaf and shoot expression would be necessary for explaining the phenotype of the studied populations.

Regarding to the Cl^- exclusion, both in DV and BC_t tolerant populations, lower content in Cl^- can be associated with the lower relative values of g_s and E compared to the control populations (Figures 17 and 19, Table 7). Cl^- exclusion has been described as a passive mechanism linked to anion transporters downregulated by ABA (Munns and Tester, 2008; Henderson et al., 2014), which also downregulates the stomatal aperture of the plant, limiting the water and ion uptake. Therefore, the reduction on whole-plant transpiration driven by stomatal regulation would contribute to the reduction of Cl^- in persimmon tolerant plants. Furthermore, an upregulation on PIP1 and PIP2 aquaporin families has been observed in DV population when exposed to saline conditions (Figure 22). This response has been linked with salinity tolerance in other species (Rodríguez-Gamir et al., 2012) as a regulation of the ion imbalance and water flow inside the plant to adapt the ionic and osmotic stresses caused by salinity (Vitali et al., 2015). The other ion content measured (Ca^{2+}, P, Mg^{2+}, S) was not affected by salinity treatment (Table 7).

In conclusion, persimmon salinity tolerance is based on the reduction of stomatal conductance and decrease of transpiration, preventing the osmotic stress. Beside the reduction, the leaf net photosynthesis was higher in tolerant plants and the growth rate was less affected.

The leaf content of toxic ions as Na^+ and Cl^- was lower in tolerant plants. Necrosis on old leaves for accumulation of toxic ions was observed only in sensitive plants. A mechanism of exclusion should be involved. The transcriptomic data obtained does not allow to link expression of *SOS1* to salinity tolerance (Figure 21). A potential involvement of *HKT* is suggested but data of expression of different tissues (roots and leaves) would be necessary. Additionally, the upregulation on *PIP1* and *PIP2* aquaporin families detected in tolerant plants exposed to salinity could contribute to regulate the ion imbalance by water flow (Figure 23). Further analysis of the isoforms within PIP families could reveal more information. However, the lack of availability of persimmon genome makes difficult these transcriptomic approaches.

This is the first approach into the possible mechanism regulating tolerance to salinity of persimmon. Tolerance in hybrids from *D. kaki* is being identified. This fact opens the opportunity of breeding for salinity tolerance and made possible to initiate further studies based on the selected genotypes to dig into the mechanisms of salinity tolerance present in this species. The selected tolerant individuals will be tested for graft-compatibility with *D. kaki* for its use as potential salt-tolerant rootstocks

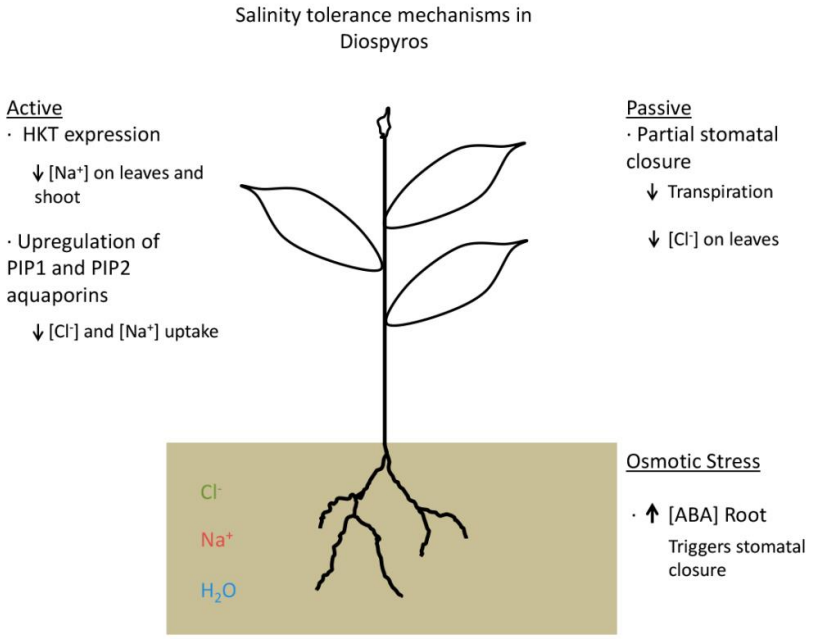

Figure 23. Schematic representation of the salt tolerance mechanisms present in *Diospyros* species.

Intra and inter-specific variability of salt tolerance mechanisms in *Diospyros* genus

Abstract

Saline stress is one of the problems that agriculture must face within the climatic change. In the Mediterranean, persimmon production can be compromised by this effect, as availability of salt tolerant rootstocks is limited. Seedlings coming from four populations from the *Diospyros* genus have been exposed to salt stress in order to find salt tolerance variability within populations. Morphological, physiological and transcriptomic approaches have revealed different mechanisms present on each population. An *HKT1-like* gene probably plays an important role in determining salinity tolerance among and within populations. This variability can be generated through crossings or naturally exploited. Furthermore, *PIP* aquaporins might play a role in Na^+ traslocation to the leaves. Furthermore, differences in water use efficiency (WUE) have been revealed between and within populations. The information obtained of the natural and inheritable variability among *Diospyros* genus will be useful for salt-tolerant rootstock breeding programs.

Introduction

Persimmon (*Diospyros kaki*) production in the Mediterranean has increased by five times in the last 20 years (Perucho, 2018). In fact, it became an important alternative to citrus production and shares the same crop areas. However, in the recent years, cultural practices and climate change have modified rainfall distribution and have increased salt content in the irrigation water (Visconti et al., 2015). Several approaches can be applied to alleviate the salinization problems caused in the crop, for instance changes in crop management and irrigation methods could minimize the problem, however the most effective method is to use salt-tolerant genotypes.

In tree crops composed by rootstock and scion, the best approach to overcome soil salinity is to use salt-tolerant rootstocks compatible with the scion (Forner-Giner and Ancillo, 2013). There are three species of *Diospyros* genus used as rootstocks: *D. kaki*, *D. lotus* and *D. virginiana* (Badenes et al., 2015). *D. lotus* is the most commonly used rootstock in the Mediterranean area due to its tolerance to lime-filled soils, adaptability and absence of basal shoots. However, it is high sensitive to salinity (de Paz et al., 2016; Visconti et al., 2017). *D. virginiana*, is tolerant to salinity and has a good development in lime-filled soils, but it confers too much vigour to the scion and produces basal shoots, both traits difficult crop management (Incesu et al., 2014; De Paz et al., 2016). *D. kaki* is the most used rootstock species around the world, because its compatibility with all the cultivars. This rootstock is not used in the Mediterranean basin because its sensitivity to lime-filled soils and develops a weak root system that

causes pour and slow development in nurseries (Bellini and Giordani, 2002).

An additional problem for persimmon crop is the origin of the rootstocks; all of them come from seedlings, never from clonal propagation, which implies a high genetic heterozygosity among rootstocks. There are not clonal rootstocks available, neither selected clones from breeding programs, despite micropropagation methods have been developed for some genotypes of *D. lotus* and *D. virginiana* (Giordani et al., 2012). Regarding to saline-stress performance, *D. virginiana* has been identified as the most salt-tolerant species and *D. lotus* the most sensitive, being *D. kaki* intermediate (De Paz et al., 2016; Visconti et al., 2017; Gil-Muñoz et al., 2018a). However, information about the salt tolerance diversity into each rootstock species is not available. To unravel this question is the key for developing genotypes tolerant to salinity Moreover, to determine the salt tolerance mechanisms among the persimmon rootstock species would allow to define strategies for managing the crop in saline environments and to design interspecific crosses that combined different tolerance mechanisms.

Salt stress tolerance is a polygenic and quantitative trait highly influenced by the environment (Tiwari et al., 2016). Therefore, discovering the salinity tolerance mechanism or even the genes underlying to the tolerant phenotypes might help to avoid the environment effect in the first steps of a breeding program. Salt stress causes dehydration, metabolic toxicity, nutrient imbalances, membrane dysfunction and oxidative stress (Essah et al., 2003).

Furthermore, it compromises several types of stress: osmotic stress caused by the more negative osmotic pressure of the soil water and ionic stress caused by the accumulation of toxic ions in the plant (Munns and Tester, 2008).

Under salinity conditions, osmotic stress causes drought-like effects in the plant. It causes changes in the stomatal aperture of the plant via abscisic acid (ABA) route (Fricke et al., 2006). Independently to the water ion profile, this mechanism is activated and might be a drought response effect, as it has been observed that it is regulated by root signals that are also triggered in drought conditions (Termaat et al., 1985; Davies et al., 2005). Photosynthesis of the plant can be severely affected by salinity stress, but the causes are not yet fully known (Gil-Muñoz et al., 2020). Some studies have related salinity stress with an increase in stored carbohydrate (Munns et al., 2000), indicating a reduction in sink demand that may downregulate photosynthesis.

Regulation of water transport, small solutes and hydric balance through the plant is a mechanism to overcome salinity stress. Maurel et al., (2008) described membrane intrinsic proteins named aquaporins that play a central role in water relations of roots, leaves and seeds, hence, involved in this regulation. Several studies described changes in aquaporin Plasma membrane intrinsic protein (PIPs) family activity under salt stress (Martínez-Ballesta et al., 2003; Boursiac et al., 2005; López-Pérez et al., 2009) linked to a reduction in hydraulic conductivity (Joly, 1989; Zekri and Parsons, 1989). Furthermore, in citrus rootstocks, it has been observed different

aquaporin activity in salt-tolerant genotypes compared to sensitive (Rodríguez-Gamir et al., 2012). Furthermore, experiments on yeast and *Xenopus oocytes* have shown increased Na^+ conductance when overexpressing *AtPIP2;1* from *Arabidopsis thaliana*, suggesting a possible function for Na^+ influx into the plant (Chaumont and Tyerman, 2014).

Several genes have been identified in the model species *Arabidopsis thaliana* with salt tolerance, mainly with ionic stress overcame by avoiding toxic ion inflow, transport or by balancing ion homeostasis. The Salt Overly Sensitive (SOS) signaling pathway is responsible of maintaining ion homeostasis during salt stress (Zhu et al., 1998). In this pathway, myristoylated calcium-binding protein CBL4 (SOS3) acts as a sensor to perceive the Na^+-mediated Ca^{2+} spike. After activation, it interacts with a serine/threonine protein kinase (SOS2) (Liu and Zhu, 1998; Halfter, 2000; Liu, 2000; Hrabak et al., 2003) that mediates the activation of the target gene *SOS1* (Shi et al., 2000; Qiu et al., 2002; Quintero et al., 2002, 2011; Quan et al., 2007), a plasma membrane encoding gene with Na^+/H^+ antiporter activity (Qiu et al., 2003) that mediates the retrieval of Na^+ from the cytosol. However, this pathway has a high demand of energy and can compromise plant growth (Isayenkov and Maathuis, 2019). Other genes related with salt stress tolerance participate in different tolerance mechanisms. Some members of the HKT (High affinity potassium transporter) family have been linked with Na^+ exclusion (Byrt et al., 2007; Munns and Tester, 2008; Almeida et al., 2013; Isayenkov and Maathuis, 2019). Also, a member from the Na^+/H^+ exchanger family (NHX) has

been liked to salinity tolerance (Apse et al., 1999), possibly via a role in stomatal regulation (Barragán et al., 2012). Furthermore, the ALMT (Aluminum-activated Malate Transporter) protein family encodes anion transmembrane channels (Barbier-Brygoo et al., 2011) that have been proposed to have a role in Cl^- and Na^+ sequestration in vacuoles of salt tolerant plants (Baetz et al., 2016).

Plants have developed extensive Na^+ tolerance mechanisms. Therefore, in saline environments Cl^- can become potentially more harmful than Na^+, as Cl^- influx is believed to be mediated by passive mechanisms through anion channels regulated by ABA (Munns and Tester, 2008).

In a previous study, variability of salt tolerance in two *Diospyros* genus species was exploited and studied through interspecific crossings (Gil-Muñoz et al., 2020). However, the facts acting under osmotic and ionic stress within the species used as rootstock in persimmon remain not fully known. Understanding and identifying the mechanisms of salt tolerance present in the natural variability of these species will help to advance in rootstock breeding programs. Screening of physiological parameters and genetic expression of genes involved in tolerance is the strategy proposed for selecting genetic-dependent salt tolerant individuals. Results will provide an hypothesis of the mechanism of tolerance in all persimmon species used as rootstocks. The discovery of the mechanisms for salt tolerance will provide tools for breeding *Diospyros* rootstocks better adapted to the saline conditions present in the Mediterranean basin environment.

Materials and methods

Plant material and salinity treatment

Four populations were used for the salinity tolerance study: Seedlings from different accessions of *D. kaki,* (DK) pollinated with male-flowering D. kaki accessions from the IVIA germplasm bank, seedlings from open pollination family of *D. virginiana* (DV), seedlings from a half-sibling backcross family between *D. kaki x D. virginiana* (BC) and a population from *D. lotus* (DL), a full sibling family from a cross between two *D. lotus* trees at the IVIA persimmon germplasm bank was added to the study. At the end of March, seeds were stratified for 30 days in plastic bags filled with perlite in a cold chamber at 4ºC. After stratification, seeds were transferred to peat-moss and perlite (4:1 ratio, respectively) and kept in a greenhouse at 18-24 ºC during two months (from April, 24, to June, 26, 2017).

One hundred and twenty-seven seedlings of each population were transplanted into 1-L pots containing coarse sand. The plants were distributed randomly in the greenhouse and watered with a nutrient solution (3% Cristaljisa 18-18-18, soluble fertilizer with micronutrients) until apical meristem growth was observed. The plants were acclimated before exposition to salinity treatment, meaning that they were watered with the nutrient solution until normal growth was observed. After acclimation, plants were submitted to a salinity treatment during 60 days. The treatment consisted in 40 mM NaCl added to the nutrient solution. The control plants remained watered with the standard nutrient solution.

Agro-morphological data

The parameters total height (cm), leaves (no.), nodes (no.), internodes (cm) and defoliation (1-no. leaves/no. nodes) were measured at days 0, 30 and 45 for all plants. Twenty plants (10 tolerant and 10 sensitive) of each family were selected based on salt tolerance according to the visual and agro-morphological data for further analyses. For the *D. lotus* family only 5 plants could be selected as tolerant. Ten control plants of each population were randomly selected. At the end of the salinity treatment (day 60), prior parameters were also measured for selected plants. Variables related to growth were calculated as the ratio between initial and final value. Relative growth rate (RGR) was calculated as follows:

$$\text{RGR} = \frac{Ln(Height\ 2 - Height\ 1)}{t2 - t1}$$

Being Height 1 the height of the plant at the day 1 and Height 2 the height at the day 2. t2 – t1 is the time between measurements.

Based on visual symptoms, salinity injury was rated from 0 to 4: 0 – no symptoms, 1 – leaf turgor loss, 2 – leaf tip necrosis, 3 – leaf margin necrosis, 4 – defoliated plant.

Stem water potential

Stem water potential **(**ψ_H, MPa) was measured in fully expanded leaf of the control and selected plants in a sunny day using a Model 600 Schölander Pressure Chamber (PMS Instrument Company, Albany, OR, USA) at the end of the salinity treatment (day 60). Previously, the

leaf was kept in a reflective plastic bag for 30 minutes to remove water loss (Levin, 2019).

Leaf gas exchange parameters

Leaf net CO_2 assimilation rate (A_{CO2}), stomatal conductance (g_s), leaf transpiration rate (E) and internal CO_2 concentration (C_i) were measured on single attached leaves from selected (tolerant, sensitive and control) plants. Determinations were performed using uniform fully expanded leaves from the mid-stem zone. Intrinsic leaf water use efficiency (WUE) was calculated as A_{CO2} and g_s ratio. All measurements were carried out in a sunny day between 9:30 a.m. and 12:30 p.m. at the end of the salt treatment (day 60). Photosynthetically active radiation (PAR) at the leaf surface was adjusted to a photon flux density of 1.000 µmol m^{-2} s^{-1}. A CIRAS-2 Portable Photosynthesis System (PP Systems, Amesbury, Massachusetts, USA) was used for the measurements. Leaf laminae were fully enclosed within a PLC 6 (U) universal leaf autocuvette in a closed-circuit model and kept at 25 ± 0.5 ºC, with a leaf-to-air vapor deficit of about 1.7 kPa. The air flow rate through the cuvette was 0.5–1.5 L min^{-1}.

Ion content analysis

After saline treatment, three leaves from each selected plant (control, tolerant and sensitive plants) were collected. Sample pre-treatments for ion content measurement were performed as described in Gil-Muñoz et al (2018). Chloride concentration (mg ml^{-1}) was determined by silver ion-titration (Gilliam, 1971) with a Corning

926 automatic chloridometer (Corning Ltd. Halstead Essex, UK). Na^+, Ca^{2+}, K^+, Mg^{2+}, P and S ions were quantified (mg g^{-1} dry w.t.) using a multiple-collector inductively coupled plasma mass spectrometry (MC-ICP MS, Thermo Finnigan Neptune).

Gene expression analysis

Young fully expanded leaves and root tip tissue was collected after 60 days of salt treatment and immediately frozen and powdered using liquid nitrogen. Control samples from all populations were also collected and processed. RNA was isolated according to Gambino et al. (2008). DNA was removed with the RNase-Free DNase Set (Qiagen, Valencia, CA, USA), using the RNeasy Plant Mini Kit (Qiagen). Purified RNA (500 ng) was reverse transcribed with PrimeScript RT Reagent Kit (Takara Bio, Otsu, Japan) in a total volume of 10 µL.

Six putative orthologous genes involved in different mechanisms leading to salt tolerance were analyzed *SOS1*, *SOS2*, *SOS3*, *NHX1*, *HKT1* and *ALMT9* with primers designed from *D. lotus* SRA archive (SRA ID: SRP045872) *cv*. Kunsenshi (Akagi et al., 2014). For the *PIP* aquaporin expression analysis, *Arabidopsis thaliana* PIP genes from the PIP1 and PIP2 families were blasted against the *D. lotus* (SRA ID: SRP045872) *cv*. Kunsenshi (Akagi et al., 2014). The output fragments were manually assembled to complete putative orthologous genes. Specific persimmon primers were designed using the sequences obtained (Table 8).

Table 8. Primers used for RT-qPCR analysis

Gene name	Sequence (5'-3')
SOS1-Like	F: GGATTTTCTCTGGAAGGAAAGTGCTA R: GGAGATGTAATCAGTTCCTCTTTGACAC
SOS2-Like	F: TTAGAGTTTGTTACTGGAGGGGAACT R: CACTCAGTCCAAAGTCAGAAACCTTCA
SOS3-Like	F: GAAGTTGAGGCCTTGTATGAGCTATTT R: CCTAATGAACGAACAAATTCTCCAAACTC
HKT1-Like	F: GATTCCTAACCCTGCAGATAAACCCATT R: GTTGCAGACACAGAGGTAAAGAACAAG
NHX1-Like	F: CACCAAAGAACTTGACAAGAATGCTG R: CCAATAGTAGTGCACGGTACGAG
ALMT9-Like	F: ACTTATGCAAAACTATACCCCACAATG R: TAGATAAACATATTCACCACCAAACACAC
PIP1-1-Like	F: CCCCAACAAGTGCTCCAGC R: CTTGGTGTAGCCGGAGCTG
PIP1-2-Like	F: TCACCTAGCAAGTGTGCCTCC R: CCTTGGTGTAGCCATGCTGC
PIP1-3-Like	F: GGCTCCCAACAAGTGTGCTT R: CCTTGGTGTAGCCATGTGCA
PIP1-4-Like	F: TCAGGTCTCCTACCAAGTGTGG R: CCCTTGGTATAGCCAGGGTTT
PIP2-1-Like	F: AAGTGAGCGAAGAGGGCCAAAC R: GTAGCGACGGTGACGTAGAGG
PIP2-2-Like	F: ATCTGAGCGAGGAAGGCCAAG R: GTGGCGACGGTGACGTAGAGA
PIP2-3-Like	F: CCACATTAACCCAGCAGTGACA R: CCGATGATCTCAGCTCCGAGT
PIP2-4-Like	F: AGGAAAGTGTCGCTGATCCGG

	R: TTGCTGTAGCCGTGAGCCACCGAA
PIP2-5-Like	F: GAGGAAGGTGTCGCTGATCAGA
	R: TGTTGTAGCCTGACGCCACCTCA
PIP2-6-Like	F: ATTGCTCTTCCTCTACGTCTCAGTG
	R: GCGACACCTTCCTGGCTAACAG

The first-strand cDNA was 30-fold diluted, using 1 µL as template in a final volume of 20 µL. Quantitative real-time PCR was performed on a StepOnePlus Real-Time PCR System (Life Technologies, Carlsbad, CA, USA), using SYBR premix Ex Taq (Tli RNaseH plus) (Takara Bio). The PCR protocol consisted of 10 min at 95 ºC, followed by 40 cycles of 15 s at 95 ºC, and 1 min at 60 ºC. The specificity of the reaction was assessed by the presence of a single peak in the dissociation curve and through size estimation of the amplified product by agarose electrophoresis. *DkACT* (Akagi et al., 2009b) and *DkTUA* (Wang et al., 2016) were used as reference genes. The normalization factor was calculated by the geometric mean of the values of relative expression of both genes. Expression analysis was carried out in 5 plants of each subgroup (tolerant, sensitive and control) for each population. Results were the average of 3 technical replicates.

Statistical analyses

All the data analysis and graphics were made using RStudio v1.1.447 (2018) with packages from the Comprehensive R Archive Network (CRAN). Parameters for all the populations were statistically tested by Kruskal-Wallis test ($P \leq 0.05$) and averages were compared with the Pairwise Wilcoxon-Mann-Whitney test at 95% confidence level

(P≤0.05) using the packages *dplyr* (Wickham et al., 2018), *ggplot2* (Wickham, 2016), *FSA* (Ogle et al., 2018), *DescTools* (Signorell, 2017), *rcompanion* (Mangiafico, 2018), *RColorBrewer* (Neuwirth, 2014) and *multcompView* (Graves et al., 2015). Principal component analysis (PCA) and correlogram were carried out using the packages *ggplot2* (Wickham, 2016), *factoextra* (Kassambara and Mundt, 2017) and *corrplot* (Wei and Simko, 2016). The variables included were the agro-morphological traits measured before the selection. A biplot of individual scores and loadings was obtained. For representation of the RNA expression data, packages *gplots* (Warnes et al., 2016) and *RColorBrewer* (Neuwirth, 2014) were used.

Results

Saline stress effect among populations

Initial morphological parameters from the four populations were measured before salinity treatment began (Figure 24). The number of days from sowing to germination showed differences between all the populations. *D. kaki* (DK) population resulted in the smallest plants and *D. lotus* (DL) plants the highest, backcross (BC) and *D. virginiana* (DV) populations had a similar initial height. No differences were observed in initial node number between DK and BC population and between DL and DV. Interestingly, the highest variability in initial phenotype was found in DV and BC populations compared to DK and DL populations.

After 45 days of saline stress, differences were noticeable among the four populations (Figure 25). DV and BC reached higher height than

DL and DK populations. The BC population reached the highest internode length compared to other populations, suggesting higher vigour under salinity conditions. Again, more variability was observed among DV and BC populations compared to DK and DL regarding to morphological parameters. Furthermore, some of the plants did not survive to the salt stress treatment. The survival rate after 45 days of saline treatment was 100% for BC, 87% for DV, 89% for DK and 98% for DL. Comparing the morphological traits before and after the saline treatment, DV and BC populations had less detrimental effects than DK and DL populations that showed significantly reduced height and severe salt stress damage (Figure 26).

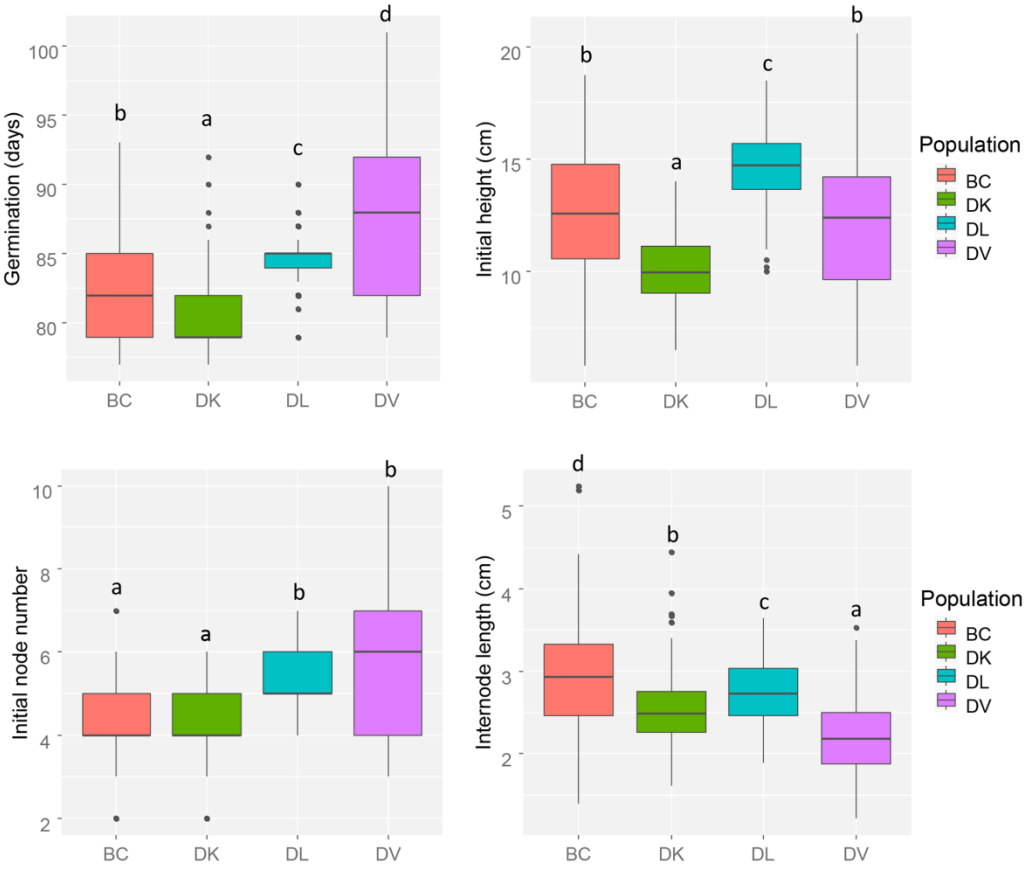

Figure 24. Box and whisker representation of initial morphologic parameters of the four populations (n=128). Different letters mean statistical differences between populations.

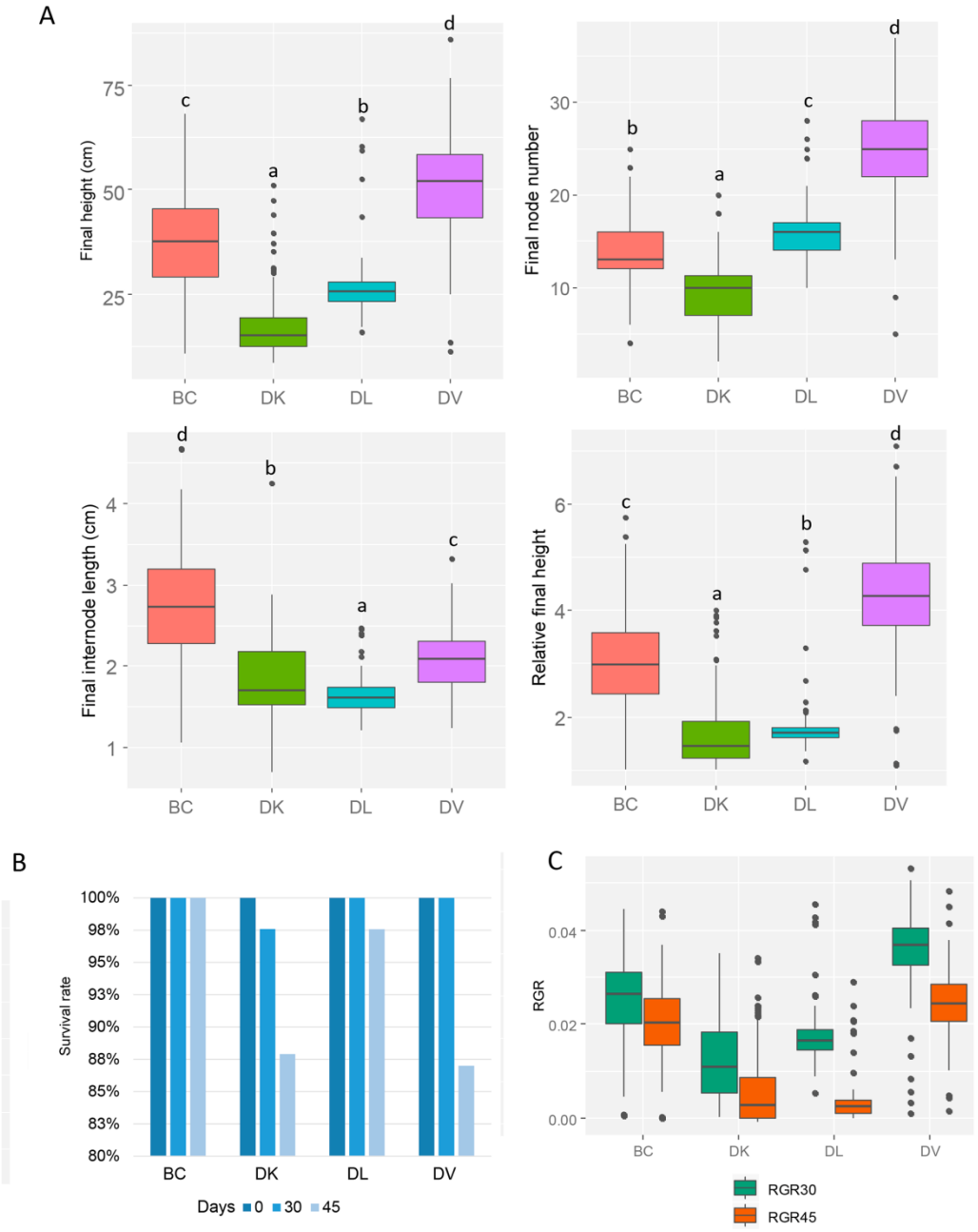

Figure 25. Box and whisker representation of morphologic parameters of the four populations (n=128) after 45 days of salt treatment (A). Different letters mean statistical differences between populations. Relative final height is the ratio between final and initial height. Percentage of plants that were still alive after 30 and 45 days of treatment (B). Relative growth rate of 0-30 days and 30-45 days (C).

Figure 26. Representation of mean plants from each population with and without salt (control) after 45 days of treatment (prior to plant selection). Height (cm) number of nodes, defoliation (as missing leaves) and salinity injury are depicted.

All the morphological variables measured during the stress treatment were submitted to a Principal Component Analysis (PCA) (Figure 27). The first two components explained almost 60% of total variability. The PCA grouped clearly the individuals according to the population they belonged, but separated the populations DV, DK and DL. The backcross population that combines genetic background from *D. kaki* and *D. virginiana* is located at equidistance from DK and DV populations. Furthermore, the DL dispersion was the narrowest. DV, BC and DK population are separated by the PC1. The variables contributing to the PC1 were final plant height, final number of nodes and relative final height (Supplementary Figure S1). DL population was separated from the other three by variables contributing to the PC2, final internode length, height growth and defoliation.

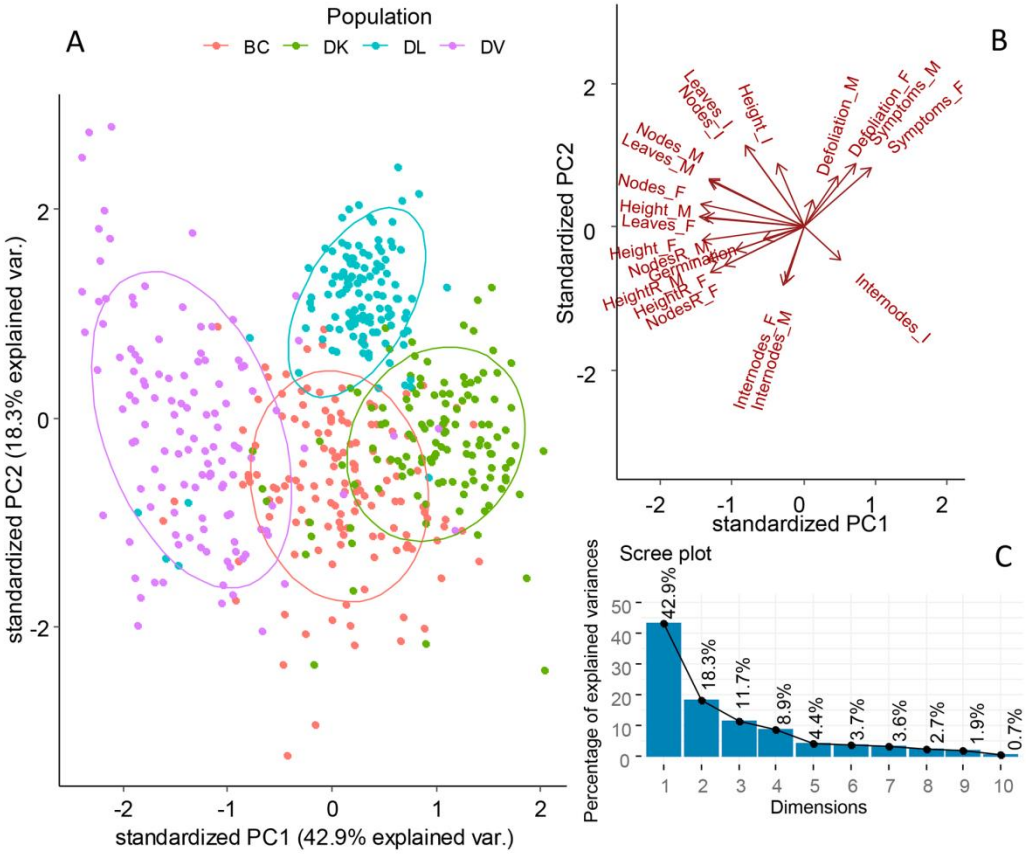

Figure 27. Plot of the first 2 components from Principal Component Analysis of the morphological variables (A). Projection of the variables on the first 2 components (B). Scree plot of the dimensions and explained variability for each component (C).

Saline stress tolerance variability within populations

Using the symptoms and overall plant status, subsets of tolerant and sensitive plants were chosen from each population. These subsets were submitted to a PCA using the morphological variables, but removing those that showed a high collinearity in the previous PCA (Figure 28A). In the four populations sensitive and tolerant plants were grouped apart. DK, BC and DL were separated on similar directions, according to the PCA variables final height and height growth (Figure 28B). DV population showed less clear separation between tolerant and sensitive plants, mainly in the PC2 axis. All the populations showed a coherency in the separation between tolerant and sensitive plants (Figure 28C), which implies that the morphological traits used are a useful tool for phenotyping salt tolerance. Due to the higher tolerance to salinity in the DV population, the discrimination by phenotype was weaker

A correlogram using the morphological variables was done, including the leaf damage symptoms (Supplementary Figure S2). The height growth parameter and the relative final height were the variables more correlated with final salt damage symptoms. Differences for both variables were found between tolerant and sensitive individuals in the DK, DL and BC populations (Figure 29). Furthermore, in these populations, the control plants had higher values than both the tolerant and sensitive subsets, except for the DK population in which the control plants were statistical identical to the tolerant subset regarding to height. No significant differences were found within the DV population.

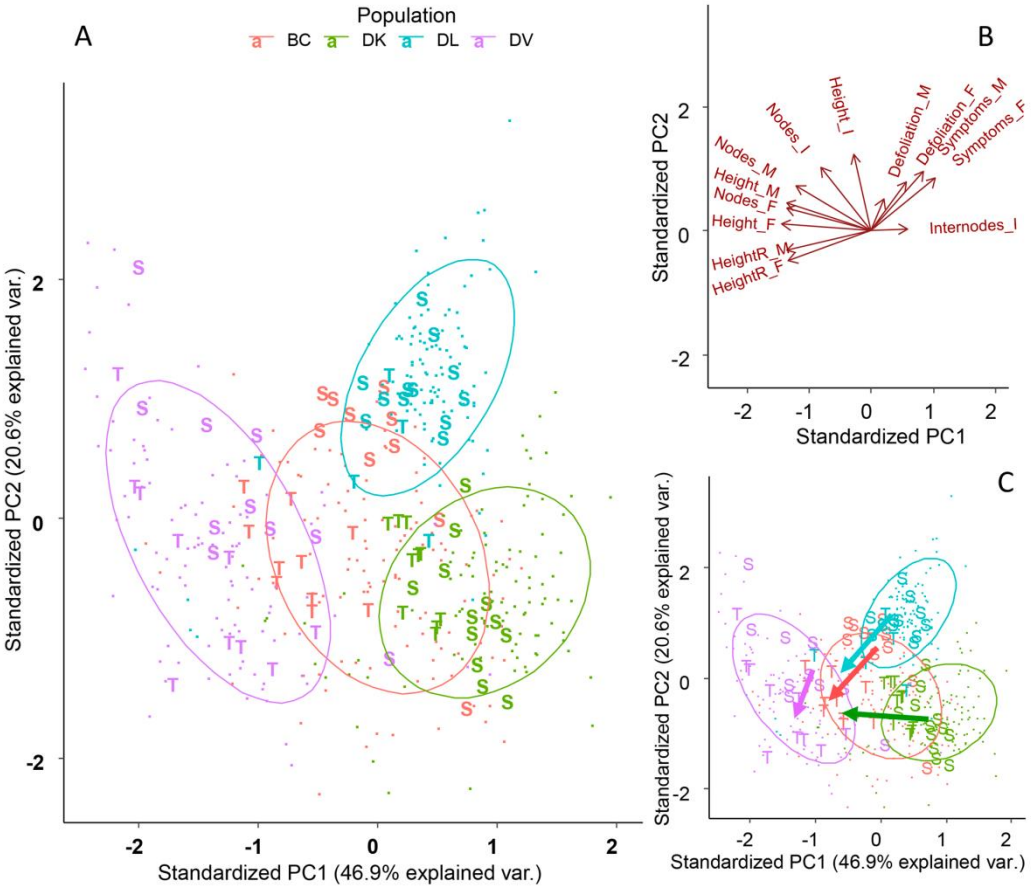

Figure 28. Plot of the first 2 components from Principal Component (PC) Analysis of the morphological variables after removal of highly collinear variables (A). Plants selected as Tolerant and Sensitive according its phenotype have been represented. Projection of the variables on the first 2 components (B). Dimensional division between tolerant and sensitive subsets for each population (C).

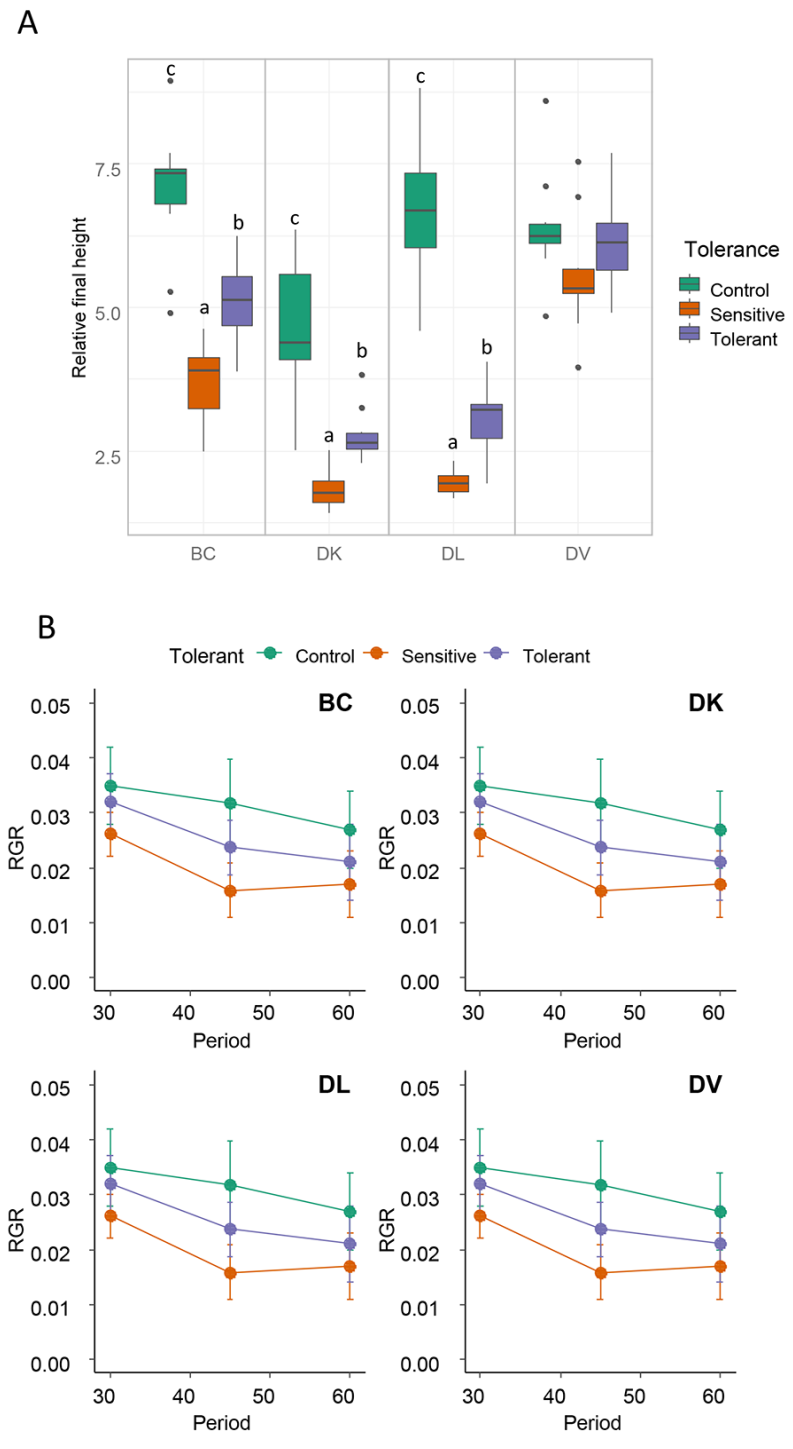

Figure 29.A) Box and whisker representation of relative final height (ratio between final and initial) of the four populations after 60 days of salt treatment. Individuals from each population were grouped into tolerant and sensitive according to its phenotype. Control plants were included. Different letters mean statistical differences between populations. B) Representation of the Relative Growth Ratio (RGR) for the subsets of the four populations in the periods of 0-30, 30-45 and 45-60 days.

Physiological and nutritional effects related to salinity tolerance

In order to elucidate the salinity tolerance mechanisms within each species and population, once the populations were divided into subsets of tolerant and sensitive plants to saline stress, we analyzed plant water status, leaf gas exchange and nutritional parameters for each subset after 60 days of saline stress.

Stem water potential was measured to determine differences in plant water status between the different populations. Sensitive plants showed significant better plant water status (higher values of stem water potential) than the tolerant in both DK and DL populations (Figure 30). In addition, in these populations, the values of stem water potential from the tolerant subset and the control were statistically identical. Respect to the leaf gas exchange parameters, all tolerant populations maintained similar values of A_{CO2} and g_s than control plants, whereas in sensitive subsets from DK and DL were significantly decreased (Figure 31). The C_i was significantly higher in both sensitive and tolerant DK and DL populations than in control plants (Figure 31). In the case of BC populations, C_i were significantly lower in tolerant than in sensitive plants, whereas C_i remained unaltered in DV plants. On the other hand, the DK and DL populations showed lower WUE in both tolerant and sensitive plants than in the control (Figure 31). The BC population had higher WUE in tolerant plants than in sensitive. No differences were observed between any population subset of DV.

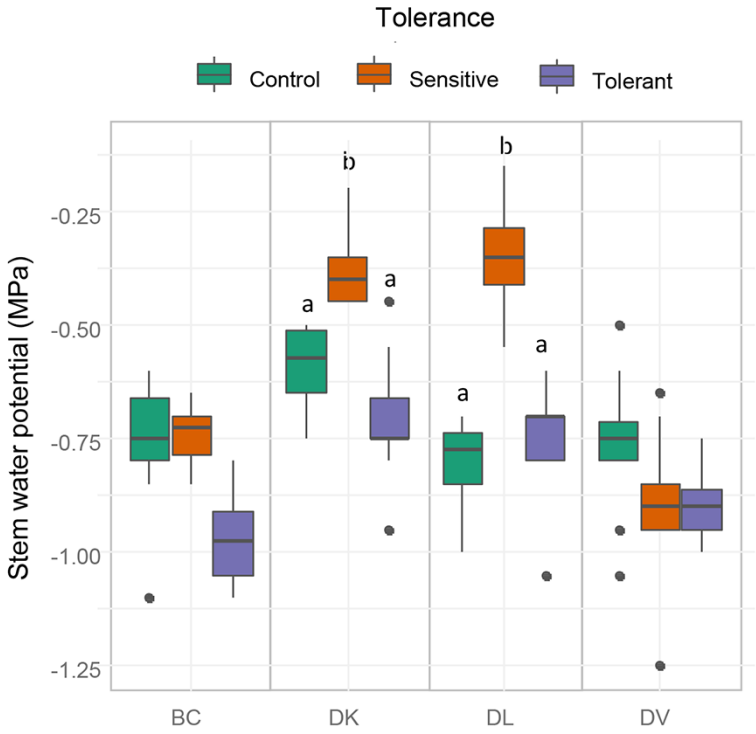

Figure 30. Box and whisker representation of stem water potential of the four populations after 60 days of salt treatment. Genotypes were grouped into tolerant and sensitive according to its phenotype. Control plants were included. Different letters mean statistical differences between populations.

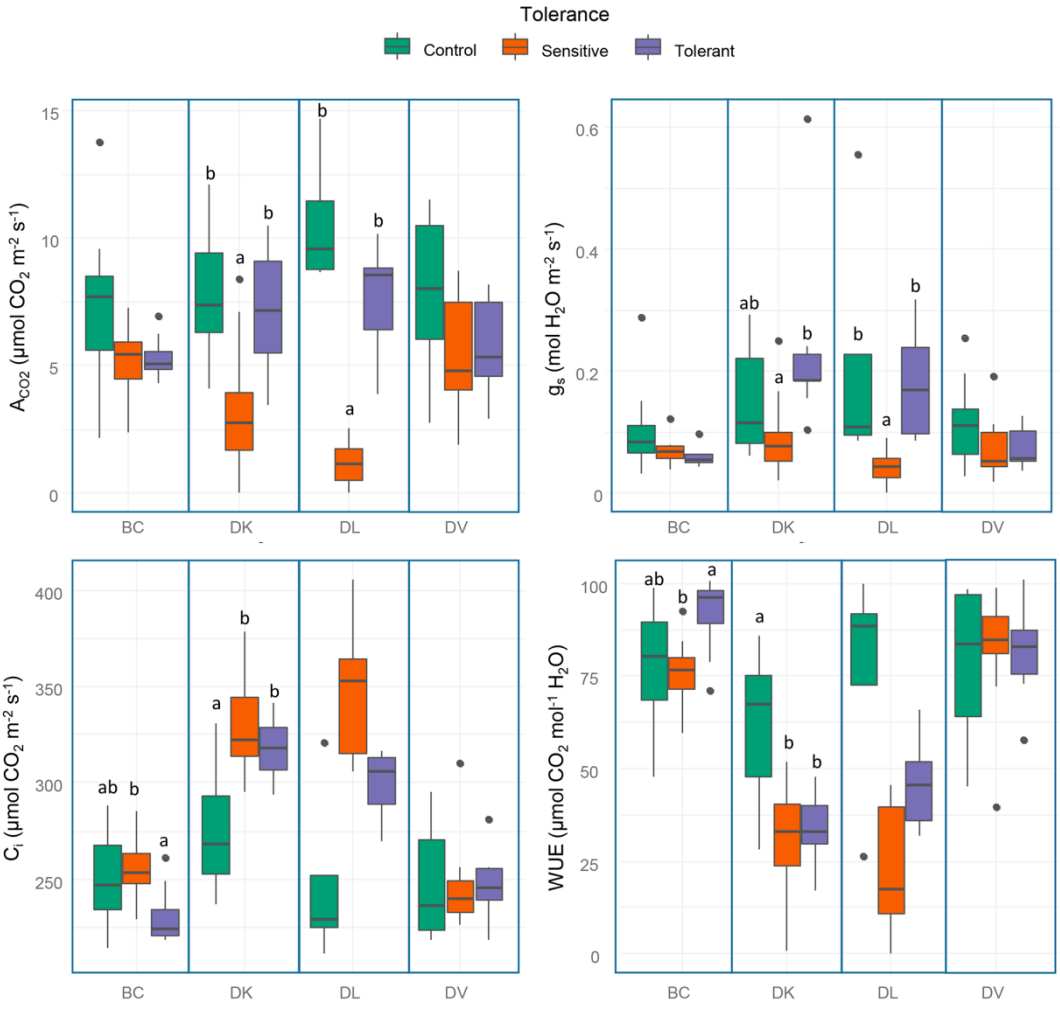

Figure 31. Box and whisker representation of leaf net CO_2 assimilation rate (A_{CO2}), stomatal conductance (g_s), internal CO_2 concentration (C_i) and intrinsic water use efficiency (WUE) of the four populations after 60 days of salt treatment. Genotypes were grouped into tolerant and sensitive according to its phenotype. Control plants were included. Different letters mean statistical differences between populations.

Leaf ions content were analyzed to quantify toxic ion accumulation (Cl^- and Na^+) and nutritional imbalances (K^+ and Ca^{2+}) caused by saline stress. Leaf Cl^- accumulation significantly increased in both sensitive and tolerant populations (Figure 32), but in DL populations sensitive plants had higher leaf Cl^- content than tolerant plants (Table 2). Regarding to leaf Na^+ accumulation, on DV and BC populations, Na^+ foliar content was higher on sensitive than tolerant subsets (Table 9; Figure 32), whereas on DK and DL populations no differences were observed between tolerant and sensitive subsets. Comparing leaf Na^+ accumulation between populations, DV showed the lowest values. Control plants had lower Na^+ content in all populations (Figure 32).

Table 9. Relative ionic content of each tolerant and sensitive populations compared to control. 'Tol' and 'Sens' mean Tolerant and Sensitive subsets. The representation of the subset vs control levels are as follows: '+' more concentration '=', similar concentration and '-' less concentration. Different number of signs between tolerant and sensitive refer to statistically different concentrations between tolerant and sensitive (Kruskal-Wallis test).

	BC		***D. kaki***		***D. lotus***		***D. virginiana***	
	Tol	Sens	Tol	Sens	Tol	Sens	Tol	Sens
Cl^-	+	+	+	+	+	++	+	+
Na^+	+	++	+	+	+	+	+	++
K^+	++	+	+	+	=	=	=	=
Ca^{2+}	-	-	-	=	=	-	=	-

Analyzing the nutritional imbalances caused by salinity, the K^+ content in the BC population was higher in tolerant plants than sensitive ones, being both significantly higher than the control plants. However, in the DK a lower K^+ is observed in the control plants compared to the sensitive and tolerant subsets. No significant differences are observed in DL and DV populations (Table 9).

Regarding to Ca^{2+} content, it was lower in tolerant plants than in control, but without differences with the sensitive subset. Nutrient balances were also calculated for Na^+/K^+, Na^+/Ca^{2+}. The Na^+/K^+ balance increased in all salinized plants, but differences between tolerant and sensitive plants were only observed in the BC population (Figure 33). In all populations the control plants had the lowest Na^+/K^+ ratio. Similar results were obtained for Na^+/Ca^{2+}, except that in DV population: significant differences were observed among all subsets.

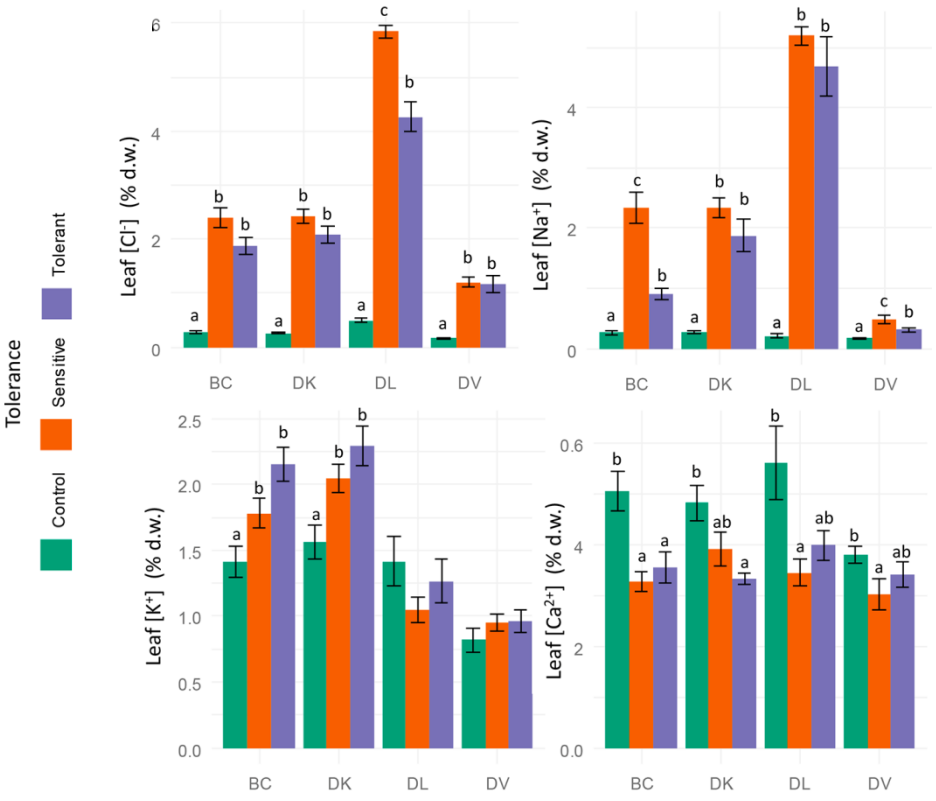

Figure 32. Leaf ion content measurements after 60 days of salinity treatment. Genotypes were grouped into tolerant and sensitive according to its phenotype.

Control plants were included. Different letters mean statistical differences between populations.

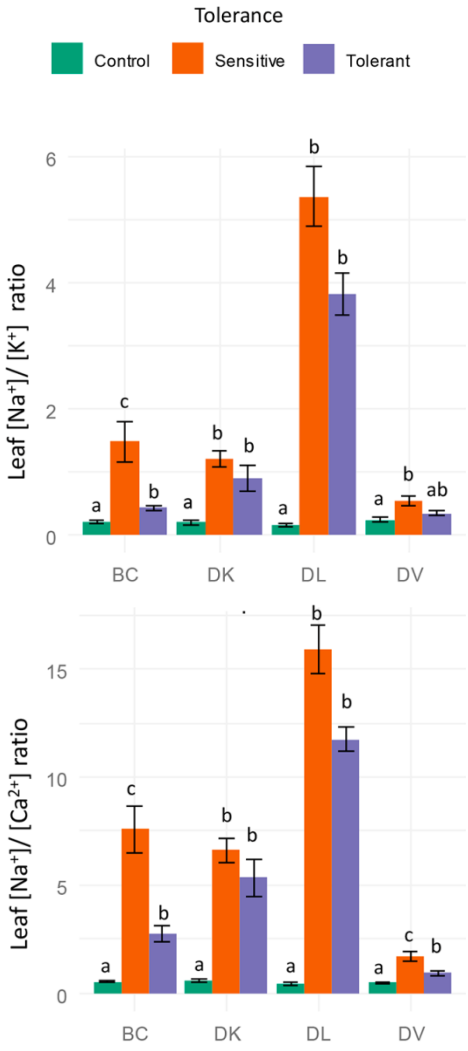

Figure 33. Leaf Na^+/K^+ and Na^+/Ca^{2+} ratios Genotypes were grouped into tolerant and sensitive according to its phenotype. Control plants were included Different letters mean statistical differences between populations.

Differential expression of genes related to salinity tolerance

Differential expression of genes related to salt-tolerance was analyzed in leaves and roots of 5 individuals of each subset at the end of the salt treatment (60 days). Control plants were included in the analysis (Supplementary Figure 3). Leaf expression of *SOS1-like*,

SOS2-like and ALMT9-like was similar among all the populations and different in root tissue. *HKT1-like* expression on leaf was undetectable in all populations, but detectable in roots, being the lowest expression in DL. On the other hand, *NHX1.1-like* highest expression in leaf corresponded to DV population and in roots to BC. In order to compare between tolerant and sensitive subsets, all gene expression was relative to the control plants of each population and a heatmap was constructed using the Log2fold change (Figure 34). On leaves, SOS3-like expression was downregulated on both subsets of DK population under salt treatment, whereas an upregulation was observed in the DL population. Interestingly, an upregulation was observed only in the sensitive subset of the BC population on 4/5 plants. Regarding to roots, *SOS2-like* expression was downregulated under salt treatment on the BC population, whereas *SOS3-like* was upregulated. *ALMT9-like* gene expression was upregulated on sensitive BC subset. About *HKT1-like* gene expression, a downregulation has observed in sensitive subset of BC and DL populations, whereas in tolerant DL subset and DV population a higher expression has been observed.

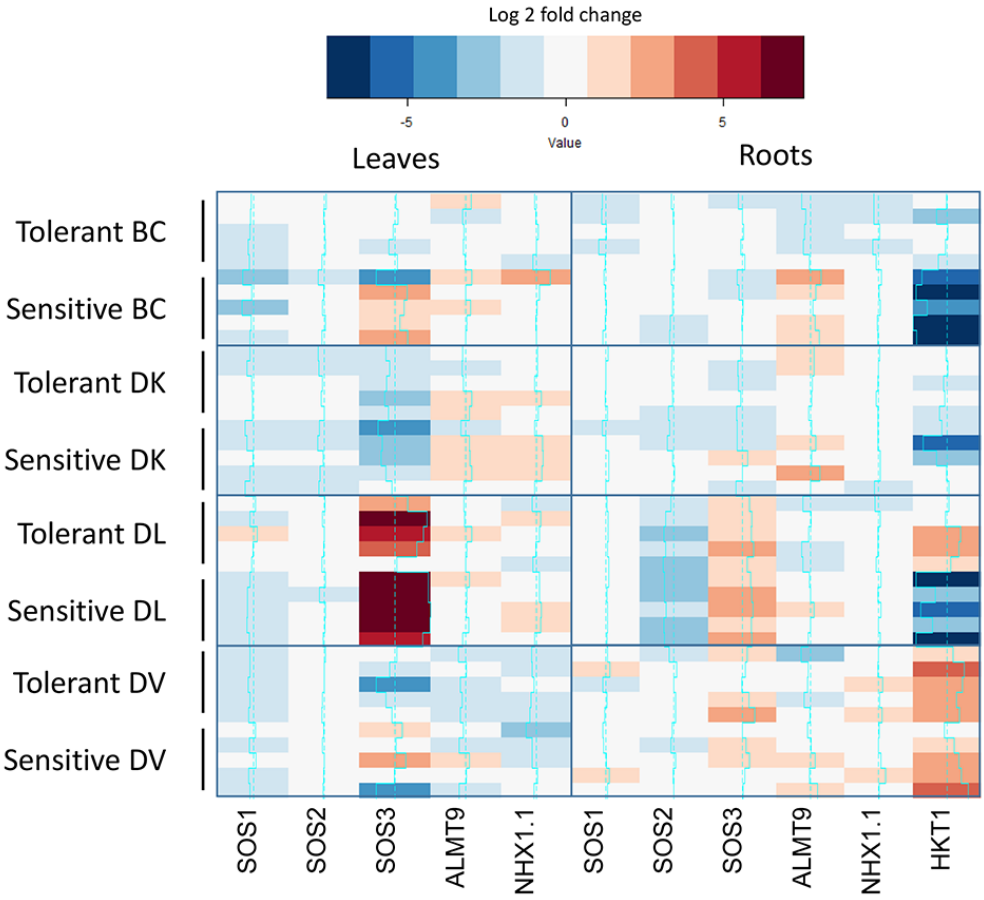

Figure 34. Expression analysis of salt tolerance related-like genes from control and treated subsets of tolerant and sensitive plants from each population. Only significant differences between control and treated subsets are colored.

After obtaining the sequences of the putative orthologues of *PIPs* in *Diospyros lotus*, a phylogenetic tree was constructed (Supplementary Figure 4). *PIP1-like* family of *D. lotus* was grouped together with the *PIP1 Arabidopsis thaliana* genes, whereas *D. lotus PIP2-like* genes were grouped with the *A. thaliana PIP2* genes. Expression of *PIP1-like* and *PIP2-like* aquaporin families were analyzed and compared between tolerant and sensitive subset bulks for each population. A heat map was constructed using the control bulk for normalizing within populations (Figure 35). On the BC population, *PIP2-like 5* showed a 4-fold upregulation on leaves from sensitive plants compared to tolerant, Furthermore, *PIP2-like 6* and *PIP1-like 1* showed a downregulation in sensitive plants compared to tolerant in leaves and roots, respectively. For these genes, the tolerant plants had similar levels of expression to the control plants. Regarding to the DK population; comparing sensitive to tolerant leaves, *PIP1-like 1* and *PIP2-like 5* showed a downregulation, whereas *PIP2-like 3* showed an upregulation. In roots, a strong (32 fold) downregulation was shown in *PIP2-like 6*. Both *PIP1-like 3* and *PIP2-like 3* presented a downregulation in sensitive plants. The DL population showed similar expression differences in roots between tolerant and sensitive to the DK population. In addition, *PIP2-like 5* showed less expression in sensitive roots. In leaves of DV population, the only differential *PIP-like* expression between tolerant and sensitive plants was in *PIP2-like 1*, where the sensitive plants showed a strong upregulation.

On roots, *PIP1-like 1*, *PIP2-like 3* and *PIP2-like 5* exhibited lower expression in tolerant plants. Regarding to the salt induction of this genes, *PIP1-like 1* has shown opposite expression patterns in the BC and DK population than the DL and DV populations.

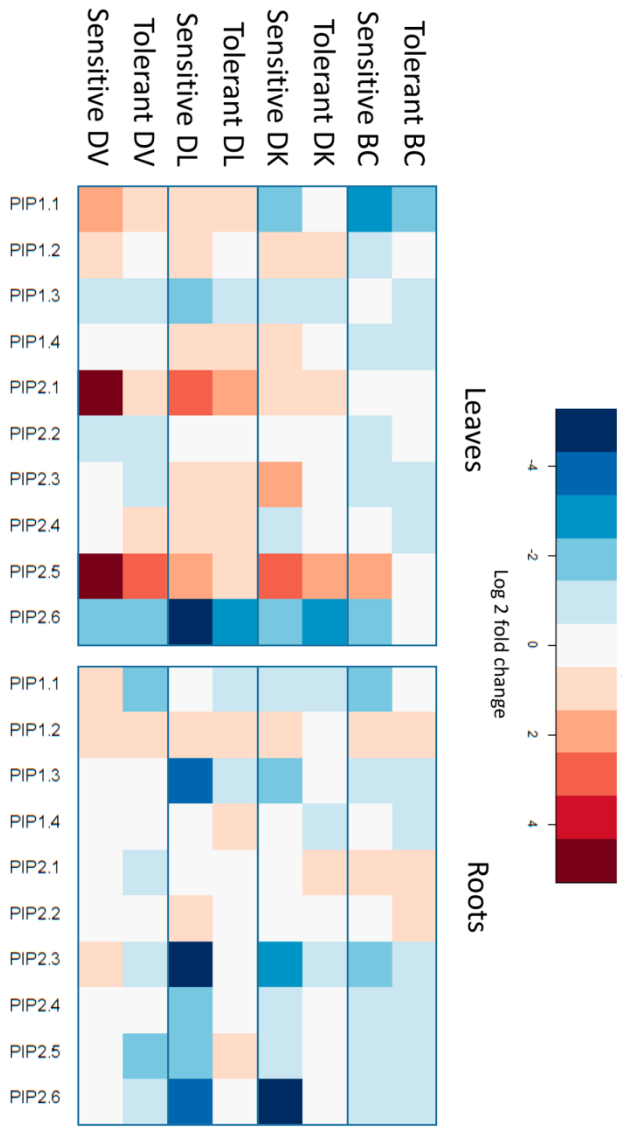

Figure 35. PIP aquaporin-like genes expression changes between control and treated subsets of tolerant and sensitive plants from each population. Only significant differences between control and treated subsets are colored

Discussion

Saline stress effect among populations

The severity of the symptoms in the different populations is coherent with the described differences between these species regarding to salinity tolerance, being *D. virginiana* the most tolerant specie among populations followed by *D. kaki* and *D. lotus* (De Paz et al., 2016; Visconti et al., 2017; Gil-Muñoz et al., 2018a). All the populations exhibited a reduction in the internode length compared to the control. This effect is believed to be caused by the salinity stress response mechanism mediated by DELLA proteins (Achard et al., 2006) as adaption to both saline and osmotic stress via ROS detoxification (Achard et al., 2008). The side effect of DELLA expression would be a reduction in bioactive GAs (Achard et al., 2006; Magome et al., 2008) causing a reduction in the internode length.

Saline stress tolerance variability within populations

Differences related to the variability of morphological parameters among the four populations studied were obtained. Furthermore, the Principal Component Analysis (PCA), showed the widest distribution in the DV population, whereas the narrowest corresponded to the DL population. Differences in variability can be explained by the genetic structure of each population; DV population comes from an open pollination family, whereas DL is formed by full siblings. Interestingly, DK population is an open pollination family, but shows narrower variability than DV population. This fact can be explained by the low genetic variability previously described for *D. kaki* (Naval et al., 2010;

Parfitt et al., 2015; Gil-Muñoz et al., 2018b). BC population shows an intermediate variability between DV and DK as expected because it combines both genetic backgrounds.

The variability observed in the analyzed parameters is consistent with the population genetic structures. This fact can indicate that a significant percentage of the observed variability might be controlled by genetic traits. The PCA analysis has been also consistent with the genetic structure of the populations, and it can be a useful tool to aid selection during a plant breeding program, as it extracts, compresses, simplifies and analyzes complex multidimensional datasets (Das et al., 2017). Furthermore, with large datasets, some collinearity is expected to be present among the measured variables. Thus, measurement errors and phenotyping noise can be reduced by PCA projection, providing more precise individual phenotyping. Furthermore, the PCA can provide the importance of easy-measurable variables to the overall desired trait, giving a powerful aid in the selection.

Physiological and nutritional effects related to salinity tolerance

Differences in vegetative development between tolerant and sensitive subsets in both DL and DK populations can be explained by the effect of a poor adaption to the osmotic stress, as shown by changes in plant water status and the lower photosynthesis rate. However, which one is the cause and which one the effect is not yet known (Munns and Tester, 2008). Nevertheless, ABA contributes to stress tolerance by regulating water balance and stomatal closure (Lim et al., 2015a). However, our results show higher stomatal

closure in sensitive than in tolerant plants, indicating that the sensitive populations have suffered higher saline stress. On the other hand, differences in photosynthesis, stomatal aperture or water relations between tolerant and control plants are not observed, indicating that the tolerant subsets had a better response to the osmotic stress than the sensitive subsets in both populations. Furthermore, differences were neither observed between tolerant and control final internode relative length, discarding DELLA response as a mechanism effect. All facts indicate that the observed differences in growth rate and relative final height between tolerant and control plants must be mainly related to ionic stress, which affects growth in a different way than osmotic stress (Munns and Tester, 2008). Respect to the BC population, no differences in parameters as relative growth and growth rate, photosynthesis, stomatal aperture or water relations were obtained in the analyzed subsets. This may indicate that both tolerant and sensitive plants are not strongly affected by the osmotic stress but rather the ionic stress and differences between these groups might be related to ion exclusion. The DV population has proven to be highly tolerant to saline stress as previously described (De Paz et al., 2016; Gil-Muñoz et al., 2018a). The similar growth rates and relative final weight among the subsets while maintaining photosynthesis, stomatal aperture and plant water status indicate the presence of highly efficient mechanisms to overcome osmotic and saline stress.

As foliar contents of Na^+ and Cl^- have been analyzed, other mechanisms such as vacuolar sequestration have not been detected

that could further explain the differences observed. Our aim has been to study intake and root to shoot exclusion mechanisms taking into account the background objective of breeding rootstock plant, as different scions might have different responses mechanisms of vacuolar ion sequestration. Variability in osmotic stress tolerance is present within DK, DL and BC populations and in Cl^- uptake within DL population. The differences for Na^+ exclusion observed within BC population but not in DV and DK populations indicate that DV and DK populations have different Na^+ exclusion mechanisms, being the DV mechanism more efficient. Further crosses between DL and DV might reveal variability in Cl^- exclusion mechanisms that might help to untangle the salt tolerance mechanisms present in *Diospyros* genus.

Differential expression of genes related to salinity tolerance

Regarding to salt tolerance-related genes expression, a strong upregulation of *SOS3-like* gene has been observed in the DL population on both tolerant and sensitive plants. This gene is responsible for activating the SOS salinity response mechanism when a low Ca^{2+} concentration is detected in the cell (Gong et al., 2004). Interestingly, DL population showed similar Na^+ accumulation on leaves from control plants than leaves from the end of the salinity experiment. This population presented the highest Na^+ concentration in leaves and both the highest Na^+/K^+ and Na^+/Ca^{2+}. Furthermore, the higher *SOS3-like* expression present in the sensitive plants leaves of the BC population, but not in the DK in despite of similar Na^+, Ca^{2+} and Na^+/Ca^{2+} levels are observed in the DK population and BC sensitive plants. Surprisingly, differences in *SOS3-like* response are

present even though 75% of the BC population genome comes from DK population. *SOS3-like* expression level is upregulated on plants where seems to be a response caused by the toxic Na^+ concentrations in leaves and not as a direct indicator of salinity tolerance, although DK population may have a deficient SOS response compared to the other populations. BC population might have inherited the more sensitive SOS response mechanism present on DV population, whose response has not been observed due to the low levels of Na^+ in leaves. On the other hand, *HKT1-like* gene expression differences on roots observed between tolerant and sensitive subsets in BC population can be linked to the variability for Na^+ accumulation, as *HKT1* gene is responsible to avoid Na^+ translocation from roots to shoot via xylem transport (Hanin et al., 2016). A difference in the DL population for Na^+ accumulation might not have been observed in despite of differences in *HKT1-like* root expression between tolerant and sensitive because the higher transpiration rate that would increase the water flow and solute passive intake into the plants. PIP gene expression has been linked to an increase in osmotic stress tolerance (Katsuhara et al., 2014; Afzal et al., 2016; Alavilli et al., 2016). In our study, a downregulation in several PIPs has been observed in roots of sensitive subsets of both DL and DK populations where lower stem water potential values were measured. This may indicate the activation of passive mechanisms for avoiding saline-water intrusion into the plant at the cost of hydric stress. Furthermore, a strong upregulation was observed in some *PIP2-like* family members on leaves of the sensitive DV subset, that may act as

a Na^+ gate to the leaves similarly to the Na^+ influx effect associated to AtPIP2.1 (Chaumont and Tyerman, 2014).

To sum up, in DK population, we have not observed variability in active Na^+ or Cl^- exclusion mechanisms, but they are present for osmotic stress tolerance via water balance regulation. Regarding to the DL population, the lowest basal expressions of *SOS1-like* gene and *HKT1-like* in roots compared to the other populations might explain its poor ability to exclude Na^+ ions and prevent toxic concentrations. However, variability in both osmotic stress tolerance via water balance regulation is present. Cl^- exclusion variability in this population has been observed, but the mechanism is yet unknown. The DV population tolerance to salinity can also be related to the higher *SOS1-like* basal expression that might contribute to Na^+ extrusion to the soil and *HKT1-like* upregulation in roots that would prevent Na^+ translocation to the shoots when exposed to saline stress (Hanin et al., 2016). In addition, variability in the indicators used in this work to identify mechanisms related to salt stress tolerance are not observed within this population.

Conclusions

Among the different populations studied, different mechanism of tolerance could be hypothesized, providing different strategies for breeding for salinity tolerance.

BC tolerant population: The mechanism of tolerance to osmotic stress found was based in the water use efficiency (WUE). BC tolerant population has shown to have better tolerance to saline stress than sensitive BC through a higher WUE, which agrees with previous results on *Diospyrus* genus (Gil-Muñoz et al., 2020). Since the lack of variability for this character in the DV and DK populations, we can conclude the variability into BC has been generated through crossing. We have generated a tolerant population by back crossing in which the water use efficiency is higher than in DV population, which might be a sign of transgressive segregation through expressing the DV higher tolerance under the DK genetic background. Concerning to ionic stress, the Na^+ accumulation was higher in the BC than in the DV population, indicating other factors involved in Na^+ absorption. The transcriptomic study resulted in a high expression of HKT1-like in roots of DV population; this gene is being involved in Na^+ exclusion, which might be a mechanism of preventing Na^+ translocation to the higher parts of the plant in *D. virginiana* species.

DK population: Little variability was found within the DK population regarding to salinity tolerance, neither by ion leaf content nor salt tolerance gene expression. In this case, the observed differences between tolerant and sensitive subsets might be explained by

differences in osmotic stress tolerance, but not in ionic stress. In this population, the tolerance might be based only in plant water regulation via stomatal aperture and water flow as indicated by differential expression in *PIP-like* genes.

DL population: Similarly, to the DK population, the tolerance observed in DL population for Na^+ might be based in passive mechanisms through water regulation. In despite of DL population was the most susceptible to salinity, is the only population that has shown differences in Cl^- accumulation. However, with the analyzed data we cannot provide a hypothesis that can explain this fact, as water flow differences were similar than the observed in DK population and this differences in Cl^- accumulation were not detected. Also, the transcriptomic approach revealed high expression of *HKT1-like* in roots of the tolerant subset despite of it cannot be linked to lower Na^+ leaf content.

DV population: In this population, variability for saline tolerance was low, most of the plants showed high saline tolerance. Significant Na^+ accumulation might be explained by higher *PIP2-like* family (*PIP2-like 1* and *PIP2-like 5* isoforms) expression in leaves, acting as a gate of Na^+ influx into the leaves.

As a result of the comparison between physiological parameters, transcriptomic analysis and phenotypes under saline conditions, we can conclude that interspecific crosses of *D. virginiana* can be an option for breeding persimmon rootstocks tolerant to salinity. Crosses with *D. kaki* can provide better rootstock-scion compatibility

with varieties than genotypes from *D. virginiana*. However, selection of agronomic traits that improve crop management would be most necessary.

Supplementary material

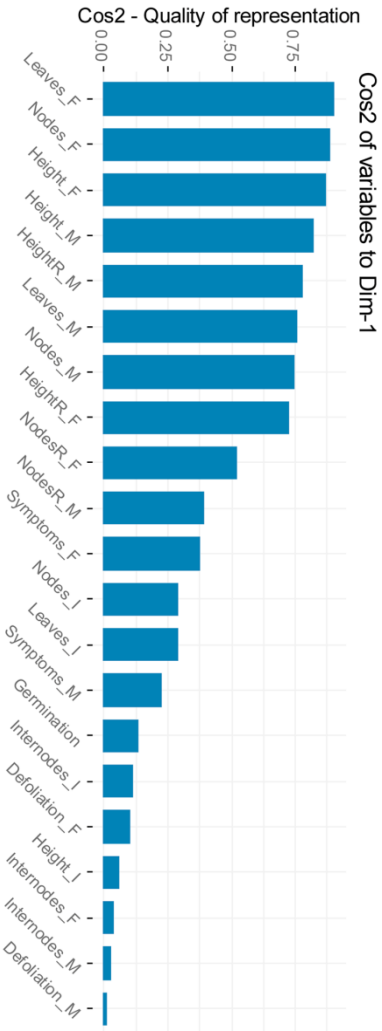

Supplementary Figure 1. Contribution of the variables to the first dimension of the Principal Component Analysis.

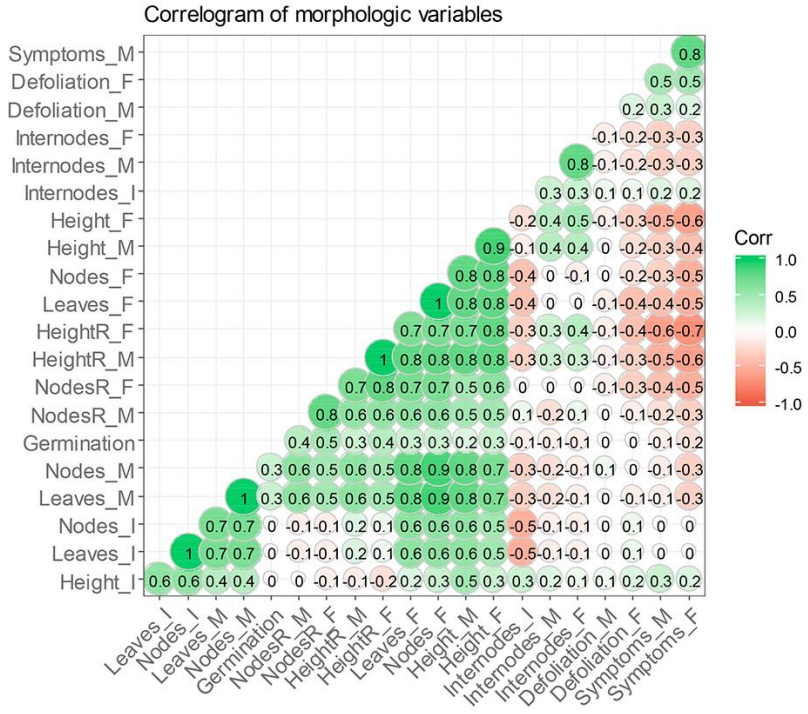

Supplementary Figure 2. Correllogram of the morphological variables measured during the saline stress treatment.

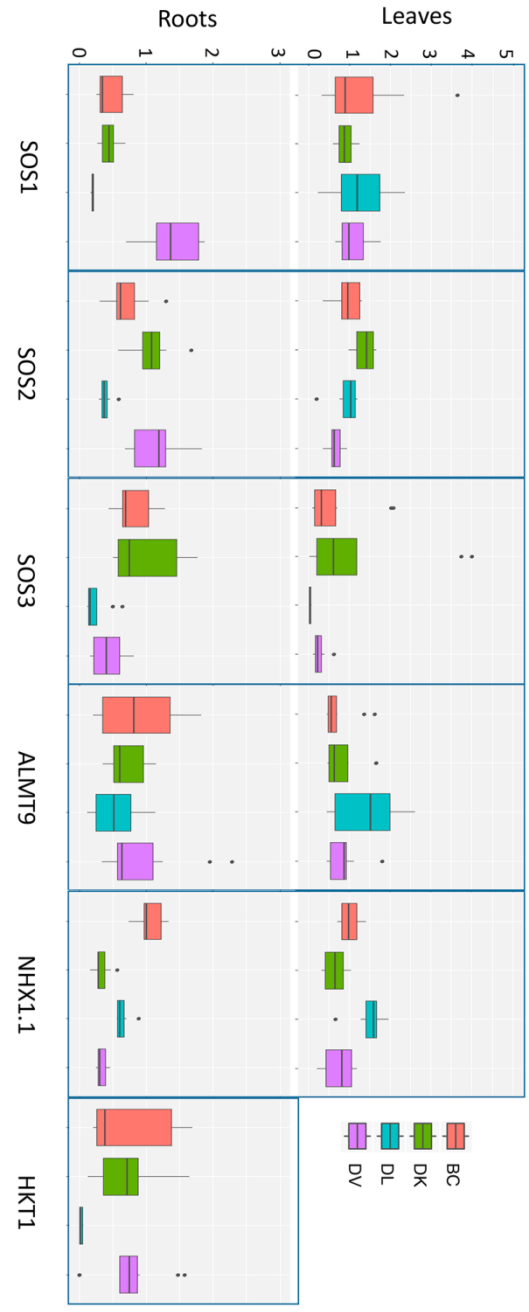

Supplementary Figure 3. Box and whisker representation of the expression levels of salt-tolerance-related genes in leaves and roots.

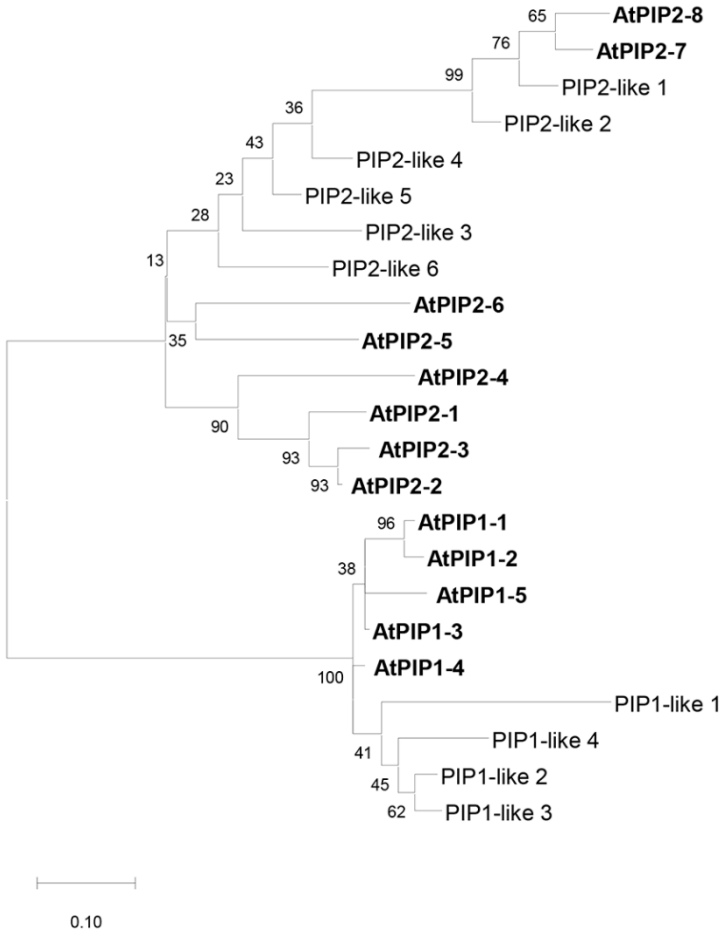

Supplementary Figure 4. Neighbor-Joining tree with 1000 bootstraps showing the relationship between the sequences of PIP-like putative proteins from *D. lotus* and PIP proteins from *A. thaliana*

Transcriptomic analysis reveals salt tolerance mechanisms present in date-plum persimmon rootstock (*Diospyros lotus*)

Abstract

Agriculture is in dire need for effective solutions to adapt to the increasing salinity in soils and water reservoirs. The increase in salinity is already affecting crop production due to osmotic and ionic stresses. Research on the physiological and molecular responses activated by salinity is needed to elucidate the mechanism of tolerance to salinity. Such knowledge is essential to design solutions to be implemented into operational agriculture. Transcriptome profiling (RNA-Seq) has been proven a powerful tool to study physiological changes at the molecular level, and it has already been applied to study the transcriptomic profile of genotypes under varied stress conditions. In temperate fruit tree species, tree grafting on salinity tolerant rootstocks is a common method to compensate for the cultivar saline sensitivity. Persimmon species have different levels of tolerance to salinity, making them an appropriate model to study the mechanism of salinity tolerance, and to provide knowledge on persimmon species´ potential as salt tolerant rootstock. In this study, we conducted a physiological and transcriptomic profiling of roots and leaves in a persimmon species commonly used as rootstock, *Diospyros lotus*, grown under saline and control condition. Characterization of the physiological responses associated to saline-stress tolerance along with the genes expression changes in roots and leaves allowed

identifying several salt-tolerance mechanisms: Ion transport, photosynthesis and respiration systems, ROS signaling, and thermospermine synthesis. Differences were clearly observed in putative genes related to both Ca^{2+} and K^{+} transport. Chloride channel protein-like genes were upregulated in leaves and roots of sensitive plants and correlated with chlorine leaf accumulation. With regard to photosynthesis and respiration genes, all differentially expressed genes in leaves were upregulated in the tolerant plants compared to the sensitive ones, where a reduced metabolism supported by lowered photosynthesis and respiration genes expression as well as a significant reduction in carbon fixation was detected. The data suggest that ROS detoxification was, also, upregulated in both control and tolerant leaves resulting in higher ROS content in the leaves of sensitive plants, probably as a part of a signalling mechanism that indicates high level of stress. Furthermore, an overexpression of thermospermine synthase was found in the roots of tolerant plants, which may be an indication that alterations in root architecture could act as an additional mechanism of response to salt stress. This work has contributed with novel knowledge on the main molecular networks involved in tolerance to salinity and unrevealed genes acting in the mechanism. We have also provided a framework for designing strategies for dealing with salinity stress in other tree species.

Introduction

Drought and salinity are two of the main challenges in agriculture. Reduction of water availability and increase of salinity in soils and water reservoirs can limit crop production due to severe inhibition of plant growth and development via osmotic and ionic stresses (Flowers and Colmer, 2008; Munns and Tester, 2008). The negative effect of salinity in photosynthesis is caused either by a reduction in available water, by the toxic accumulation of ions in the cell, or both. Furthermore an attenuated photosynthesis leads to an increase in Reactive Oxygen Species (ROS) and a consequent oxidative damage of the cells (Bose et al., 2014). The cultivated surface affected by either stresses increases year after year as a consequence of more frequent drought episodes associated to climate change. Among the affected areas, the Mediterranean basin registered a significant increase in salinity in soils and water reservoirs in the last 10 years (Libutti et al., 2018). Therefore, there is a pressing need to find solutions to alleviate the negative impact on plant production in an area dominated by fruit tree crops. Controlled crosses and selection (plant breeding) has proven an efficient method to develop new cultivars with improved characteristics such as salinity tolerance in several species (Ashrai and McNelly, 1990; Saranga et al., 1992; Cuartero et al., 2006; Forner-Giner and Ancillo, 2013). In the case of temperate fruit trees, salinity stress can also be overcome by means of tree grafting on tolerant rootstocks (Shahid et al., 2019). This method provides a solution for dealing with the two components of salinity stress: the osmotic effect, or water balance loss, through decreasing the area of stomatal aperture via phytohormonal root

signalling (Daszkowska-Golec and Szarejko, 2013; Lim et al., 2015b) and ionic toxicity, by maintaining the ion homeostasis in the cell of the aerial parts (Tester and Davenport, 2003). Furthermore, grafting of existing varieties on rootstocks contributes to avoid losing the current genetic diversity.

Previous studies have contributed knowledge about the molecular mechanisms that regulate plant´s physiological responses to salinity in both model and economically important crops (Gong et al., 2002; Martínez-Atienza et al., 2007; Hsu et al., 2009). Those mechanisms involve changes in gene expression associated to several biological processes such as ionic transport and exchange mechanisms (Volkov, 2015), photosynthesis (Yang et al., 2020), flavonoid biosynthesis (Chen et al., 2019), ROS scavenging and detoxification (Nguyen et al., 2017), ethylene production (Tao et al., 2015), signalling networks related to ABA (Abscisic Acid) (Suzuki et al., 2016) and protein refolding (Yu et al., 2018). Expression of different functional genes related to osmoregulation and cell protection as dehydrins and aquaporins are involved as well in salinity response (Hanin et al., 2011; Kapilan et al., 2018; Yu et al., 2018).

One of the most prompt physiological response following exposure to saline environments is the differential regulation of growth water balance and uptake, and the activation of different cascades of molecular networks that result in the expression changes of specific stress-related genes, and their encoded metabolites (Boudsocq and Laurière, 2005; Isah, 2019). Studies focused on model plants revealed the involvement of several transduction pathways in salt stress

response, including SOS (Saline Overly Sensitive) (Quan et al., 2007), ABA (Lim et al., 2015b) and ethylene signalling pathways (Luo et al., 2017). Additional cell wall changes result in differential growth responses required to adapt to saline environments (Shafi and Zahoor, 2019). Significant amount of data concerns the role of plant mitogen-activated protein kinases (MAPKs) in osmoregulation. MAPK cascades are now recognized as major signal transduction mechanisms to regulate gene expression, multiple cell activities and protein functions in various developmental and adaptive processes (Moustafa et al., 2014), including salt stress (Sinha et al., 2011). Ion toxicity caused by Na^+ and Cl^- accumulation also affects plant photosynthesis, which can lead to leaf and stem necrosis. Mechanisms to limit Na^+ uptake and translocation are therefore linked to salinity tolerance. Several genes have been identified in *Arabidopsis*, such as the Na^+/H^+ antiporter responsible for the exclusion of sodium from the cytosol (Shi et al., 2000) in the SOS response pathway. In Arabidopsis thaliana, the serine/threonine type protein kinase SOS2 (CBL-interacting serine/threonine-protein kinase 24) interacts with the calcium sensor SOS3 (Calcineurin B-like protein 4) to regulate the Na^+/H^+ antiporter SOS1, thereby conferring salt tolerance (Liu, 2000; Mahajan et al., 2008). Na^+/K^+ homeostasis in poplar is regulated by CIPK (CBL-interacting serine/threonine-protein kinase) genes which interact with CBL1 (Calcineurin B-like protein 1) (Zhang et al., 2013). The CIPK genes from wild barley and maize are also known to be implicated in salt tolerance responses (Li et al., 2012; Chen et al., 2014). Furthermore, in tolerant persimmon species such as *Diospyros virginiana*, salt stress tolerance is believed to be

caused by a high affinity potassium transporter HKT-1-like gene in roots (Gil-Muñoz et al., 2020), which was previously described in other species as key factor in salinity tolerance (Garciadeblás et al., 2003; Huang et al., 2006; Horie et al., 2007; Almeida et al., 2013). Although Na^+ ion translocation and regulation mechanisms have previously been reported in several species, little is known about Cl^- transport and regulation. It has been suggested that Cl^- uptake occurs mainly through passive water intake (Munns and Tester, 2008), although chloride channels are also suggested to be able to sequestrate Cl^- ions (Isayenkov and Maathuis, 2019). Chloride accumulation effect is also especially important in persimmon where it causes a decrease in fruit quality and a shorter post-harvest life (Besada et al., 2016).

In this study, the main objective is aimed at unravelling the mechanism of salinity tolerance in persimmon rootstock. Persimmon species have different levels of tolerance to salinity, making them an appropriate model to study the mechanisms of salinity tolerance, and to provide knowledge on persimmon species´ potential as salt tolerant rootstock. Transcriptome profiling (RNA-Seq) using next-generation sequencing technologies has proven a powerful tool to detect changes in gene expression associated to physiological responses to salt stress (Formentin et al., 2018; Tian et al., 2018; Wang et al., 2018; Amirbakhtiar et al., 2019; Zeng et al., 2019). In this study, we conducted physiological and RNA-Seq analyses of roots and leaves in persimmon rootstocks (*Diospyros lotus*) grown under saline and control conditions.

Material and Methods

Plant material and RNA extraction

A full-sib progeny of *Diospyros lotus* (DL) obtained from a cross between two *D. lotus* trees at the Instituto Valenciano de Investigaciones Agrarias (IVIA) persimmon germplasm bank was used in this study. At the end of March, seeds were stratified for 30 days in plastic bags filled with perlite in a cold chamber at 4ºC. After stratification, seeds were transferred to peat-moss and perlite (4:1 ratio, respectively) and kept in a greenhouse at 18-24ºC during two months (from April, 24, to June, 26, 2017).

One hundred and fifty seedlings were transplanted into 1L pots containing coarse sand. The plants were distributed randomly in the greenhouse and watered with a nutrient solution (3% Cristaljisa 18-18-18, soluble fertilizer with micronutrients) until apical meristem growth was observed. The plants were acclimated before exposition to salinity treatment. After acclimation, plants were submitted to a salinity treatment during 60 days. The treatment consisted in 40 mM NaCl added to the nutrient solution. The control plants remained watered with the standard nutrient solution.

Three of the plants were kept in control treatment, and six treated plants (three tolerant, three sensitive) seedlings were selected based on salt tolerance according to the visual and agro-morphological data.

Plant phenotyping

The morphological parameters total height (cm), leaves (no.), nodes (no.), internodes (cm) and defoliation (1-no. leaves/no. nodes) were measured at days 0, 30, 45 and 60. Relative growth rate (RGR) was calculated as follows:

$$\text{RGR} = \frac{Ln(Height\ 2 - Height\ 1)}{t2 - t1}$$

Stem water potential (**(**ψ_H, MPa) was measured in fully expanded leaves using a Model 600 Schölander Pressure Chamber (PMS Instrument Company, Albany, OR, USA). Measured leaves were kept in reflective plastic bags for 30 minutes (Levin, 2019). Furthermore, leaf net CO_2 assimilation rate (A_{CO2}), stomatal conductance (g_s), leaf transpiration rate (E) and internal CO_2 concentration (C_i) were measured on three single leaves of each plant. Determinations Measurements were performed using uniform fully expanded leaves from the mid-stem zone. Intrinsic leaf water use efficiency (WUE) was calculated as A_{CO2} and g_s ratio. Photosynthetically active radiation (PAR) at the leaf surface was adjusted to a photon flux density of 1.000 µmol m^{-2} s^{-1}. A CIRAS-2 Portable Photosynthesis System (PP Systems, Amesbury, Massachusetts, USA) was used for the measurements. Leaf laminae were fully enclosed within a PLC 6 (U) universal leaf autocuvette in a closed-circuit model and kept at 25 ± 0.5 ºC, with a leaf-to-air vapor deficit of about 1.7 kPa. The air flow rate through the cuvette was 0.5–1.5 L min^{-1}. All measurements were carried out in a sunny day between 9:30 a.m. and 12:30 p.m. at the end of the salt treatment (day 60).

After saline treatment, three leaves from each plant were collected. Sample pre-treatments were performed as described in Gil-Muñoz et al. (2020). Na^+, Ca^{2+}, K^+, Mg^{2+}, P and S content was determined (mg g^{-1} dry w.t.) using a multiple-collector inductively coupled plasma mass spectrometry (MC-ICP MS, Thermo Finnigan Neptune). Chloride concentration (mg ml^{-1}) was quantified by silver ion-titration (Gilliam, 1971) with a Corning 926 automatic chloridometer (Corning Ltd. Halstead Essex, UK).

RNA extraction

After 60 days of salt treatment young fully expanded leaves and root tip tissue were collected and immediately frozen and powdered using liquid nitrogen. Control samples from all populations were also collected and processed. The samples of each of the three individuals were mixed. The three biological replicates were made resampling and mixing new tissue samples. RNA was isolated according to Gambino et al. (2008). DNA was removed with the RNase-Free DNase Set (Qiagen, Valencia, CA, USA), using the RNeasy Plant Mini Kit (Qiagen). Purified RNA (500 ng) was reverse transcribed with PrimeScript RT Reagent Kit (Takara Bio, Otsu, Japan) in a total volume of 10 µl.

RNA Sequencing

RNA samples were sequenced by Novogene ® using the following procedure: mRNA was enriched using oligo(dT) beads and fragmented randomly using a fragmentation buffer. cDNA was synthetized using random hexamers and reverse transcriptase. A

second strand was generated using nick-translation with RNAse H and Escherichia coli Polymerase I with Illumina second strand synthesis buffer and dNTPs .AMPure XP beads were used to purify the cDNA and the first strand was degraded with USER enzyme. Then, the resulting cDNA was purified, terminal repaired, A-tailed, ligated to the sequencing adapters, size-selected and enriched with PCR. The resulting library was sequence using Illumina.

Pre-processing of RNA-Seq data

The data pre-processing was performed as described here: http://www.epigenesys.eu/en/protocols/bio-informatics/1283-guidelines-for-rna-seq-data-analysis. Briefly, the quality of the raw sequence data was assessed using FastQC (http://www.bioinformatics.babraham.ac.uk/projects/fastqc/).

Residual ribosomal RNA (rRNA) contamination was assessed and filtered using SortMeRNA (v2.1; settings --log --paired_in --fastx--sam --num_alignments 1) (Kopylova et al., 2012) using the rRNA sequences provided with SortMeRNA. Data was subsequently trimmed for adapters and quality using Trimmomatic (v0.36; settings TruSeq3-PE-2.fa:2:30:10 LEADING:3 SLIDINGWINDOW:5:20 MINLEN:50) (Bolger et al., 2014). After both filtering steps, FastQC was run again to ensure that no technical artefacts were introduced.

Transcriptome de novo assembly and annotation

As there was no transcriptome assembly for any *Diospyros* species, a *de novo* transcriptome was built using the sequences from the RNA-Seq data. For transcriptome assembly, Trinity (v2.8.3.1) (Haas et al.,

2013) was used inside a Singularity (v2.5.2) (Kurtzer et al., 2017) container for ensuring reproducibility. Protein sequences were also putatively predicted. Assembled transcriptome was then annotated using Blast2GO (Conesa et al., 2005), Blast+ (v2.6.0; using blastp) (Camacho et al., 2009) against UniRef90 database (10th October 2018) (Suzek et al., 2015), HMMER (v3.1) (http://hmmer.org/), Trinotate (Bryant et al., 2017), PFAM (v3.1;) (El-Gebali et al., 2019) and signalP (Trinity package v.2.8.3.1) (Haas et al., 2013).

Differential expression analyses

Filtered reads were pseudo-aligned to the obtained transcriptome using kallisto (v0.44, non default settings: -b 100 --rf-stranded -t 8) (Bray et al., 2016). Statistical analysis of single-gene differential expression between conditions was performed in R (v3.6.0; R Core Team 2019) using the Bioconductor (v3.9) (Gentleman et al., 2004) DESeq2 package (v1.24.1) (Love et al., 2014). FDR adjusted p-values were used to assess significance; a common threshold of 1% was used throughout. For the data quality assessment (QA) and visualisation, the read counts were normalised using a variance stabilising transformation as implemented in DESeq2. The biological relevance of the data - e.g. biological replicates similarity - was assessed by Principal Component Analysis (PCA) and other visualisations (e.g. heatmaps), using custom R scripts

Results

Plant physiological responses associated to salt stress tolerance

Plants exposed to saline treatment showed significant reduction in growth, increased leaf damage and defoliation, and altered ion concentration. Among the treated plants, those physiological responses were especially pronounced in a subset of plants which we hereafter categorized as sensitive to salinity (Table 10). As compared to tolerant plants the sensitive ones showed a significantly higher Cl^- concentration. Interestingly, no significant differences were observed for Na^+ accumulation, neither were differences significant for Na^+/K^+ and Na^+/Ca^{2+} ratios. Moreover, P accumulation was more pronounced in tolerant plants. The overall reduction in carbon fixation capacity and water potential due to salinity were significantly more pronounced in the sensitive plants.

Table 10. Physiological responses under control and saline conditions. Asterisk (*) indicates significant differences between tolerant and sensitive groups (Kruskal-Wallis test, $p<0.05$).

	Non-saline	Saline	
	Control	**Sensitive**	**Tolerant**
Initial height (cm)	11.5 ± 1.4	14.9 ± 1.1	12.8 ± 1.4
Initial node number (nº)	4.7 ± 0.6	5.0 ± 0.0	5.0 ± 0.0
Initial internode length (cm)	2.5 ± 0.4	3.0 ± 0.2	2.6 ± 0.3
Final height (cm) *	76 ± 20	28 ± 4	39 ± 2
Final node number (nº) *	35 ± 6	19.0 ± 1.0	24 ± 3
Final internode length (cm)	2.2 ± 0.4	1.47 ± 0.18	1.62 ± 0.14
Defoliation (leaves/nodes) *	0.0 ± 0.0	0.33 ± 0.13	0.12 ± 0.03
Stem water potential (MPa) *	-0.82 ± 0.16	-0.35 ± 0.05	-0.73 ± 0.06
ACO_2 (μmol CO_2/m^2s) *	11.3 ± 3.1	1.1 ± 1.3	9.2 ± 0.9
g_s (mmol H_2O/m^2s) *	254 ± 262	40 ± 21	242 ± 74
C_i (μmol CO_2/m^2s)	254 ± 59	357 ± 47	306 ± 15
WUE (μmol CO_2/mol H_2O) *	70 ± 4	20 ± 20	40 ± 10
Cl^- (mg/g d.w.) *	0.49 ± 0.09	5.5 ± 0.2	4.0 ± 0.3
Ca^{2+} (mg/g d.w.)	0.63 ± 0.07	0.32 ± 0.06	0.42 ± 0.08
K^+ (mg/g d.w.)	1.6 ± 0.2	0.99 ± 0.19	1.4 ± 0.3
Mg^{2+} (mg/g d.w.)	0.179 ± 0.013	0.17 ± 0.02	0.21 ± 0.04
Na^+ (mg/g d.w.)	0.21 ± 0.07	4.9 ± 0.3	5.0 ± 1.4
P (mg/g d.w.) *	0.064 ± 0.016	0.12 ± 0.01	0.15 ± 0.02
S (mg/g d.w.)	0.12 ± 0.02	0.06 ± 0.02	0.07 ± 0.02
Na^+/K^+	0.13 ± 0.04	5.1 ± 1.2	3.63 ± 0.18
Na^+/Ca^{2+}	0.34 ± 0.14	15.9 ± 4.3	11.8 ± 1.2

The morphological differences between tolerant and sensitive plants were clearly significant for the Relative Growth Rate (RGR) (Figure 36). The sensitive plants showed less RGR than the tolerant ones at the end of the saline treatment (day 60).

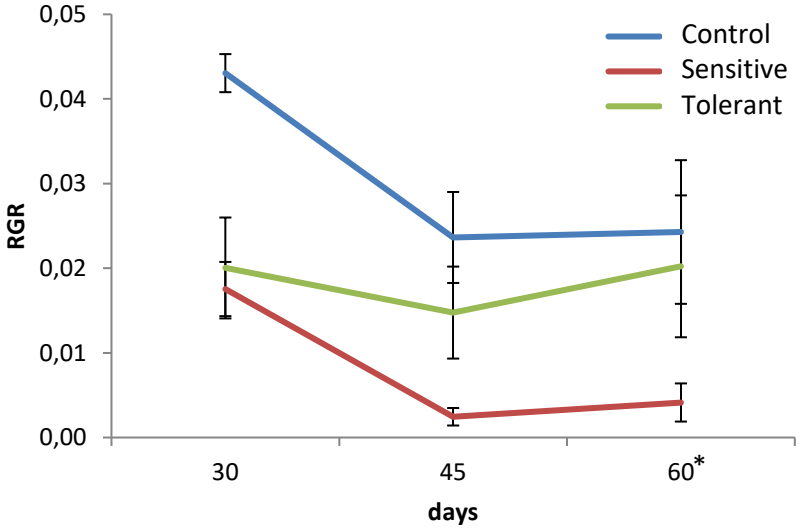

Figure 36. Relative growth rate (RGR) of the groups. Bar represents standard deviation. Asterisk (*) indicates significant differences between tolerant and sensitive groups (Kruskal-Wallis test, $p<0.05$).

Gene expression changes in response to salinity

Regarding to the gene expression profile, a principal component analysis (PCA) was conducted using the transcriptomic data for all samples. In this analysis, a clear separation was shown between roots and leaves. Leaves showed little variability between the three categories (Figure 37). However, the percentage of variability explained between control and treated roots was of the same order of magnitude as that between leaves and roots. Furthermore, the separation between tolerant and sensitive plants was also evident

based on root transcriptomic data as shown in Figure 37. This separation was consistent with the phenotypic data previously exposed.

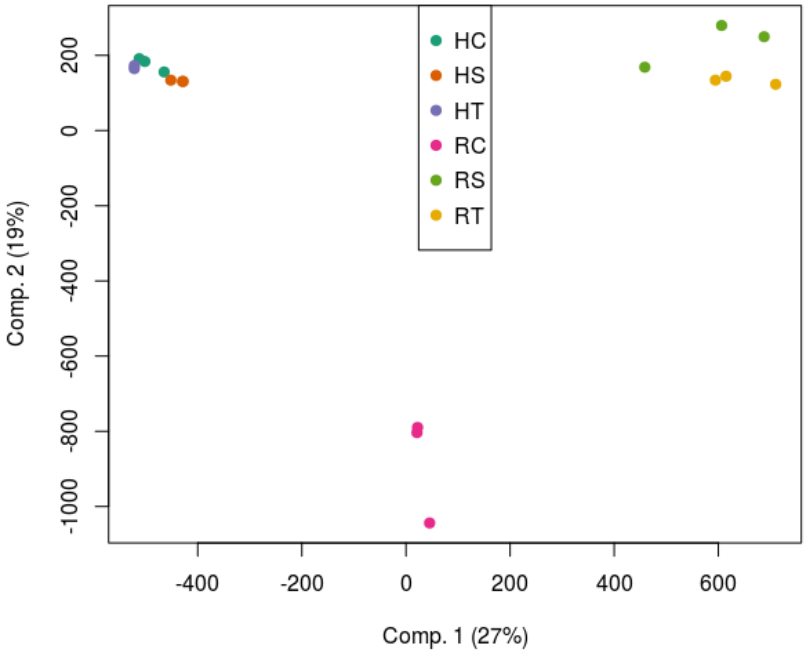

Figure 37. Principal component analysis of the whole transcriptomic profiles of the six analyzed samples with its three biological replicates

The comparison between expression in tolerant *vs* sensitive plants revealed 2901 differentially expressed genes. These genes were further filtered using the BLAST results and annotations to look for putative genes related to salinity tolerance. Additionally, an orthogonal design analysis was conducted to be able to differentiate

gene expression differences specific to roots or to leaves. The orthogonal analysis identified 1277 genes differentially expressed between tolerant and sensitive leaves (Supplementary Figure 5). Also, 1395 genes were differentially expressed between tolerant vs sensitive roots (Supplementary Figure 6).

Differentially expressed genes were divided according to several salt-tolerance mechanisms: Ion transport, photosynthesis and respiration systems, and ROS detoxification. No water transport related genes were found differentially expressed. Ion transport related genes were divided according to each ion type (Table 11). Among Ca^{2+} transport related genes, a calcium ATPase-like gene was down-regulated in the leaves of sensitive plants as compared to those in tolerant plants, whereas the opposite was true for the roots. Furthermore, a calcium uniporter protein-like gene was found to be upregulated in the leaves of sensitive plants. Potassium channels SKOR and KAT3-like genes were downregulated in the leaves of sensitive plants, whereas a probable potassium transporter was upregulated in the leaves of sensitive plants. With regard to ionic channels, vacuolar cation/proton exchangers were upregulated in the leaves of sensitive plants. Other cation/proton antiporters did not show a clear response to salinity stress, as some isoforms had different expression patterns. On the other hand, chloride channel protein-like genes were upregulated in both leaves and roots of sensitive plants and downregulated in tolerant leaves. Phosphate, magnesium and boron transport-related genes were upregulated in tolerant roots. Phosphate, zinc and ammonium transport-related genes were also

upregulated in tolerant leaves. Regarding ATPases, Plasma membrane ATPase-like genes were strongly upregulated in the roots of tolerant plants and downregulated in sensitive leaves. Furthermore, a V-type proton ATPase subunit G-like gene was strongly upregulated in leaves of tolerant plants as compared to the sensitive ones.

Table 11. Log2 FC and adjusted p-value for genes associated to ion transport which are differentially expressed in tolerant vs sensitive plants. Colors represent relative differences in expression according to the read counts: red color is assigned to the lowest count value and blue color is assigned to the highest count value. Leaves and roots are represented by the columns with letters "L" and "R". Brown columns correspond to the relative mean expression in control plants, blue tolerant plants and red sensitive plants. Tissue column indicates tissue specificity of the tolerant vs sensitive expression

Sequence Description	log2 FC	p-value (adj)	L R	Tissue
CALCIUM				
Mitochondrial calcium uptake protein 1 -like	0.93	1.1E-08		L
Cation/calcium exchanger 3-like	0.75	5.7E-03		
Extracellular calcium sensing receptor-like	0.85	1.0E-04		L
Calcium-transporting ATPase-like 1	1.25	3.0E-04		
Calcium-transporting ATPase-like 2	1.28	5.3E-07		
Calcium-transporting ATPase-like 3	1.30	1.6E-05		
Calcium uniporter protein-like	-1.50	1.2E-03		L
SODIUM				
Sodium/hydrogen exchanger 2-like-1	0.60	1.5E-05		
Sodium/hydrogen exchanger 2-like-2	-0.74	3.6E-16		

POTASSIUM				
Chloroplastic K^+ efflux antiporter 3, -like	0.95	2.1E-03		
Potassium channel AKT2/3 like 1	1.83	1.3E-14		
Potassium channel AKT2/3 like 2	1.90	3.5E-11		
Probable potassium transporter like	-2.21	2.2E-14		
Potassium channel KAT3-like	1.44	3.5E-03		
Potassium channel SKOR-like 1	3.16	6.9E-04		L
Potassium channel SKOR-like 2	4.13	5.3E-04		L
CATIONS				
Mechanosensitive ion channel-like	1.10	3.0E-12		
Chloroplastic mechanosensitive ion channel 2-like	0.70	2.0E-04		
Cation/H(+) antiporter like-1	1.75	1.1E-03		
Cation/H(+) antiporter 18-like	-1.07	7.2E-03		
Cation/H(+) antiporter like-2	-1.82	8.3E-03		
Cation/H(+) antiporter 14-like	-1.64	4.4E-03		
Vacuolar cation/proton exchanger-like	-2.98	2.5E-04		L
Vacuolar cation/proton exchanger 3-like 1	-2.83	7.6E-04		L
Vacuolar cation/proton exchanger 3-like 2	-2.71	2.6E-03		L
ANIONS				
S-type anion channel SLAH1-like	-1.70	1.0E-03		
Voltage-dependent anion-selective channel 2-like	5.32	5.8E-04		L
Chloride channel protein-like 1	-0.88	3.4E-09		
Chloride channel protein-like 2	-0.64	5.5E-03		L
Voltage dependent anion channel 1-like	1.24	5.8E-06		L
Aluminum-activated malate	3.58	2.3E-10		L

transporter-like				
OTHER NUTRIENTS				
Ammonium transporter-like	1.91	2.3E-09	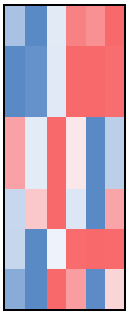	L
Ammonium transporter 1 member 1-like	1.94	8.9E-04		L
Magnesium/proton exchanger-like	1.12	2.8E-08		L
Boron transporter 1-like	1.56	5.3E-04		
Zinc transporter like	2.79	1.8E-05		L
Phosphate transporter PHO1-like	3.82	1.1E-18		
H+ ATPases				
Plasma membrane H+-ATPase-like	0.85	1.5E-03	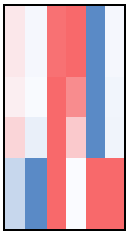	
Plasmalemma H+-ATPase 1-like	0.92	4.2E-03		
Plasma membrane ATPase 4-like	1.17	1.9E-05		
V-type proton ATPase subunit G-like	7.33	2.9E-04		L

Regarding photosynthesis and respiration genes, all genes were downregulated in roots from all plants in comparison to the leaf expression levels. Differentially expressed genes in leaves were all upregulated in the tolerant plants as compared to the sensitive ones, while the expression levels of the tolerant plants were similar to the control plants (Table 12).

Table 12 Log2 FC and adjusted p-value for genes associated to photosynthesis and respiration which are differentially expressed in tolerant vs sensitive plants. Colors represent relative differences in expression according to the read counts: red color is assigned to the lowest count value and blue color is assigned to the highest count value. Leaves and roots are represented by the columns with letters "L" and "R". Brown columns correspond to the relative mean expression in control plants, blue tolerant plants and red sensitive plants. Tissue column indicates tissue specificity of the tolerant vs sensitive expression

Sequence Description	log2 FC	p-value (adj)	L R	Tissue
PHOTOSYNTHESIS AND RESPIRATION				
PSI reaction center subunit N-like-1	2.32	2.5E-07		L
PSI reaction center subunit N-like-2	2.13	1.5E-08		L
PSI reaction center subunit III-like	2.26	1.8E-08		L
PSI reaction center subunit V-like	1.86	3.2E-06		L
PSII reaction center W-like	1.66	1.2E-06		L
PSII PsbY-like	1.75	1.5E-06		L
PSII repair protein PSB27-H1-like	0.93	4.6E-03		L
Cytochrome c oxidase subunit 5A-like	6.86	5.4E-03		L

About ROS detoxification genes (Table 13), except Thermospermine synthase ACAULIS5-like, all of them were mostly expressed in the leaves. Peroxiredoxin-like and peroxidase-like genes were upregulated in the tolerant plants except for one peroxidase-like that was upregulated in sensitive plants. Thermospermine synthase ACAULIS5-like was strongly upregulated in the roots of the tolerant plants and strongly downregulated in the leaves of the sensitive leaves.

Table 13. Log2 FC and adjusted p-value for genes associated to photosynthesis and respiration which are differentially expressed in tolerant vs sensitive plants. Colors represent relative differences in expression according to the read counts: red color is assigned to the lowest count value and blue color is assigned to the highest count value. Leaves and roots are represented by the columns with letters "L" and "R". Brown columns correspond to the relative mean expression in control plants, blue tolerant plants and red sensitive plants. Tissue column indicates tissue specificity of the tolerant vs sensitive expression

Sequence Description	Log2 FC	p-value (adj)	L R	Tissue
ROS DETOXIFICATION				
Peroxiredoxin 1-like	4.49	8.4E-04		L
Type II Peroxiredoxin 2-like	1.18	7.3E-08		L
Peroxidase-like	-1.03	1.1E-03		L
Peroxidase 12-like 1	3.89	4.0E-18		L
Peroxidase 12-like 2	5.09	6.2E-03		L
Spermidine synthase-like	1.95	8.7-05		L
Thermospermine synthase ACAULIS5-like	2.12	2.4E-11		

Discussion

Ion Transport

Following salt treatment, no significant differences between salt tolerant and sensitive plants were observed for Na^+, Ca^{2+} or K^+ accumulation in leaves. However, a higher K^+ and Ca^{2+} accumulation in the leaves of tolerant plants coincides with a higher leaf expression of several potassium channels and calcium transporting ATPases in the tolerant plants.

In our study, the total content of Na^+ and Cl^- was analysed and therefore a possible vacuolar compartmentalization could not be detected. However, we observed higher expression of all the analysed H^+-ATPases in tolerant plants. This suggest the involvement of these genes in the compartmentalization mechanism of cell protection from Na^+ toxicity. In spite of that the responsible proteins of the removal of sodium ions from the cytoplasm into the apoplast or vacuole are the specific plasma membrane Na^+/H^+ antiporters, the activity of this protein depends on the electrochemical proton gradient between membranes. The H^+-ATPases are the only proteins that are able to generate the adequate electrochemical proton gradient that allows these antiporters to perform the Na^+ extrusion (Palmgren, 2001). Furthermore, the upregulation of this protein under salt conditions has been previously reported (Niu et al., 1993; Vera-Estrella et al., 1994; Chen et al., 2007; Sahu and Shaw, 2009) and its critical role on the Na+ extrusion has been confirmed using transgenic plants (Gévaudant et al., 2007; Shen et al., 2011).

Another ion directly involved in damage caused by toxicity is Cl^-, especially in the case of persimmon as previously shown by others (Besada et al., 2016; de Paz et al., 2016). In our study, we observed a direct relationship between expression of chloride channel proteins and chlorine accumulation in leaf. Recently, chloride channels were proposed as key transporters of Cl^- into the higher parts of the plant (Isayenkov and Maathuis, 2019). In persimmon, our results suggest that these channels might be playing a key role in avoiding high Cl^- leaf accumulation in tolerant plants.

Photosynthesis, respiration systems and ROS signalling

A decreased metabolism in sensitive plants is supported both by the downregulation of photosynthetic and respiratory genes, and by a significant reduction in carbon fixation. This effect might be caused by a combination of reduced transpiration and cell damage caused by the accumulation of toxic ions causing leaf necrosis and defoliation (Munns and Tester, 2008). ROS inactivation is also higher in both control and tolerant leaves an effect that probably leads to higher leaf ROS content in the sensitive plants. Although ROS can cause toxic effect in the leaves, it is a part of a signalling mechanism that may not be key to explaining the salinity tolerance, as an efficient ROS detoxification is essential for plant survival under natural conditions (Munns and Tester, 2008). ROS are known to trigger programmed cell death (Petrov et al., 2015) and tissue necrosis and defoliation, which are believed to be a mechanism for protecting the most photosynthetically active cells (Baetz et al., 2016).

Root architecture involvement

Under stress conditions, thermospermine synthesis and K^+ uptake are linked to the inhibition of lateral root formation (Osakabe et al., 2013; Tong et al., 2014). Although root architecture was not characterized in this study, transcriptomic data revealed thermospermine synthesis and K^+ transport activation by salinity in roots of tolerant plants, which suggests that root architecture may also play a role in the mechanism of tolerance to salt stress. Although previous reports have pointed out the association between reduced lateral root growth and sensitivity to saline stress trough better maintenance of Na^+/K^+ ratio by accumulating Na^+ in the secondary root stele (Julkowska et al., 2014), other studies have pointed that in some cases, such as in seedlings, accumulation of Na^+ in the stele can cause lateral root quiescence or even lateral root primordia damage (Julkowska et al., 2017) and therefore reduced root development. In this line, *D. virginiana*, which is considered a salt-tolerant persimmon rootstock the root system is characterized by a well-developed taproot (Incesu et al., 2014). *D. lotus*, a salt-sensitive rootstock, is characterized by a fibrous root system as compared to *D. virginiana* that presents a well-developed taproot (Intrigliolo et al., 2018), this morphological differences are believed to play an important role in the salinity tolerance in *Diospyros* rootstocks (Visconti et al., 2017). Our expression results indicate a possible association between root architecture and tolerance to salinity warrants further studies.

Strategies present in Diospyros lotus to overcome saline stress

To sum up, in *Diospyros lotus* several mechanisms are present to overcome the saline stress. In these paper we could elucidate the ones that present variability within these species and therefore could be exploited for breeding new salt-tolerant rootstocks. At root level, thermospermine might play a role in root architecture, whose involvement in salt tolerance among *Diospyros* species has been previously pointed by other authors (Visconti et al., 2017). On the other hand, chloride channel expression could facilitate Cl^- transport inside the plant, and therefore cause higher Cl^- accumulation in the higher parts of the plant. Finally, in the leaves, H^+-ATPases seems to be crucial to be able to generate the electrochemical membrane gradient to allow Na^+ extrusion from the cytoplasm.

Supplementary material

Supplementary Figure 5. Venn diagram of the orthogonal analysis for identification of leaf-specific differential expressed genes between tolerant and sensitive plants

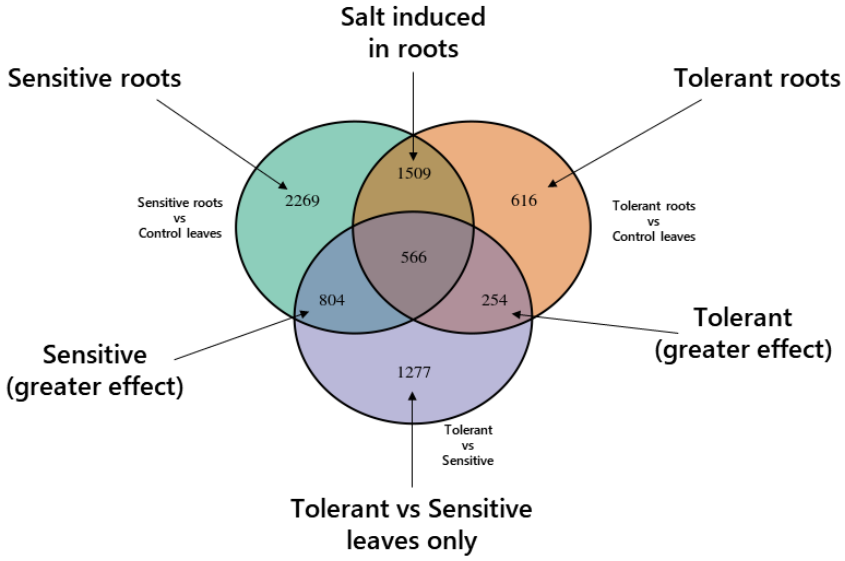

Supplementary Figure 6. Venn diagram of the orthogonal analysis for identification of leaf-specific differential expressed genes between tolerant and sensitive plants

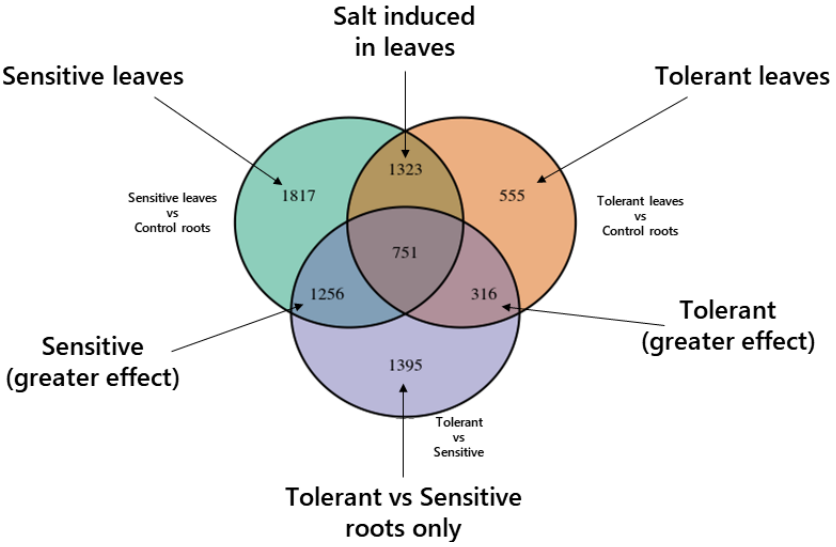

CHAPTER 3: Studies of a MBW complex role in proanthocyanidin synthesis regulation on persimmon

The results presented in this chapter were published in two scientific papers and a proceeding:

María del Mar Naval, Francisco Gil-Muñoz, Alba Lloret, Cristina Besada, Alejandra Salvador, María Luisa Badenes, Gabino Ríos. 2016. A WD40-repeat protein from persimmon interacts with the regulators of proanthocyanidin biosynthesis *DkMYB2* and *DkMYB4.* Tree Genetics and Genomes. 12: 13. doi:10.1007/s11295-016-0969-z

Francisco Gil-Muñoz, Jesús Ángel Sánchez-Navarro, Cristina Besada, Alejandra Salvador, María Luisa Badenes, María del Mar Naval, Gabino Ríos. 2020. MBW complexes impinge on anthocyanidin reductase gene regulation for proanthocyanidin biosynthesis in persimmon fruit. *Sci Rep* **10,** 3543. https://doi.org/10.1038/s41598-020-60635-w

María del Mar Naval, Francisco Gil-Muñoz, Alba Lloret, Maria Luisa Badenes, Gabino Ríos. 2016. Molecular Characterization of a TTG1-like Gene Expressed in Persimmon Fruit. Acta Horticulturae. doi 10.17660/ActaHortic.2017.1172.67

The WD40-repeat protein DkTTG1 from persimmon interacts with the regulator of proanthocyanidin biosynthesis DkMYB4

Abstract

MBW ternary complexes composed of MYB domain proteins, basic helix-loop-helix (bHLH) transcription factors, and WD40-repeat proteins are involved in the transcriptional regulation of anthocyanin and proanthocyanidin (PA) biosynthesis pathways in distinct plant species. DkMYB4 (MYB type) and DkMYC1 (bHLH type) genes have been related to the synthesis of PAs in persimmon fruit, which are the compounds responsible for its strong astringent taste. We have identified a WD40-repeat gene from persimmon (DkTTG1) coding for a protein highly similar to TTG1 from Arabidopsis thaliana and other components of distinct MBW complexes. DkTTG1 expression was detected in different tissues, and was essentially constant during fruit development. DkMYB4 interacted with both DkTTG1 and DkMYC1 in the two-hybrid system, suggesting that an MBW-like complex could be involved in PAs accumulation in persimmon fruit.

Introduction

Persimmon (*Diospyros kaki* Thunb.) is a hexaploid fruit crop originated in Eastern Asia (2n = 6x = 90) (Zhuang et al., 1990; Tamura et al., 1998), with increasing economic importance worldwide (FAOSTAT, http://faostat.fao.org/faostat). Persimmon fruit accumulates large amounts of proanthocyanidins (PAs) or condensed tannins in large cells named “tannin cells” during the process of fruit ripening, which cause a strong astringent taste when consumed (Yonemori and Matsushima, 1985, 1987). Persimmon cultivars are classified into four groups depending on the effect of pollination on flesh colour and their patterns of astringency-loss (Yonemori et al., 2000): pollination-constant non-astringent (PCNA), pollination-variant non-astringent (PVNA), pollination-variant astringent (PVA) and pollination-constant astringent (PCA). Among these groups, only PCNA-type genotypes lost the ability to produce PA at an early stage of fruit development on the tree. Other fruit types remain astringent until ripening on the tree, hence they need a postharvest treatment to be edible.

PAs are oligomeric and polymeric end products synthesized via the flavonoid biosynthetic pathway (Winkel-Shirley, 2001; Dixon et al., 2005; Lepiniec et al., 2006). PAs are widespread throughout the plant kingdom and generally have protective functions against predation and pathogen attack (Scalbert, 1991; Harborne and Grayer, 1993). Furthermore, their beneficial effects on human health have been demonstrated in several studies (Bagchi et al., 2000; Manach et al., 2005; Georgiev et al., 2014). PA biosynthesis is modulated by

structural genes encoding enzymes that directly participate in the synthesis of PAs and regulatory genes that control the transcription of structural genes (Lepiniec et al., 2006; Akagi et al., 2011a). Many of the structural genes common to both PA and anthocyanin biosynthesis, such as chalcone synthase (CHS), chalcone isomerase (CHI), flavonoid 3´-hydroxylase (F3´H), dihydroflavonol reductase (DFR), and anthocyanidin synthase (ANS) have been identified using different *Arabidopsis thaliana* mutants (Jende-Strid, 1993; Abrahams et al., 2002; Cone, 2007). The products of the enzymatic reactions catalysed by DFR and ANS lead to PA precursors (before polymerization/oxidation) by leucoanthocyanidin reductase (LAR) converting leucoanthocyanidin to (+)-catechin (Tanner et al., 2003), and anthocyanidin reductase (ANR) converting anthocyanidin to (-)-catechin (Xie et al., 2003). The PA-specific genes *DkANR* and *DkLAR* have been already identified in persimmon (Ikegami et al., 2005; Akagi et al., 2009a; Wang et al., 2010).

The transcriptional regulators involved in PA biosynthesis have been categorized into different families according to their protein structure and functional domains (Marles et al., 2003; Dixon et al., 2005), including WD40-repeat proteins and bHLH, MYB, WRKY, MADS-box, and Zn-finger transcription factors among others. In *Arabidopsis*, the transcription of genes involved in PA biosynthesis is regulated by a ternary MYB-bHLH-WD40 (MBW) protein complex (Baudry et al., 2004; Gonzalez et al., 2008), composed of TT2 (Nesi et al., 2001), TT8 (Nesi et al., 2000) and TTG1 (Walker et al., 1999). This complex is necessary for activating the expression of *BANYULS* (*BAN*)

gene, which encodes an ANR involved in PAs biosynthesis in the *Arabidopsis* seed coat (Baudry et al., 2004). Similar MBW complexes have been found in petunia and strawberry, among other plant species (Spelt et al., 2002; Schaart et al., 2013).

In persimmon, MYB-like (*DkMYB2, DkMYB4*) and bHLH-like (*DkMYC1*) genes have been postulated to regulate PA biosynthesis and astringency in fruit by sequence similarity and functional studies (Akagi et al., 2009b, 2010a; Su et al., 2012). However, no WD40-like genes have been related to MBW complexes in this species. In this study, we report the characterization of a WD40-**R**epeat gene (*DkWDR1*) and postulate its participation in putative MBW complexes involved in PAs accumulation in persimmon fruit.

Materials and methods

Plant material

Diospyros kaki Thunb. cvs 'Hachiya' and 'Hana Fuyu' were grown in the same orchard located in Museros (Spain; 39º 34' 40" N, 0º 21' 46" W) under standard agricultural practices, according to Bellini and Giordani (Bellini and Giordani, 2002). Fruit samples were collected on the following dates in 2011: July 12 and 21, August 30, and September 16 and 30. Sets of four seedless fruit (naturally parthenocarpic) per cultivar were collected on each harvest day. Leaves and flowers (five per sample) were collected on May 6, 2014. Buds were pooled from 4-5 shoots obtained on January 9, 2015.

Measurement of fruit development parameters

At each developmental stage, fruit weight and colour were measured. The analyses were done within 6 hours after harvesting. Fruit skin colour was evaluated using a Minolta Colorimeter (Model CR-300, Ramsey, NY, USA). The 'L', 'a', 'b' Hunter parameters were measured and the results were expressed as a skin Colour Index (CI) = (1000a)/(Lb) (Salvador et al., 2007). In addition, flesh samples were frozen and stored for the measurement of soluble tannin content and expression studies (see below). Soluble tannins were evaluated using the Folin-Denis method (Taira, 1996), as described previously (Arnal and Del Rio, 2004), and results were expressed as percentage of fresh weight (FW). Measurements from four independent fruits were made per sample.

Cloning of full-length DkWDR1 and sequence analysis

The primers designed for cloning of full-length *DkWDR1* into two-hybrid vectors were also used for allele sequence analysis (Online Resource Table S1). The coding region of *DkWDR1* was amplified using cDNA from 'Hachiya' fruit flesh (see below) as template, and Pwo SuperYield DNA Polymerase (Roche, Basel, Switzerland) under the following PCR conditions: 2 min at 94 ºC, 5 cycles of 15 s at 94 ºC, 30 s at 60 ºC, and 2 min 30 s at 72 ºC, followed by 33 cycles of 15 s at 94 ºC, 30 s at 63 ºC, and 2 min 30 s at 72 ºC, and a final step of 7 min at 72 ºC. The PCR product was digested with enzymes *Nde*I and *Bam*HI (Roche), purified with High Pure PCR Product Purification Kit (Roche), and ligated to *Nde*I/*Bam*HI digested plasmid pGADT7 (Clontech-Takara Bio, Otsu, Japan) with T4 DNA ligase (Roche).

Competent JM109 *Escherichia coli* cells (Promega, Madison, WI, USA) were transformed with the ligation product, and positive colonies were selected for gene sequencing. The presence of WD40 repeats in the deduced amino acid sequence of DkWDR1 was predicted by WDSP software (Wang et al. 2013). For the phylogenetic analysis, TTG1 and TTG1-like proteins were aligned using ClustalW algorithm (opening=10, extension=0.2). The *Arabidopsis* proteins most similar to TTG1, LWD1 and LWD2, were also included as external controls. A phylogenetic tree was elaborated using the Maximum Likelihood method, and tested using Bootstrap method with 1000 replicates. Both, alignment and phylogenetic analysis were performed using MEGA version 6 (Tamura et al., 2013).

Isolation of RNA and quantitative real-time RT-PCR

Total RNA was isolated from 150 mg of plant tissue using a rapid cetyltrimethylammonium bromide (CTAB)-based procedure (Gambino et al., 2008). Contaminant genomic DNA was removed with the RNase-Free DNase Set (Qiagen, Valencia, CA, USA), by on-column digestion using the RNeasy Plant Mini Kit (Qiagen), according to manufacturer's instructions. Purified RNA (500 ng) was reverse transcribed with PrimeScript RT Reagent Kit (Takara Bio, Otsu, Japan) in a total volume of 10 µl. The first-strand cDNA was 20-fold diluted, and 1.5 µl used as template for quantitative real-time RT-PCR in a final volume of 20 µl. The primers employed are listed in Online Resource Table S1. Quantitative real-time PCR was performed on a StepOnePlus Real-Time PCR System (Life Technologies, Carlsbad, CA, USA), using SYBR premix Ex Taq (Tli RNaseH plus) (Takara Bio). The

PCR protocol consisted of 10 min at 95 ºC, followed by 40 cycles of 15 s at 95 ºC, and 1 min at 60 ºC. The specificity of the reaction was assessed by the presence of a single peak in the dissociation curve and through size estimation of the amplified product by agarose electrophoresis. *DkActin* transcript, amplified with specific primers, was used as reference gene (Akagi et al., 2009b). Relative expression was measured by the relative standard curve procedure. Results were the average of two independent biological replicates with 2–3 technical replicates each.

Analysis of protein interactions by yeast two-hybrid system

DkMYB2, *DkMYB4* and *DkMYC1* coding regions were PCR-amplified from cDNA obtained from fruit flesh of 'Hachiya', using the specific two-hybrid primers listed in Online Resource Table S1, and following the same PCR conditions used for amplification of *DkWDR1* (see above). *DkMYB2* and *DkMYB4* fragments were digested with *Eco*RI and *Bam*HI enzymes and cloned between the *Eco*RI/*Bam*HI restriction sites of pGADT7 vector; whereas *DkMYC1* fragment was digested with *Nde*I and *Bam*HI and cloned into pGADT7 treated with *Nde*I and *Bam*HI. In order to construct the protein fusions to the DNA-binding domain (BD), *DkWDR1*, *DkMYB2*, *DkMYB4* and *DkMYC1* genes were obtained from pGADT7-derived plasmids, and cloned into the *Nde*I/*Bam*HI (*DkWDR1* and *DkMYC1*) or *Eco*RI/*Bam*HI (*DkMYB2* and *DkMYB4*) sites of pGBKT7 vector (Clontech-Takara Bio). The pGBKT7 and pGADT7-derived plasmids were sequentially introduced into the Saccharomyces cerevisiae strain Y2HGold by yeast transformation

with the Matchmaker Gold Yeast Two-Hybrid System (Clontech-Takara Bio), following manufacturer's protocols.

The autoactivation of transcription of pGBKT7-DkWDR1, pGBKT7-DkMYB2, pGBKT7-DkMYB4 and pGBKT7-DkMYC1, in the absence of proteins fused to the activation domain (AD), was assayed in minimal medium supplemented with the antibiotic Aureobasidin A (AbA) and the chromogenic substrate X-α-Gal at the recommended concentrations (Clontech-Takara Bio). Two-hybrid interactions were tested in minimal medium without histidine and adenine, and supplemented with AbA and X-α-Gal. Three independent transformants of each combination of BD and AD plasmids were tested.

Measurement of α-galactosidase activity in yeast two-hybrid strains

The colorimetric method for the quantification of the MEL1 reporter gene in yeast, coding for a secreted α-galactosidase enzyme, was performed according to the Clontech Yeast Protocols Handbook (PT3024-1). Briefly, the rate of hydrolysis of p-nitrophenyl-α-D-galactoside (PNP-α-Gal) yielding the yellow product p-nitrophenol was calculated in cell-free culture media by recording the absorbance at 410 nm. Four independent yeast colonies per genotype were grown overnight in liquid minimal medium until an optical density at 600 nm (OD_{600}) of 0.5-1. Cells were pelleted by centrifugation for 2 min at 10,000 x g.

The enzymatic assay was performed in microtiter plates, in a total volume of 200 µl. We added 48 µl of assay buffer (mix of sodium

acetate 0.5 M pH 4.5 and PNP-α-Gal 100 mM in a ratio 2:1) to 16 µl of cell-free sample, and incubated it at 30 ºC for 60 min. The reaction was terminated by adding 136 µl of Na_2CO_3 1 M. The OD_{410} was recorded and used to calculate the enzymatic activity relative to OD_{600} to normalize to the number of cells in each culture. We made three replicates per sample.

Results

Molecular cloning of DkWDR1

We used a recently released sequence of persimmon (GenBank HQ880577) to amplify the whole coding region of *DkWDR1* from the astringent fruit of cultivar 'Hachiya'. We sequenced 11 independent clones, which corresponded to four different alleles, named from *DkWDR1*a to *DkWDR1*d (Annexed Table S2). *DkWDR1*b showed two base substitutions with respect to *DkWDR1*a, but the deduced protein was identical in both. *DkWDR1*c had five and *DkWDR1*d had four base replacements, leading to one and two amino acid changes, respectively (Annexed Fig. S1). *DkWDR1*a allele was used in subsequent experiments. Amplification of *DkWDR1* in the non-astringent variety 'Hana Fuyu', and sequencing of a pooled PCR sample allowed the identification of six single nucleotide polymorphisms (SNP) also found in 'Hachiya' alleles (Online Resource Fig. S2), which excluded any mutation in *DkWDR1* as the origin of fruit astringency loss in this variety.

DkWDR1 encodes a WD40 domain protein similar to TTG1

The WDSP program predicted the presence of seven WD40 repeats in DkWDR1 (Figure 38). Thus, DkWDR1 could be able to form a 7-bladed β-propeller, the most typical structure of WD40 proteins (Wang et al. 2013). The conservation of amino acid sequence was very high in WD40 repeats 3-7 when comparing TTG1-like proteins from persimmon, *Arabidopsis*, cotton (*Gossypium hirsutum*), apple (*Malus x domestica*), and peach (*Prunus persica*) (Figure 38). The percentage of amino acid identity ranged from 79% between DkWDR1 and *Arabidopsis* TTG1 to 87% between DkWDR1 and peach PpTTG1.

DkWDR1 was more similar to TTG1 than to other related WD40 proteins, such as LWD1 and LWD2, and clustered into a TTG1-like group of proteins by phylogenetic analysis (Figure 39). Thus, DkWDR1 was structurally related to TTG1 and its orthologs in other species.

Analysis of DkWDR1 expression

We studied the tissue-dependent expression of DkWDR1 by quantitative real-time RT-PCR. DkWDR1 was similarly expressed in leaves, reproductive buds and flowers; whereas its expression was slightly lower in fruit flesh (Figure 40). *DkWDR1* expression was not impaired in the non-astringent variety ‘Hana Fuyu’.

Figure 38. Protein sequence alignment of DkWDR1 and selected WD40-repeat proteins. The deduced protein sequence of DkWDR1 (shown as DkTTG1) was compared to PpTTG1 (*Prunus persica*), MdTTG1 (*Malus* x *domestica*), GhTTG1 (*Gossypium hirsutum*), and TTG1 (*Arabidopsis thaliana*). Identical residues in four and five of the protein sequences are shown in grey and black respectively. Predicted WD40 repeats are labelled (WD-1 to WD-7)

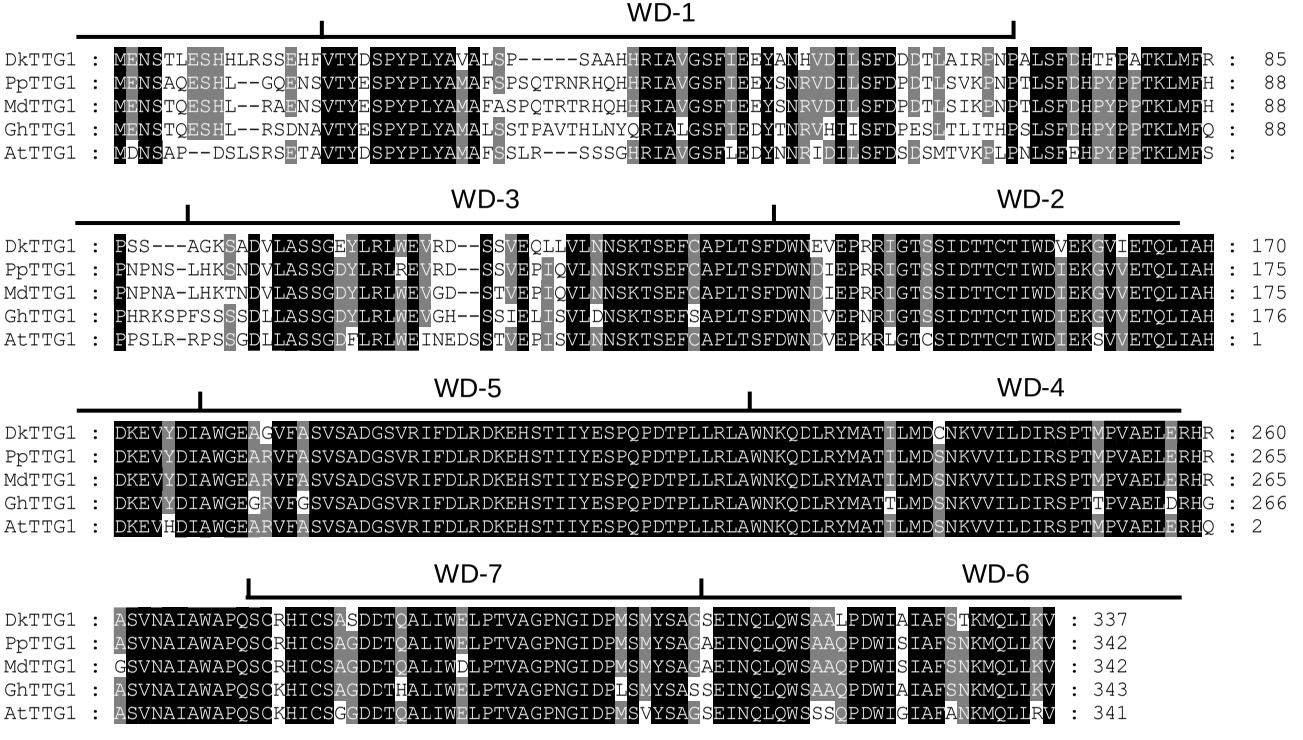

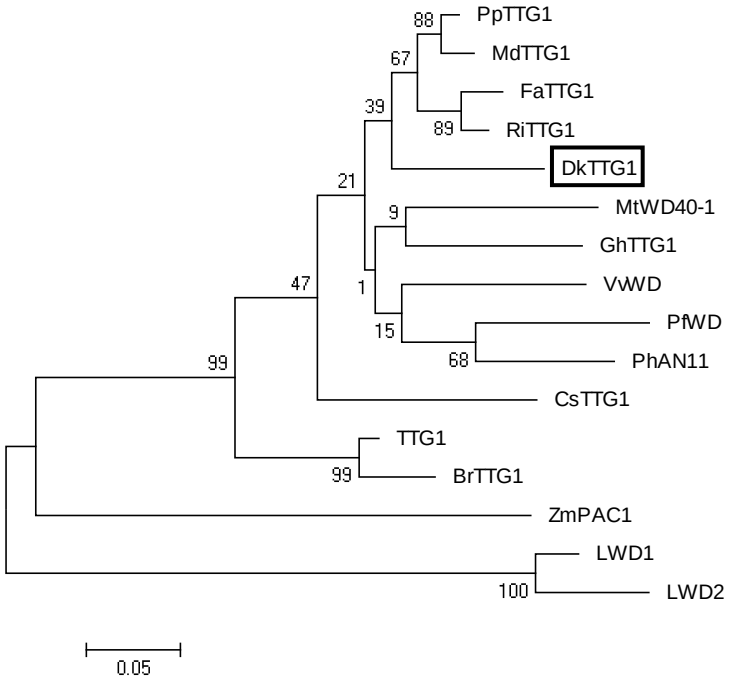

Figure 39. Phylogenetic tree of selected WD40-repeat proteins. The tree was constructed using the Maximum Likelihood method and bootstrapped with 1000 replicates. Numbers next to each node represent the bootstrap values in percentage. The scale bar indicates the branch length that corresponds to the number of substitutions per amino acid position. GenBank accession numbers: *Arabidopsis thaliana* TTG1 (CAB45372), *Malus x domestica* MdTTG1 (ADI58760), *Fragaria x ananassa* FaTTG1 (AFL02466), *Cucumis sativus* CsTTG1 (ABY64743), *Rubus idaeus* RiTTG1 (AEI55401), *Prunus persica* PpTTG1 (ACQ65867), *Gossypium hirsutum* GhTTG1 (AAM95641), *Arabidopsis thaliana* LWD1 (AEE28948), *Arabidopsis thaliana* LWD2 (AEE77190), *Zea mays* ZmPAC1 (AAM76742), *Vitis vinifera* WDR1 (ABF66625), *Brassica rapa* BrTTG1 (XP_009150977), *Medicago* truncatula MtWD40-1 (XP_003602392), *Perilla frutescens* PfWD (BAB58883), and *Petunia hybrida* PhAN11 (AAC18914)

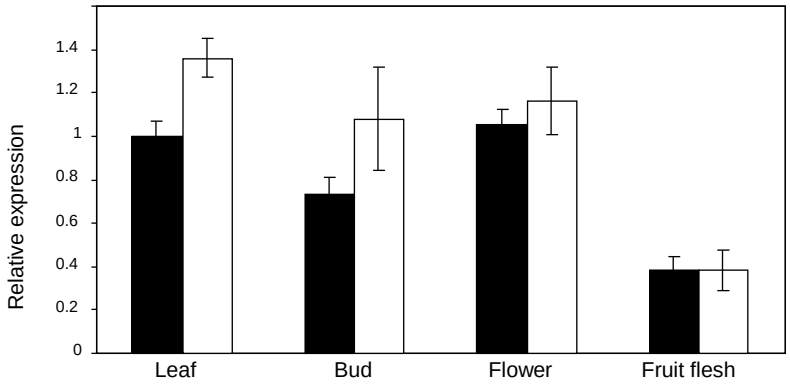

Figure 40. Relative expression of *DkWDR1* in different tissues. The expression of *DkWDR1* in cultivars 'Hachiya' (black bars) and 'Hana Fuyu' (white bars) is shown. Expression levels are relative to *DkActin*. An expression value of one is assigned to the leaf sample from 'Hachiya'. Data are means from two biological replicates with 2–3 technical replicates each, with error bars representing standard deviations

Certain regulatory factors and PA biosynthesis genes have been found mis-regulated during fruit development in non-astringent mutants of persimmon. In close agreement with published data, the expression of *DkMYB4* and *DkMYC1* genes, coding for putative regulators of PA and anthocyanin biosynthesis in persimmon fruit (Akagi et al., 2009b; Su et al., 2012), was lower in the non-astringent fruit of 'Hana Fuyu' than in the astringent fruit of 'Hachiya' (Figure 41). Also the *DkF3H* and *DkANS* genes, coding respectively for flavonoid 3-hydroxylase and anthocyanidin synthase in the PA pathway (Akagi et al., 2009b, 2009a), showed lower expression in 'Hana Fuyu' fruit. Such differences were higher in early stages of fruit development, where fruits were greenish and lighter, and the relative accumulation of soluble tannins was higher (Figure 42). However, the relative expression of *DkWDR1* did not change drastically during fruit

development, and it was not systematically lower in the 'Hana Fuyu' variety, contrarily to observations from previous genes (Figure 41).

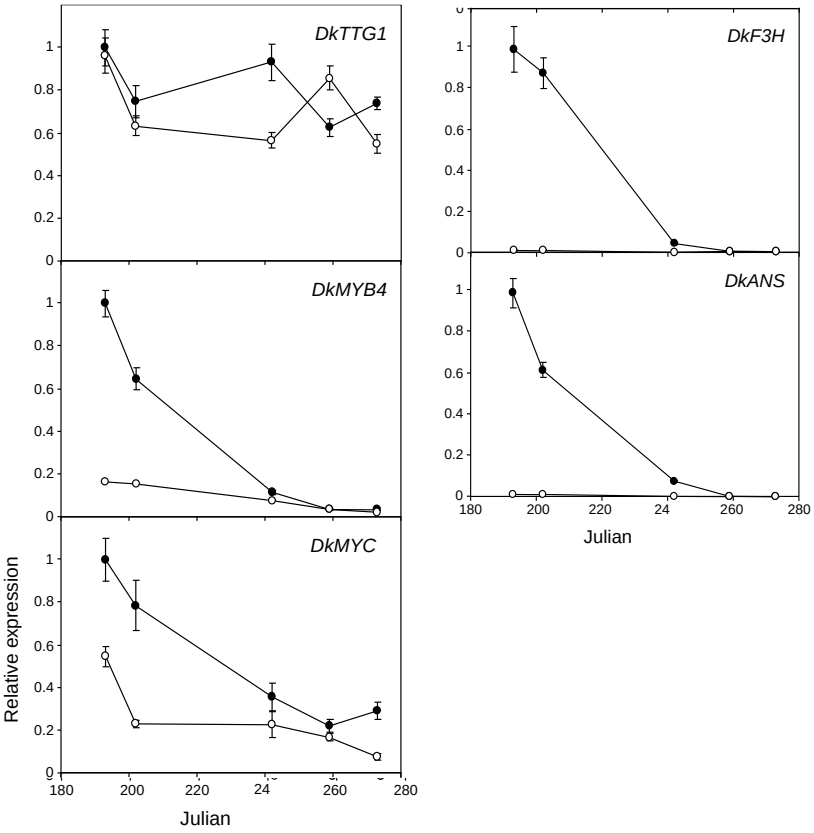

Figure 41. Relative expression of DkWDR1 and other genes involved in PA biosynthesis during fruit development in cultivars 'Hachiya' (black symbols) and 'Hana Fuyu' (white symbols). Expression levels are relative to *DkActin*. An expression value of one is assigned to the first fruit sample from 'Hachiya'. Data are means from two biological replicates with 2–3 technical replicates each, with error bars representing standard deviations

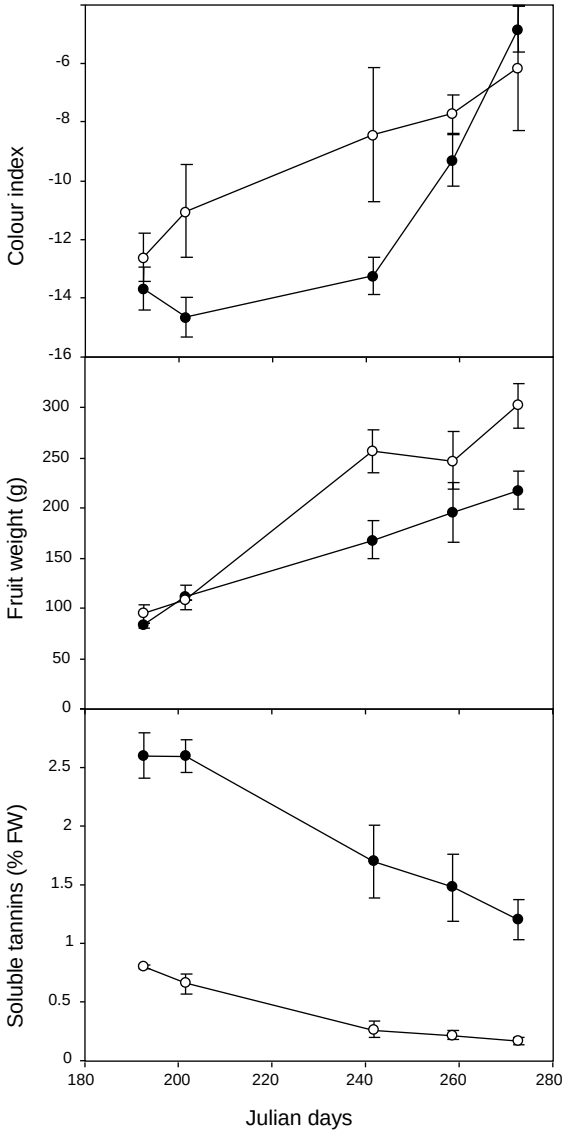

Figure 42. Development parameters of persimmon fruit samples used in this study. Colour index, fruit weight and content of soluble tannins were measured in cultivars 'Hachiya' (black symbols) and 'Hana Fuyu' (white symbols). Data are means from four different fruits, with error bars representing standard deviations.

DkWDR1 interacts with DkMYB2 and DkMYB4

We used a two-hybrid strategy to study the ability of DkWDR1 to interact with DkMYB2, DkMYB4 and DkMYC1, analogous to the MYB and bHLH components of MBW ternary complexes in persimmon. The cloning of *DkMYB2*, *DkMYB4* and *DkMYC1* into two-hybrid vectors allowed the identification of 'Hachiya' alleles different to the ones reported in databases. The cloned 'Hachiya' *DkMYB2* had three base substitutions with respect to *DkMYB2* from databases (GenBank AB503699; (Akagi et al., 2009b), A to T in position 39 from the ATG, C to T in position 496, and G to A in position 600, leading to two amino acid changes. Four different clones of *DkMYB4* sequenced in 'Hachiya' had an A to G conversion in residue 716 from the ATG, causing an amino acid change of D to G in the published sequence of *DkMYB4* (GenBank AB503701; (Akagi et al., 2009b). The three sequenced clones of *DkMYC1* were identical to each other (GenBank KR057234), but showed 26 nucleotide substitutions and an insertion of a twice-repeated GAA with respect to the 2,160 bp-long *DkMYC1* identified in the variety 'Luotiantianshi' (GenBank JF411059; (Su et al., 2012)). Such variations led to nine amino acid changes and an insertion of two residues in 'Hachiya' DkMYC1 protein.

The reporter yeast strain was transformed with the plasmids pGBKT7-*DkWDR1*, pGBKT7-*DkMYB2*, pGBKT7-*DkMYB4* and pGBKT7-*DkMYC1*, containing a fusion of the four factors with the BD, in order to check for the autonomous activation of reporter transcription. The constructs pGBKT7-*DkMYB2* and pGBKT7-*DkMYB4* transactivated the different two-hybrid reporters in the absence of a prey protein fused

to the AD (Figure 43). This confirmed that DkMYB2 and DkMYB4 proteins are able to activate the transcription of a gene when bound to its promoter, but made pGBKT7-*DkMYB2* and pGBKT7-*DkMYB4* strains useless for subsequent studies of protein interactions by growth and qualitative colorimetric assays. The subsequent transformation with pGADT7-*DkWDR1*, pGADT7-*DkMYB2*, pGADT7-*DkMYB4*, and pGADT7-*DkMYC1* fusions with AD resulted in four positive interactions measured by yeast growth in the presence of the antibiotic AbA, and the chromogenic reaction. DkWDR1 and DkMYC1 interacted with DkMYB2 and DkMYB4, but they did not interact with each other (Figure 44).

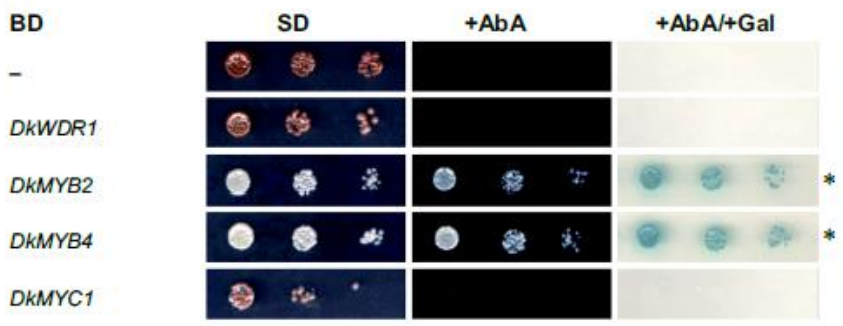

Figure 43. Two-hybrid system analysis of protein interaction. An assay of autonomous transactivation in the absence of activation domain (AD). Yeast strains were grown on a nonselective medium (SD), a growth-selective medium containing Aureobasidin A with (+AbA) or with chromogenic medium containing Aureobasidin A and X-α-Gal with (+AbA/+Gal). Positive interactions in media containing X-α-Gal are labelled with an asterisk (*)

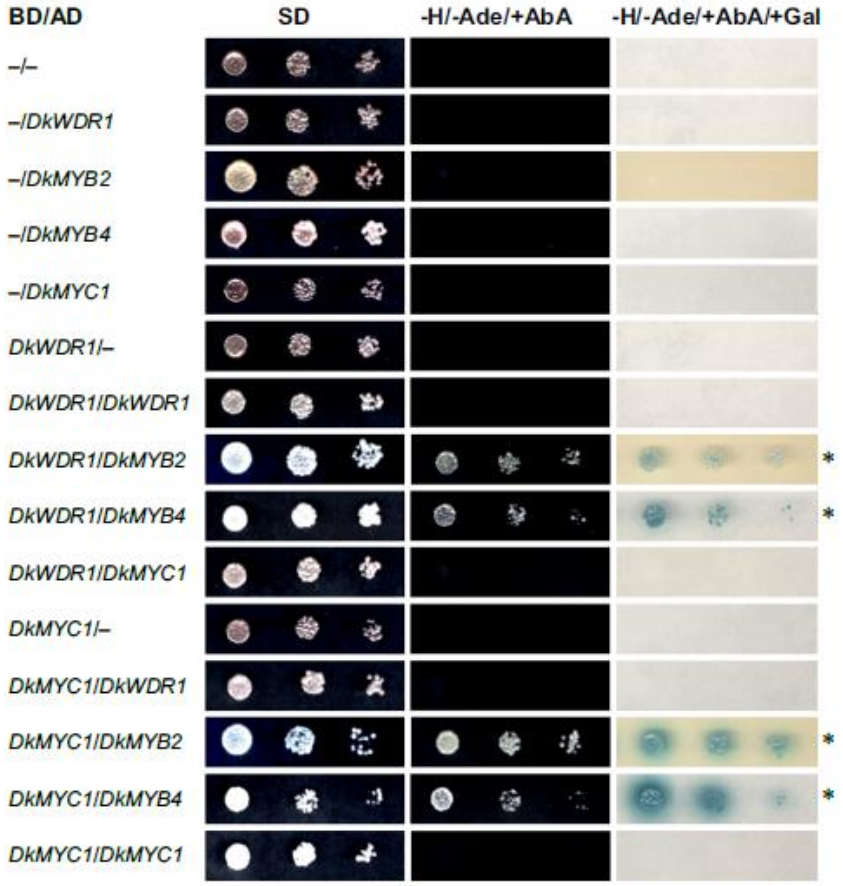

Figure 44. Two-hybrid assay using different combinations of DNA-binding domain (BD) and AD fused with DkWDR1, DkMYB2, DkMYB4 and DkMYC1. Yeast strains were grown on a nonselective medium (SD), a growth-selective medium containing Aureobasidin A with (+AbA) or without histidine and adenine (−H/−Ade/+AbA) and a chromogenic medium containing Aureobasidin A and X-α-Gal with without histidine and adenine (−H/ −Ade/+AbA/+Gal). Positive interactions in media containing X-α-Gal are labelled with an asterisk (*)

Quantitative analysis of DkMYB4 interactions

Due to the autonomous activation of reporter transcription by DkMYB2 and DkMYB4, we could not test the formation of MYB homo and heterodimers with standard qualitative assays involving growth of yeast colonies on dropout synthetic media and media containing the antibiotic AbA. However, the relative expression of the reporter *MEL1*, coding for a α-galactosidase enzyme leading to blue colonies after X-α-Gal hydrolysis in the qualitative assay used in Figure 44, can also be measured in quantitative liquid assays.

Yeast strains containing DkMYB4 fused to BD were employed to check if protein interactions significantly increased *MEL1* expression, measured as the rate of PNP-α-Gal hydrolysis in a colorimetric reaction. Yeast strains with the control pGBKT7 plasmid and the different pGADT7 vectors containing *DkWDR1*, *DkMYB2*, *DkMYB4* or *DkMYC1*did not show detectable α-galactosidase activity when compared with a reference medium sample (data not shown). However, pGBKT7-*DkMYB4* strains expressing a BD fusion of DkMYB4 were positive in the quantitative assay, and remarkably the AD fusion partner strongly influenced α-galactosidase activity. The co-expression of BD-*DkMYB4* with AD*DkMYB2*, AD-*DkMYB4*, and AD-*DkMYC1* significantly increased *MEL1* reporter expression, which provides evidences on the protein interactions DkMYB4-DkMYB2, DkMYB4-DkMYB4 and DkMYB4-DkMYC1 (Figure 45). On the other side, AD-*DkWDR1* did not apparently modify the quantitative transcriptional activation of MEL1 by BD-DkMYB4.

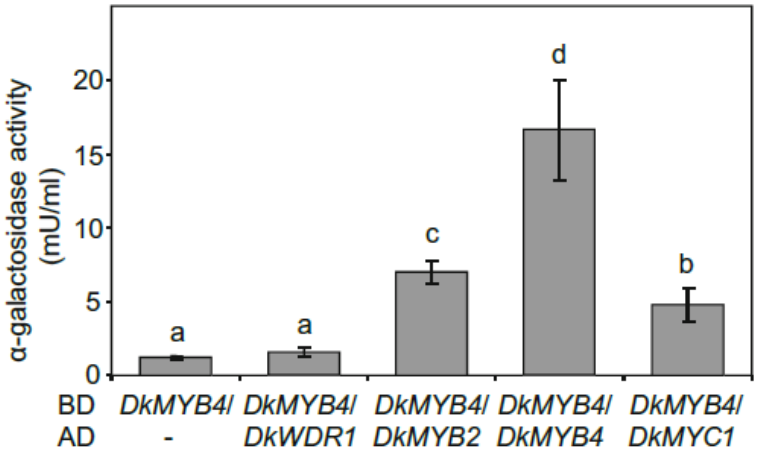

Figure 45. Evaluation of protein interaction by quantitative α-galactosidase assay. Enzyme activity was measured in DNA-binding domain (BD)- DkMYB4 yeast strains transformed with control plasmid and the activation domain (AD) fused with DkWDR1, DkMYB2, DkMYB4 or DkMYC1 genes. The α-galactosidase activity of the different media was made relative to the optical density at 600 nm. Data are means from four independent clones with three replicates each, with error bars representing standard deviations. Non-overlapping letters indicate significant difference between samples with a confidence level of 95 %

Discussion

We have described a *WD40-repeat* gene from persimmon related to Arabidopsis *TTG1* and *TTG1-like* genes from other species at the sequence level. Some of the TTG1-like proteins clustering with DkWDR1 in the phylogenetic tree have been functionally characterized by complementation of the trichome-defective and seed colouration phenotypes of *ttg1-1* mutant of *Arabidopsis* (Walker et al., 1999; Humphries et al., 2005; Brueggemann et al., 2010; Taheri et al., 2012; Schaart et al., 2013), and their effect on the transcriptional activation of the promoter of *BANYULS* (Baudry et al., 2004; Brueggemann et al., 2010; Schaart et al., 2013). Thus, DkWDR1 was similar to WD40 proteins involved in PA biosynthesis and proteins able to restore PA biosynthesis in a PA-defective mutant.

DkWDR1 expression was essentially constant along fruit development and was not tissue-specific, in close agreement with the reported expression of other WD40 genes involved in anthocyanin and PA biosynthesis in other species, such as *TTG1* from *Arabidopsis* (Walker et al., 1999) and *AN11* from petunia (De Vetten et al., 1997). On the contrary, *TT2* (MYB) and *TT8* (bHLH) from *Arabidopsis* and their counterparts in persimmon, *DkMYB4* and *DkMYC1*, showed narrower time and tissue-specific expression patterns (Nesi et al., 2000, 2001; Akagi et al., 2009b; Su et al., 2012). It suggests some degree of functional diversification in WD40-repeat genes, expressed in tissues where they are required for PAs and anthocyanin biosynthesis, and others where they could perform a different function.

The fact that DkWDR1 expression and its allelic diversity were comparable between the astringent cultivar 'Hachiya' and the non-astringent 'Hana Fuyu' indicates that *DkWDR1* gene is not the causal origin of the non-astringent phenotype of 'Hana Fuyu' and related cultivars. Recent attempts to isolate factors involved in *DkMYB4* expression (Akagi et al., 2011b, 2012) could provide new clues about the origin of this mutation. TTG1 protein is involved in PAs biosynthesis in the seed coat of *Arabidopsis* by means of its interaction with MYB and bHLH transcription factors to form a MBW ternary complex (Baudry et al., 2004; Xu et al., 2014b). Multiple reports describe the function of related MBW complexes, arguing for the presence of similar regulatory mechanisms orchestrating the temporal and spatial expression of genes involved in anthocyanin and PA biosynthesis in different species (Hichri et al., 2011; Xu et al., 2015). Since the characterization of MYB-type transcription factors involved in PAs biosynthesis in fruit (Akagi et al., 2009b, 2010a), and a bHLH gene (*DkMYC1*) differentially expressed in astringent and nonastringent fruit (Su et al., 2012), MBW complexes have been also postulated to drive PAs biosynthesis in persimmon fruit. However this idea has not been supported by experimental studies until now.

In the yeast two-hybrid system DkMYB2 and DkMYB4 interacted with DkMYC1 and the WD40-repeat protein encoded by the gene identified in this study *DkWDR1*. Thus, these factors could form different ternary complexes similar to other described MBWs, due to their confluent expression in early stages of fruit development, with a potential impact on PAs accumulation by virtue of the differential

expression of *DkMYB4* and *DkMYC1* in astringent and non-astringent fruit. Contrarily to the interaction of WD40 and bHLH proteins observed in different MBW models (Payne et al., 2000; Baudry et al., 2004; An et al., 2012; Liu et al., 2013; Schaart et al., 2013), DkWDR1 and DkMYC1 did not interact in the yeast two-hybrid system. In *Perilla frutescens*, the interaction of MYC-RP (bHLH) with PFWD (WD-40) has been proposed to mediate the nuclear localization of PFWD (Sompornpailin et al., 2002). Under our results the translocation of DkWDR1 to the nucleus could require alternative mechanisms.

The yeast reporters were strongly transactivated by *DkMYB2* and *DkMYB4* fused to BD (Figure 43), as similarly observed in the anthocyanin biosynthesis regulators *FaMYB5*, *FaMYB9* and *FaMYB11* from strawberry (Schaart et al., 2013), and *C1* from maize (Goff et al., 1992). On the contrary, *TT2* from *Arabidopsis* did not autoactivate the yeast two-hybrid reporter (Baudry et al., 2004). Thus, the transactivation response of DkMYB2 and DkMYB4 when targeted to a gene promoter seems to be a quite usual but not general feature of MYB components from MBW complexes.

Quantitative liquid assays of α-galactosidase activity additionally confirmed the interaction of DkMYB4 with DkMYC1, and the probable occurrence of homo- and heterodimers of MYB proteins (Figure 45). However, the interaction of DkWDR1 and DkMYB4 when using DkWDR1 fused to BD (Figure 44) was not confirmed in these quantitative experiments using BD-DkMYB4 (Figure 45). Such one-direction interactions have been often encountered in yeast two-hybrid experiments. The protein interaction data obtained in this

study support the occurrence of MBW complexes in persimmon fruit, composed of fixed or variable combinations of at least four different proteins containing MYB, bHLH and WD40-repeat domains. Contrarily to other species studies, our data suggest a key structural role of the MYB proteins DkMYB2 and DkMYB4 in the formation of MBW complexes, due to the lack of observable interaction between the other two putative components, DkWDR1 and DkMYC1 (Figure 46). Functionally different complexes could be formed containing either DkMYB2 or DkMYB4, plausibly affecting different gene targets or combining the inputs of different regulatory signals. Alternatively, DkMYB2 and DkMYB4 could be both essential for a fully functional complex; or they could perform interchangeable roles. In non-astringent varieties, the impaired expression of both *DkMYB4* and *DkMYC1* would ensure a low activity of proposed MBW complexes even under the scenario of functional redundancy between MYB proteins.

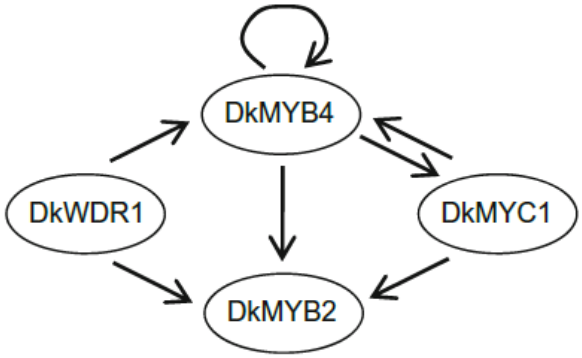

Figure 46. Schematic representation of the two-hybrid interactions identified in this study. Arrowheads indicate the protein fused to the activation domain (AD). DkMYB2 fused to the DNA-binding domain (BD) was not tested

These complexes have been postulated to regulate the biosynthesis of PAs leading to the astringent taste of persimmon fruit. Thus, a deeper knowledge of the components of these complexes and their regulation may provide plant biotechnologists with suitable tools for breeding related to fruit astringency in persimmon.

MBW complexes impinge on anthocyanidin reductase gene regulation for proanthocyanidin biosynthesis in persimmon fruit

Abstract

MBW protein complexes containing MYB, bHLH and WD40 repeat factors are known transcriptional regulators of secondary metabolites production such as proanthocyanidins and anthocyanins, and developmental processes such as trichome formation in many plant species. DkMYB2 and DkMYB4 (MYB-type), DkMYC1 (bHLH-type) and DkWDR1 (WD40-type) factors have been proposed by different authors to take part of persimmon MBW complexes for proanthocyanidin accumulation in immature fruit, leading to its characteristic astringent flavour with important agronomical and ecological effects. We have confirmed the nuclear localization of these proteins and their mutual physical interaction by bimolecular fluorescence complementation analysis. In addition, transient expression of *DkMYB2*, *DkMYB4* and *DkMYC1* cooperatively increase the expression of a persimmon anthocyanidin reductase gene (*ANR*), involved in the biosynthesis of *cis*-flavan-3-ols, the structural units of proanthocyanidin compounds. Collectively, these data support the presence of MBW complexes in persimmon fruit and suggest their coordinated participation in *ANR* regulation for proanthocyanidin production.

Introduction

Proanthocyanidins (PAs), or condensed tannins, are flavonoid polymers that accumulate in fruits, leaves, seeds and other tissues of many plants, providing protection against pathogens and herbivores. PAs also contribute to fruit flavour and colour and are considered beneficial for human health in virtue of their antioxidant properties, among other salutary attributes (Dixon et al., 2005). In persimmon (*Diospyros kaki*), the microstructure and accumulation of soluble PAs of the so called tannin cells has been found related to fruit astringent taste (Yonemori and Matsushima, 1985; Salvador et al., 2007), potentially affecting fruit palatability for frugivorous animals (Bernays et al., 1989). Interestingly, soluble tannins are reduced throughout persimmon fruit development and maturation (Salvador et al., 2007; Tessmer et al., 2016), providing a way to channel the action of frugivores when seeds are fully viable and ready for dispersal. In addition to a poorly known mechanism involving the transcriptional repression of PA biosynthetic enzymes (Nishiyama et al., 2018), soluble PA content is reduced during fruit ripening by the production of acetaldehyde by seeds, leading to PA insolubilization and the subsequent astringency loss (Sugiura et al., 1979; Sugiura & Tomana, 1983). Although the content of soluble tannins becomes undetectable from a sensory point of view at overripening stages, the concomitant loss of fruit firmness importantly limits fruit postharvest life and therefore the commercialization opportunities. To overcome this limitation, the fruit is harvested before overripening and subjected to deastringency postharvest treatments to remove astringency while maintaining high firmness (Ben-Arie and Sonego,

1993). Most of deastringency methods in persimmon are based on maintaining the fruit under anaerobic conditions or exposing them to products that induce anaerobic respiration. Under these conditions, soluble tannins are polymerized by acetaldehyde accumulated in the flesh (Matsuo and Itoo, 1982; Pesis and Ben-Arie, 1984). Furthermore, natural non-astringent mutants exist into persimmon germplasm collections. Several of these non-astringent cultivars are hypothesized to carry a recessive mutation in a single gene known as *AST* (Kanzaki et al., 2001; Yamada and Sato, 2002), but the molecular function and identity of this gene remain unknown. Postharvest treatments of astringent varieties improve the postharvest life and the organoleptic quality of treated fruit, however these treatments represent an important production cost and are often a challenge for new varieties or stressed orchards (Besada et al., 2016). Thus, studying PAs biosynthesis and metabolism in persimmon fruit may help to better understand the different mechanisms employed by plants to drive frugivore-dependent dispersal of seeds, and to improve deastringency treatments and crop management with the aim to reduce costs and increase the sustainability of persimmon production.

The pathway of PAs biosynthesis has been genetically dissected by the analysis of different seed mutants in *Arabidopsis thaliana*, barley and maize among other species (Lepiniec et al., 2006). PAs are formed by condensation of *trans*- and *cis*-flavan-3-ols units, synthesized respectively by stereospecific leucoanthocyanidin reductase (LAR) and anthocyanidin reductase (ANR) enzymes (Tanner

et al., 2003; Xie et al., 2003). These PA biosynthetic activities and genes are essentially conserved in persimmon, with some regulatory particularities (Ikegami et al., 2007). In persimmon fruit, *ANR* gene is much more expressed than its counterpart *LAR*, consistent with the higher content of *cis*-flavan-3-ols stereoisomers in PA composition (Akagi et al., 2009a). In addition, *ANR* is strongly repressed in advanced steps of fruit maturation, concomitantly with tannin decrease, which points to a role of *ANR* as a major integrative target of PA regulatory pathways in persimmon.

In *Arabidopsis*, regulation of the *ANR* orthologous gene *BANYULS* (*BAN*) and PA accumulation in seed coat requires the concerted action of *TRANSPARENT TESTA2* (*TT2*), *TRANSPARENT TESTA8* (*TT8*) and *TRANSPARENT TESTA GLABRA1* (*TTG1*), encoding respectively a R2R3-MYB transcription factor, a basic helix-loop-helix (bHLH) transcription factor and a WD40-repeat (WDR) protein (Baudry et al., 2004). These regulatory factors form a ternary complex named MYB-bHLH-WD40 (MBW) that may invoke the participation of alternative MYB and bHLH components for the regulation of particular steps of PA and anthocyanin biosynthetic pathways (Xu et al., 2014a, 2015). MBW complexes also contribute to PAs production in edible fruits of crop plants such as grapevine (Hichri et al., 2010), strawberry (Schaart et al., 2013), apple (Gesell et al., 2014) and persimmon (Naval et al., 2016).

In persimmon, *DkMYB2* and *DkMYB4* genes cause an altered pattern of PAs accumulation and expression of biosynthetic enzymes when misexpressed, and increase *ANR* promoter transcriptional activity in

transient reporter assays when combined with a heterologous bHLH factor from *Arabidopsis* (Akagi et al., 2009b, 2010a). Interestingly, DkMYB2 and DkMYB4 specifically recognize different MYB-binding cis-elements by electrophoretic mobility shift assays, arguing for certain degree of subfunctionalization (Akagi et al., 2010a). On the other hand, a persimmon bHLH encoding gene named *DkMYC1* is underexpressed in non-astringent cultivars, following an expression pattern in fruit similar to *DkMYB4* (Su et al., 2012). DkMYC1 protein interacts with DkMYB2 and DkMYB4, and these, in turn, interact with the WD40-repeat protein DkWDR1 by two-hybrid analysis, suggesting the conserved participation of MBW complexes in PA synthesis regulation in persimmon fruit (Naval et al., 2016). In this study, we go further on the cytological and molecular characterization of MBW complex in persimmon by approaching the subcellular localization, protein interaction and transcriptional regulation effects of these MYB (DkMYB2 and DkMYB4), bHLH (DkMYC1) and WD40 (DkWDR1) components.

Material and methods

Plant material

Diospyros kaki Thunb. cvs 'Hachiya' (astringent fruit) and 'Hana Fuyu' (non-astringent fruit) were grown in an orchard located in Museros (Spain; 39° 34' 40" N, 0° 21' 46" W) under standard agricultural practices (Bellini and Giordani, 2002). Four fruit samples per cultivar were collected at different maturation stages on the following dates in 2011: July 12, July 21, August 30, September 16 and September 30 (Naval et al., 2016). Soluble tannins were evaluated using the Folin-Denis method (Taira, 1996), as described previously (Arnal and Del Rio, 2004), and results were expressed as percentage of fresh weight (FW).

Gene isolation

The *Diospyros kaki* (cv. 'Hachiya') genes *DkMYB2* (AB503699.1), *DkMYB4* (KR057233.1), *DkMYC1* (KR057234.1) and *DkWDR1* (KR057229.1) were obtained from pGADT7 plasmids described in a previous study (Naval et al., 2016). In order to identify *DkMYB4* and *DkMYC1* promoter sequences, a manual assembly of *D. lotus* cv. Kunsenshi genome reads stored in the Sequence Read Archive (SRA) database (ID: SRP045872) was performed (Akagi et al., 2014). For amplifying *ANR* promoter, we designed primers (Supplementary Table 1) from the previously published sequence of *D. lotus* gene (AB504523.1). *ANR* promoter amplification was not possible in *D. kaki*, and therefore the *D. lotus* promoter was used in the analysis. *DkMYB4* and *DkMYC1* promoters were amplified from *D. kaki* cv. 'Hachiya' genomic DNA (Supplementary Table 1). The DNA of both *D.*

kaki and *D. lotus* was extracted from fresh leaves following a standard CTAB DNA extraction protocol (Doyle and Doyle, 1987).

Plasmid construction

For the construction of subcellular localization and BiFC vectors, each of the four genes were amplified (Supplementary Table 1) with a 15 bp target vector residue at the 5' end needed for recombination with the In-Fusion HD Cloning kit (Takara Bio, Otsu, Japan). Fragments were purified and cloned into ampicillin resistant pSK+35S-eGFP-PoPit vectors (Herranz et al., 2005) and two cassettes for each protein were made for subcellular localization. Four cassettes for each protein were made with ampicillin resistant pSK+35S-(N-YFP or C-YFP)-PoPit vector (Leastro et al., 2015) for BiFC analysis. The fragments containing the expression cassette from pSK vectors were digested with *Hin*dIII and subcloned into the kanamycin resistant pMOG800 vector (Knoester et al., 1998).

In order to construct the vectors for transient expression, the four genes contained in pGADT7 plasmids (Naval et al., 2016) were digested with *Sac*I and *Xho*I to release the insert. The fragments were purified and inserted in a pGreenII-62-SK kanamycin resistant vector (Hellens et al., 2000), previously linearized with *Sac*I/*Xho*I. The promoter sequences were amplified from vectors using specific primers with restriction enzyme sequences tails at 5' (Supplementary Table 1). The purified PCR products were digested (*Hin*dIII/*Pst*I for *ANR* and *DkMYC1* promoters and *Hin*dIII/*Nco*I for *DkMYB4* promoter), purified and cloned into linearized pGreenII-0800-LUC kanamycin resistant vector (Hellens et al., 2000).

All the described vectors were provided by Dr. J. A. Sánchez-Navarro (Instituto de Biología Molecular y Celular de Plantas "Primo Yúfera", Valencia, Spain). Plasmids containing gene and promoter constructs were finally transferred to *Agrobacterium tumefaciens* strain C58 by electroporation. For pMOG800 vectors, transformation was carried out in bacteria containing the virulence helper plasmid pCH32 (Hamilton et al., 1996). All DNA constructions were verified by plasmid DNA sequencing.

Subcellular localization of MBW complex proteins in vivo

To characterize the subcellular localization of the MBW complex components, each protein was fused at either the Nt or the Ct of eGFP and transiently expressed *in planta*. For a better visualization of the fluorescence signal, all proteins were co-expressed with the silencing suppressor HC-Pro protein from the *Tobacco Etch Virus* (Leastro et al., 2015). *A. tumefaciens* C58 strains were grown overnight in LB media supplemented with kanamycin and rifampicin, at 28 ºC. Cultures were centrifuged 5 min at 4,000 x g, and pellets were resuspended in infiltration media ($MgCl_2$ 10 mM + MES 10 mM pH 5.6) to an OD_{600} of 0.5 for each construct and an OD_{600} of 0.1 for the HC-Pro. *N. benthamiana* young plants (2 pairs of leaves) were agroinfiltrated as previously described (Genoves et al., 2011). Plants remained in a greenhouse at 24 ºC (day) and 18 ºC (night) with a 16 h light photoperiod. Three days after infiltration, leaf samples were collected and mounted in a microscope slide with a drop of water. Observation of the fluorescence in the underside epidermis was performed with a Leica TCS SL confocal microscope (λ_{exc} = 488 nm;

λe_m = 492–533 nm for eGFP). For the nucleus and nucleolus subcellular colocalization, the proteins were coinfiltrated with cultures (OD_{600} 0.1) expressing the NLS of SV40 large T antigen fused to the red fluorescent protein and the fibrillarin fused to the cherry fluorescent protein, respectively (λ_{exc} = 561 nm; λe_m = 588-634 nm).

Bimolecular fluorescence complementation assays (BiFC)

In the BiFC assay (Aparicio et al., 2006), addressed to characterize the interaction between the components of the hypothetical MBW complex, all the possible two-by-two combinations of homodimers and heterodimers were assayed *in planta*. Chimeric proteins were transiently co-expressed in *N. benthamiana* using *A. tumefaciens* (strain C58) cultures (OD_{600} = 0.4) transformed with the corresponding binary plasmids pMOG800, as previously described (Genoves et al., 2011). To increase the expression of the different proteins, we included an *A. tumefaciens* culture (OD_{600} = 0.1) expressing the HC-Pro. At 3 days post-infiltration, the fluorescence reconstitution was monitored in the confocal Leica TCS SL (λexc = 488 nm; λem = 492-533 nm).

Western blot assay

Samples from the BiFC assay were immediately frozen in liquid nitrogen. Frozen leaves (50 mg) were ground and proteins were extracted with 200 µl of Laemmli buffer (Laemmli, 1970), boiled for 5 min and centrifuged for 1 min at 15,800 × g to pellet cellular debris. For protein separation, 25 µl of the mixture was subjected to 12 % sodium dodecylsulphate-polyacrylamide gel electrophoresis (SDS-PAGE). Gels were electrotransferred to nitrocellulose membranes

following the manufacturer's recommendations. Proteins were detected on western blots using an anti-GFP N-terminal antibody (Sigma, St. Louis, MO, USA; cat. no. G1544) for N-terminal yellow fluorescent protein (NtYFP) fusions, and anti-GFP antibody (Roche, Basel, Switzerland; cat. no. 11814460001) for C-terminal YFP (CtYFP) fusions, followed by a secondary peroxidase-labelled antibody and incubation with a chemiluminescence substrate (Amersham™ ECLTM Prime Western Blotting Detection Reagent). The chemiluminescence was detected exposing photographic film to the membranes.

Dual luciferase assay

To determine the effects of the hypothetical MBW protein complex on the promoters of *ANR*, *DkMYB4* and *DkMYC1* genes, a dual luciferase assay was performed. The effect of the homo and heterodimers formed by two and three proteins was assayed by the co-expression of the promoter and protein vectors as previously described in *N. benthamiana* with *A. tumefaciens* strain C58. HC-Pro was also used for enhancing the transient expression of the different proteins. After 3 days, 30 mg of agroinfiltrated leaves from 3 biological replicates, were sampled for each combination. Samples were immediately frozen in liquid nitrogen. For measuring promoter activity, samples were ground to powder and then Firefly (LUC) and Renilla (REN) luciferase activity was measured following the Dual-Luciferase Reporter Assay System (Promega, Madison, WI, USA) with the aid of a Promega GloMax Multi Microplate Reader luminometer. Promoter activity was measured as the quotient between the

LUC/REN ratio of promoter plus transcription factors samples and the LUC/REN ratio of promoter without additional factors.

Isolation of RNA and quantitative real-time RT-PCR (qRT-PCR)

Total RNA was isolated from 150 mg of fruit flesh using a cetyltrimethylammonium bromide (CTAB)-based procedure (Gambino et al., 2008). Genomic DNA was removed with the RNase-Free DNase Set (Qiagen, Hilden, Germany) according to manufacturer's instructions. Purified RNA was reverse transcribed with PrimeScript RT Reagent Kit (Takara Bio). qRT-PCR was performed in a StepOnePlus Real-Time PCR System (Life Technologies, Carlsbad, CA, USA), using 1-2 µl of 10X diluted cDNA, SYBR premix Ex Taq (Tli RNaseH plus) (Takara Bio) and primers shown in Supplementary Table 1, in a total volume of 20 µl. The PCR protocol consisted of 10 min at 95 °C, followed by 40 cycles of 15 s at 95 °C, and 1 min at 60 °C. PCR specificity was confirmed by the presence of a single peak in the dissociation curve and by agarose electrophoresis. We used *DkActin* as reference gene (Akagi et al., 2009b; Naval et al., 2016). A relative standard curve procedure was employed for measuring relative expression. Results were the average of two independent biological replicates with 2–3 technical replicates each.

Results

Subcellular localization of MBW complex components

As transcription factors belonging to a hypothetical regulatory protein complex, DkMYB2, DkMYB4, DkMYC1 and DkWDR1 are expected to co-localize temporarily in the cell nucleus where they

interact and perform their regulatory role within the framework of a developmental programme. The subcellular localization of these four putative MBW components in persimmon has been elucidated by transient expression in *Nicotiana benthamiana* leaves of the four corresponding genes fused to enhanced green fluorescent protein (eGFP) gene. According to the localization of specific nucleus and nucleolus markers, DkMYB2, DkMYB4 and DkMYC1 show differential nucleus/nucleolus partitioning when eGFP fusion is either at the N-terminal (Nt) or C-terminal (Ct), suggesting that eGFP position affects protein targeting (Figure 47). Protein fusions with higher abundance in the nucleolus are DkMYB2-eGFP, DkMYB4-eGFP and eGFP-DkMYC1, whereas DkWDR1-eGFP shows appreciable presence in the cytoplasm in spite of its predominant localization in the nucleus. Overall, these four transcription factors show preferential localization in the nuclear compartment, and consequently physical interactions at the protein level occur most plausibly in the nucleus.

In vivo interaction of DkMYB2, DkMYB4, DkMYC1 and DkWDR1

Physical protein interactions among members of MBW complex involved in PAs accumulation in persimmon fruit has been only previously tested by the two-hybrid system in the yeast model, however no additional *in planta* evidences have been obtained on the formation of this complex. To asses this issue, we have assayed pair-wise interactions between DkMYB2, DkMYB4, DkMYC1 and DkWDR1 factors by bimolecular fluorescence complementation (BiFC) and transient expression in *N. benthamiana*. The Nt and Ct fragments of the yellow fluorescent protein (YFP), required for

reassembling of the fluorescent reporter, have been tested on both Nt and Ct sides of each transcription factor. Positive protein interactions by BiFC are shown in Figure 48a. According to these results, DkMYB4 and DkMYC1 are able to interact with the rest of the factors and with themselves, and DkWDR1 does not reconstitute YFP fluorescence when paired with DkMYB2 and itself. This reproduces previous yeast two-hybrid results with few exceptions (Figure 48b). Particularly, DkMYC1 homodimerization was not observed, and DkMYB2 self-interaction was not assayed due to autoactivation issues in former yeast-two hybrid experiments. Moreover, DkMYB2-DkWDR1 and DkMYC1-DkWDR1 interactions have been exclusively detected by yeast-two hybrid and BiFC analysis, respectively. A western analysis of transiently transformed leaves confirms that *DkWDR1* and *DkMYB2* were successfully co-expressed in different construct combinations and hence, the absent interaction of DkWDR1 with itself and DkMYB2 are not due to deficient protein synthesis or accumulation (Supplementary Figure 7). Overall, these data support the biochemical ability of these factors to associate in a putative MBW complex *in planta*.

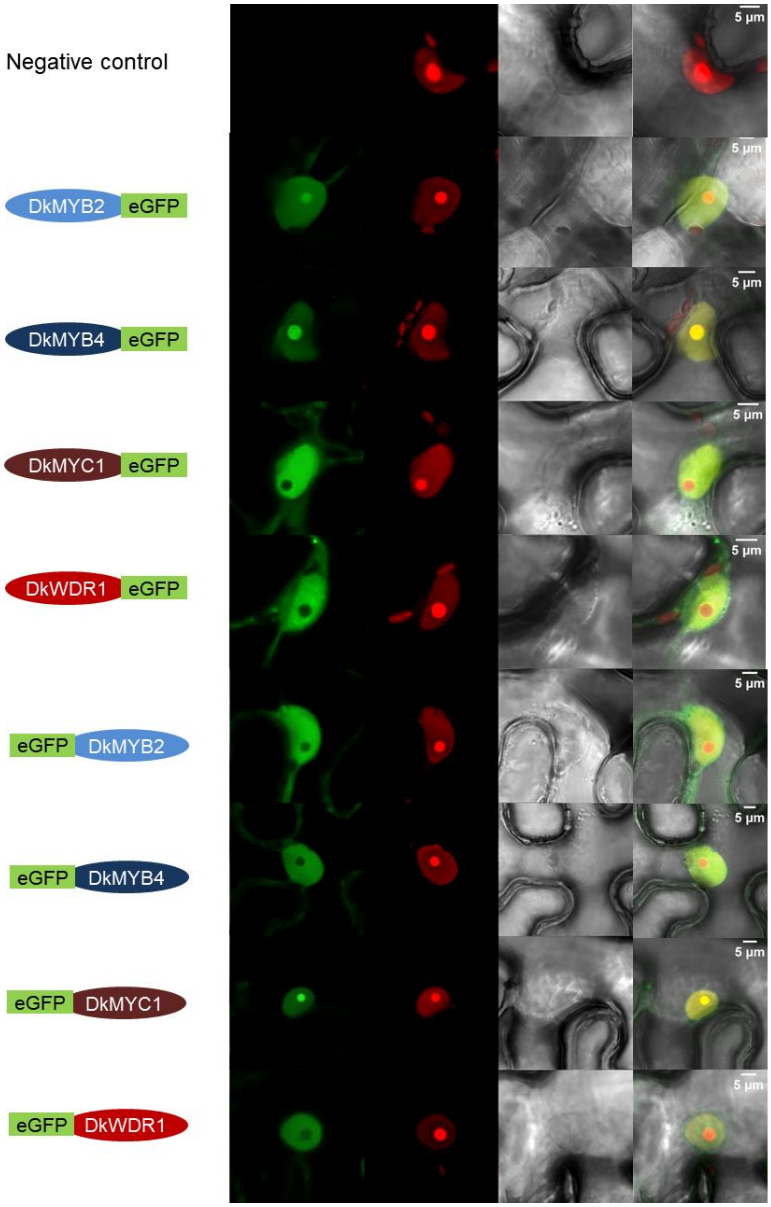

Figure 47. Nuclear localization of MBW factors. *Nicotiana benthamiana* leaves agroinfiltrated with *DkMYB2*, *DkMYB4*, *DkMYC1* and *DkWDR1* constructs containing Ct (right green label) or Nt (left green label) eGFP tags, were co-expressed with nucleus/nucleolus markers. The green (GFP), red (nucleus/nucleolus marker), transmitted light (TL) channels and merged images are shown in the figure. The fluorescent signals were visualized at 72 hours post-infiltration. Scale bars are shown in merged images.

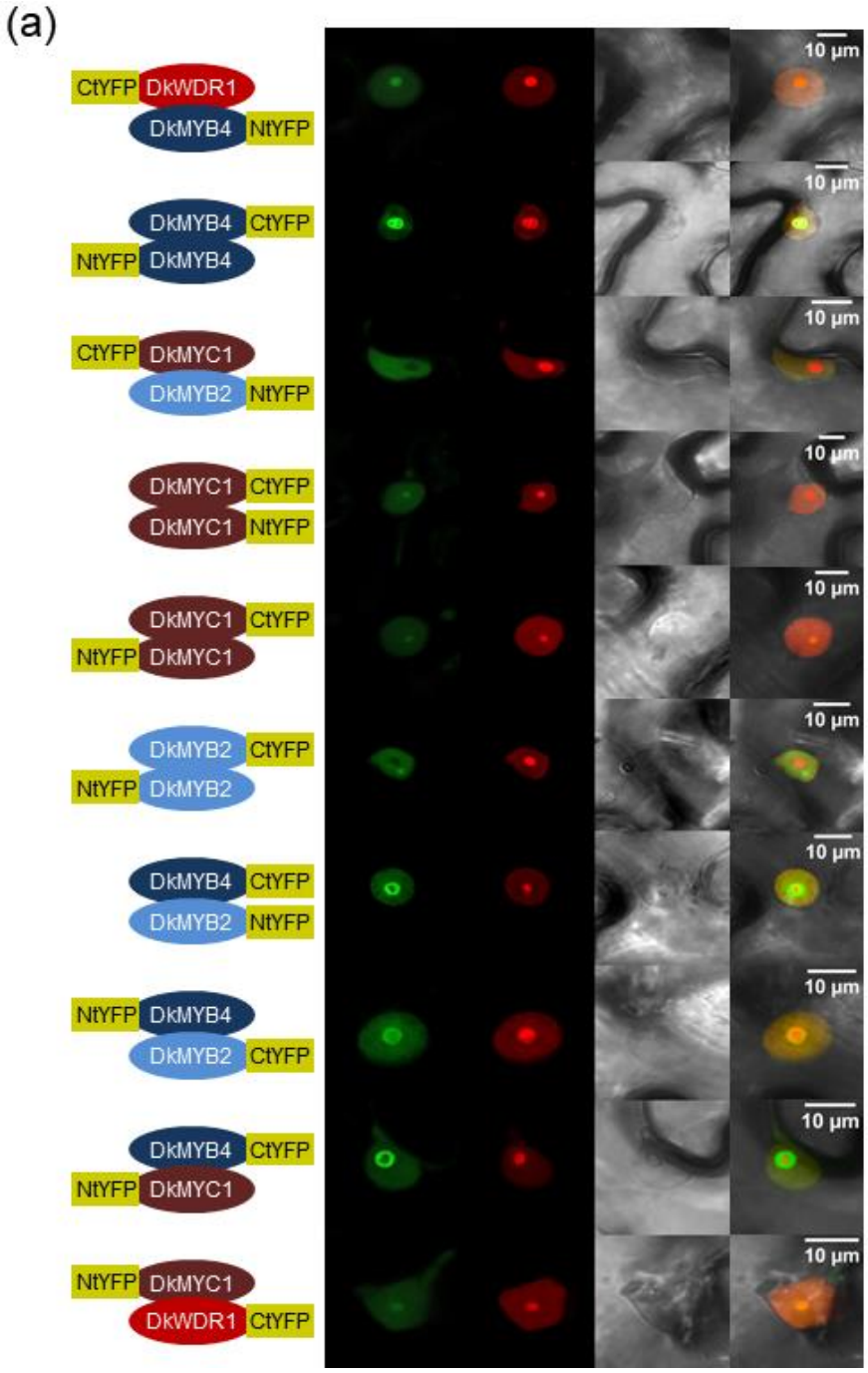
(a)
CtYFP DkWDR1
DkMYB4 NtYFP
DkMYB4 CtYFP
NtYFP DkMYB4
CtYFP DkMYC1
DkMYB2 NtYFP
DkMYC1 CtYFP
DkMYC1 NtYFP
DkMYC1 CtYFP
NtYFP DkMYC1
DkMYB2 CtYFP
NtYFP DkMYB2
DkMYB4 CtYFP
DkMYB2 NtYFP
NtYFP DkMYB4
DkMYB2 CtYFP
DkMYB4 CtYFP
NtYFP DkMYC1
NtYFP DkMYC1
DkWDR1 CtYFP
10 µm

(b)

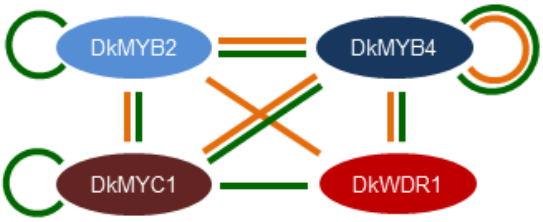

Figure 48. a) Protein interactions of MBW factors by bimolecular fluorescence complementation assays (BiFC). *N. benthamiana leaves* agroinfiltrated with different combinations of MBW factors fused to NtYFP or CtYFP peptides in Ct (right yellow label) or Nt (left yellow label) positions together with nucleus/nucleolus markers. The green reconstituted fluorescence (YFP), red (nucleus/nucleolus marker), transmitted light (TL) channels and merged images are shown in the figure. b) A diagram of previous yeast two-hybrid (orange lines) and positive BiFC interactions obtained in this study (green lines). The fluorescent signals were visualized at 72 hours post-infiltration. Scale bars are shown in merged images.

DkANR expression correlates well with PA accumulation and astringency

PA content has been measured at different points of fruit development in 'Hachiya' cultivar, starting in July and finishing in September, after external colour change has been initiated and before ripening leads to fruit softening and natural deastringency (Figure 49a). During that period fruit average weight increases three-fold and the percentage of PA decreases concomitantly (Figure 49a). Fruit soluble PA content is a balance between PA biosynthesis and insolubilization. PA insolubilization is mediated by acetaldehyde accumulation as a result of ripening and deastringency treatments (Matsuo and Itoo, 1982; Pesis and Ben-Arie, 1984). Acetaldehyde content in these 'Hachiya' fruit samples reaches values around 0.1 mg per 100 ml of juice (Figure 49b), which is by far lower than acetaldehyde produced in stored fruit and fruit treated for deastringency (Hribar et al., 2000; Salvador et al., 2007). Thus, PA

insolubilization due to acetaldehyde accumulation is not expected to contribute significantly to reduce soluble PA level in our samples, and PA content is mostly dependent on its biosynthesis rate. When representing the total estimated amount of PAs per fruit instead of its relative percentage, PA amount remains almost unchanged during the whole interval, with the exception of an initial increase in July samples (Figure 49b). As we consider that PA reduction by acetaldehyde-dependent insolubilization is relatively low, the observed decrease in relative PA content in Figure 49a must be mostly due to a growth dilution effect, and the rate of PA biosynthesis is expected to be also low in this period. As anthocyanidin reductase encoded by *ANR* gene has been postulated to perform a key role in PA biosynthesis, we have measured *DkANR* expression in 'Hachiya' fruit samples by qRT-PCR. *DkANR* transcript sharply decreases until a 0.01-fold change during the whole period (Figure 49c), which cannot be explained by just growth dilution effects. On the contrary, it indicates a strong transcriptional repression in advanced developmental stages. The higher expression of *DkANR* in initial samples is in close agreement with the concurrent increase in total PA content per fruit (Figure 49c). Then PA content remains steady in concordance with *DkANR* down-regulation (Figure 49b and c). Such a positive correlation between *DkANR* expression and astringent-responsible PAs is confirmed in the low-PA non-astringent cultivar 'Hana Fuyu', which shows a constantly low *DkANR* expression during fruit development stages (Figure 49c).

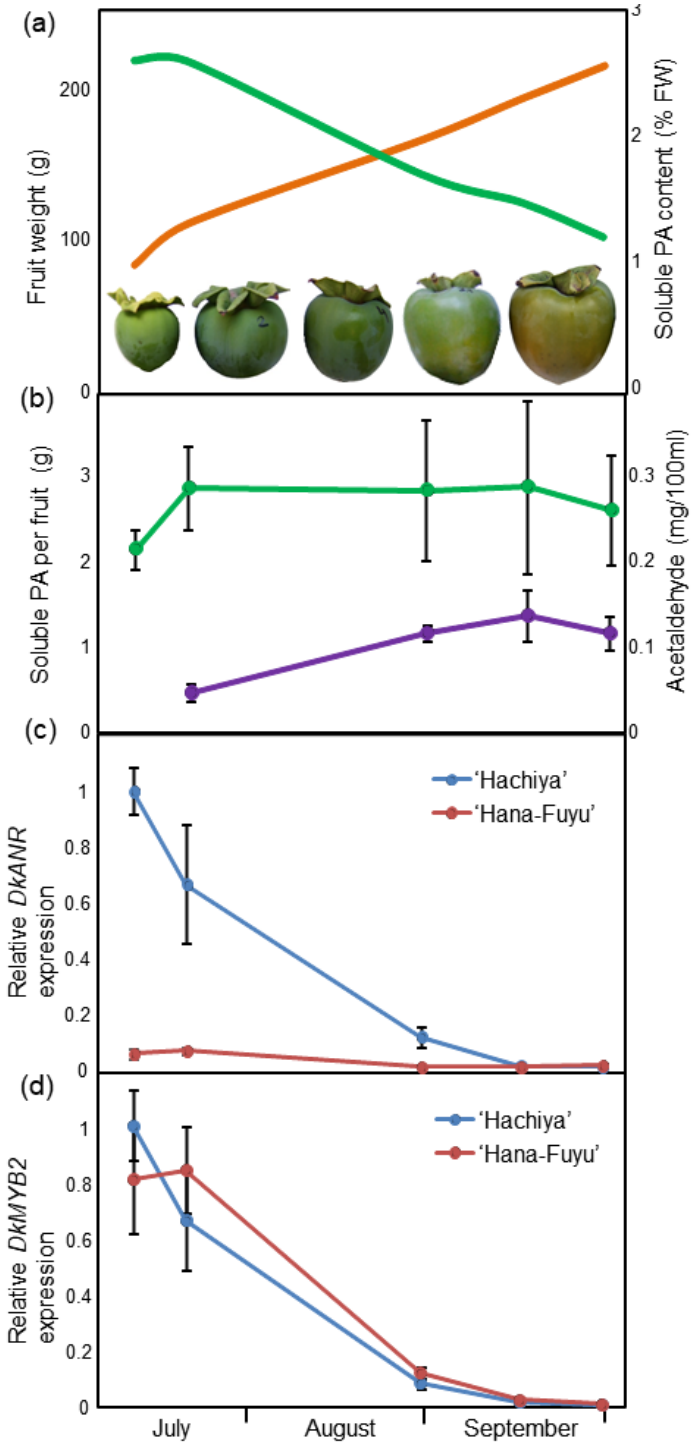

Figure 49. Proanthocyanidin (PA) content and gene expression during fruit development in persimmon. Fruit weight (orange line) and PA relative content (green line) in 'Hachiya' cultivar at different fruit development stages (a). Acetaldehyde accumulation (violet label) and total estimated PA content per fruit unit (green label) in 'Hachiya' (b). Relative gene expression of *DkANR* (c) and *DkMYB2* (d) by qRT-PCR in the fruit samples shown in (a) and (b). The astringent cultivar 'Hachiya' (blue label) and the non-astringent cultivar 'Hana Fuyu' with the *ast* mutation (red label) have been analyzed. Data are means from four different fruits for anatomical and chemical analysis, and two biological replicates for gene expression. Error bars represent standard deviations.

Other PA biosynthetic regulators, such as *DkMYB4* and *DkMYC1*, reproduce well this low expression profile in 'Hana Fuyu' and other non-astringent cultivars, as shown in previous studies (Akagi et al., 2009b; Su et al., 2012; Naval et al., 2016). However, *DkMYB2* relative expression decays in a similar way in both astringent and non-astringent cultivars (Figure 49d), suggesting a common mechanism involving *AST* locus-dependent regulation of *DkMYB4* and *DkMYC1*, with no impact on *DkMYB2* expression.

Effect of MBW factors on the activity of ANR promoter

Based on PA-linked expression of these genes, we have cloned three DNA fragments (1.2-1.4 kb) of the promoter and 5' UTR of *DkMYB4*, *DkMYC1* and the *D. lotus ANR*, in the pGreenII-0800-LUC vector. These vectors synthesize luciferase reporter (LUC) under the action of our selected promoters, in order to test the regulatory effect of individual and combined MBW factors on the activity of these promoters by a dual luciferase assay, using expression of the REN reporter gene as internal reference.

DkMYB2 transient expression in *N. benthamiana* leaves increases *ANR* promoter transcriptional activity three-fold, whereas *DkMYB4*, *DkMYC1* and *DkWDR1* do not modify it significantly (Figure 50a). Interestingly, any combination of two or three elements containing both *DkMYC1* and a MYB gene (*DkMYB2* or *DkMYB4*), strongly increases LUC/REN ratio, being highest when *DkMYC1* and *DkMYB2* are co-expressed. On the contrary, *DkWDR1* does not improve *ANR* promoter expression under any gene combination.

As *DkMYB4* and *DkMYC1* genes are similarly down-regulated during fruit development concomitantly with PA reduction, and are differentially expressed in a non-astringent cultivar (Akagi et al., 2009b; Su et al., 2012; Naval et al., 2016), their promoters have been also cloned and tested by dual luciferase assays in *N. benthamiana*. MBW factors assayed in the experiment do not increase the activity of *DkMYB4* nor *DkMYC1* promoters, however *DkWDR1* transient expression associates with a significant decrease in LUC expression driven by *DkMYB4* promoter (Figure 50b and c).

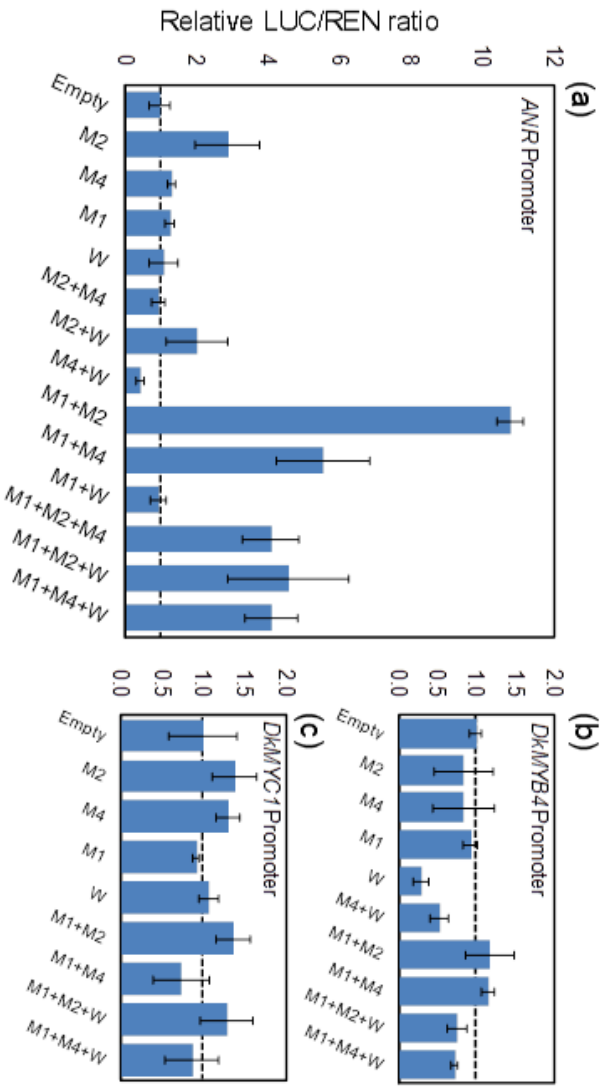

Figure 50.. Analysis of the transcriptional activity of relevant PA biosynthesis regulatory promoters by dual luciferase assay. The LUC/REN ratio of *N. benthamiana* cells agroinfiltrated with *ANR* (a), *DkMYB4* (b) and *DkMYC1* (c) promoters driving the LUC gene reporter, and regulatory genes *DkMYB2* (M2), *DkMYB4* (M4), *DkMYC1* (M1) and *DkWDR1* (W) under different combinations, was made relative to mock agroinfiltrations with pGreenII-62-SK (value of 1 labelled with a discontinuous line). Data are means from three replicates. Error bars represent standard deviations.

Discussion

DkMYB2, DkMYB4, DkMYC1 and DkWDR1 have been postulated to co-regulate the expression of PA biosynthesis genes in persimmon as a complex (Naval et al., 2016), and hence a coordinated nuclear co-localization of them is expected. Related components of MBW complexes in other species have been found located in the nucleus (TT2) (Nesi et al., 2001), or partitioned in nucleus and cytoplasm (TTG1 and VvMYC1) (Gonzalez et al., 2008; Hichri et al., 2010). In this study, DkMYB2, DkMYB4, DkMYC1 and DkWDR1 have been mostly localized in the cell nucleus, but DkMYB2, DkMYB4, DkMYC1 show a differential nucleus-nucleolus partitioning depending on the Nt or Ct position of the eGFP fusion. To our knowledge, this has not been previously observed in other MBW factors, although in most of these cases, only one Nt or Ct fusion is assayed. Indeed, a systematic approach in yeast has shown that a high percentage of proteins display different subcellular localization when GFP is tagged at either the Nt or Ct (Weill et al., 2019).

Transient expression in *N. benthamiana* and BiFC analysis support the ability of DkMYB2, DkMYB4, DkMYC1 and DkWDR1 proteins to interact with each other *in vivo*, which in fact reinforces previous two-hybrid data in the yeast *Saccharomyces cerevisiae* (Naval et al., 2016). The only combinatorial interactions not confirmed by BiFC are DkMYB2-DkWDR1 and DkWDR1 with itself. DkMYB2-DkWDR1 interaction was observed in a previous two-hybrid study, thus only homodimerization of DkWDR1 is not sustained on experimental evidences. These BiFC and yeast two-hybrid interaction data are

compatible with a multitude of possible combinations and sizes of the complex, which presumably enable a high degree of functional and regulatory versatility. Physical interactions among MBW factors involved in PA production have been also verified in *Arabidopsis* (Baudry et al., 2004), grapevine (Hichri et al., 2010), strawberry (Schaart et al., 2013), and tea plant (Wang et al., 2019) among other PA and flavonoid biosynthesis complexes.

These BiFC and subcellular localization results strongly support the formation *in vivo* of protein complexes comprising at least several of these factors, but conclusive functional evidences about their coordinated recruitment to modify the expression of PA biosynthetic genes in persimmon fruit are scarce. Anthocyanidin reductase is the main enzyme specifically involved in PA production in persimmon, and its coding *ANR* gene is considered a major target of transcriptional regulation (Akagi et al., 2009a), being consequently a proper candidate gene for studying PA biosynthesis regulation. Previous dual luciferase assays in *N. benthamiana* have shown that *DkMYB2* and *DkMYB4* increase the activity of *ANR* promoter when co-expressed with *Arabidopsis AtEGL3* gene coding for a bHLH protein involved in regulation of the flavonoid pathway, but not when expressed individually (Akagi et al., 2010a). On the contrary, in our hands, *DkMYB2* is able to increase *ANR* promoter activity three-fold in the absence of other factors, which suggests that DkMYB2 does not require a complete MBW complex to enhance, at some level, *ANR* expression and consequently improve PA production (Figure 51). Interestingly, the ectopic expression of *DkMYB2* in

kiwifruit calluses induces PA accumulation without additional MBW components (Akagi et al., 2010a). *DkMYB2* expression is regulated by fruit maturation factors in persimmon that markedly reduce it in advanced stages of development, similarly to *ANR*, *DkMYB4* and *DkMYC1*, but in contrast to these genes it seems not to be impaired in *ast* non-astringent mutants. Unexpectedly, *DkMYB2* has only a minor contribution to PA accumulation in these mutants, which is most likely due to its low expression level in fruit in comparison with *DkMYB4* (Akagi et al., 2009b).

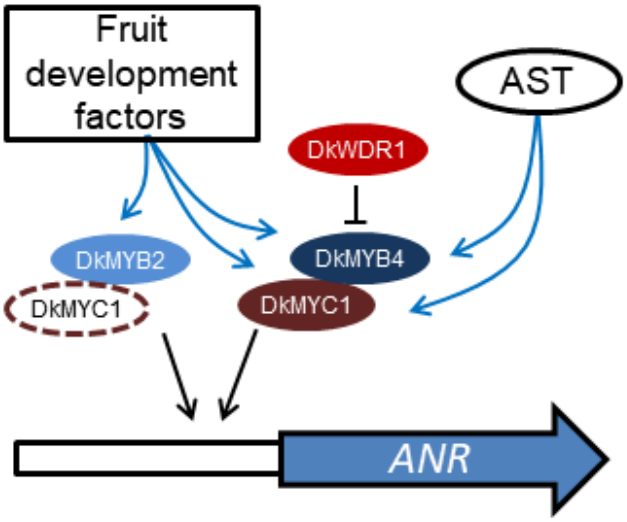

Figure 51. Diagram of regulatory factors affecting *ANR* expression. *ANR* coding gene is represented as a wide blue arrow, and its promoter as a contiguous white rectangle. Regulatory proteins are elliptic forms. The discontinuous ellipse of DkMYC1 indicates it is dispensable for the positive effect of DkMYB2. The transcriptional effect is labelled as a black arrow (inductive) or a black line ended in a perpendicular bar (repressive). Fruit development-dependent factors and AST locus modify the expression of MYB and bHLH factors by a yet unknown mechanism (blue arrows).

We have employed for the first time the persimmon bHLH (DkMYC1) and WD40 (DkWDR1) components in transient expression assays in combination with MYB factors, for the elucidation of the function of MBW complexes in the expression of PA responsive genes in persimmon fruit. *DkMYC1* does not affect significantly *ANR* expression on its own, but consistently intensifies the effect of *DkMYB2* and *DkMYB4*. In *Arabidopsis*, there is a similar synergistic effect of *TT2* (MYB) and *TT8* (bHLH) on the expression of *BAN* that responds to a stronger cooperative binding of the pair TT2-TT8 to *BAN* promoter (Baudry et al., 2004). Thus, the low expression of *ANR* gene from early stages of fruit development in the *ast* non-astringent cultivar 'Hana Fuyu' (Figure 49c) seems to be caused by the concomitant defective expression of *DkMYB4* and *DkMYC1* genes in this mutant (Naval et al., 2016) (Figure 5 of the paper). Contrarily to the positive effect of *TTG1* (WD40) gene overexpression, and the negative effect of *TTG1* silencing on *BAN* expression in *Arabidopsis* (Baudry et al., 2004), *DkWDR1* expression does not affect *ANR* promoter activity in our transient expression experiments. The strawberry ortholog of TTG1 also increases *Arabidopsis BAN* expression in combination with its bHLH and MYB co-interactors (Schaart et al., 2013), which suggests the presence of certain functional particularities in persimmon DkWDR1 or perhaps regulatory differences between *ANR* and *BAN* promoters. On the other side, WD40 proteins act as structural platforms for facilitating protein-protein interaction, and consequently its effect on the positive transcriptional activity of the complex could be shaded by

the ectopic overexpression of components of the complex and the presence of endogenous similar factors in *N. benthamiana* cells.

As *DkMYB4* and *DkMYC1* show a development and cultivar dependent expression profile highly similar to *ANR* (Akagi et al., 2009b; Su et al., 2012; Naval et al., 2016) (Figure 49c), we considered plausible a self-regulatory loop in the expression of these genes, similar to the positive feedback mechanism operating in *TT8* from *Arabidopsis* (Baudry et al., 2006). However, *DkMYB4* and *DkMYC1* promoters are not activated by any MBW element utilized in this study. On the contrary, *DkWDR1* reduces the expression of *DkMYB4* by itself and in combination with MYB genes. This repressive effect of *DkWDR1* resembles the activity of MBW complexes containing MYB proteins showing at the C-terminal end an ethylene-responsive element binding factor-associated amphiphilic repression (EAR) motif (Albert et al., 2014). Thus, binding of specific tobacco endogenous repressive MYB proteins has potentially the ability to turn MBW complex into a repressive factor. In light of these data we cannot discard a repressive role of *DkWDR1* on the expression of *DkMYB4* and other genes, which could depend on the binding of distinct MYB of bHLH elements with specific activating or repressive domains.

Supplementary material

Supplementary Figure 7. Western blot analysis of BiFC negative interaction combinations. Combinations are DkMYB2, DkMYB4, DkMYC1 and DkWDR1 with NtYFP (a), DkWDR1 with itself (b), and DkWDR1 with DkMYB2 (c). Molecular weight markers are shown on the left. Antibodies are shown on the right. Non-specific bands are labelled (*).

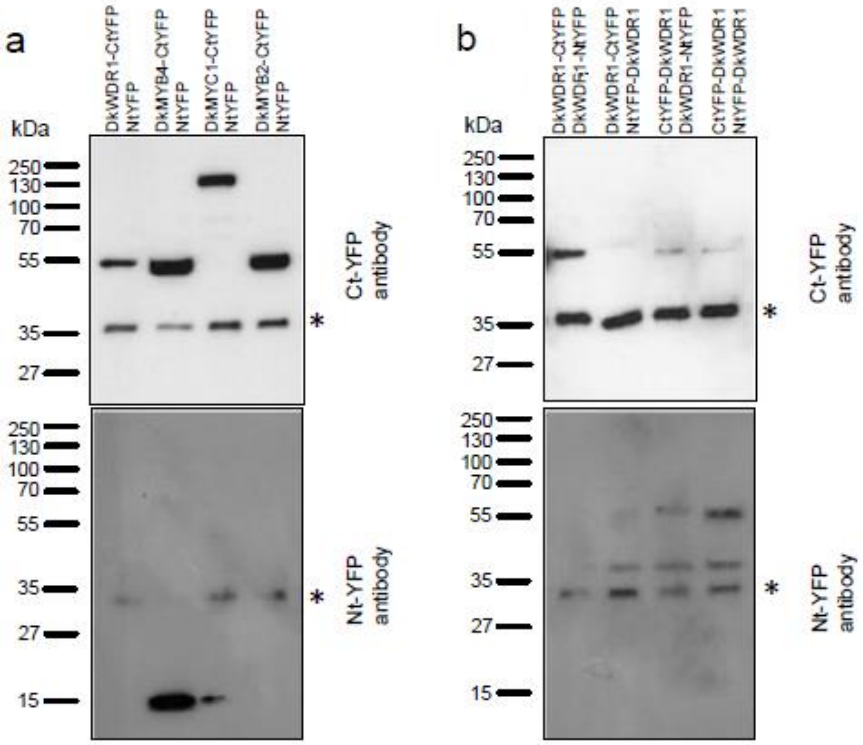

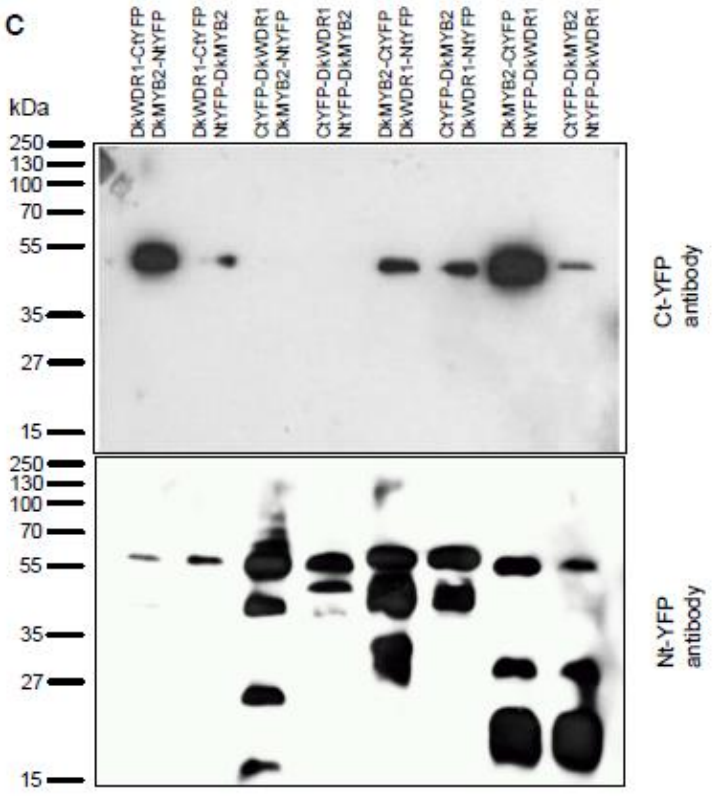
C
kDa
DkWDR1-CtYFP
DkMYB2-NtYFP
DkWDR1-CtYFP
NtYFP-DkMYB2
CtYFP-DkWDR1
DkMYB2-NtYFP
CtYFP-DkWDR1
NtYFP-DkMYB2
DkMYB2-CtYFP
DkWDR1-NtYFP
CtYFP-DkMYB2
DkWDR1-NtYFP
DkMYB2-CtYFP
NtYFP-DkWDR1
CtYFP-DkMYB2
NtYFP-DkWDR1
250
130
100
70
55
35
27
15
Ct-YFP antibody
Nt-YFP antibody

Primers used for promoter cloning		
ANR promoter (cloning)	F	AAAAGTCTTGGGAGTCGTGCCTTC
	R	ACGCTGCCTTGGCTCCTAACG
DkMYB4 promoter (cloning)	F	AATTCACGGCCATGGAAACGTGGT
	R	CTCTTCTTCTGATATTTGTGACGCAG
DkMYC1 promoter (cloning)	F	CGTGCGAGCATTCATGAGATGAGA
	R	ACTGTAAGTCCATTGCACCGTCTGA

Subcellular localization and BiFC		
DkMYB2-Fluorescent protein (FP)	F	AGGATCGGTACCATGGGAAGGAAGCCATGCTGTG
	R	CTGCACCGGCGCTAGCTGCGCCTAAACCATGGGGT
FP-DkMYB2	F	GGTGCAGGAGCCATGGGAAGGAAGCCATGCTGTG
	R	TCTAGGGAGCGCTAGCCTAGCCTAAACCATGGGGTTGG
DkMYB4-FP	F	AGGATCGGTACCATGGGAAGAGCTCCTTGTTGTTC
	R	CTGCACCGGCGCTAGCGATGAGCAATGATTCAGCAAAGG
FP-DkMYB4	F	GGTGCAGGAGCCATGGGAAGAGCTCCTTGTTGTTC
	R	TCTAGGGAGCGCTAGCTCAGATGAGCAATGATTCAGCAAAGG
DkMYC1-FP	F	AGGATCGGTACCATGGCCGCTCCGCCTAGTT
	R	CTGCACCGGCGCTAGCATGTATTATCTGATGTATCGCCCTCTTC
FP-DkMYC1	F	GGTGCAGGAGCCATGGCCGCTCCGCCTAGTT
	R	TCTAGGGAGCGCTAGCTTAATGTATTATCTGATGTATCGCCCTCTTC
DkWDR1-FP	F	AGGATCGGTACCATGGAGAATTCGACCCTAGAG
	R	CTGCACCGGCGCTAGCAACTTTTAGAAGCTGCATTTTGG
FP-DkWDR1	F	GGTGCAGGAGCCATGGAGAATTCGACCCTAGAG
	R	TCTAGGGAGCGCTAGCTTAAACTTTTAGAAGCTGCATTTTGG

Transient expression vector construction		
ANR-Luc	F	CGGAAGCTTAAAAGTCTTGGGAGTCGTGCCTTCAAC
	R	TATCTGCAGACGCTGCCTTGGCTCCTAACGTTG
DkMYB4-Luc	F	CGCAAGCTTGTATAGCTTGAATAGAATGAAACTTGTAG
	R	TAACCATGGCTCTTCTTCTGATATTTGTGACGCAG
DkMYC1-Luc	F	GCCAAGCTTCGATTTGGGATAATTTCAACTAAGGAGAAT
	R	TATCTGCAGCTACGCCGCTCTGCTAGCTGTCAC

Supplementary Table 1. Primers used in this study

General discussion

Prior to this thesis, the population structure of persimmon was already approached by different groups. The first studies targeting this topic divided persimmon populations according to the astringency type (Kajiura, 1946; Kitagawa and Glucina, 1984). More recent approaches used molecular markers, such as AFLPs (Kanzaki et al., 2000; Yonemori et al., 2008; Parfitt et al., 2015), RAPDs (Luo Zheng-Rong et al., 1995; Badenes et al., 2003; Yamagishi et al., 2005) and SSRs (Naval et al. 2010). These studies showed that the traditional division of persimmon population according to its astringency type is a coarse indication of their genetic differences. In this study, these differences have been confirmed employing new varieties from different origins. The population structure and genetic relationships among accessions established in these studies will be useful for a more efficient use of the IVIA persimmon germplasm bank towards breeding. In coming studies, these results will be used for targeting genetic traits of interest in persimmon breeding. Furthermore, the estimation of the genetic values of traits of interest for each accession will be higly useful, and its estimation could be more precisely done through the populations coming from the crosses of the breeding program.

Currently, few studies regarding salt tolerance in *Diospyros* species are available. These studies established the basis for understanding the salinity problem in these species and indicated differences of salt tolerance among them (De Paz et al., 2016; Visconti et al., 2017; Gil-Muñoz et al., 2018a). However, there is no information about the possibilities of intraspecific variability and even less about the

mechanisms of salt tolerance in persimmon. This work has contributed to understand the basic mechanisms of salt tolerance which will contribute to more efficient saline assays and reliable selections of tolerance based on specific phenotypical traits. Even more, the knowledge generated on the tolerance mechanisms into each species and population is of major interest for planning further crossings in order to take benefit of the different salinity-tolerance mechanisms. Furthermore, the use of biostatistical tools such as PCA has been proven useful as an aid for breeding. In our case it has been used as a tool for the selection of complicated phenotypes such the ones behind saline stress tolerance. Furthermore, this study provides a transcriptome of *Diospyros lotus* available for the use as a tool in molecular studies. Previously, neither complete assembled genomes nor transcriptomes were available in any *Diospyros* species. Regarding to the discovery of chloride tolerance mechanisms in *Diospyros*, further crossings between *D. lotus* and salt-tolerant populations such as the available *D. virginiana* or *D. kaki* x *D. virginiana* backcrosses could reveal the relevance of these genes outside the salt sensitive genetic background of *D. lotus*. The present study provides the first selected clones for future salt-tolerant rootstocks. In addition, the selections obtained with these assays will be micropropagated and tested in field conditions in order to develop the first persimmon clonal rootstocks.

Concerning the knowledge about PA biosynthesis, the regulation of this pathway is well known in *Arabidopsis thaliana* seeds (Jende-Strid, 1993; Abrahams et al., 2002; Tanner et al., 2003; Xie et al., 2003;

Baudry et al., 2004 Cone, 2007; Gonzalez et al., 2008). Furthermore, orthologues of these genes were identified in persimmon (Ikegami et al., 2005; Akagi et al., 2009a; Wang et al., 2010, Akagi et al., 2011a). In *Arabidopsis*, a ternary MYB-bHLH-WD40 (MBW) protein complex regulates the transcription of genes involved in PA biosynthesis, and orthologues of the genes of this complex have been discovered in persimmon. MYB-like (*DkMYB2, DkMYB4*) and bHLH-like (*DkMYC1*) genes have been postulated to regulate PA biosynthesis and astringency in fruit (Akagi et al., 2009b, 2010a; Su et al., 2012). However, at the beginning of the realization of this thesis, no *WD40* gene related to this complex had been discovered in persimmon. In addition, the mechanism behind the mutation of the non-astringent persimmon was also unknown. In this thesis, we have identified a putative orthologue of *Arabidopsis TTG1* gene, and we have shown that this gene is not responsible for the non-astringent trait. Furthermore, we have obtained *in vivo* and *in vitro* evidences of the MBW complex in persimmon and the direct action of these genes and its interaction in the activation and regulation of PA biosynthesis. Finally, we have shown that the regulation of *DkMYB4* gene might give more clues about the non-astringent trait mutation. Our results give a model for astringency regulation trough a genetic interaction network slightly different to the one described and indicate the possibility that the non-astringent mutation is directly or indirectly related to DkMYB4 regulation. This study will continue using other model species via searching for genes responsible for the regulation of *DkMYB4* expression. Although now we have more information about PA biosynthesis, more studies will be performed around PA

insolubilization mechanisms which are also an important factor regarding deastringency treatments, that can interact with salt-stress affected fruits. More information about these metabolic networks and additional transcriptomic studies in varieties with different behavior in deastringency treatments will be useful for increasing knowledge on this important persimmon trait.

Conclusions

Genetic analysis of variability using SSR markers among persimmon cultivars coincides with the phenotypical division according to astringency type.

Backcrosses between *D. kaki* and *D. virginiana* have much higher salt tolerance and less Na^+ and Cl^- leaf accumulation than the D. kaki parental.

Saline tolerance in *D. virginiana* and the aforementioned backcrosses is driven by the higher root expression of an *HKT-1-like* gene for Na^+ and stomatal regulation for Cl^- altogether with a higher WUE.

Variability for the salinity tolerance trait has been found within D. kaki, *D. lotus*, *D. virginiana* and the *D. kaki* x *D. virginiana* backcross populations.

Salinity tolerance within *D. kaki* population is driven by the osmotic stress tolerance via water flow regulation and stomatal regulation mechanisms.

Salinity tolerance within *D. virginiana* population is driven by the leaf expression of *PIP2*-like genes that may act as Na^+ gates into the leaves.

Salinity tolerance within *D. kaki* x *D. virginiana* backcross population is driven by differences in WUE and root *HKT-1-like* gene expression.

Despite *D. lotus* population showed increased Na^+ and Cl^- leaf accumulation compared with the other populations, was the only population with observed variability for Cl^- leaf accumulation.

RNAseq revealed that salinity tolerance within *D. lotus* population is driven by the leaf expression of *chloride channel* like genes. Possibly this tolerance is also driven by leaf vacuolar sequestration allowed through electrochemical gradients generated by H^+-ATPase pumps and changes in root architecture via thermospermine synthesis.

The sequenced *DkWDR1* gene is highly similar to the *TTG1* gene of *Arabidopsis thaliana* and other *WD-40* genes involved in proanthocyanidin synthesis from other species.

Allele analysis on astringent and non-astringent accessions has shown that DkWDR1 gene is not the responsible for the non-astringent *ast* mutation.

Expression analysis in fruit development over astringent and non-astringent accessions have shown that the *ast* mutation is linked to the downregulation of *DkMYC1* and *DkMYB4* genes.

Proanthocyanidin synthesis related proteins DkWDR1, DkMYB4, DkMYB2 and DkMYC1 have shown to have *in-vitro* interaction trough yeast (*Saccharomyces cerevisae*) two-hybrid system.

The interaction between DkMYB2/DkMYB4, DkMYB4/DkMYC1 and DkMYB4/DkMYB4 showed increased reporter expression in the *in-vitro* yeast (*S. cerevisae*) α-galactosidase assay.

The in-vivo expression of DkWDR1, DkMYB4, DkMYB2 and DkMYC1 fused to eGFP has shown the localization of the proteins inside the nucleus in *Nicotiana benthamiana* leaves.

Except DkMYB2 and DkWDR1 combinations, DkWDR1, DkMYB4, DkMYB2 and DkMYC1 proteins have shown to interact between them in the in-vivo BiFC assay in *N. benthamiana* leaves. Furthermore DkMYB4, DkMYB2 and DkMYC1 have shown homodimerization. All the interactions were also located inside the nucleus.

DkMYB2 is able to upregulate persimmon ANR expression by interacting with its promoter in the in-vivo assay in *N. benthamiana* leaves using persimmon ANR promoter and a luciferase reporter. The protein coexpression of DkMYC1/DkMYB2, DkMYC1/DkMYB4, DkMYC1/DkMYB2/DkMYB4, DkMYC1/DkMYB4/DkWDR1 and DkMYC1/DkMYB2/DkWDR1 also resulted in increased reporter expression.

DkWDR and DkMYB4 interaction have resulted in ANR downregulation. Also, DkWDR1 itself and the coexpression of DkWDR1/DkMYB4, DkMYC1/DkMYB2/DkWDR1 and DkMYC1/DkMYB4/DkWDR1 resulted in a downregulation of the reporter using DkMYB4 persimmon promoter. This indicates a possible role of DkWDR1 in proanthocyanidin synthesis regulation.

References

Abrahams, S., Tanner, G. J., Larkin, P. J., and Ashton, A. R. (2002). Identification and biochemical characterization of mutants in the proanthocyanidin pathway in Arabidopsis. *Plant Physiol.* 130, 561–576. doi:10.1104/pp.006189.

Achard, P., Cheng, H., De Grauwe, L., Decat, J., Schoutteten, H., Moritz, T., et al. (2006). Integration of plant responses to environmentally activated phytohormonal signals. *Science (80-.).* 311, 91–94. doi:10.1126/science.1118642.

Achard, P., Renou, J. P., Berthomé, R., Harberd, N. P., and Genschik, P. (2008). Plant DELLAs Restrain Growth and Promote Survival of Adversity by Reducing the Levels of Reactive Oxygen Species. *Curr. Biol.* 18, 656–660. doi:10.1016/j.cub.2008.04.034.

Acosta-Motos, J. R., Ortuño, M. F., Bernal-Vicente, A., Diaz-Vivancos, P., Sanchez-Blanco, M. J., and Hernandez, J. A. (2017). Plant responses to salt stress: Adaptive mechanisms. *Agronomy* 7, 18. doi:10.3390/agronomy7010018.

Afzal, Z., Howton, T. C., Sun, Y., and Mukhtar, M. S. (2016). The roles of aquaporins in plant stress responses. *J. Dev. Biol.* 4. doi:10.3390/jdb4010009.

Akagi, T., Henry, I. M., Kawai, T., Comai, L., and Tao, R. (2016). Epigenetic regulation of the sex determination gene megi in polyploid persimmon. *Plant Cell* 28, 2905–2915. doi:10.1105/tpc.16.00532.

Akagi, T., Henry, I. M., Tao, R., and Comai, L. (2014). A y-chromosome-encoded small RNA acts as a sex determinant in persimmons. *Science (80-.).* 346, 646–650. doi:10.1126/science.1257225.

Akagi, T., Ikegami, A., Suzuki, Y., Yoshida, J., Yamada, M., Sato, A., et al. (2009a). Expression balances of structural genes in shikimate and flavonoid biosynthesis cause a difference in proanthocyanidin accumulation in persimmon (Diospyros kaki Thunb.) fruit. *Planta* 230, 899–915. doi:10.1007/s00425-009-0991-6.

Akagi, T., Ikegami, A., Tsujimoto, T., Kobayashi, S., Sato, A., Kono, A.,

et al. (2009b). DkMyb4 is a Myb transcription factor involved in proanthocyanidin biosynthesis in persimmon fruit. *Plant Physiol.* 151, 2028–2045. doi:10.1104/pp.109.146985.

Akagi, T., Ikegami, A., and Yonemori, K. (2010a). DkMyb2 wound-induced transcription factor of persimmon (Diospyros kaki Thunb.), contributes to proanthocyanidin regulation. *Planta* 232, 1045–1059. doi:10.1007/s00425-010-1241-7.

Akagi, T., Katayama-Ikegami, A., Kobayashi, S., Sato, A., Kono, A., and Yonemori, K. (2012). Seasonal abscisic acid signal and a basic leucine zipper transcription factor, DkbZIP5, regulate proanthocyanidin biosynthesis in persimmon fruit. *Plant Physiol.* 158, 1089–1102. doi:10.1104/pp.111.191205.

Akagi, T., Katayama-Ikegami, A., and Yonemori, K. (2011a). Proanthocyanidin biosynthesis of persimmon (Diospyros kaki Thunb.) fruit. *Sci. Hortic. (Amsterdam).* 130, 373–380. doi:10.1016/j.scienta.2011.07.021.

Akagi, T., Takeda, Y., Yonemori, K., Ikegami, A., Kono, A., Yamada, M., et al. (2010b). Quantitative genotyping for the astringency locus in hexaploid persimmon cultivars using quantitative real-time PCR. *J. Am. Soc. Hortic. Sci.* 135, 59–66. doi:10.21273/jashs.135.1.59.

Akagi, T., Tsujimoto, T., Ikegami, A., and Yonemori, K. (2011b). Effects of seasonal temperature changes on DkMyb4 expression involved in proanthocyanidin regulation in two genotypes of persimmon (Diospyros kaki Thunb.) fruit. *Planta* 233, 883–894. doi:10.1007/s00425-010-1346-z.

Alavilli, H., Awasthi, J. P., Rout, G. R., Sahoo, L., Lee, B. H., and Panda, S. K. (2016). Overexpression of a Barley aquaporin gene, HvPIP2;5 confers salt and osmotic stress tolerance in yeast and plants. *Front. Plant Sci.* 7. doi:10.3389/fpls.2016.01566.

Albert, N. W., Davies, K. M., Lewis, D. H., Zhang, H., Montefiori, M., Brendolise, C., et al. (2014). A conserved network of transcriptional activators and repressors regulates anthocyanin pigmentation in Eudicots. *Plant Cell* 26, 962–980.

doi:10.1105/tpc.113.122069.

Almeida, P., Katschnig, D., and de Boer, A. H. (2013). HKT transporters-state of the art. *Int. J. Mol. Sci.* 14, 20359–20385. doi:10.3390/ijms141020359.

Amirbakhtiar, N., Ismaili, A., Ghaffari, M. R., Firouzabadi, F. N., and Shobbar, Z. S. (2019). Transcriptome response of roots to salt stress in a salinity-tolerant bread wheat cultivar. *PLoS One* 14, e0213305. doi:10.1371/journal.pone.0213305.

Amtmann, A., and Sanders, D. (1998). Mechanisms of Na+ Uptake by Plant Cells. *Adv. Bot. Res.* 29, 75–112. doi:10.1016/S0065-2296(08)60310-9.

An, D., Chen, J. G., Gao, Y. Q., Li, X., Chao, Z. F., Chen, Z. R., et al. (2017). AtHKT1 drives adaptation of Arabidopsis thaliana to salinity by reducing floral sodium content. *PLoS Genet.* 13. doi:10.1371/journal.pgen.1007086.

An, X. H., Tian, Y., Chen, K. Q., Wang, X. F., and Hao, Y. J. (2012). The apple WD40 protein MdTTG1 interacts with bHLH but not MYB proteins to regulate anthocyanin accumulation. *J. Plant Physiol.* 169, 710–717. doi:10.1016/j.jplph.2012.01.015.

Andersen, C. L., Jensen, J. L., and Ørntoft, T. F. (2004). Normalization of real-time quantitative reverse transcription-PCR data: A model-based variance estimation approach to identify genes suited for normalization, applied to bladder and colon cancer data sets. *Cancer Res.* 64, 5245–5250. doi:10.1158/0008-5472.CAN-04-0496.

Aparicio, F., Sánchez-Navarro, J. A., and Pallás, V. (2006). In vitro and in vivo mapping of the Prunus necrotic ringspot virus coat protein C-terminal dimerization domain by bimolecular fluorescence complementation. *J. Gen. Virol.* 87, 1745–1750. doi:10.1099/vir.0.81696-0.

Apse, M. P., Aharon, G. S., Snedden, W. A., and Blumwald, E. (1999). Salt tolerance conferred by overexpression of a vacuolar Na+/H+ antiport in Arabidopsis. *Science (80-.).* 285, 1256–1258. doi:10.1126/science.285.5431.1256.

Arnal, L., and Del Rio, M. A. (2004). Quality of persimmon fruit cv. Rojo brillante during storage at different temperatures. *Spanish J. Agric. Res.* 2, 243. doi:10.5424/sjar/2004022-78.

Arnal, L., and Del Río, M. A. (2003). Removing astringency by carbon dioxide and nitrogen-enriched atmospheres in persimmon fruit cv. "Rojo brillante." *J. Food Sci.* 68, 1516–1518. doi:10.1111/j.1365-2621.2003.tb09676.x.

Ashrai, M., and McNelly, T. (1990). Improvement of Salt Tolerance in Maize by Selection and Breeding. *Plant Breed.* 104, 101–107. doi:10.1111/j.1439-0523.1990.tb00410.x.

Badenes, M., Garcés, A., Romero, C., Romero, M., Clavé, J., Rovira, M., et al. (2003). Genetic diversity of introduced and local Spanish persimmon cultivars revealed by RAPD markers. *Genet. Resour. Crop Evol.* 50, 579–585. doi:10.1023/A:1024474719036.

Badenes, M. L., Naval, M. M., Martínez-Calvo, J., and Giordani, E. (2015). "Material Vegetal y Mejora Genetica," in *El cultivo del caqui*, eds. M. L. Badenes, D. Intrigliolo, A. Salvador, and A. Vicent (Generalitat Valenciana), 58–80.

Baetz, U., Eisenach, C., Tohge, T., Martinoia, E., and De Angeli, A. (2016). Vacuolar chloride fluxes impact ion content and distribution during early salinity stress. *Plant Physiol.* 172, 1167–1181. doi:10.1104/pp.16.00183.

Bagchi, D., Bagchi, M., Stohs, S. J., Das, D. K., Ray, S. D., Kuszynski, C. A., et al. (2000). Free radicals and grape seed proanthocyanidin extract: Importance in human health and disease prevention. in *Toxicology*, 187–197. doi:10.1016/S0300-483X(00)00210-9.

Barbier-Brygoo, H., De Angeli, A., Filleur, S., Frachisse, J.-M., Gambale, F., Thomine, S., et al. (2011). Anion Channels/Transporters in Plants: From Molecular Bases to Regulatory Networks. *Annu. Rev. Plant Biol.* 62, 25–51. doi:10.1146/annurev-arplant-042110-103741.

Barragán, V., Leidi, E. O., Andrés, Z., Rubio, L., de Luca, A., Fernández, J. A., et al. (2012). Ion exchangers NHX1 and NHX2 mediate active potassium uptake into vacuoles to regulate cell turgor

and stomatal function in arabidopsis. *Plant Cell* 24, 1127–1142. doi:10.1105/tpc.111.095273.

Bates, L. S., Waldren, R. P., and Teare, I. D. (1973). Rapid determination of free proline for water-stress studies. *Plant Soil* 39, 205–207. doi:10.1007/BF00018060.

Baudry, A., Caboche, M., and Lepiniec, L. (2006). TT8 controls its own expression in a feedback regulation involving TTG1 and homologous MYB and bHLH factors, allowing a strong and cell-specific accumulation of flavonoids in Arabidopsis thaliana. *Plant J.* 46, 768–779. doi:10.1111/j.1365-313X.2006.02733.x.

Baudry, A., Heim, M. A., Dubreucq, B., Caboche, M., Weisshaar, B., and Lepiniec, L. (2004). TT2, TT8, and TTG1 synergistically specify the expression of BANYULS and proanthocyanidin biosynthesis in Arabidopsis thaliana. *Plant J.* 39, 366–380. doi:10.1111/j.1365-313X.2004.02138.x.

Bellini, E., and Giordani, E. (2002). Cultural practices for persimmon production. *CIHEAM Options Mediterr.*, 39–52.

Ben-Arie, R., and Sonego, L. (1993). Temperature Affects Astringency Removal and Recurrence in Persimmon. *J. Food Sci.* 58, 1397–1400. doi:10.1111/j.1365-2621.1993.tb06191.x.

Berthomieu, P., Conéjéro, G., Nublat, A., Brackenbury, W. J., Lambert, C., Savio, C., et al. (2003). Functional analysis of AtHKT1 in Arabidopsis shows that Na+ recirculation by the phloem is crucial for salt tolerance. *EMBO J.* 22, 2004–2014. doi:10.1093/emboj/cdg207.

Besada, C., Gil, R., Bonet, L., Quiñones, A., Intrigliolo, D., and Salvador, A. (2016). Chloride stress triggers maturation and negatively affects the postharvest quality of persimmon fruit. Involvement of calyx ethylene production. *Plant Physiol. Biochem.* 100, 105–112. doi:10.1016/j.plaphy.2016.01.006.

Bolger, A. M., Lohse, M., and Usadel, B. (2014). Trimmomatic: A flexible trimmer for Illumina sequence data. *Bioinformatics*. doi:10.1093/bioinformatics/btu170.

Bose, J., Rodrigo-Moreno, A., and Shabala, S. (2014). ROS homeostasis in halophytes in the context of salinity stress tolerance. *J. Exp. Bot.* 65, 1241–1257. doi:10.1093/jxb/ert430.

Boudsocq, M., and Laurière, C. (2005). Osmotic signaling in plants. Multiple pathways mediated by emerging kinase families. *Plant Physiol.* 138, 1185–1194. doi:10.1104/pp.105.061275.

Boursiac, Y., Chen, S., Luu, D. T., Sorieul, M., Van Den Dries, N., and Maurel, C. (2005). Early effects of salinity on water transport in Arabidopsis roots. Molecular and cellular features of aquaporin expression. *Plant Physiol.* 139, 790–805. doi:10.1104/pp.105.065029.

Bray, N. L., Pimentel, H., Melsted, P., and Pachter, L. (2016). Near-optimal probabilistic RNA-seq quantification. *Nat. Biotechnol.* doi:10.1038/nbt.3519.

Brecht, H., Dasgupta, S., Laplante, B., Murray, S., and Wheeler, D. (2012). Sea-Level Rise and Storm Surges: High Stakes for a Small Number of Developing Countries. *J. Environ. Dev.* 21, 120–138. doi:10.1177/1070496511433601.

Brini, F., Gaxiola, R. A., Berkowitz, G. A., and Masmoudi, K. (2005). Cloning and characterization of a wheat vacuolar cation/proton antiporter and pyrophosphatase proton pump. *Plant Physiol. Biochem.* 43, 347–354. doi:10.1016/j.plaphy.2005.02.010.

Brueggemann, J., Weisshaar, B., and Sagasser, M. (2010). A WD40-repeat gene from Malus × domestica is a functional homologue of Arabidopsis thaliana TRANSPARENT TESTA GLABRA1. *Plant Cell Rep.* 29, 285–294. doi:10.1007/s00299-010-0821-0.

Brugnoli, E., and Lauteri, M. (1991). Effects of salinity on stomatal conductance, photosynthetic capacity, and carbon isotope discrimination of salt-tolerant (Gossypium hirsutum L.) and salt-sensitive (Phaseolus vulgaris L.) C3 non-halophytes. *Plant Physiol.* 95, 628–635. doi:10.1104/pp.95.2.628.

Bryant, D. M., Johnson, K., DiTommaso, T., Tickle, T., Couger, M. B., Payzin-Dogru, D., et al. (2017). A Tissue-Mapped Axolotl De Novo Transcriptome Enables Identification of Limb

Regeneration Factors. *Cell Rep.* doi:10.1016/j.celrep.2016.12.063.

Buntjer, J. B. (1997). Phylogenetic computer tools (PhylTools), version 1.32 for Windows.

Byrt, C. S., Platten, J. D., Spielmeyer, W., James, R. A., Lagudah, E. S., Dennis, E. S., et al. (2007). HKT1;5-like cation transporters linked to Na+ exclusion loci in wheat, Nax2 and Kna1. *Plant Physiol.* 143, 1918–1928. doi:10.1104/pp.106.093476.

Callister, A. N., Arndt, S. K., and Adams, M. A. (2006). Comparison of four methods for measuring osmotic potential of tree leaves. *Physiol. Plant.* 127, 383–392. doi:10.1111/j.1399-3054.2006.00652.x.

Camacho, C., Coulouris, G., Avagyan, V., Ma, N., Papadopoulos, J., Bealer, K., et al. (2009). BLAST+: Architecture and applications. *BMC Bioinformatics*. doi:10.1186/1471-2105-10-421.

Cellier, F., Conéjéro, G., Ricaud, L., Doan, T. L., Lepetit, M., Gosti, F., et al. (2004). Characterization of AtCHX17, a member of the cation/H+ exchangers, CHX family, from Arabidopsis thaliana suggests a role in K + homeostasis. *Plant J.* 39, 834–846. doi:10.1111/j.1365-313X.2004.02177.x.

Chambers, J. M., Cleveland, W. S., Kleiner, B., and Tukey, P. A. (2018). *Graphical methods for data analysis*. doi:10.1201/9781351072304.

Chaumont, F., and Tyerman, S. D. (2014). Aquaporins: Highly regulated channels controlling plant water relations. *Plant Physiol.* 164, 1600–1618. doi:10.1104/pp.113.233791.

Chen, S., Wu, F., Li, Y., Qian, Y., Pan, X., Li, F., et al. (2019). NTMYB4 and NTCHS1 are critical factors in the regulation of flavonoid biosynthesis and are involved in salinity responsiveness. *Front. Plant Sci.* 10, 178. doi:10.3389/fpls.2019.00178.

Chen, X., Huang, Q., Zhang, F., Wang, B., Wang, J., and Zheng, J. (2014). ZmCIPK21, a Maize CBL-Interacting Kinase, Enhances Salt Stress Tolerance in Arabidopsis Thaliana. *Int. J. Mol. Sci.* 15,

14819–14834. doi:10.3390/ijms150814819.

Chen, Z., Pottosin, I. I., Cuin, T. A., Fuglsang, A. T., Tester, M., Jha, D., et al. (2007). Root plasma membrane transporters controlling K+/Na+ homeostasis in salt-stressed barley. *Plant Physiol.* 145, 1714–1725. doi:10.1104/pp.107.110262.

Cho, S. K., and Cho, T. H. (1965). Studies on the local varieties of persimmon. *Korea Res. Reports Off. Rural Dev.* 8, 147–190.

Cone, K. C. (2007). Anthocyanin synthesis in maize aleurone tissue. *Plant Cell Monogr.* 8, 121–139. doi:10.1007/7089_2007_117.

Conesa, A., Götz, S., García-Gómez, J. M., Terol, J., Talón, M., and Robles, M. (2005). Blast2GO: A universal tool for annotation, visualization and analysis in functional genomics research. *Bioinformatics*. doi:10.1093/bioinformatics/bti610.

Cuartero, J., Bolarín, M. C., Asíns, M. J., and Moreno, V. (2006). Increasing salt tolerance in the tomato. *J. Exp. Bot.* 57, 1045–1058. doi:10.1093/jxb/erj102.

Das, S., D., S., Chakraborti, I., Roy, N., and Das, S. S. (2017). Principal Component Analysis in Plant Breeding. *Biomol. Reports*.

Dasgupta, S., Hossain, M. M., Huq, M., and Wheeler, D. (2015). Climate change and soil salinity: The case of coastal Bangladesh. *Ambio* 44, 815–826. doi:10.1007/s13280-015-0681-5.

Daszkowska-Golec, A., and Szarejko, I. (2013). Open or close the gate - Stomata action under the control of phytohormones in drought stress conditions. *Front. Plant Sci.* 4, 138. doi:10.3389/fpls.2013.00138.

Davies, W. J., Kudoyarova, G., and Hartung, W. (2005). Long-distance ABA signaling and its relation to other signaling pathways in the detection of soil drying and the mediation of the plant's response to drought. *J. Plant Growth Regul.* 24, 285–295. doi:10.1007/s00344-005-0103-1.

de Paz, J. M., Visconti, F., Chiaravalle, M., and Quiñones, A. (2016). Determination of persimmon leaf chloride contents using near-

infrared spectroscopy (NIRS). *Anal. Bioanal. Chem.* 408, 3537–3545. doi:10.1007/s00216-016-9430-2.

De Paz, J., Visconti, F., Tudela, L., Quiñones Oliver, A., Intrigliolo, D., Jordà, M., et al. (2016). *La fitotoxicidad por cloruro en el cultivo del caqui: descripción del problema*.

De Vetten, N., Quattrocchio, F., Mol, J., and Koes, R. (1997). The an11 locus controlling flower pigmentation in petunia encodes a novel WD-repeat protein conserved in yeast, plants, and animals. *Genes Dev.* 11, 1422–1434. doi:10.1101/gad.11.11.1422.

Diospyros - Wikipedia Available at: https://en.wikipedia.org/wiki/Diospyros [Accessed July 18, 2020].

Dixon, R. A., Xie, D. Y., and Sharma, S. B. (2005). Proanthocyanidins - A final frontier in flavonoid research? *New Phytol.* 165, 9–28. doi:10.1111/j.1469-8137.2004.01217.x.

Doyle, J. J., and Doyle, J. L. (1987). A rapid DNA isolation procedure for small quantities of fresh leaf tissue. *Phytochem. Bull.* 19, 11–15. doi:10.2307/4119796.

El-Gebali, S., Mistry, J., Bateman, A., Eddy, S. R., Luciani, A., Potter, S. C., et al. (2019). The Pfam protein families database in 2019. *Nucleic Acids Res.* doi:10.1093/nar/gky995.

Essah, P. A., Davenport, R., and Tester, M. (2003). Sodium influx and accumulation in arabidopsis. *Plant Physiol.* 133, 307–318. doi:10.1104/pp.103.022178.

Evanno, G., Regnaut, S., and Goudet, J. (2005). Detecting the number of clusters of individuals using the software STRUCTURE: A simulation study. *Mol. Ecol.* 14, 2611–2620. doi:10.1111/j.1365-294X.2005.02553.x.

Evans, A. R., Hall, D., Pritchard, J., and Newbury, H. J. (2012). The roles of the cation transporters CHX21 and CHX23 in the development of Arabidopsis thaliana. *J. Exp. Bot.* 63, 59–67. doi:10.1093/jxb/err271.

Excoffier, L., Smouse, P. E., and Quattro, J. M. (1992). Analysis of molecular variance inferred from metric distances among DNA haplotypes: Application to human mitochondrial DNA restriction data. *Genetics* 131, 479–491. doi:10.5962/bhl.title.86657.

Falush, D., Stephens, M., and Pritchard, J. K. (2003). Inference of population structure using multilocus genotype data: Linked loci and correlated allele frequencies. *Genetics* 164, 1567–1587. doi:10.1080/13235818.1996.10673675.

Felsenstein, J. (2005). PHYLIP (Phylogeny Inference Package) version 3.6.

Flowers, T. J., and Colmer, T. D. (2008). Salinity tolerance in halophytes. *New Phytol.* 179, 945–963. doi:10.1111/j.1469-8137.2008.02531.x.

Formentin, E., Sudiro, C., Perin, G., Riccadonna, S., Barizza, E., Baldoni, E., et al. (2018). Transcriptome and cell physiological analyses in different rice cultivars provide new insights into adaptive and salinity stress responses. *Front. Plant Sci.* 9, 204. doi:10.3389/fpls.2018.00204.

Forner-Giner, M. A., and Ancillo, G. (2013). "Breeding salinity tolerance in citrus using rootstocks," in *Salt Stress in Plants: Signalling, Omics and Adaptations*, 355–376. doi:10.1007/978-1-4614-6108-1_14.

Fricke, W., Akhiyarova, G., Wei, W., Alexandersson, E., Miller, A., Kjellbom, P. O., et al. (2006). The short-term growth response to salt of the developing barley leaf. in *Journal of Experimental Botany*, 1079–1095. doi:10.1093/jxb/erj095.

Gambino, G., Perrone, I., and Gribaudo, I. (2008). A rapid and effective method for RNA extraction from different tissues of grapevine and other woody plants. *Phytochem. Anal.* 19, 520–525. doi:10.1002/pca.1078.

Garciadeblás, B., Senn, M. E., Bañuelos, M. A., and Rodríguez-Navarro, A. (2003). Sodium transport and HKT transporters: The rice model. *Plant J.* 34, 788–801. doi:10.1046/j.1365-

313X.2003.01764.x.

Gaxiola, R. A., Li, J., Undurraga, S., Dang, L. M., Allen, G. J., Alper, S. L., et al. (2001). Drought- and salt-tolerant plants result from overexpression of the AVP1 H+-pump. *Proc. Natl. Acad. Sci. U. S. A.* 98, 11444–11449. doi:10.1073/pnas.191389398.

Genoves, A., Pallas, V., and Navarro, J. A. (2011). Contribution of Topology Determinants of a Viral Movement Protein to Its Membrane Association, Intracellular Traffic, and Viral Cell-to-Cell Movement. *J. Virol.* 85, 7797–7809. doi:10.1128/jvi.02465-10.

Gentleman, R. C., Carey, V. J., Bates, D. M., Bolstad, B., Dettling, M., Dudoit, S., et al. (2004). Bioconductor: open software development for computational biology and bioinformatics. *Genome Biol.* doi:10.1186/gb-2004-5-10-r80.

Georgiev, V., Ananga, A., and Tsolova, V. (2014). Recent advances and uses of grape flavonoids as nutraceuticals. *Nutrients* 6, 391–415. doi:10.3390/nu6010391.

Gesell, A., Yoshida, K., Tran, L. T., and Constabel, C. P. (2014). Characterization of an apple TT2-type R2R3 MYB transcription factor functionally similar to the poplar proanthocyanidin regulator PtMYB134. *Planta* 240, 497–511. doi:10.1007/s00425-014-2098-y.

Gévaudant, F., Duby, G., Von Stedingk, E., Zhao, R., Morsomme, P., and Boutry, M. (2007). Expression of a constitutively activated plasma membrane H +-ATPase alters plant development and increases salt tolerance. *Plant Physiol.* doi:10.1104/pp.107.103762.

Gil-Muñoz, F., Peche, P. M., Climent, J., Forner, M. A., Naval, M. M., and Badenes, M. L. (2018a). Breeding and screening persimmon rootstocks for saline stress tolerance. *Acta Hortic.* 1195, 105–110. doi:10.17660/ActaHortic.2018.1195.18.

Gil-Muñoz, F., Pérez-Pérez, J. G., Quiñones, A., Primo-Capella, A., Cebolla, J., Ángeles Forner-Giner, M., et al. (2020). A cross population between D. Kaki and D. Virginiana shows high

variability for saline tolerance and improved salt stress tolerance. *PLoS One* 15, e0229023. doi:10.1371/journal.pone.0229023.

Gil-Muñoz, F., Zuriaga, E., Badenes, M. L., and Naval, M. M. (2018b). Analysis of genetic diversity among a set of accessions from the IVIA's persimmon collection. *Acta Hortic.* 1195, 43–50. doi:10.17660/ActaHortic.2018.1195.7.

Gilliam, J. W. (1971). Rapid Measurement of Chlorine in Plant Materials1. *Soil Sci. Soc. Am. J.* 35, 512. doi:10.2136/sssaj1971.03615995003500030051x.

Gimenez, C., Gallardo, M., and Thompson, R. B. (2004). "Plant-Water Relations," in *Encyclopedia of Soils in the Environment* (Elsevier), 231–238. doi:10.1016/B0-12-348530-4/00459-8.

Giordani, E., Naval, M., and Benelli, C. (2012). "In Vitro Propagation of Persimmon (Diospyros kaki Thunb.)," in *Methods in molecular biology (Clifton, N.J.)*, 89–98. doi:10.1007/978-1-62703-074-8_7.

Goff, S. A., Cone, K. C., and Chandler, V. L. (1992). Functional analysis of the transcriptional activator encoded by the maize B gene: Evidence for a direct functional interaction between two classes of regulatory proteins. *Genes Dev.* 6, 864–875. doi:10.1101/gad.6.5.864.

Gong, D., Guo, Y., Jagendorf, A. T., and Zhu, J. K. (2002). Biochemical characterization of the Arabidopsis protein kinase SOS2 that functions in salt tolerance. *Plant Physiol.* 130, 256–264. doi:10.1104/pp.004507.

Gong, D., Guo, Y., Schumaker, K. S., and Zhu, J. K. (2004). The SOS3 family of calcium sensors and SOS2 family of protein kinases in arabidopsis. *Plant Physiol.* 134, 919–926. doi:10.1104/pp.103.037440.

Gonzalez, A., Zhao, M., Leavitt, J. M., and Lloyd, A. M. (2008). Regulation of the anthocyanin biosynthetic pathway by the TTG1/bHLH/Myb transcriptional complex in Arabidopsis seedlings. *Plant J.* 53, 814–827. doi:10.1111/j.1365-313X.2007.03373.x.

Graves, S., Piepho, H.-P., Selzer With Help From Sundar, L., Maintainer, D.-R., and Selzer, L. (2015). Package "multcompView" Visualizations of Paired Comparisons. *R Packag. http//CRAN.R-project.org/package=multcompView*.

Haas, B. J., Papanicolaou, A., Yassour, M., Grabherr, M., Blood, P. D., Bowden, J., et al. (2013). De novo transcript sequence reconstruction from RNA-seq using the Trinity platform for reference generation and analysis. *Nat. Protoc.* doi:10.1038/nprot.2013.084.

Halfter, U. (2000). The Arabidopsis SOS2 protein kinase physically interacts with and is activated by the calcium-binding protein SOS3. *Proc. Natl. Acad. Sci.* 97, 3735–3740. doi:10.1073/pnas.040577697.

Hamilton, C. M., Frary, A., Lewis, C., and Tanksley, S. D. (1996). Stable transfer of intact high molecular weight DNA into plant chromosomes. *Proc. Natl. Acad. Sci. U. S. A.* 93, 9975–9979. doi:10.1073/pnas.93.18.9975.

Han, Y., Yin, S., Huang, L., Wu, X., Zeng, J., Liu, X., et al. (2018). A sodium transporter HvHKT1;1 confers salt tolerance in barley via regulating tissue and cell ion homeostasis. *Plant Cell Physiol.* 59, 1976–1989. doi:10.1093/pcp/pcy116.

Hanin, M., Brini, F., Ebel, C., Toda, Y., Takeda, S., and Masmoudi, K. (2011). Plant dehydrins and stress tolerance: Versatile proteins for complex mechanisms. *Plant Signal. Behav.* 6, 1503–1509. doi:10.4161/psb.6.10.17088.

Hanin, M., Ebel, C., Ngom, M., Laplaze, L., and Masmoudi, K. (2016). New insights on plant salt tolerance mechanisms and their potential use for breeding. *Front. Plant Sci.* 7. doi:10.3389/fpls.2016.01787.

Harborne, J. B., and Grayer, R. J. (1993). "Flavonoids and insects," in *The Flavonoids*, 589–618. doi:10.1007/978-1-4899-2911-2_14.

Hazzouri, K. M., Khraiwesh, B., Amiri, K. M. A., Pauli, D., Blake, T., Shahid, M., et al. (2018). Mapping of HKT1;5 gene in barley using gwas approach and its implication in salt tolerance

mechanism. *Front. Plant Sci.* 9. doi:10.3389/fpls.2018.00156.

Hellens, R. P., Anne Edwards, E., Leyland, N. R., Bean, S., and Mullineaux, P. M. (2000). pGreen: A versatile and flexible binary Ti vector for Agrobacterium-mediated plant transformation. *Plant Mol. Biol.* 42, 819–832. doi:10.1023/A:1006496308160.

Henderson, S. W., Baumann, U., Blackmore, D. H., Walker, A. R., Walker, R. R., and Gilliham, M. (2014). Shoot chloride exclusion and salt tolerance in grapevine is associated with differential ion transporter expression in roots. *BMC Plant Biol.* 14, 273. doi:10.1186/s12870-014-0273-8.

Herranz, M. C., Sanchez-Navarro, J. A., Aparicio, F., and Pallás, V. (2005). Simultaneous detection of six stone fruit viruses by non-isotopic molecular hybridization using a unique riboprobe or "polyprobe." *J. Virol. Methods* 124, 49–55. doi:10.1016/j.jviromet.2004.11.003.

Hichri, I., Barrieu, F., Bogs, J., Kappel, C., Delrot, S., and Lauvergeat, V. (2011). Recent advances in the transcriptional regulation of the flavonoid biosynthetic pathway. *J. Exp. Bot.* 62, 2465–2483. doi:10.1093/jxb/erq442.

Hichri, I., Heppel, S. C., Pillet, J., Léon, C., Czemmel, S., Delrot, S., et al. (2010). The basic helix-loop-helix transcription factor MYC1 is involved in the regulation of the flavonoid biosynthesis pathway in grapevine. *Mol. Plant* 3, 509–523. doi:10.1093/mp/ssp118.

Horie, T., Costa, A., Kim, T. H., Han, M. J., Horie, R., Leung, H. Y., et al. (2007). Rice OsHKT2;1 transporter mediates large Na+ influx component into K+-starved roots for growth. *EMBO J.* 26, 3003–3014. doi:10.1038/sj.emboj.7601732.

Horie, T., Sugawara, M., Okunou, K., Nakayama, H., Schroeder, J. I., Shinmyo, A., et al. (2008). Functions of HKT transporters in sodium transport in roots and in protecting leaves from salinity stress. *Plant Biotechnol.* 25, 233–239. doi:10.5511/plantbiotechnology.25.233.

Hrabak, E. M., Chan, C. W. M., Gribskov, M., Harper, J. F., Choi, J. H., Halford, N., et al. (2003). The Arabidopsis CDPK-SnRK

superfamily of protein kinases. *Plant Physiol.* 132, 666–680. doi:10.1104/pp.102.011999.

Hribar, J., Zavrtanik, M., Simčič, M., and Vidrih, R. (2000). Changes during storing and astringency removal of persimmon fruit (Diospyros Kaki L.). *Acta Aliment.* 29, 123–136. doi:10.1556/aalim.29.2000.2.3.

Hsu, J. L., Wang, L. Y., Wang, S. Y., Lin, C. H., Ho, K. C., Shi, F. K., et al. (2009). Functional phosphoproteomic profiling of phosphorylation sites in membrane fractions of salt-stressed Arabidopsis thaliana. *Proteome Sci.* 7, 42. doi:10.1186/1477-5956-7-42.

Huang, C. X., and Van Steveninck, R. F. M. (1989). Maintenance of Low Cl − Concentrations in Mesophyll Cells of Leaf Blades of Barley Seedlings Exposed to Salt Stress . *Plant Physiol.* 90, 1440–1443. doi:10.1104/pp.90.4.1440.

Huang, S., Spielmeyer, W., Lagudah, E. S., James, R. A., Platten, J. D., Dennis, E. S., et al. (2006). A sodium transporter (HKT7) is a candidate for Nax1, a gene for salt tolerance in durum wheat. *Plant Physiol.* 142, 1718–1727. doi:10.1104/pp.106.088864.

Huang, S., Spielmeyer, W., Lagudah, E. S., and Munns, R. (2008). Comparative mapping of HKT genes in wheat, barley, and rice, key determinants of Na+ transport, and salt tolerance. *J. Exp. Bot.* 59, 927–937. doi:10.1093/jxb/ern033.

Humphries, J. A., Walker, A. R., Timmis, J. N., and Orford, S. J. (2005). Two WD-repeat genes from cotton are functional homologues of the Arabidopsis thaliana TRANSPARENT TESTA GLABRA1 (TTG1) gene. *Plant Mol. Biol.* 57, 67–81. doi:10.1007/s11103-004-6768-1.

Ikeda, I., Yamada, M., Kurihara, A., and Nishida, T. (1985). Inheritance of Astringency in Japanese Persimmon. *J. Japanese Soc. Hortic. Sci.* 54, 39–45. doi:10.2503/jjshs.54.39.

Ikegami, A., Eguchi, S., Kitajima, A., Inoue, K., and Yonemori, K. (2007). Identification of genes involved in proanthocyanidin biosynthesis of persimmon (Diospyros kaki) fruit. *Plant Sci.* 172,

1037–1047. doi:10.1016/j.plantsci.2007.02.010.

Ikegami, A., Kitajima, A., and Yonemori, K. (2005). Inhibition of flavonoid biosynthetic gene expression coincides with loss of astringency in pollination-constant, non-astringent (PCNA)-type persimmon fruit. *J. Hortic. Sci. Biotechnol.* 80, 225–228. doi:10.1080/14620316.2005.11511921.

Incesu, M., Cimen, B., Yesiloglu, T., and Yilmaz, B. (2014). Growth and photosynthetic response of two persimmon rootstocks (Diospyros kaki and D. virginiana) under different salinity levels. *Not. Bot. Horti Agrobot. Cluj-Napoca* 42, 386–391. doi:10.1583/nbha4229471.

Intrigliolo, D. S., Visconti, F., Bonet, L., Parra, M., Besada, C., Abrisqueta, I., et al. (2018). "Persimmon (Diospyros kaki) trees responses to restrictions in water amount and quality," in *Water Scarcity and Sustainable Agriculture in Semiarid Environment: Tools, Strategies, and Challenges for Woody Crops* (Elsevier), 149–177. doi:10.1016/B978-0-12-813164-0.00008-9.

Isah, T. (2019). Stress and defense responses in plant secondary metabolites production. *Biol. Res.* 52, 39. doi:10.1186/s40659-019-0246-3.

Isayenkov, S. V., and Maathuis, F. J. M. (2019). Plant salinity stress: Many unanswered questions remain. *Front. Plant Sci.* 10. doi:10.3389/fpls.2019.00080.

James, R. A., Munns, R., Von Caemmerer, S., Trejo, C., Miller, C., and Condon, T. (2006). Photosynthetic capacity is related to the cellular and subcellular partitioning of Na+, K+ and Cl- in salt-affected barley and durum wheat. *Plant, Cell Environ.* 29, 2185–2197. doi:10.1111/j.1365-3040.2006.01592.x.

Jende-Strid, B. (1993). Genetic Control of Flavonoid Biosynthesis in Barley. *Hereditas* 119, 187–204. doi:10.1111/j.1601-5223.1993.00187.x.

Ji, H., Pardo, J. M., Batelli, G., Van Oosten, M. J., Bressan, R. A., and Li, X. (2013). The salt overly sensitive (SOS) pathway: Established and emerging roles. *Mol. Plant* 6, 275–286.

doi:10.1093/mp/sst017.

Jia, B., Sun, M., Duanmu, H., DIng, X., Liu, B., Zhu, Y., et al. (2017). GsCHX19.3, a member of cation/H+ exchanger superfamily from wild soybean contributes to high salinity and carbonate alkaline tolerance. *Sci. Rep.* 7. doi:10.1038/s41598-017-09772-3.

Johanson, U., Karlsson, M., Johansson, I., Gustavsson, S., Sjövall, S., Fraysse, L., et al. (2001). The complete set of genes encoding major intrinsic proteins in arabidopsis provides a framework for a new nomenclature for major intrinsic proteins in plants. *Plant Physiol.* 126, 1358–1369. doi:10.1104/pp.126.4.1358.

Joly, R. J. (1989). Effects of Sodium Chloride on the Hydraulic Conductivity of Soybean Root Systems. *Plant Physiol.* 91, 1262–1265. doi:10.1104/pp.91.4.1262.

Julkowska, M. M., Hoefsloot, H. C. J., Mol, S., Feron, R., De Boer, G. J., Haring, M. A., et al. (2014). Capturing arabidopsis root architecture dynamics with root-fit reveals diversity in responses to salinity. *Plant Physiol.* 166, 1387–1402. doi:10.1104/pp.114.248963.

Julkowska, M. M., Koevoets, I. T., Mol, S., Hoefsloot, H., Feron, R., Tester, M. A., et al. (2017). Genetic components of root architecture remodeling in response to salt stress. *Plant Cell* 29, 3198–3213. doi:10.1105/tpc.16.00680.

Kajiura, M. (1946). Persimmon cultivars and their improvement 2 (In japanese). *Breed. Hort.* 1, 175–182.

Kanzaki, S., Yonemori, K., Sato, A., Yamada, M., and Sugiura, A. (2000). Analysis of the genetic relationships among pollination-constant and non-astringent (PCNA) cultivars of persimmon (Diospyros kaki Thunb.) from Japan and China using Amplified Fragment Length Polymorphism (AFLP). *J. Japanese Soc. Hortic. Sci.* 69, 665–670. doi:10.2503/jjshs.69.665.

Kanzaki, S., Yonemori, K., Sugiura, A., Sato, A., and Yamada, M. (2001). Identification of molecular markers linked to the trait of natural astringency loss of Japanese persimmon (Diospyros kaki) fruit. *J. Am. Soc. Hortic. Sci.* 126, 51–55.

doi:10.21273/jashs.126.1.51.

Kapilan, R., Vaziri, M., and Zwiazek, J. J. (2018). Regulation of aquaporins in plants under stress. *Biol. Res.* 51. doi:10.1186/s40659-018-0152-0.

Karley, A. J., Leigh, R. A., and Sanders, D. (2000a). Differential ion accumulation and ion fluxes in the mesophyll and epidermis of barley. *Plant Physiol.* 122, 835–844. doi:10.1104/pp.122.3.835.

Karley, A. J., Leigh, R. A., and Sanders, D. (2000b). Where do all the ions go? The cellular basis of differential ion accumulation in leaf cells. *Trends Plant Sci.* 5, 465–470. doi:10.1016/S1360-1385(00)01758-1.

Kassambara, A., and Mundt, F. (2017). Package "factoextra" for R: Extract and Visualize the Results of Multivariate Data Analyses. *R Packag. version*.

Katsuhara, M., Tsuji, N., Shibasaka, M., and Panda, S. K. (2014). Osmotic stress decreases PIP aquaporin transcripts in barley roots but H2O2 is not involved in this process. *J. Plant Res.* 127, 787–792. doi:10.1007/s10265-014-0662-y.

Kikuchi (1948). *Pomology-part I (in Japanese)*. Tokyo: Yokendo.

Kitagawa, H., and Glucina, P. G. (1984). *Persimmon culture in New Zealand*. Wellington: Science Information Publishing Centre.

Kitajima, A., Akuta, H., Yoshioka, T., Entani, T., Nakano, M., and Ishida, M. (1992). Influence of Seeded Fruit on Seedless Fruit Set in Japanese Persimmon cv. Fuyu (Diospyros kaki L. f.). *Engei Gakkai zasshi* 61, 499–506. doi:10.2503/jjshs.61.499.

Knoester, M., van Loon LC, L. C. van, van den Heuvel J, J. van den, Hennig, J., Bol, J. F., and Linthorst, H. J. (1998). Ethylene-insensitive tobacco lacks nonhost resistance against soil-borne fungi. *Proc. Natl. Acad. Sci. U. S. A.* 95, 1933–7. Available at: http://www.ncbi.nlm.nih.gov/pubmed/9465120 [Accessed September 17, 2018].

Kono, A., Kobayashi, S., Onoue, N., and Sato, A. (2016).

Characterization of a highly polymorphic region closely linked to the AST locus and its potential use in breeding of hexaploid persimmon (Diospyros kaki Thunb.). *Mol. Breed.* 36, 1–13. doi:10.1007/s11032-016-0480-0.

Kopylova, E., Noé, L., and Touzet, H. (2012). SortMeRNA: Fast and accurate filtering of ribosomal RNAs in metatranscriptomic data. *Bioinformatics*. doi:10.1093/bioinformatics/bts611.

Koyro, H. W. (2006). Effect of salinity on growth, photosynthesis, water relations and solute composition of the potential cash crop halophyte Plantago coronopus (L.). *Environ. Exp. Bot.* 56, 136–146. doi:10.1016/j.envexpbot.2005.02.001.

Kurtzer, G. M., Sochat, V., and Bauer, M. W. (2017). Singularity: Scientific containers for mobility of compute. *PLoS One*. doi:10.1371/journal.pone.0177459.

Laemmli, U. K. (1970). Cleavage of structural proteins during the assembly of the head of bacteriophage T4. *Nature* 227, 680–685. doi:10.1038/227680a0.

Leastro, M. O., Pallás, V., Resende, R. O., and Sánchez-Navarro, J. A. (2015). The movement proteins (NSm) of distinct tospoviruses peripherally associate with cellular membranes and interact with homologous and heterologous NSm and nucleocapsid proteins. *Virology* 478, 39–49. doi:10.1016/j.virol.2015.01.031.

Lepiniec, L., Debeaujon, I., Routaboul, J.-M., Baudry, A., Pourcel, L., Nesi, N., et al. (2006). Genetics and Biochemistry of Seed Flavonoids. *Annu. Rev. Plant Biol.* 57, 405–430. doi:10.1146/annurev.arplant.57.032905.105252.

Levin, A. D. (2019). Re-evaluating pressure chamber methods of water status determination in field-grown grapevine (Vitis spp.). *Agric. Water Manag.* 221, 422–429. doi:10.1016/j.agwat.2019.03.026.

Li, R., Zhang, J., Wu, G., Wang, H., Chen, Y., and Wei, J. (2012). HbCIPK2, a novel CBL-interacting protein kinase from halophyte Hordeum brevisubulatum, confers salt and osmotic stress tolerance. *Plant, Cell Environ.* doi:10.1111/j.1365-

3040.2012.02511.x.

Libutti, A., Cammerino, A. R. B., and Monteleone, M. (2018). Risk assessment of soil salinization due to tomato cultivation in mediterranean climate conditions. *Water (Switzerland)* 10. doi:10.3390/w10111503.

Lim, C. W., Baek, W., Jung, J., Kim, J. H., and Lee, S. C. (2015a). Function of ABA in stomatal defense against biotic and drought stresses. *Int. J. Mol. Sci.* 16, 15251–15270. doi:10.3390/ijms160715251.

Lim, C. W., Baek, W., Jung, J., Kim, J. H., and Lee, S. C. (2015b). Function of ABA in stomatal defense against biotic and drought stresses. *Int. J. Mol. Sci.* 16, 15251–15270. doi:10.3390/ijms160715251.

Liu, J. (2000). The Arabidopsis thaliana SOS2 gene encodes a protein kinase that is required for salt tolerance. *Proc. Natl. Acad. Sci.* 97, 3730–3734. doi:10.1073/pnas.060034197.

Liu, J., and Zhu, J. K. (1998). A calcium sensor homolog required for plant salt tolerance. *Science (80-.).* 280, 1943–1945. doi:10.1126/science.280.5371.1943.

Liu, X., Feng, C., Zhang, M., Yin, X., Xu, C., and Chen, K. (2013). The MrWD40-1 Gene of Chinese Bayberry (Myrica rubra) Interacts with MYB and bHLH to Enhance Anthocyanin Accumulation. *Plant Mol. Biol. Report.* 31, 1474–1484. doi:10.1007/s11105-013-0621-0.

López-Pérez, L., Martínez-Ballesta, M. del C., Maurel, C., and Carvajal, M. (2009). Changes in plasma membrane lipids, aquaporins and proton pump of broccoli roots, as an adaptation mechanism to salinity. *Phytochemistry* 70, 492–500. doi:10.1016/j.phytochem.2009.01.014.

Love, M. I., Anders, S., and Huber, W. (2014). *Differential analysis of count data - the DESeq2 package*. doi:110.1186/s13059-014-0550-8.

Luo, Y., Reid, R., Freese, D., Li, C., Watkins, J., Shi, H., et al. (2017). Salt

tolerance response revealed by RNA-Seq in a diploid halophytic wild relative of sweet potato. *Sci. Rep.* 7. doi:10.1038/s41598-017-09241-x.

Luo Zheng-Rong, Yonemori, K., and Sugiura, A. (1995). Evaluation of RAPD analysis for cultivar identification of persimmons. *J. Japanese Soc. Hortic. Sci.* 64, 535–541. doi:10.2503/jjshs.64.535.

Lyman, B. J., and Green, B. G. (1990). Oral astringency: Effects of repeated exposure and interactions with sweeteners. *Chem. Senses*. doi:10.1093/chemse/15.2.151.

Magome, H., Yamaguchi, S., Hanada, A., Kamiya, Y., and Oda, K. (2008). The DDF1 transcriptional activator upregulates expression of a gibberellin-deactivating gene, GA2ox7, under high-salinity stress in Arabidopsis. *Plant J.* 56, 613–626. doi:10.1111/j.1365-313X.2008.03627.x.

Mahajan, S., Pandey, G. K., and Tuteja, N. (2008). Calcium- and salt-stress signaling in plants: Shedding light on SOS pathway. *Arch. Biochem. Biophys.* 471, 146–158. doi:10.1016/j.abb.2008.01.010.

Manach, C., Williamson, G., Morand, C., Scalbert, A., and Rémésy, C. (2005). Bioavailability and bioefficacy of polyphenols in humans. I. Review of 97 bioavailability studies. *Am. J. Clin. Nutr.* 81. doi:10.1093/ajcn/81.1.230s.

Mangiafico, S. (2018). rcompanion: Functions to Support Extension Education Program Evaluation. Available at: http://rcompanion.org.

Marles, M. A. S., Ray, H., and Gruber, M. Y. (2003). New perspectives on proanthocyanidin biochemistry and molecular regulation. *Phytochemistry* 64, 367–383. doi:10.1016/S0031-9422(03)00377-7.

Martínez-Atienza, J., Jiang, X., Garciadeblas, B., Mendoza, I., Zhu, J. K., Pardo, J. M., et al. (2007). Conservation of the salt overly sensitive pathway in rice. *Plant Physiol.* 143, 1001–1012. doi:10.1104/pp.106.092635.

Martínez-Ballesta, M. C., Aparicio, F., Pallás, V., Martínez, V., and Carvajal, M. (2003). Influence of saline stress on root hydraulic conductance and PIP expression in Arabidopsis. *J. Plant Physiol.* 160, 689–697. doi:10.1078/0176-1617-00861.

Mäser, P., Eckelman, B., Vaidyanathan, R., Horie, T., Fairbairn, D. J., Kubo, M., et al. (2002). Altered shoot/root Na+ distribution and bifurcating salt sensitivity in Arabidopsis by genetic disruption of the Na+ transporter AtHKT1. *FEBS Lett.* 531, 157–161. doi:10.1016/S0014-5793(02)03488-9.

Matsuo, T., and Itoo, S. (1982). A model experiment for de-astringency of persimmon fruit with high carbon dioxide treatment: In vitro gelation of kaki-tannin by reacting with acetaldehyde. *Agric. Biol. Chem.* 46, 683–689. doi:10.1080/00021369.1982.10865131.

Maurel, C., Verdoucq, L., Luu, D.-T., and Santoni, V. (2008). Plant Aquaporins: Membrane Channels with Multiple Integrated Functions. *Annu. Rev. Plant Biol.* 59, 595–624. doi:10.1146/annurev.arplant.59.032607.092734.

Mimi, Z. A., and Jamous, S. A. (2010). Climate change and agricultural water demand: Impacts and adaptations. *African J. Environ. Sci. Technol.* 4, 183–191. doi:10.4314/AJEST.V4I4.56351.

Moustafa, K., AbuQamar, S., Jarrar, M., Al-Rajab, A. J., and Trémouillaux-Guiller, J. (2014). MAPK cascades and major abiotic stresses. *Plant Cell Rep.* 33, 1217–1225. doi:10.1007/s00299-014-1629-0.

Munns, R. (2002). Comparative physiology of salt and water stress. *Plant, Cell Environ.* 25, 239–250. doi:10.1046/j.0016-8025.2001.00808.x.

Munns, R., Guo, J., Passioura, J. B., and Cramer, G. R. (2000). Leaf water status controls day-time but not daily rates of leaf expansion in salt-treated barley. *Aust. J. Plant Physiol.* 27, 949–957. doi:10.1071/pp99193.

Munns, R., Passioura, J. B., Colmer, T. D., and Byrt, C. S. (2020). Osmotic adjustment and energy limitations to plant growth in

saline soil. *New Phytol.* 225, 1091–1096. doi:10.1111/nph.15862.

Munns, R., and Tester, M. (2008). Mechanisms of Salinity Tolerance. *Annu. Rev. Plant Biol.* 59, 651–681. doi:10.1146/annurev.arplant.59.032607.092911.

Naval, M. del M., Gil-Muñoz, F., Lloret, A., Besada, C., Salvador, A., Badenes, M. L., et al. (2016). A WD40-repeat protein from persimmon interacts with the regulators of proanthocyanidin biosynthesis DkMYB2 and DkMYB4. *Tree Genet. Genomes* 12, 13. doi:10.1007/s11295-016-0969-z.

Naval, M. del M., Zuriaga, E., Pecchioli, S., Llácer, G., Giordani, E., and Badenes, M. L. (2010). Analysis of genetic diversity among persimmon cultivars using microsatellite markers. *Tree Genet. Genomes* 6, 677–687. doi:10.1007/s11295-010-0283-0.

Nei, M. (1972). Genetic Distance between Populations. *Am. Nat.* 106, 283–292. doi:10.1086/282771.

Nesi, N., Debeaujon, I., Jond, C., Pelletier, G., Caboche, M., and Lepiniec, L. (2000). The TT8 gene encodes a basic helix-loop-helix domain protein required for expression of DFR and BAN genes in Arabidopsis siliques. *Plant Cell* 12, 1863–1878. doi:10.1105/tpc.12.10.1863.

Nesi, N., Jond, C., Debeaujon, I., Caboche, M., and Lepiniec, L. (2001). The Arabidopsis TT2 Gene Encodes an R2R3 MYB Domain Protein That Acts as a Key Determinant for Proanthocyanidin Accumulation in Developing Seed . *Plant Cell* 13, 2099–2114. doi:10.1105/tpc.010098.

Neuwirth, E. (2014). RColorBrewer: ColorBrewer palettes. *R Packag. version 1.1-2*, https://cran.R-project.org/package=RColorBrewer. Available at: https://cran.r-project.org/web/packages/RColorBrewer/index.html.

Nguyen, H. M., Sako, K., Matsui, A., Suzuki, Y., Mostofa, M. G., Van Ha, C., et al. (2017). Ethanol enhances high-salinity stress tolerance by detoxifying reactive oxygen species in arabidopsis thaliana and rice. *Front. Plant Sci.* 8, 1001.

doi:10.3389/fpls.2017.01001.

Niu, X., Narasimhan, M. L., Salzman, R. A., Bressan, R. A., and Hasegawa, P. M. (1993). NaCl regulation of plasma membrane H+-ATPase gene expression in a glycophyte and a halophyte. *Plant Physiol.* doi:10.1104/pp.103.3.713.

Ogle, D. H., Wheeler, P., and Dinno, A. (2018). FSA: Fisheries Stock Analysis. R package version 0.8.22. Available at: https://github.com/droglenc/FSA.

Osakabe, Y., Arinaga, N., Umezawa, T., Katsura, S., Nagamachi, K., Tanaka, H., et al. (2013). Osmotic stress responses and plant growth controlled by potassium transporters in Arabidopsis. *Plant Cell* 25, 609–624. doi:10.1105/tpc.112.105700.

Padmanaban, S., Chanroj, S., Kwak, J. M., Li, X., Ward, J. M., and Sze, H. (2007). Participation of endomembrane cation/H+ exchanger AtCHX20 in osmoregulation of guard cells. *Plant Physiol.* 144, 82–93. doi:10.1104/pp.106.092155.

Palmgren, M. G. (2001). Plant Plasma Membrane H+/-ATPases: Powerhouses for Nutrient Uptake. *Annu. Rev. Plant Physiol. Plant Mol. Biol.* 52, 817–845. doi:10.1146/annurev.arplant.52.1.817.

Pardo, J. M., Cubero, B., Leidi, E. O., and Quintero, F. J. (2006). Alkali cation exchangers: Roles in cellular homeostasis and stress tolerance. in *Journal of Experimental Botany*, 1181–1199. doi:10.1093/jxb/erj114.

Parfitt, D. E., Yonemori, K., Honsho, C., Nozaka, M., Kanzaki, S., Sato, A., et al. (2015). Relationships among Asian persimmon cultivars, astringent and non-astringent types. *Real-Time Syst.* 51, 1–9. doi:10.1007/s11295-015-0848-z.

Payne, C. T., Zhang, F., and Lloyd, A. M. (2000). GL3 encodes a bHLH protein that regulates trichome development in arabidopsis through interaction with GL1 and TTG1. *Genetics* 156, 1349–1362.

Peakall, R., and Smouse, P. E. (2012). GenALEx 6.5: Genetic analysis in

Excel. Population genetic software for teaching and research-an update. *Bioinformatics* 28, 2537–2539. doi:10.1093/bioinformatics/bts460.

Perucho, R. (2015). “El cultivo del caqui. Antecedentes e importancia económica,” in *El cultivo del caqui*, eds. M. L. Badenes, D. S. Intrigliolo, A. Salvador, and A. Vicent (Generalitat Valenciana), 17–34.

Perucho, R. (2018). Evolution of production of the ‘Rojo Brillante’ cultivar in Spain and its impact on markets. in *Acta Horticulturae* (International Society for Horticultural Science (ISHS), Leuven, Belgium), 1–8. doi:10.17660/ActaHortic.2018.1195.1.

Pesis, E., and Ben-Arie, R. (1984). Involvement of Acetaldehyde and Ethanol Accumulation During Induced Deastringency of Persimmon Fruits. *J. Food Sci.* 49, 896–899. doi:10.1111/j.1365-2621.1984.tb13236.x.

Petrov, V., Hille, J., Mueller-Roeber, B., and Gechev, T. S. (2015). ROS-mediated abiotic stress-induced programmed cell death in plants. *Front. Plant Sci.* 6, 69. doi:10.3389/fpls.2015.00069.

Plett, D. C., and Møller, I. S. (2010). Na+ transport in glycophytic plants: What we know and would like to know. *Plant, Cell Environ.* 33, 612–626. doi:10.1111/j.1365-3040.2009.02086.x.

Postiglione, L. (2002). “Soil salinization in the Mediterranean: Soils, processes and implications,” in *Mediterranean desertification: A mosaic of processes and responses*, eds. N. A. Geeson, C. J. Brandt, and J. B. Thornes (John Wiley & Sons, Inc.), 163–173.

Pritchard, J. K., Stephens, M., and Donnelly, P. (2000). Inference of population structure using multilocus genotype data. *Genetics* 155, 945–959.

Qiu, Q. S., Barkla, B. J., Vera-Estrella, R., Zhu, J. K., and Schumaker, K. S. (2003). Na+/H+ exchange activity in the plasma membrane of Arabidopsis. *Plant Physiol.* 132, 1041–1052. doi:10.1104/pp.102.010421.

Qiu, Q. S., Guo, Y., Dietrich, M. A., Schumaker, K. S., and Zhu, J. K.

(2002). Regulation of SOS1, a plasma membrane Na+/H+ exchanger in Arabidopsis thaliana, by SOS2 and SOS3. *Proc. Natl. Acad. Sci. U. S. A.* 99, 8436–8441. doi:10.1073/pnas.122224699.

Quan, R., Lin, H., Mendoza, I., Zhang, Y., Cao, W., Yang, Y., et al. (2007). SCABP8/CBL10, a putative calcium sensor, interacts with the protein kinase SOS2 to protect Arabidopsis shoots from salt stress. *Plant Cell* 19, 1415–1431. doi:10.1105/tpc.106.042291.

Quintero, F. J., Martinez-Atienza, J., Villalta, I., Jiang, X., Kim, W. Y., Ali, Z., et al. (2011). Activation of the plasma membrane Na/H antiporter salt-overly-sensitive 1 (SOS1) by phosphorylation of an auto-inhibitory C-terminal domain. *Proc. Natl. Acad. Sci. U. S. A.* 108, 2611–2616. doi:10.1073/pnas.1018921108.

Quintero, F. J., Ohta, M., Shi, H., Zhu, J. K., and Pardo, J. M. (2002). Reconstitution in yeast of the Arabidopsis SOS signaling pathway for Na+ homeostasis. *Proc. Natl. Acad. Sci. U. S. A.* 99, 9061–9066. doi:10.1073/pnas.132092099.

Rahnama, A., James, R. A., Poustini, K., and Munns, R. (2010). Stomatal conductance as a screen for osmotic stress tolerance in durum wheat growing in saline soil. *Funct. Plant Biol.* 37, 255–263. doi:10.1071/FP09148.

Reig, C., Martínez-Fuentes, A., Mesejo, C., and Agustí, M. (2018). Hormonal control of parthenocarpic fruit set in 'Rojo Brillante' persimmon (Diospyros kaki Thunb.). *J. Plant Physiol.* 231, 96–104. doi:10.1016/j.jplph.2018.09.004.

Rodríguez-Gamir, J., Ancillo, G., Legaz, F., Primo-Millo, E., and Forner-Giner, M. A. (2012). Influence of salinity on pip gene expression in citrus roots and its relationship with root hydraulic conductance, transpiration and chloride exclusion from leaves. *Environ. Exp. Bot.* 78, 163–166. doi:10.1016/j.envexpbot.2011.12.027.

Rus, A., Lee, B. H., Muñoz-Mayor, A., Sharkhuu, A., Miura, K., Zhu, J. K., et al. (2004). AtHKT1 facilitates Na+ homeostasis and K+ nutrition in planta. *Plant Physiol.* 136, 2500–2511.

doi:10.1104/pp.104.042234.

Sahu, B. B., and Shaw, B. P. (2009). Salt-inducible isoform of plasma membrane H+ATPase gene in rice remains constitutively expressed in natural halophyte, Suaeda maritima. *J. Plant Physiol.* doi:10.1016/j.jplph.2008.12.001.

Salvador, A., Arnal, L., Besada, C., Larrea, V., Quiles, A., and Pérez-Munuera, I. (2007). Physiological and structural changes during ripening and deastringency treatment of persimmon fruit cv. "Rojo Brillante." *Postharvest Biol. Technol.* 46, 181–188. doi:10.1016/j.postharvbio.2007.05.003.

Saranga, Y., Cahaner, A., Zamir, D., Marani, A., and Rudich, J. (1992). Breeding tomatoes for salt tolerance: inheritance of salt tolerance and related traits in interspecific populations. *Theor. Appl. Genet.* 84, 390–396. doi:10.1007/BF00229498.

Sato, A., and Yamada, M. (2016). Persimmon breeding in Japan for pollination-constant non-astringent (PCNA) type with marker-assisted selection. *Breed. Sci.* 66, 60–68. doi:10.1270/jsbbs.66.60.

Scalbert, A. (1991). Antimicrobial properties of tannins. *Phytochemistry* 30, 3875–3883. doi:10.1016/0031-9422(91)83426-L.

Schaart, J. G., Dubos, C., Romero De La Fuente, I., van Houwelingen, A. M. M. L., de Vos, R. C. H., Jonker, H. H., et al. (2013). Identification and characterization of MYB-bHLH-WD40 regulatory complexes controlling proanthocyanidin biosynthesis in strawberry (Fragaria × ananassa) fruits. *New Phytol.* 197, 454–467. doi:10.1111/nph.12017.

Schuelke, M. (2000). An economic method for the fluorescent labeling of PCR fragments. *Nat. Biotechnol.* 18, 233–234. doi:10.1038/72708.

Shafi, A., and Zahoor, I. (2019). "Plant Survival and Tolerance Under High Salinity: Primary and Secondary Cell Wall-Sensing Mechanism," in *Salt Stress, Microbes, and Plant Interactions: Causes and Solution*, 129–146. doi:10.1007/978-981-13-8801-

9_6.

Shahid, M. A., Balal, R. M., Khan, N., Simón-Grao, S., Alfosea-Simón, M., Cámara-Zapata, J. M., et al. (2019). Rootstocks influence the salt tolerance of Kinnow mandarin trees by altering the antioxidant defense system, osmolyte concentration, and toxic ion accumulation. *Sci. Hortic. (Amsterdam).* 250, 1–11. doi:10.1016/j.scienta.2019.02.028.

Shapira, O., Khadka, S., Israeli, Y., Shani, U., and Schwartz, A. (2009). Functional anatomy controls ion distribution in banana leaves: Significance of Na + seclusion at the leaf margins. *Plant, Cell Environ.* 32, 476–485. doi:10.1111/j.1365-3040.2009.01941.x.

Shen, P., Wang, R., Jing, W., and Zhang, W. (2011). Rice Phospholipase Dα is Involved in Salt Tolerance by the Mediation of H+-ATPase Activity and Transcription. *J. Integr. Plant Biol.* doi:10.1111/j.1744-7909.2010.01021.x.

Shi, H., Ishitani, M., Kim, C., and Zhu, J. K. (2000). The Arabidopsis thaliana salt tolerance gene SOS1 encodes a putative Na+/H+ antiporter. *Proc. Natl. Acad. Sci. U. S. A.* 97, 6896–6901. doi:10.1073/pnas.120170197.

Shi, H., Quintero, F. J., Pardo, J. M., and Zhu, J. K. (2002). The putative plasma membrane NA+/H+ antiporter SOS1 controls long-distance NA+ transport in plants. *Plant Cell* 14, 465–477. doi:10.1105/tpc.010371.

Sibole, J. V., Cabot, C., Poschenrieder, C., and Barceló, J. (2003). Ion allocation in two different salt-tolerant Mediterranean Medicago species. *J. Plant Physiol.* 160, 1361–1365. doi:10.1078/0176-1617-00811.

Signorell, A. (2017). DescTools: Tools for descriptive statistics. R package version 0.99.20. *CRAN*. doi:10.1016/j.foreco.2014.09.033.

Sinha, A. K., Jaggi, M., Raghuram, B., and Tuteja, N. (2011). Mitogen-activated protein kinase signaling in plants under abiotic stress. *Plant Signal. Behav.* 6, 196–203. doi:10.4161/psb.6.2.14701.

Sompornpailin, K., Makita, Y., Yamazaki, M., and Saito, K. (2002). A WD-repeat-containing putative regulatory protein in anthocyanin biosynthesis in Perilla frutescens. *Plant Mol. Biol.* 50, 485–495. doi:10.1023/A:1019850921627.

Song, C. P., Guo, Y., Qiu, Q., Lambert, G., Galbraith, D. W., Jagendorf, A., et al. (2004). A probable Na+(K+)/H+ exchanger on the chloroplast envelope functions in pH homeostasis and chloroplast development in Arabidopsis thaliana. *Proc. Natl. Acad. Sci. U. S. A.* 101, 10211–10216. doi:10.1073/pnas.0403709101.

Soriano, J. M., Pecchioli, S., Romero, C., Vilanova, S., Llácer, G., Giordani, E., et al. (2006). Development of microsatellite markers in polyploid persimmon (Diospyros kaki Thunb) from an enriched genomic library. *Mol. Ecol. Notes* 6, 368–370. doi:10.1111/j.1471-8286.2006.01236.x.

Spelt, C., Quattrocchio, F., Mol, J., and Koes, R. (2002). ANTHOCYANIN1 of petunia controls pigment synthesis, vacuolar pH, and seed coat development by genetically distinct mechanisms. *Plant Cell* 14, 2121–2135. doi:10.1105/tpc.003772.

Su, F., Hu, J., Zhang, Q., and Luo, Z. (2012). Isolation and characterization of a basic Helix-Loop-Helix transcription factor gene potentially involved in proanthocyanidin biosynthesis regulation in persimmon (Diospyros kaki Thunb.). *Sci. Hortic. (Amsterdam).* 136, 115–121. doi:10.1016/j.scienta.2012.01.013.

Sugiura, A., and Tomana, T. (1983). Relationships of ethanol production by seeds of different types of Japanese persimmons and their tannin content. *HortSci*, 319–321.

Sugiura, A., Yonemori, K., Harada, H., and Tomana, T. (1979). Changes of ethanol and acetaldehyde contents in Japanese persimmon fruits and their relation to natural deastringency. *Stud Inst Hortic Kyoto Univ*, 41–47.

Sunarpi, Horie, T., Motoda, J., Kubo, M., Yang, H., Yoda, K., et al. (2005). Enhanced salt tolerance mediated by AtHKT1 transporter-induced Na + unloading from xylem vessels to

xylem parenchyma cells. *Plant J.* 44, 928–938. doi:10.1111/j.1365-313X.2005.02595.x.

Suzek, B. E., Wang, Y., Huang, H., McGarvey, P. B., and Wu, C. H. (2015). UniRef clusters: A comprehensive and scalable alternative for improving sequence similarity searches. *Bioinformatics*. doi:10.1093/bioinformatics/btu739.

Suzuki, N., Bassil, E., Hamilton, J. S., Inupakutika, M. A., Zandalinas, S. I., Tripathy, D., et al. (2016). ABA is required for plant acclimation to a combination of salt and heat stress. *PLoS One* 11, e0147625. doi:10.1371/journal.pone.0147625.

Szczerba, M. W., Britto, D. T., and Kronzucker, H. J. (2009). K+ transport in plants: Physiology and molecular biology. *J. Plant Physiol.* 166, 447–466. doi:10.1016/j.jplph.2008.12.009.

Taheri, A., Jayasankar, S., Cline, J. A., Raizada, M. N., and Pauls, P. K. (2012). A WD-repeat gene from peach (Prunus persica L.) is a functional ortholog of Arabidopsis thaliana TRANSPARENT TESTA GLABRA1. *Vitr. Cell. Dev. Biol. - Plant* 48, 23–29. doi:10.1007/s11627-011-9390-3.

Taira, S. (1996). “Astringency in Persimmon,” in, 97–110. doi:10.1007/978-3-642-79660-9_6.

Tamura, K., Stecher, G., Peterson, D., Filipski, A., and Kumar, S. (2013). MEGA6: Molecular evolutionary genetics analysis version 6.0. *Mol. Biol. Evol.* 30, 2725–2729. doi:10.1093/molbev/mst197.

Tamura, M., Tao, R., Yonemori, K., Utsunomiya, N., and Sugiura, A. (1998). Ploidy Level and Genome Size of Several Diospyros Species. *J. Japanese Soc. Hortic. Sci.* 67, 306–312. doi:10.2503/jjshs.67.306.

Tanner, G. J., Francki, K. T., Abrahams, S., Watson, J. M., Larkin, P. J., and Ashton, A. R. (2003). Proanthocyanidin biosynthesis in plants. Purification of legume leucoanthocyanidin reductase and molecular cloning of its cDNA. *J. Biol. Chem.* 278, 31647–31656. doi:10.1074/jbc.M302783200.

Tao, J. J., Chen, H. W., Ma, B., Zhang, W. K., Chen, S. Y., and Zhang, J. S. (2015). The role of ethylene in plants under salinity stress. *Front. Plant Sci.* 6, 1–12. doi:10.3389/fpls.2015.01059.

Termaat, A., Passioura, J. B., and Munns, R. (1985). Shoot Turgor Does Not Limit Shoot Growth of NaCl-Affected Wheat and Barley. *Plant Physiol.* 77, 869–872. doi:10.1104/pp.77.4.869.

Tester, M., and Davenport, R. (2003). Na+tolerance and Na+transport in higher plants. *Ann. Bot.* 91, 503–527. doi:10.1093/aob/mcg058.

Tian, X., Wang, Z., Zhang, Q., Ci, H., Wang, P., Yu, L., et al. (2018). Genome-wide transcriptome analysis of the salt stress tolerance mechanism in Rosa chinensis. *PLoS One* 13, e0200938. doi:10.1371/journal.pone.0200938.

Tiwari, S., Sl, K., Kumar, V., Singh, B., Rao, A. R., Sv, A. M., et al. (2016). Mapping QTLs for Salt Tolerance in Rice (Oryza sativa L.) by Bulked Segregant Analysis of Recombinant Inbred Lines Using 50K SNP Chip. *PLoS One* 11, e0153610. doi:10.1371/journal.pone.0153610.

Tong, W., Yoshimoto, K., Kakehi, J.-I., Motose, H., Niitsu, M., and Takahashi, T. (2014). Thermospermine modulates expression of auxin-related genes in Arabidopsis. *Front. Plant Sci.* 5, 94. doi:10.3389/fpls.2014.00094.

Uozumi, N., Kim, E. J., Rubio, F., Yamaguchi, T., Muto, S., Tsuboi, A., et al. (2000). The Arabidopsis HKT1 gene homolog mediates inward Na+ currents in Xenopus laevis oocytes and Na+ uptake in Saccharomyces cerevisiae. *Plant Physiol.* 122, 1249–1259. doi:10.1104/pp.122.4.1249.

Vera-Estrella, R., Barkla, B. J., Higgins, V. J., and Blumwald, E. (1994). Plant defense response to fungal pathogens. Activation of host-plasma membrane H+-ATPase by elicitor-induced enzyme dephosphorylation. *Plant Physiol.* doi:10.1104/pp.104.1.209.

Visconti, F., de Paz, J. M., Bonet, L., Jordà, M., Quiñones, A., and Intrigliolo, D. S. (2015). Effects of a commercial calcium protein hydrolysate on the salt tolerance of Diospyros kaki L. cv. “Rojo

Brillante" grafted on Diospyros lotus L. *Sci. Hortic. (Amsterdam).* 185, 129–138. doi:10.1016/j.scienta.2015.01.028.

Visconti, F., Intrigliolo, D. S., Quiñones, A., Tudela, L., Bonet, L., and de Paz, J. M. (2017). Differences in specific chloride toxicity to Diospyros kaki cv. "Rojo Brillante" grafted on D. lotus and D. virginiana. *Sci. Hortic. (Amsterdam).* 214, 83–90. doi:10.1016/j.scienta.2016.11.025.

Vitali, V., Bellati, J., Soto, G., Ayub, N. D., and Amodeo, G. (2015). Root hydraulic conductivity and adjustments in stomatal conductance: hydraulic strategy in response to salt stress in a halotolerant species. *AoB Plants* 7, plv136. doi:10.1093/aobpla/plv136.

Volkov, V. (2015). Salinity tolerance in plants. Quantitative approach to ion transport starting from halophytes and stepping to genetic and protein engineering for manipulating ion fluxes. *Front. Plant Sci.* 6, 873. doi:10.3389/fpls.2015.00873.

Walker, A. R., Davison, P. A., Bolognesi-Winfield, A. C., James, C. M., Srinivasan, N., Blundell, T. L., et al. (1999). The TRANSPARENT TESTA GLABRA1 locus, which regulates trichome differentiation and anthocyanin biosynthesis in arabidopsis, encodes a WD40 repeat protein. *Plant Cell* 11, 1337–1349. doi:10.1105/tpc.11.7.1337.

Wang, J., Zhu, J., Zhang, Y., Fan, F., Li, W., Wang, F., et al. (2018). Comparative transcriptome analysis reveals molecular response to salinity stress of salt-tolerant and sensitive genotypes of indica rice at seedling stage. *Sci. Rep.* 8, 1–13. doi:10.1038/s41598-018-19984-w.

Wang, P., Ma, G., Zhang, L., Li, Y., Fu, Z., Kan, X., et al. (2019). A Sucrose-Induced MYB (SIMYB) Transcription Factor Promoting Proanthocyanidin Accumulation in the Tea Plant (Camellia sinensis). *J. Agric. Food Chem.* 67, 1418–1428. doi:10.1021/acs.jafc.8b06207.

Wang, P., Xiong, A., Gao, Z., Yu, X., Li, M., Hou, Y., et al. (2016). Selection of suitable reference genes for RTqPCR normalization

under abiotic stresses and hormone stimulation in persimmon (Diospyros kaki Thunb). *PLoS One* 11. doi:10.1371/journal.pone.0160885.

Wang, R. (1983). The origin of “Luo Tian Tian Shi” (in Chinese). *Chinese Fruit tree* 2, 16–19.

Wang, R., Yang, T., and Ruan, X. (2013). Industry history and culture of persimmon (Diospyros kaki Thunb.) in China. *Acta Hortic.* 996, 49–54. doi:10.17660/ActaHortic.2013.996.3.

Wang, R., Yang, Y., and Li, G. (1997). Chinese persimmon germplasm resources. *Acta Hortic.* 436, 43–50.

Wang, Y., Zhang, Q. L., and Luo, Z. R. (2010). Isolation and expression of gene encoding leucoanthocyanidin reductase from Diospyros kaki during fruit development. *Biol. Plant.* 54, 707–710. doi:10.1007/s10535-010-0125-9.

Warnes, G. R., Bolker, B., Bonebakker, L., Gentleman, R., Liaw, W. H. A., Lumley, T., et al. (2016). Package “gplots”: Various R programming tools for plotting data. *R Packag. version 2.17.0.* doi:10.1111/j.0022-3646.1997.00569.x.

Wei, T., and Simko, V. (2016). Visualization of a Correlation Matrix: Package “corrplot.” *CRAN*, 1–17. Available at: https://cran.r-project.org/package=corrplot.

Weill, U., Krieger, G., Avihou, Z., Milo, R., Schuldiner, M., and Davidi, D. (2019). Assessment of GFP Tag Position on Protein Localization and Growth Fitness in Yeast. *J. Mol. Biol.* 431, 636–641. doi:10.1016/j.jmb.2018.12.004.

Weir, B. S. (1990). Genetic data analysis : methods for discrete population genetic data. 377.

Wickham, H. (2016). *ggplot2 Elegant Graphics for Data Analysis*. doi:10.1007/978-3-319-24277-4.

Wickham, H., François, R., Henry, L., and Müller, K. (2018). *Package “dplyr.”*

Winkel-Shirley, B. (2001). Flavonoid biosynthesis. A colorful model for genetics, biochemistry, cell biology, and biotechnology. *Plant Physiol.* 126, 485–493. doi:10.1104/pp.126.2.485.

Xie, D. Y., Sharma, S. B., Paiva, N. L., Ferreira, D., and Dixon, R. A. (2003). Role of anthocyanidin reductase, encoded by BANYULS in plant flavonoid biosynthesis. *Science (80-.).* 299, 396–399. doi:10.1126/science.1078540.

Xu, L. Q., Zhang, Q. L., and Luo, Z. R. (2008). Occurrence and cytological mechanism of 2n pollen formation in Chinese Diospyros spp. (Ebenaceae) staminate germplasm. *J. Hortic. Sci. Biotechnol.* 83, 668–672. doi:10.1080/14620316.2008.11512441.

Xu, Q., Yin, X. R., Zeng, J. K., Ge, H., Song, M., Xu, C. J., et al. (2014a). Activator-and repressor-type MYB transcription factors are involved in chilling injury induced flesh lignification in loquat via their interactions with the phenylpropanoid pathway. *J. Exp. Bot.* 65, 4349–4359. doi:10.1093/jxb/eru208.

Xu, W., Dubos, C., and Lepiniec, L. (2015). Transcriptional control of flavonoid biosynthesis by MYB-bHLH-WDR complexes. *Trends Plant Sci.* 20, 176–185. doi:10.1016/j.tplants.2014.12.001.

Xu, W., Grain, D., Bobet, S., Le Gourrierec, J., Thévenin, J., Kelemen, Z., et al. (2014b). Complexity and robustness of the flavonoid transcriptional regulatory network revealed by comprehensive analyses of MYB-bHLH-WDR complexes and their targets in Arabidopsis seed. *New Phytol.* 202, 132–144. doi:10.1111/nph.12620.

Yakushiji, H., and Nakatsuka, A. (2007). Recent persimmon research in Japan. *Japan J. Plant Sci.* 1, 43–62.

Yamada, M. (1993). Persimmon breeding in Japan. *Japan Agric. Res. Q.* 27, 33.

Yamada, M. (2005). Persimmon genetic resources and breeding in Japan. in *Acta Horticulturae*, 51–64. doi:10.17660/actahortic.2005.685.5.

Yamada, M., Giordani, E., and Yonemori, K. (2012). “Persimmon,” in *Fruit breeding, Handbook of plant breeding*, eds. M. L. Badenes and D. H. Byrne (New York: Springer), 663–693.

Yamada, M., and Sato, A. (2002). Segregation for fruit astringency type in progenies derived from crosses of “Nishimurawase” x pollination constant non-astringent genotypes in oriental persimmon (Diospyros kaki Thunb.). *Sci. Hortic. (Amsterdam).* 92, 107–111. doi:10.1016/S0304-4238(01)00285-0.

Yamada, M., Sato, A., Yakushiji, H., Yoshinaga, K., Yamane, H., and Endo, M. (1993). Characteristics of" Luo Tian Tian Shi", a non-astringent cultivar of oriental persimmon (Diospyros kaki Thunb.) of Chinese origin in relation to non-astringent cultivars of Japanese origin. *Bull. Fruit Tree Res. Stn.*

Yamada, M., Yamane, H., and Ukai, Y. (1994). Genetic analysis of Japanese persimmon fruit weight. *J. Am. Soc. Hortic. Sci.* 119, 1298–1302. doi:10.21273/jashs.119.6.1298.

Yamagishi, M., Matsumoto, S., Nakatsuka, A., and Itamura, H. (2005). Identification of persimmon (Diospyros kaki) cultivars and phenetic relationships between Diospyros species by more effective RAPD analysis. *Sci. Hortic. (Amsterdam).* 105, 283–290. doi:10.1016/j.scienta.2005.01.020.

Yang, Z., Li, J. L., Liu, L. N., Xie, Q., and Sui, N. (2020). Photosynthetic Regulation Under Salt Stress and Salt-Tolerance Mechanism of Sweet Sorghum. *Front. Plant Sci.* 10, 1722. doi:10.3389/fpls.2019.01722.

Yonemori, K., Honsho, C., Kitajima, A., Aradhya, M., Giordani, E., Bellini, E., et al. (2008). Relationship of European persimmon (Diospyros kaki Thunb.) cultivars to Asian cultivars, characterized using AFLPs. *Genet. Resour. Crop Evol.* 55, 81–89. doi:10.1007/s10722-007-9216-7.

Yonemori, K., and Matsushima, J. (1985). Property of Development of the Tannin Cells in Non-Astringent Type Fruits of Japanese Persimmon (Diospyros kaki) and Its Relationship to Natural Deastringency. *J. Japanese Soc. Hortic. Sci.* 54, 201–208.

doi:10.2503/jjshs.54.201.

Yonemori, K., and Matsushima, J. (1987). Changes in tannin cell morphology with growth and development of Japanese persimmon fruit. *J. Am. Soc. Hortic. Sci.* 112, 818–821.

Yonemori, K., Sugiura, A., and Yamada, M. (2000). "Persimmon Genetics and Breeding," in *Plant Breeding Reviews* (Oxford, UK: John Wiley & Sons, Inc.), 191–225. doi:10.1002/9780470650172.ch6.

Yu, Z., Wang, X., and Zhang, L. (2018). Structural and functional dynamics of dehydrins: A plant protector protein under abiotic stress. *Int. J. Mol. Sci.* 19. doi:10.3390/ijms19113420.

Zekri, M., and Parsons, L. R. (1989). Growth and root hydraulic conductivity of several citrus rootstocks under salt and polyethylene glycol stresses. *Physiol. Plant.* 77, 99–106. doi:10.1111/j.1399-3054.1989.tb05984.x.

Zeng, A., Chen, P., Korth, K. L., Ping, J., Thomas, J., Wu, C., et al. (2019). RNA sequencing analysis of salt tolerance in soybean (Glycine max). *Genomics* 111, 629–635. doi:10.1016/j.ygeno.2018.03.020.

Zhang, H., Lv, F., Han, X., Xia, X., and Yin, W. (2013). The calcium sensor PeCBL1, interacting with PeCIPK24/25 and PeCIPK26, regulates Na+/K+ homeostasis in Populus euphratica. *Plant Cell Rep.* 32, 611–621. doi:10.1007/s00299-013-1394-5.

Zhang, N., Xu, J., Mo, R., Zhang, Q., and Luo, Z. (2016). Androecious Genotype 'Male 8' Carries the CPCNA Gene Locus Controlling Natural Deastringency of Chinese PCNA Persimmons. *Hortic. Plant J.* 2, 309–314. doi:10.1016/j.hpj.2016.11.006.

Zhu, J. K., Liu, J., and Xiong, L. (1998). Genetic analysis of salt tolerance in arabidopsis: Evidence for a critical role of potassium nutrition. *Plant Cell* 10, 1181–1191. doi:10.1105/tpc.10.7.1181.

Zhu, X., Cao, Q., Sun, L., Yang, X., Yang, W., and Zhang, H. (2018). Stomatal conductance and morphology of arbuscular

mycorrhizal wheat plants response to elevated co2 and NaCl Stress. *Front. Plant Sci.* 9, 1363. doi:10.3389/fpls.2018.01363.

Zhuang, D. H., Kitajima, A., Ishida, M., and Sobajima, Y. (1990). Chromosome Numbers of Diospyros kaki Cultivars. *J. Japanese Soc. Hortic. Sci.* 59, 289–297. doi:10.2503/jjshs.59.289.

First representation of persimmon fruit. ***Six Persimmons*** (六柿图)

Muqi Fachang. XIII century